INTERPRETATION OF A SEISMIC SURVEY OF CRUSTAL STRUCTURE IN WESTERN SCOTLAND AND THE HEBRIDES

by

PETROS E. TSOUMAKOS

B.Sc., M.Sc.

Thesis submitted for the degree of Doctor of Philosophy

in the Faculty of Science, Geology Department,

Glasgow University

September 1986

ProQuest LLC.
789 East Eisenhower Parkway
P.O. Box 1346
Ann Arbor, MI 48106 – 1346

TO MY PARENTS, STRATIS AND HELEN

without whose moral and financial support
this work would have been impossible

ACKNOWLEDGEMENTS

I would like to thank my supervisor Dr. J. Hall for his guidance during the execution of this project and his general help and encouragement.

My thanks also to the head of the Geology Department, Professor B. E. Leake, with whose permission this work was carried out.

I am also grateful to Drs D. W. Powell, B. Doody and K. Davidson for many useful discussions, to Professor G. K. Westbrook for his help during my visit to Durham, and to Dr. D. Evans (BGS) for kindly providing updated information on the shallow structure of the Sea of the Hebrides area.

Additional thanks go to G. Gordon, R. T. Cumberland, D. MacLean and S. Hall for never refusing any help within the department and to the staff of the Computing Centre, especially Messrs D. Fildes, P. Rosenberg, J. Beck and Mrs D. Worster for their help with computing problems.

And finally my gratitude goes to Julia for her continuous encouragement and help at the time when it was most needed.

CONTENTS

FIGURES

* : Back pocket

SUMMARY

The Western Isles Seismic Experiment (WISE), a seismic refraction profile, was shot perpendicular to the British Caledonides and runs from the Outer Hebrides (Isle of Barra) to the Scottish mainland (Midland Valley).

The aim of the experiment was to determine possible upper crustal velocity variations both vertical and lateral.

The ray tracing method is used as the main interpretation technique, as the known geology suggests that the time-term / plus-minus assumptions are frequently violated. This interpretation method has also allowed for the incorporation of existing geophysical and geological controls, in order to compensate for limitations due to the quality and availability of the data and to produce internally consistent models for both the shallow structure (mainly derived from closely spaced airgun data), and the deep structure (from distant explosive-shot data). In the Sea of the Hebrides, interpretation has shown a predominance of typical Laxfordian basement velocities (5.9 - 6.1 km/sec) and a lack of distinguishable lateral variations in the basement velocities, the latter being confined to basin / basement transitions. No granulite layer was detected down to 5 - 7 km depth.

The Great Glen Fault zone is shown to have produced, and probably coincides with, a near-vertical low velocity zone which can be traced with a fair degree of certainty down to about 5 - 6 km depth. That is found to be consistent with geological models of the structure of transcurrent large-scale continental faults,

but the structure at greater depth is uncertain due to limitations in the refraction method and data availability.

The strong Lewisian / Dalradian and intra-Dalradian velocity contrasts are quantified and are shown to persist to 8 - 10 km depth. The former define an interface that can be seen dipping at about 25° to the SE, while the latter are due to the high velocities (> 6.0 km/sec) of the formations interpreted as the core of the Islay Anticline and the Port Ellen phyllites, compared to those of the Jura quartzite (< 5.5 km/sec) and the rest of the Dalradian basement (5.3 - 5.8 km/sec).

Gravity models based on the seismic interpretation along the profile show a reasonable agreement with the observed field.

The variability of the upper crustal structure is finally discussed and compared to that in adjacent areas.

CHAPTER 1

GEOLOGICAL AND GEOPHYSICAL BACKGROUND

1.1 INTRODUCTION

The Western Isles Seismic Experiment (WISE), an upper crustal seismic survey, was carried out in November 1979 and August / September of 1981 in the region of the Western Isles of Scotland. The area and line of survey are shown in Figure 1.1.

The traverse was shot perpendicular to the trend of the Caledonian orogen and, starting in the NW from the Caledonian foreland, crosses the metamorphic Caledonides and finishes in the transition zone of the Midland Valley. The experiment was executed in two Phases.

During the first phase, 23 explosive shots were fired in the sea between the islands and recordings were made with recorders situated on the islands and peninsulas between Barra and Girvan.

Since the line crosses the sedimentary basins in the area (the Sea of the Hebrides basin, the Inner Hebrides basin, the Islay basin and the Arran basin), additional control over the usually rapid velocity changes within the sedimentary cover was achieved by using an airgun source firing at intervals of few minutes.

The second phase was executed in order to increase data quality and coverage in the area between Iona and Kintyre (Fig. 1.1). This time, 10 large explosive shots were fired together with air-gun and Geoflex shots.

The main aim of the survey was to map the Lewisian basement surface, investigate the existence of intra-basement velocity

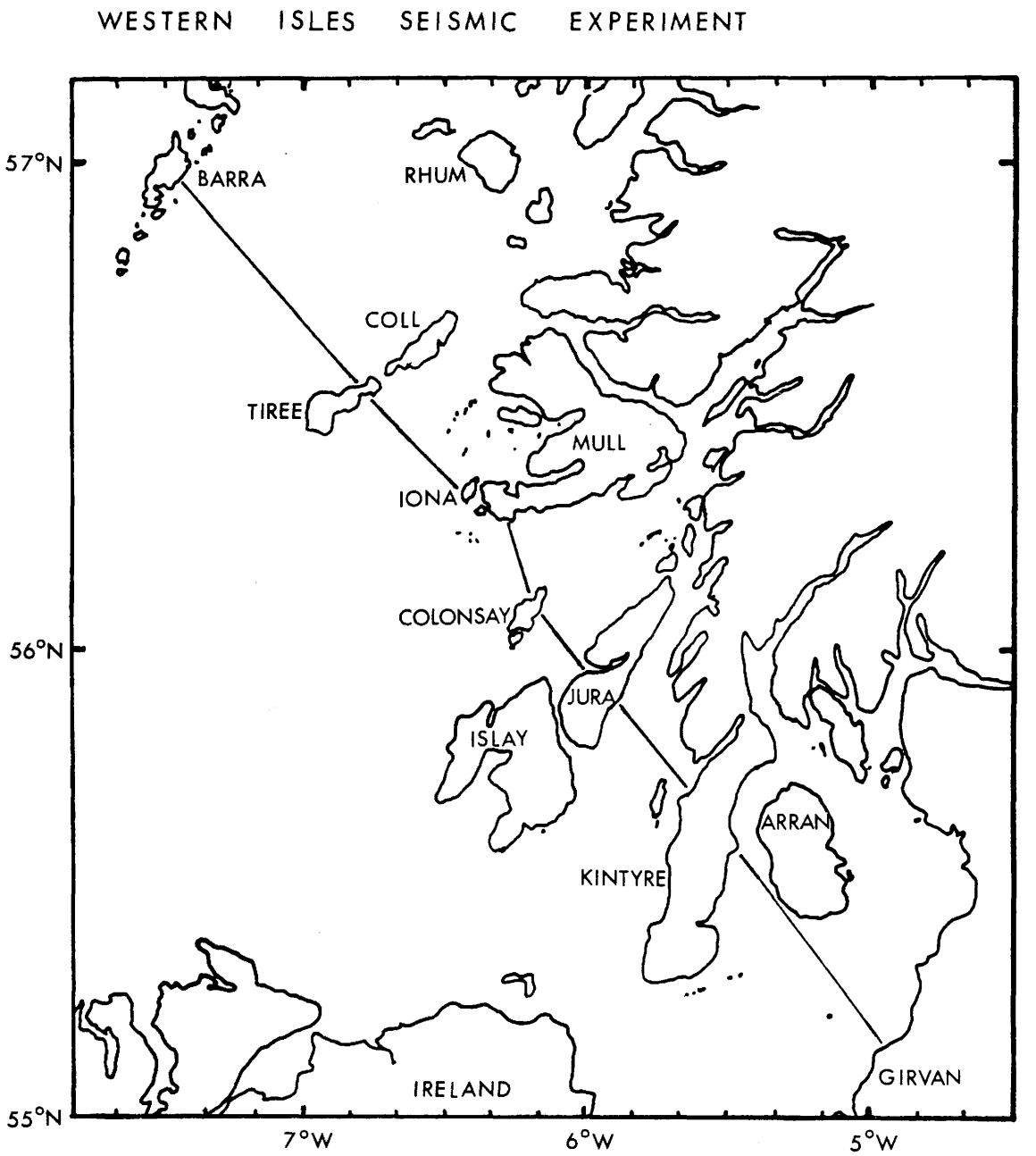

Fig. 1.1: Sketch map of the area under investigation and position of the WISE profile.

variations and define the major north-easterly trending structural blocks of the area. The structural variations within the basement might be expected to have exerted an influence on the tectonic evolution of the Mesozoic basins, of both the foreland and the Caledonian metamorphic belt.

1.2. TECTONIC SETTING AND GENERAL GEOLOGY

The most important event in the Palaeozoic history of northern Britain was the Caledonian orogeny. During the orogenic cycle the continental plates of Europe and North Atlantic collided (in late Silurian / early Devonian), closing a proto-Atlantic ocean and trapping one or more island arcs in the collision zone (Dewey 1969; Harland and Gayer 1972; Phillips et al 1976; Wright 1976; Bluck 1980; Dewey 1982; Dewey and Shackleton 1984).

The whole of Scotland and the northwestern parts of Ireland are derived from the marginal portions of the North Atlantic continent (Fig. 1.2). In the Highland region, orogenic activity began on the site of the newly formed ensialic Dalradian basin and extended progressively northwestward, towards the interior of the North Atlantic continent. Compressive deformation in the Dalradian basin (Grampian Orogeny) began in the late Cambrian when the Iapetus ocean was still very broad, due to the relative movement of the two continents. During the Ordovician and late Silurian periods, Iapetus was narrowed by subduction at one or both continental margins and the two continents were locked together and were elevated to form a single large landmass, the

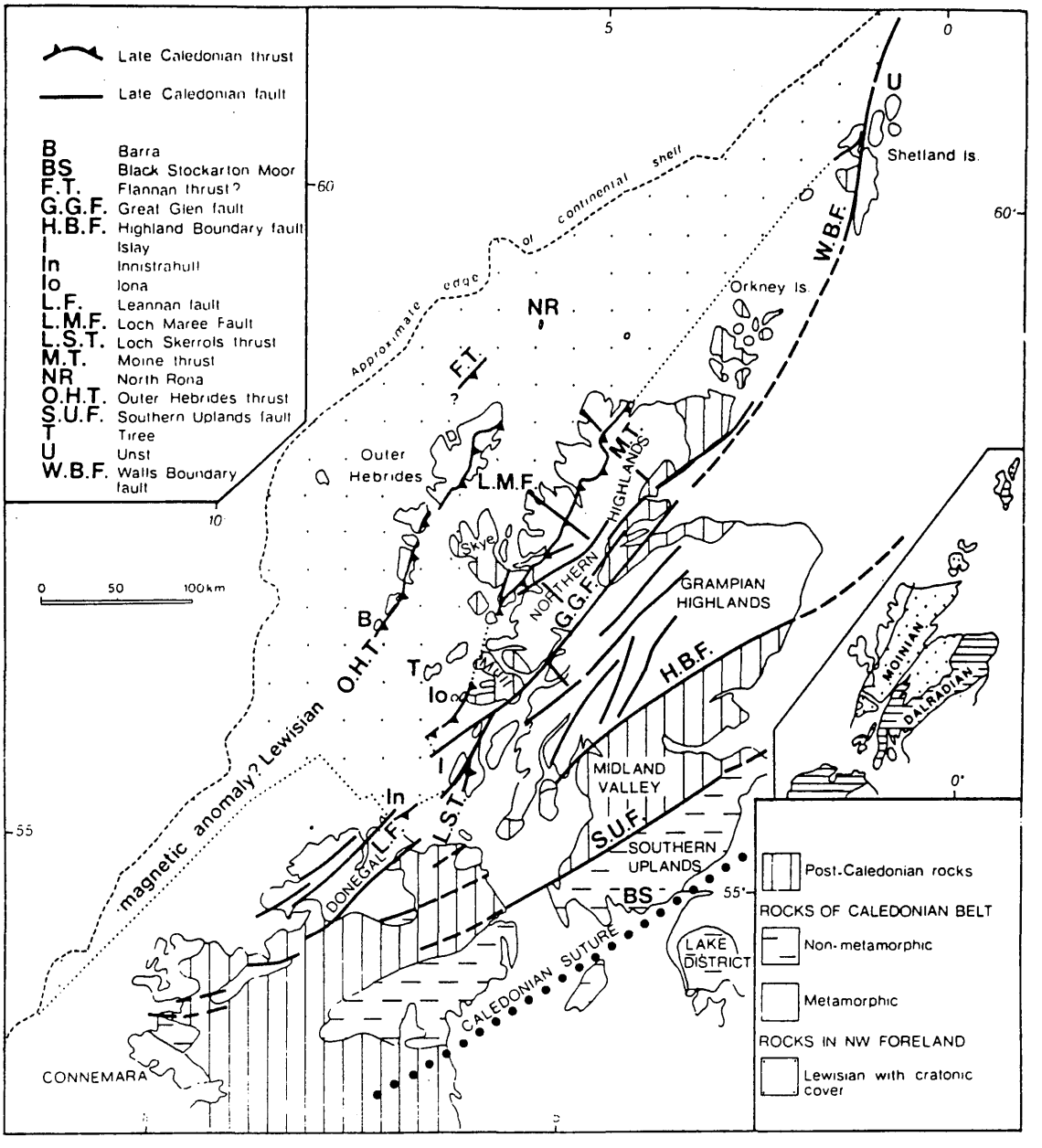

Fig. 1.2: Locality map showing the tectonic units of Scotland and NW Ireland. The inset (lower right) shows the extent of the Dalradian Supergroup (after Watson, 1984).

Old Red Sandstone continent.

Even though there are many views about the details and timing of the continental collision (for a review see Dewey and Shackleton 1984), most agree that the subduction was combined with the lateral displacement of crustal blocks and development of arc volcanos near the margin of the North Atlantic continent (Phillips et al 1976, Lambert and McKerrow 1976).

The tectonic shortening and crustal thickening during the compressive phase of the orogeny were followed by vertical isostatic movements and metamorphic reactions due to high pressure and the rise of thermal gradients. The metamorphic climax for the Dalradian of Scotland is provisionally dated at about 490 Ma. The recovery period of uplift, erosion and decline in crustal temperature lasted for about 100 Ma and by early Devonian times it was almost complete.

Meanwhile, ductile deformation had given way to brittle deformation the intensity of which decreased as the region was stabilised. The main north easterly trending fracture systems of the Highlands, the Great Glen fault and the Highland Boundary fault, were established during this late orogenic period. During the same period most of the Highland granites were emplaced.

The chronology of the Caledonian events is summarised in Figure 1.3 together with a few other details.

During post-Caledonian times the region acted as a single tectonic unit with Mesozoic sedimentation and graben formation guided along previous lines of weakness, mainly of Caledonian origin, reactivated by the tensional stresses associated with the opening of the Atlantic.

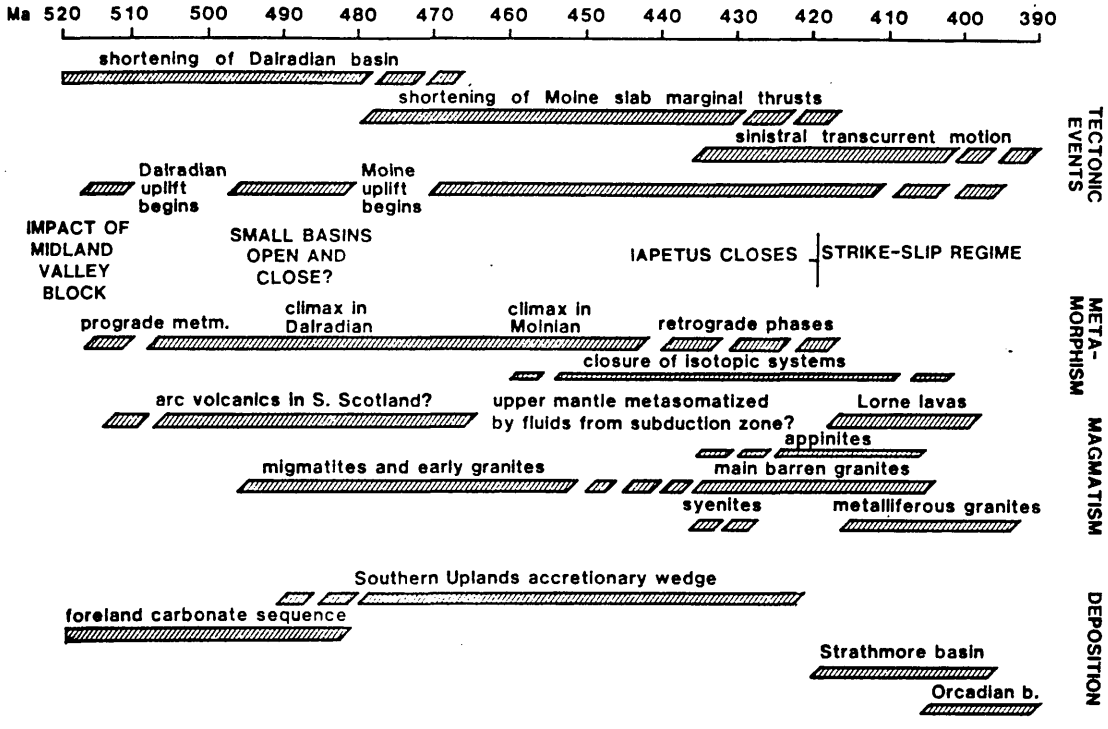

Fig. 1.3: Chart summarizing the chronology of the late Caledonian events (after Watson, 1984).

The basement of the northern craton (Hebridean craton) which constitutes the foreland of the orogen, contains Archaean to early Proterozoic gneisses and granulites (Lewisian complex) over which are thrust the metamorphosed Caledonides of the Scottish Highlands. The eastward dipping thrust belt (Moine thrust zone) divides the shelf area into two distinct regions of differing structure.

To the west, lies the Lewisian foreland basement together with its cover of late Precambrian (Torridonian) and Cambro-Ordovician unmetamorphosed sediments, having formed a stable region during Caledonian times.

To the east, lies a series of metamorphosed and folded Precambrian and Palaeozoic rocks which include reworked Lewisian basement (Northern Highlands), a cover of middle to late Proterozoic metamorphosed psammites and pelites (Moine "series"), and the Dalradian metasediments deposited in late Proterozoic to early Palaeozoic times.

The superposition of different tectonic events in the survey area have resulted in large variations in structure and rock type along the WISE line. Lewisian basement is exposed in Barra (Outer Hebrides), Coll, Tiree, Iona and Islay with Mesozoic and older sediments filling the half grabens between. Torridonian rocks lie on Lewisian basement in the area around Colonsay whereas the metasediments of the Dalradian supergroup extend from Colonsay to Kintyre. Finally, the Firth of Clyde area is characterised by Ordovician, Carboniferous and Mesozoic sedimentation and Tertiary granite intrusions.

1.3. THE HEBRIDEAN CRATON: BASEMENT

The basement consists entirely of Archaean to early Proterozoic gneisses and granulites (Lewisian complex) derived from pre-2600 Ma igneous intrusions with minor metasediments and metavolcanics (Sutton and Watson 1951, Dearnley 1962).

They were evolved during intermittent periods of metamorphic reworking down to about 1700 Ma with two main phases recognised, separated by phases of uplift erosion and dyke intrusion (Sutton and Watson 1951, Park 1970, Watson 1975, Watson and Dunning 1979).

The first phase known as Scourian occurred at about 2600 Ma (Moorbath et al 1969) and the second phase, the Laxfordian, at about 1600 Ma ago (van Breemen et al 1971). A third phase, the Inverian, is recognised by Evans (1965) and occurred between 2200 and 1950 Ma ago.

Laxfordian deformation and metamorphism in the Hebridean craton was responsible for the development of large ductile shear zones in both the Scottish mainland (Laxfordian zone) and the Outer Hebrides (South Harris zone). It was also responsible for the large scale structural pattern of the Outer Hebrides dominated by cuspate folds (Coward et al 1970, Coward 1984).

The eastern coastline of the Outer Hebrides closely parallels the Outer Isles Thrust zone, which in pre-Cambrian and again in late Caledonian times thrust dense Scourian granulites westwards over less dense amphibolite gneisses and granites (McQuillin and Watson 1973). Refined interpretation of deep seismic reflection data from north of the Hebrides (MOIST profile, see below), has

shown the thrust to extend through the crust into the upper mantle (Peddy 1984).

On the island of Barra (Fig. 1.4), a supra-structure of acid amphibolite gneiss within an infra-structure of orthopyroxene bearing gneiss can be observed (Francis 1973).

Rocks cropping out on Tiree, Coll and Iona are generally of amphibolite facies and Laxfordian in age (Bowes 1968). Westbrook (1972) and Drury (1972), however, provide evidence for an amphibolite grade of metamorphism being superimposed on a granulite texture and mineral asemblage, on Tiree and Coll.

The two facies types have been recognised to have different physical properties, the Scourian granulites having higher density (McQuillin and Watson 1973), degree of magnetisation (Powell 1978) and seismic velocity. The NASP profile (Smith and Bott 1975) and the LISPB profile (Bamford et al 1977, 1978, Bamford 1979) have shown that the 6.4 km/sec seismic layer (the deeper one in a two layered crust), in the north Scottish shelf and the north Scotland, correlates with granulites like those in Sutherland. In situ velocity measurements have confirmed that (Hall and Al-Haddad 1976, Hall 1978a).

Deep seismic reflection work (MOIST profile, Smythe et al 1982, Brewer et al 1983, Brewer and Smythe 1984) has shown the existence of another major thrust beyond the Outer Hebrides, the Flannan thrust, being roughly parallel to the Outer Isles thrust and cutting through the crust to the mantle. It has also shown that the Mesozoic basins are typical extensional features, usually half grabens, bounded by normal listric faults which sole into Caledonian thrusts.

1.4. THE HEBRIDEAN SEDIMENTARY COVER: BARRA TO IONA

On the Lewisian basement lies unconformably a cover of "Torridonian" unmetamorphosed sediments (Fig. 1.4), which includes two Proterozoic groups, the Stoer and the Torridon groups, dated respectively at about 1000 Ma and 800 Ma (Moorbath 1969).

Both groups consist of red sandstone, conglomerates and grey shales and were deposited within rifts. They are best developed in northwest Scotland and they are considered the non-metamorphic equivalent of the Moine series (Stewart 1976,1982). Rocks assigned to the Torridonian, on account of their relation to Lewisian and the Moine Thrust, include the Bowmore sandstones of Islay and the sediments of Colonsay, Oronsay and Iona. No correlation has yet been shown with the Stoer or Torridon groups of northwest Scotland (Stewart 1976).

Above the Torridonian, some Lower Palaeozoic rocks might be preserved locally but they are difficult to define geophysically.

Interpretation of the solid geology of the Sea of the Hebrides is based primarily on aeromagnetic (Institute of Geol. Sciences, Aeromagnetic map of Great Britain 1st ed. scale 1:625000 1972), gravity and magnetic surveys from ships, shallow and deep reflection seismic surveys, rock sampling and drilling (up to 70 m in the sea floor). These data were mainly collected by the Institute of Geological Sciences and are described and analysed in a number of publications (Binns et al 1973, McQuillin and

Binns 1973, McQuillin and Binns 1975, Binns et al 1975).

The geology in the area is controlled by three major faults, the Minch fault, the Camasunary-Skerryvore fault and the Great Glen fault (Fig. 1.4). These faults form margins to deep asymmetric troughs which are floored by down-thrown Torridonian.

The Sea of the Hebrides basin (south Minch basin) is bound at the northwest by the Minch fault and has a synclinal structure defined by a reflector which has been interpreted as the top of the Torridonian (Binns et al 1975). The basin reaches its maximum depth south of Skye where 2.5 km of Mesozoic sediments is believed to be preserved. On the basis of land evidence (lack of variation of strata), Jurassic and Cretaceous sediments are expected to form only a minor component of the basin infill and the presence of a thick Permo-Triassic sequence was therefore suggested (McQuillin and Binns 1973). Whitbread (1975) though states that on Skye and Raasay Jurassic sediments are about 1000 m thick.

The south margin of the basin though poorly understood from Binns et al (1975), now is believed to contain a shallow and narrow marginal basin (Coll basin) having a Caledonoid trend and filled with Triassic and Jurassic sediments (Uruski 1981).

The Inner Hebrides basin is bounded by the Camasunary-Skerryvore fault and even though it is narrower than the Sea of the Hebrides basin, the maximum thickness of the sediments is of the same order according to the gravity anomaly to the south-east of Coll and Tiree (Fig. 1.5). The basin extends from Skye to south of the Blackstones bank and is probably floored by Palaeozoic sediments upon which rest Permo-Triassic and Jurassic

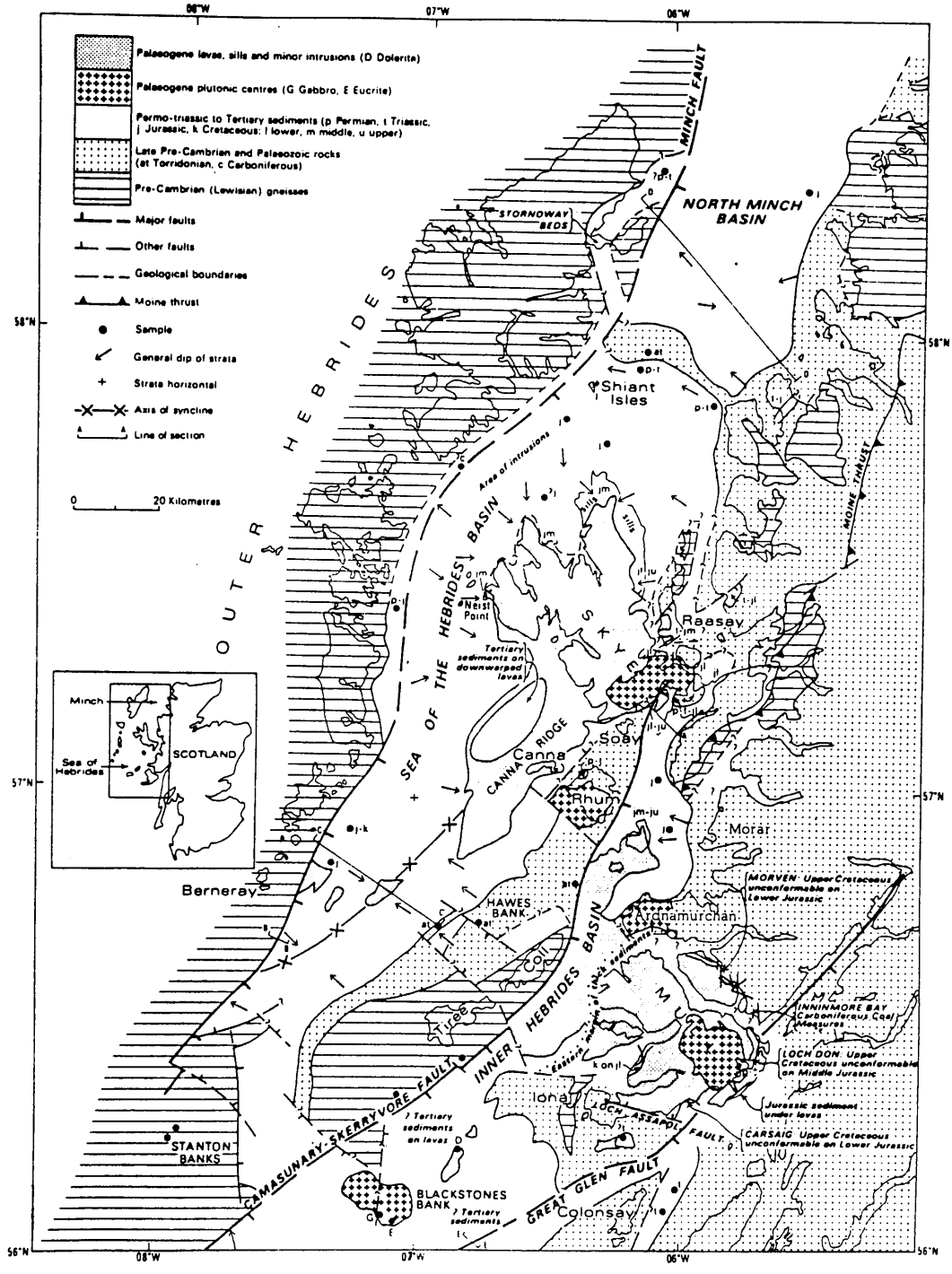

Fig. 1.4: Pre-Quaternary geology of the area between the Scottish mainland and the Outer Hebrides (after Binns et al, 1975).

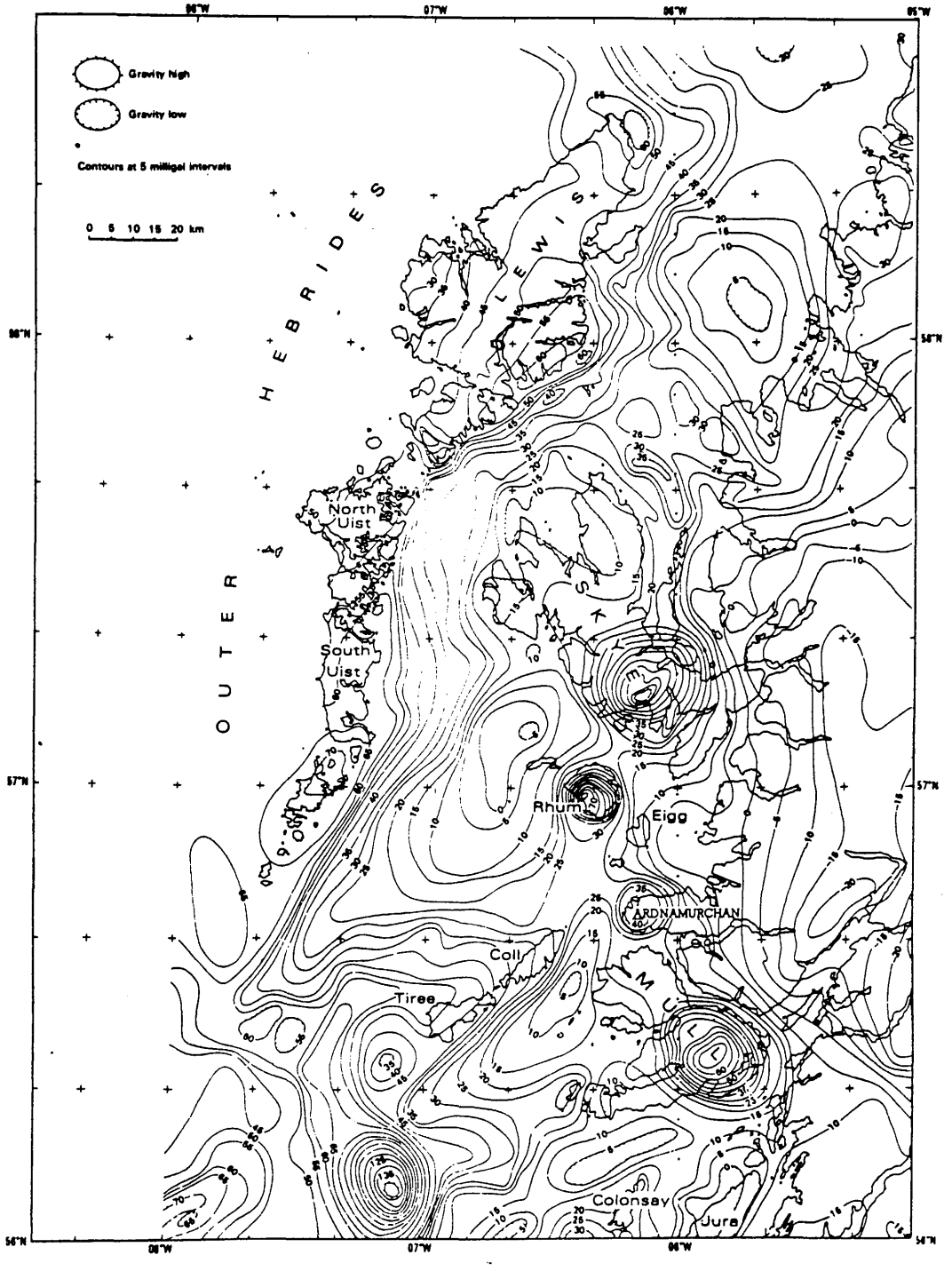

Fig. 1.5: Bouguer anomaly gravity map of the area between the Scottish mainland and the Outer Hebrides (after Binns et al, 1975).

rocks.

The Jurassic sediments of Skye can be seen to be thrown down at least 700 m to the east against the Precambrian. Alluvial fan and floodplain environments have been suggested for the Permo-Triassic sediments, the direction suggesting contemporaneous movement on the Camasunary fault (Bruck et al 1967, Steel 1971, Steel 1974).

Tertiary igneous activity and north-west faulting was superimposed on these structures. Tertiary sediments of a few hundreds of metres thickness (apart from the area west of Canna where they reach a thickness of about 1 km), are recognised in seismic reflection records and cover the Mesozoic sediments or the Tertiary lavas on the downthrown side of the Camasunary-Skerryvore fault and in the area of the Great Glen fault (Smythe and Kenolty 1975).

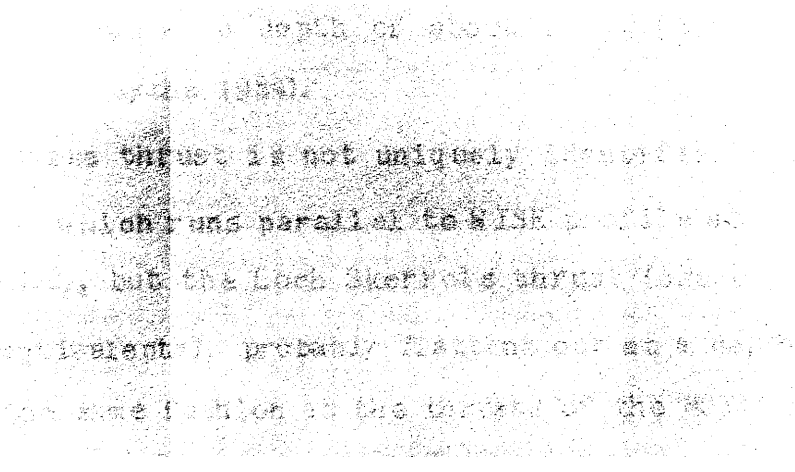

1.5. IONA TO COLONSAY: MOINE THRUST AND GREAT GLEN FAULT

The Moine Thrust (Fig. 1.2, 1.4), is the uppermost thrust of a group of sub-horizontal fracture planes known collectively as the Moine Thrust zone. The zone runs NNE-SSW and the thrust movement has brought the rocks of the orogen over Lewisian foreland during the later stages of the Caledonian orogeny. The thrust has been traced through the mainland to the offshore northern Scotland (MOIST profile, Smythe et al 1982), and probably reappears on the Shetland islands (Flinn et al 1979, Andrews 1985).

The first attempts to project its structure at depth (Elliot and Johnson 1980, Coward 1980, Soper and Barber 1982), lacked adequate subsurface control and produced widely different models from the same geophysical data. Their estimates for the extent of the foreland Lewisian basement under the orogen ranged from 70 km (Elliot and Johnson 1980) to 20-30 km (Watson and Dunning 1979).

With the MOIST profile, the thrust plane was found to have a listric form and was traced to the lower crust where it flattened out at a depth of about 18 km (Smythe et al 1982, Brewer and Smythe 1984).

The Moine thrust is not uniquely identifiable on the WINCH profile (which runs parallel to WISE profile at a 50 km offset to the SE), but the Loch Skerrols thrust (one of its supposed local equivalents), probably flattens out at a depth of about 15 km in the same fashion as the thrusts of the MOIST profile (Hall et al 1984).

In Iona, the Moine Thrust is believed to be dipping at about 25o under the Ross of Mull granite with some Torridonian rocks trapped between the Lewisian and the granite. The Ross of Mull granite has been dated to about 420 Ma (cooling age), and its ascent was probably guided by the Great Glen fault and was injected along the Moine Thrust plane (Tuson 1959, Pankhurst and Sutherland 1982).

The Great Glen fault (Fig. 1.2, 1.4), is the best known of a set of sinistral strike-slip faults including the Strathconon, Ericht Laidon and Loch Tay faults. Its physical expression on land is a striking topographic trough and is represented by a zone of intensely sheared and crushed rocks 2-3 km wide (Kennedy 1946, Eyles and MacGregor 1952). Since the paper of Kennedy suggesting pre-Upper Carboniferous sinistral movement of 100 km, all kinds of movements have been proposed including sinistral, dextral and normal and timings ranging from Caledonian to Tertiary (e.g. Holgate 1969, Garson and Plant 1972, Winchester 1974/1978, Chesher and Bacon 1975, Mykura 1975, Chinner 1978) including a 2000 km sinistral displacement (Van der Voo and Scotese 1981).

The interest reflects the significance of the scale and timing of the fault movements on the structural evolution of Britain and North Sea (Dewey 1982, Ziegler 1981).

Recent evaluation of the existing geological, geophysical and geochemical evidence concludes that the main phase of movement on the fault was pre-Devonian with sinistral displacement of 100-200 km (Smith and Watson 1983).

To the north of the Moray Firth the fault is believed to continue through the Shetland islands and to the south-west of Islay it has been traced in various surveys by following the steep banks of the fracture zone now covered by Mesozoic and/or Tertiary strata (Binns et al 1973, Rashid 1978, Wilson 1979, Barber et al 1979, Evans et al 1980, Hall et al 1984).

Between the Moine thrust and the Great Glen fault, Moine schists, comprising mainly metasediments, together with Lewisian basement inliers, form a tract that has undergone polyphase deformation and metamorphism (e.g. Powell and Phillips 1985). In the WISE area, these rocks are stacked together with granites and Tertiary basaltic lavas from the Mull Tertiary igneous centre, while to the west of the fault lie the "Torridonian" of Colonsay and Oronsay (section 1.3).

1.6. COLONSAY TO KINTYRE: THE DALRADIAN BASIN

Dalradian rocks crop out over a wide area in the Scottish Highlands immediately to the northwest of the Highland Boundary fault. They are also present on the islands of Islay and Jura (Fig. 1.6).

They form a very thick sequence of sediments, of late Precambrian to Cambrian age, which was deposited in part of the Caledonian geosyncline (section 1.2). The sequence is lithologically quite diverse and consists of conglomerates, sandstones, limestones, dolomites and shales. Their deposition was interrupted on occasion by the eruption of volcanic rocks, accompanied by the intrusion of dolerite sills. These rocks were

then deformed and metamorphosed during an early stage of the Caledonian orogeny at the end of Cambrian times.

1.6.1. Stratigraphy and depositional history

After Harris and Pitcher (1975) the Dalradian is recognised as a supergroup which includes four groups: The Grampian Group, Appin (or Lower Dalradian), Argyll (or Middle Dalradian) and the Southern Highland group (or Upper Dalradian). A generalized stratigraphy can be seen in Figure 1.7.

Little is known about the sedimentology of the Grampian group; Hickman (1975) infers shallow water, probably marine environment with intermittent terrestrial conditions. Together with the Appin group they can be stratigraphically divided from the younger Dalradian by the base of the Port Askaig tillite (Fig. 1.7). They were deposited as relatively thin units of mud, sand and carbonate on a stable continental shelf on which differential subsidence would account for lateral thickness and facies variations (Harris et al 1978).

The upper part of the Dalradian, the Argyll and Southern Highland group, starts with the Port Askaig tillite and continues with marginal to shelf sediments (Bonahaven dolomite and Jura quartzite), which are replaced upwards by deep water turbidite and basinal facies (Scarba conglomerate and Easdale slates). This change to deep water sedimentation has been interpreted as due to the initiation of major syn-depositional faulting in Argyll group times (Harris et al 1978, Anderton 1979). Lateral thickness variation of the Port Askaig tillite,

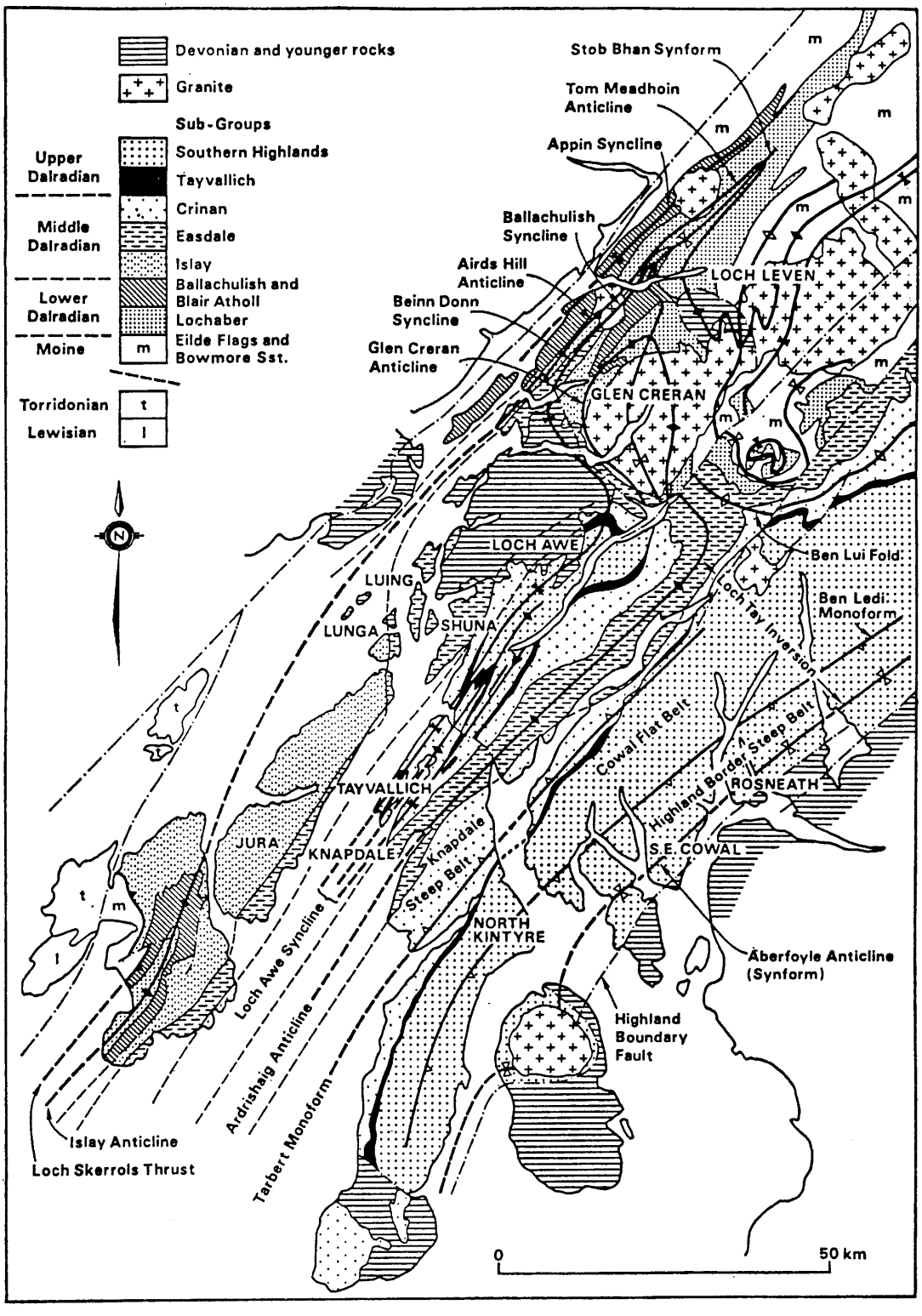

Fig. 1.6: Simplified geological map of the Dalradian rocks in the South-west Highlands of Scotland, showing the axial traces of the major folds according to Roberts and Treagus (1977). The stratigraphic units correspond to the various subgroups as given in Figure 1.9 (after Roberts and Treagus, 1977).

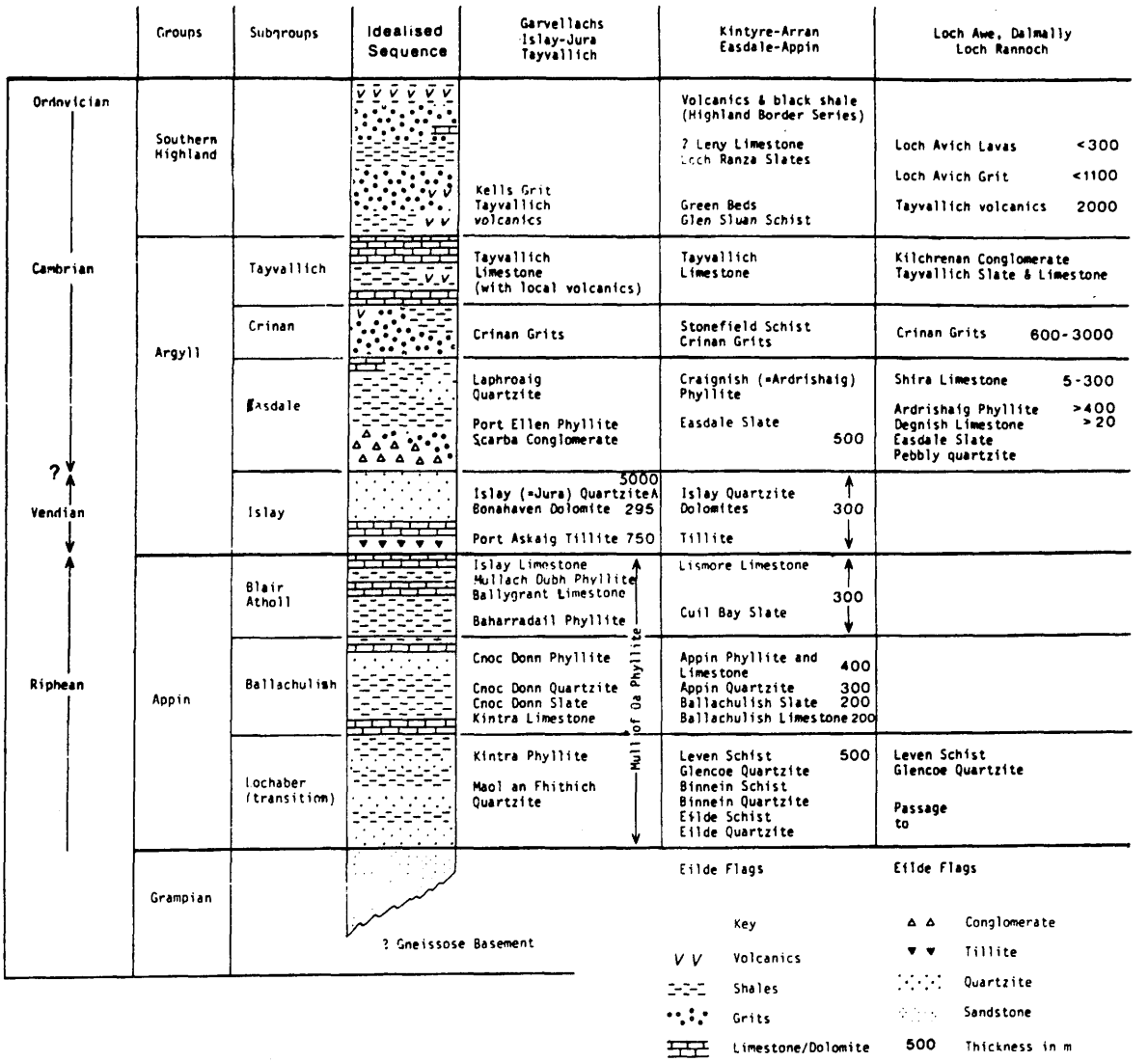

Fig. 1.7: Stratigraphic successions in the Dalradian of the South-west Highlands of Scotland (after Johnson, 1983).

Bonahaven dolomite and Jura quartzite may have resulted by less drastic fault movement, the rate of sediment influx keeping up with the rate of subsidence (Anderton 1982).

The increase in tectonic instability eventually culminated in the eruption, at the beginning of Southern Highland group times, of the tholeiitic Tayvallich lavas and the intrusion of dykes and sills in the area of the south-west Scottish Highlands. The suite indicates regional crustal extension (Graham 1976) and petrographic evidence from the Port Askaig tillite and Jura quartzite favours an opening for the Iapetus roughly contemporaneous with the Tayvallich volcanics (Anderton 1980b). This timing is in agreement with previous models (Phillips et al 1976, Scrutton 1973), as well as later ones (Dewey and Shackleton 1984).

A diagrammatic representation of the Dalradian depositional history, tectonic environment and their relation to the general time scale, is provided in Figure 1.8.

Throughout most of the time of deposition of the Appin and Argyll groups in the S.W. Highlands, it is likely that a land-mass existed to the north-west of the present outcrop and it supplied mature sediment to the subsiding Dalradian basin (Anderton 1976, 1977).

The sedimentology of the Southern Highland group rocks, showing turbidite affinities of the greywackes implying deep-sea fan sedimentation (Sutton and Watson 1955, Harris et al 1978), marks an important change in the palaeogeography. Since most of the clastic rocks are immature and contain abundant granitic

clasts and potassium feldspar fragments (Borradaile 1973), Phillips et al (1976) have postulated the creation (or uplift) of a new southern continental source area which separated the Dalradian basin from the Iapetus ocean.

1.6.2 The Structure

Within a relatively short period in late Cambrian and early Ordovician times, the Dalradian supergroup underwent polyphase deformation and regional metamorphism (the Grampian orogeny).

Each phase in the deformation history generated fold structures and cleavages parallel to the fold axial planes. The superposition of structures belonging to latter phases of deformation on structures developed in response to earlier phases of deformation has resulted in the complicated structure exhibited now by these rocks.

Four phases can be recognised in all, with the first two (D1 and D2) being the dominant deformation phases in the S.W. Highlands (Roberts and Treagus 1977a, 1977b).

Large recumbent primary folds, facing north-west and south-east away from a central zone have been interpreted as the manifestations of upward and outward expulsion of material and subsequent gravity induced collapse away from this zone, in what has been called the "fountain of nappes" hypothesis (Sturt 1961, Roberts 1974, Thomas 1979), Figures 1.6, 1.9. The alternative mechanism proposed is simply gravity-operated flow away from a tectonic elevation (Bradbury et al 1979).

The largest of the nappes, the D1 Tay nappe, is believed to

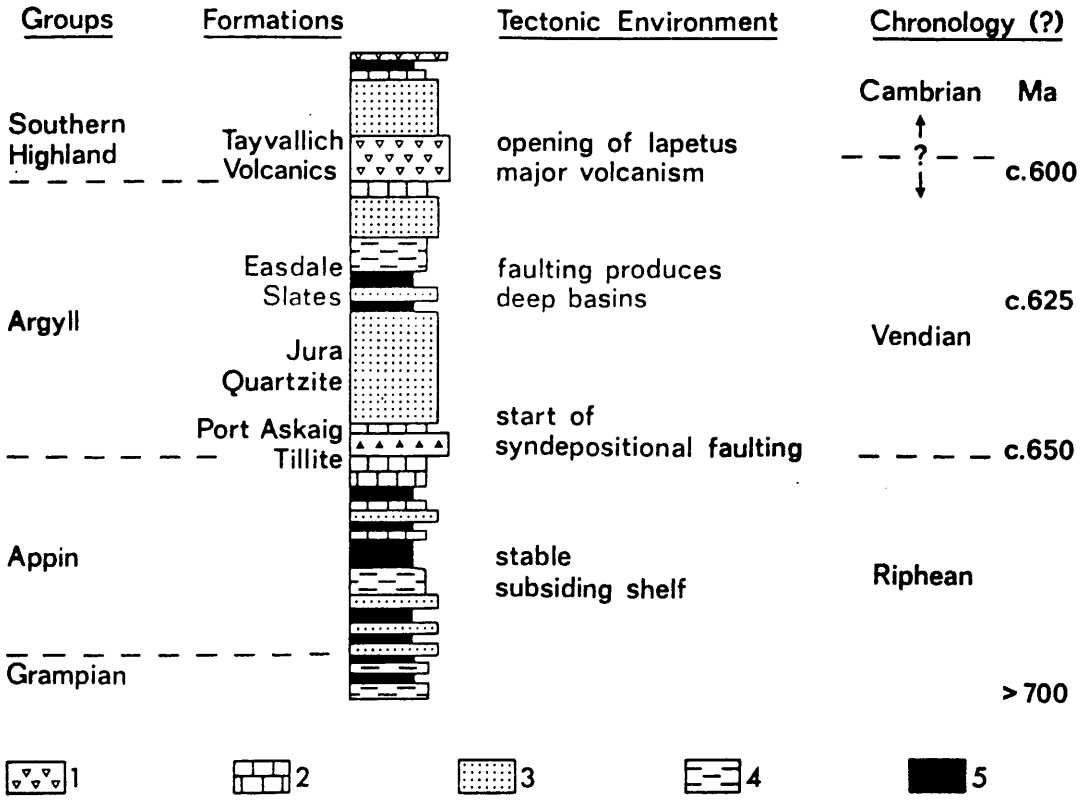

Fig. 1.8: Dalradian stratigraphy, tectonic environment and suggested chronology. Key: 1 = lavas and tuffs; 2 = limestones and dolomites; 3, 4 and 5 = predominantly sandy, silty and muddy clastic sediments, respectively (after Anderton, 1982).

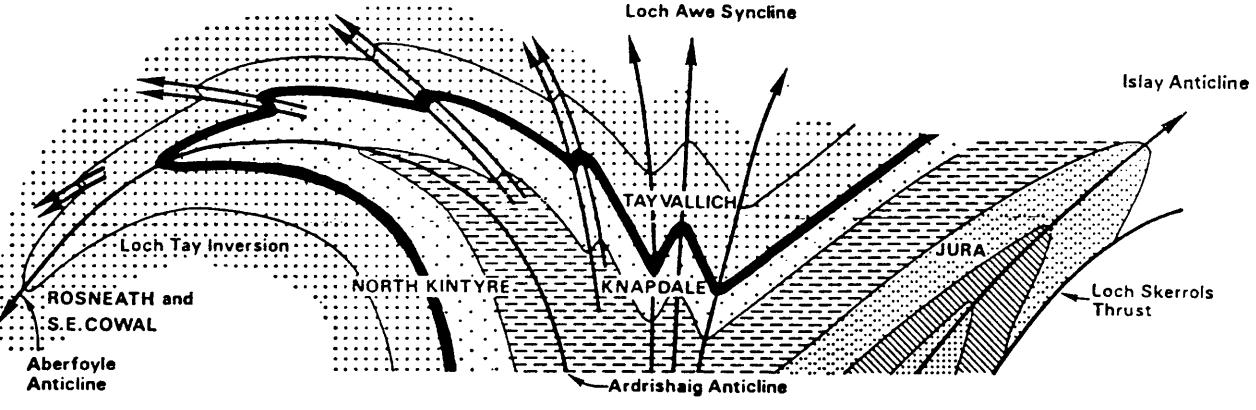

Fig. 1.9: Diagrammatic cross-section through the Dalradian rocks in the South-west Highlands of Scotland, showing the structural relations of the major folds established in Fig. 1.6 (after Roberts and Treagus 1977).

have been transported southeastwards for at least 50 km (Bradbury et al 1979, Shackleton 1979), and large areas of Dalradian rocks, including parts of the S.W. Highlands, lie on the lower inverted limb of the Tay nappe (facing northeastwards). The anticlinal core of the Tay nappe is represented by the D1 Ardrishaig anticline according to Roberts (1974), though others do not believe it represents an actual "root" of the Tay nappe.

Another recumbent fold, the Ben Lui fold can be traced for a distance of 280 km, from Kintyre to Deeside, but is now thought to be a later structure.

The D1 Islay Anticline (Bailey 1917), is another major fold and facing northwestwards is separated from the Tay nappe by the D1 Loch Awe synclinal complex (Fig. 1.9). The anticline thrusts (Loch Skerrols thrust) the Dalradian rocks of Islay over the Torridonian-like sediments of the island (Bowmore sandstones) before plunging to the north-east.

The Lewisian rocks exposed in Islay, disappear to the north under the Bowmore sandstones which form the sea-floor between Colonsay and Islay (Dobson et al 1975) and after a probable plunge depression reappear at the northern tip of Colonsay.

Geophysical surveys in the past few years (Dobson and Evans 1974, Dobson et al 1975, Evans et al 1980), have determined that the area is controlled by four faults, the Great Glen, Loch Gruinart, Lough Foyle and Tow Valley faults. The faults downthrow Mesozoic sediments against the Dalradian metasediments of Islay and Jura (Fig. 1.6, 1.10).

Of fundamental importance to the area is the Loch Gruinart

fault, which at Rinns (S.W. Islay) downthrows about 1 km of Mesozoic sediments against Lewisian gneisses, while in the area between Colonsay and Jura only a few hundred metres of Mesozoic sediments is believed to be preserved (Binns et al 1973, Wilson 1979). The fault was first considered to be a probable continuation of the Great Glen fault (Bailey 1917), but more recent geophysical surveys (e.g. Barber et al 1979, Wilson 1979) and examination of the magnetic field in Islay (Westbrook and Borradaile 1978) consider the fault to be a second-order one, associated with the Great Glen fault. The tracing of the Great Glen fault to the lower crust at the S.E. of Islay by the WINCH seismic profile (Brewer et al 1983), has finalised the matter.

Syndepositional movements along the above faults occurred during Permo-Triassic times with gentler deposition during Upper Cretaceous (Dobson and Evans 1974).

The Lewisian / Dalradian interface in Islay has been mapped by Westbrook and Borradaile (1978), while immediately to the south, just off Islay, the interpretation of the WINCH profile has supported their modelling and also showed that the crustal thickening in the Dalradian basin was achieved by oppositely dipping thrusts in a zig-zag sort of obduction (Hall et al 1984).

The Jura quartzite outcrop attains its maximum stratal thickness of about 5 km in the northern half of Jura (giving rise to a gravity low, Fig. 1.5) and rapidly thins off to the north and to the south (e.g. Anderton 1977), (Fig. 1.6).

Generally, the geology between Jura and Kintyre is believed

to be an extrapolation of the onshore geology of the S.W. Highlands (Fig. 1.6), with the Tayvallich lavas increasing their thickness considerably along the Loch Awe syncline, as they plunge to the south under the sea (Borradaile 1973, Roberts and Treagus 1977).

1.7. KINTYRE TO GIRVAN: THE OFFSHORE MIDLAND VALLEY

The solid geology of the Firth of Clyde region has been mainly determined by IGS geophysical surveys consisting of gravity, magnetic, refraction, reflection and sea-floor sampling (McLean and Deegan 1978), (Fig. 1.10). The area is bounded by the Highland Boundary fault to the north and the Southern Uplands fault to the south, creating a downthrown crustal block covered by faulted Upper Palaeozoic, Carboniferous and New Red Sandstone strata.

Two general fault trends are recognised: a set of NE-SW faults due to differential subsidence in Old Red Sandstone, early Carboniferous and Namurian times and a set of NW-SE trending faults due to movements along normal faults in late Carboniferous and Mesozoic times (McLean 1978, Mykura 1983, Francis 1983), Figure 1.10.

The Old Red Sandstone strata (Middle Old Red Sandstone missing) rest on Dalradian strata with great variations in the thickness of the Upper ORS taking place across the Highland Boundary fault. There is also a general southward increase in the thickness of the Lower ORS rocks, from 1800 m in Arran and 1200 m in Kintyre (Richey et al 1930), to about 3.5 km in the

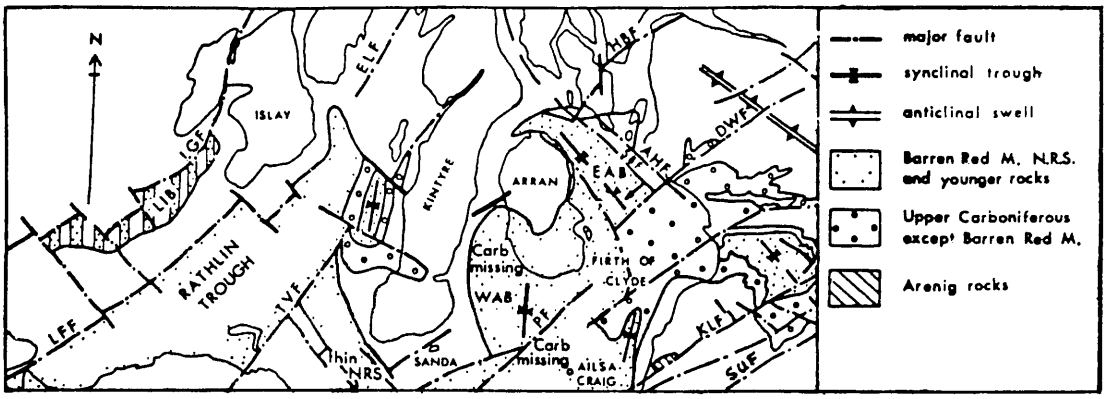

Fig. 1.10: Geological map showing the Firth of Clyde and the eastern Malin Sea. Abreviations used are: LGF = Loch Gruinart Fault; LIB = Loch Indaal Basin; LFF = Loch Foyle Fault; ELF = Ericht-Laidon Fault; TVF = Tow Valley Fault; WAB = West Arran Basin; EAB = East Arran Basin; HBF = Highland Boundary Fault; PF = Plateau Fault; KLF = Kerse Loch Fault; SUF = Southern Uplands Fault (after McLean 1978).

south part of the West Arran basin and in the area to the east of the Plateau fault (McLean and Deegan 1978).

In the West Arran basin the Carboniferous sequence is attenuated considerably or is absent towards the southwest, due to breaks in sedimentation and lateral changes combined with a lateral step of the New Red Sandstone (McLean and Deegan 1978). In contrast, further to the south the interpretation of the WINCH profile suggests about 2 km of Carboniferous rocks (Hall et al 1984). In the East Arran basin a sequence of 1.1 km of rocks of this age is preserved, on top of the Clyde Plateau lavas (Hall 1978b).

New Red Sandstone crops out over most of Arran and having a southwesterly dip covers most of the plateau areas in the Firth of Clyde. In the eastern half it oversteps the Upper Palaeozoic strata to rest on the Lower Palaeozoic. The thickness of Mesozoic strata reaches a maximum of 1.5-2 km in the West Arran basin, as inferred from gravity interpretation, and a thickness

of about 1 km on the downthrown side of the Plateau fault (McLean 1978, McLean and Deegan 1978).

There is no evidence of either Tertiary sediments or Tertiary basalts in the Firth of Clyde but the Tertiary igneous centre of Arran dominates the geology of the island and a ridge connecting the Arran and Ailsa Craig igneous rocks, has been suggested by McLean and Deegan (1978).

Though no evidence for the southward continuation of the Highland Boundary fault has been found on Kintyre, gravity and magnetics indicate that the fault is broken into distinct segments by sinistral faults causing it to step to the south (Mclean and Deegan 1978). A similar suggestion comes from Hall et al (1984), with the Plateau-Cushendall faults being in an echelon relationship with the Highland Boundary fault and thus explaining the narrowing of the Midland Valley from 70 km in Scotland to 50 km in Ireland.

1.8. GEOPHYSICAL BACKGROUND AND THE WESTERN ISLES SEISMIC EXPERIMENT

The WISE profile was executed at a time when a considerable amount of relevant geophysical data had been gathered in Scotland and the surrounding continental shelf. The various geophysical surveys of the 1970's from both IGS (Binns et al 1973, McLean and Deegan 1978,Evans et al 1980) and academic workers (e.g. Dobson and Evans 1974, Westbrook and Borradaile 1978, Barber et al 1979, Wilson 1979), provided a part of the

preliminary geophysical controls for the interpretation of the experiment. Since a number of theses from the University of Durham on the processing and initial interpretation of the WISE data already exist, this thesis will be entirely concerned with the integration of all the existing information into a refined procedure of interpretation, in order to produce geophysical models sufficiently clear to give a better appreciation of the crustal structure along the profile.

Some of the key questions to be answe red concern the definition of the NE-SW trending structural blocks, the existence of intra-basement velocity contrasts and the downward continuation of the Great Glen fault zone (Chapters 4 & 5). In addition critical appraisal is offered of the main interpretation method (ray tracing) in conjunction with other existing methods (like time-term analysis) and the various levels of accuracy and availability of refraction and other geophysical data (Chapters 2 & 3).

Comparisons will be also attempted between the crustal structure determined from the WISE and those of previous experiments in surrounding areas such as NASP (Smith and Bott 1975), LISPB (e.g. Bamford et al 1978), HMSP (Armour 1977, Bott et al 1979) -refraction profiles- MOIST (Smythe et al 1982, Brewer and Smythe 1984) and WINCH (Brewer et al 1983, Hall et al 1984) - deep reflection profiles.

CHAPTER 2

THE WISE DATA AND THEIR EVALUATION

2.1. INTRODUCTION

The data for WISE were collected during two cruises. The first one took place in November 1979 and the second in late August / early September 1981. The recording stations were positioned on the islands and peninsulas along the WISE profile (Fig. 2.1 and 2.2) and were manned by students and staff from Durham and Glasgow Universities.

2.2. DATA ACQUISITION

2.2.1. WISE Phase 1

This phase was executed between the 12th and 27th of November 1979 and provided the main body of the explosive data. Most of the stations were occupied by 3-component seismometer sets, the horizontal seismometers placed parallel and perpendicular to the line.

Two types of seismometer and recorder sets were used, either Willmore Mk.3 seismometers operating with a Geostore recorder or Willmore Mk.2 seismometers operating with the Mk.3 seismic recorder developed at Durham University. Some stations in Jura and Girvan had vertical seismometers only and the data were transmitted to a Geostore by radio link. A three-component set on Iona was recorded at Mull by the same method. Descriptions of the types of recorders used in the survey are provided by Summers (1982).

The 23 explosive shots were of variable sizes and placed at variable intervals, the former depending mainly on the desired recording distance and expected thickness of sediments under the shots, and the latter on the concepts of optimum subsurface coverage related to the geometry of the ray-paths in a refraction experiment. The shot charges were detonated on the sea-floor and the explosions were detected by a hull geophone and a hydrophone towed behind the ship, with recordings made on magnetic tape. Later, corrections were made to account for the time delays due to the distance between the moving ship and the detonation points. The timing of the shots using this method is accurate to within 0.03 seconds.

The position of the explosive shots, the airgun profiles, and the receivers are shown in Figure 2.1 together with other relevant information. Details such as the exact location of the shots and the receivers, the charge size, the water depth and firing time, are listed in Appendix 1 (Tables A.1, A.2 and A.3).

The airgun source was a 1000 cu.in. Bolt PAR airgun operating at 2000 psi and by firing approximately every 3 minutes, it provided a shot separation of about 300 m. Because of shallow water near to Kintyre, the line from Jura to Kintyre was completed by firing 12 small explosive (Geoflex) charges. Their details also appear in Appendix 1 (Table A.4).

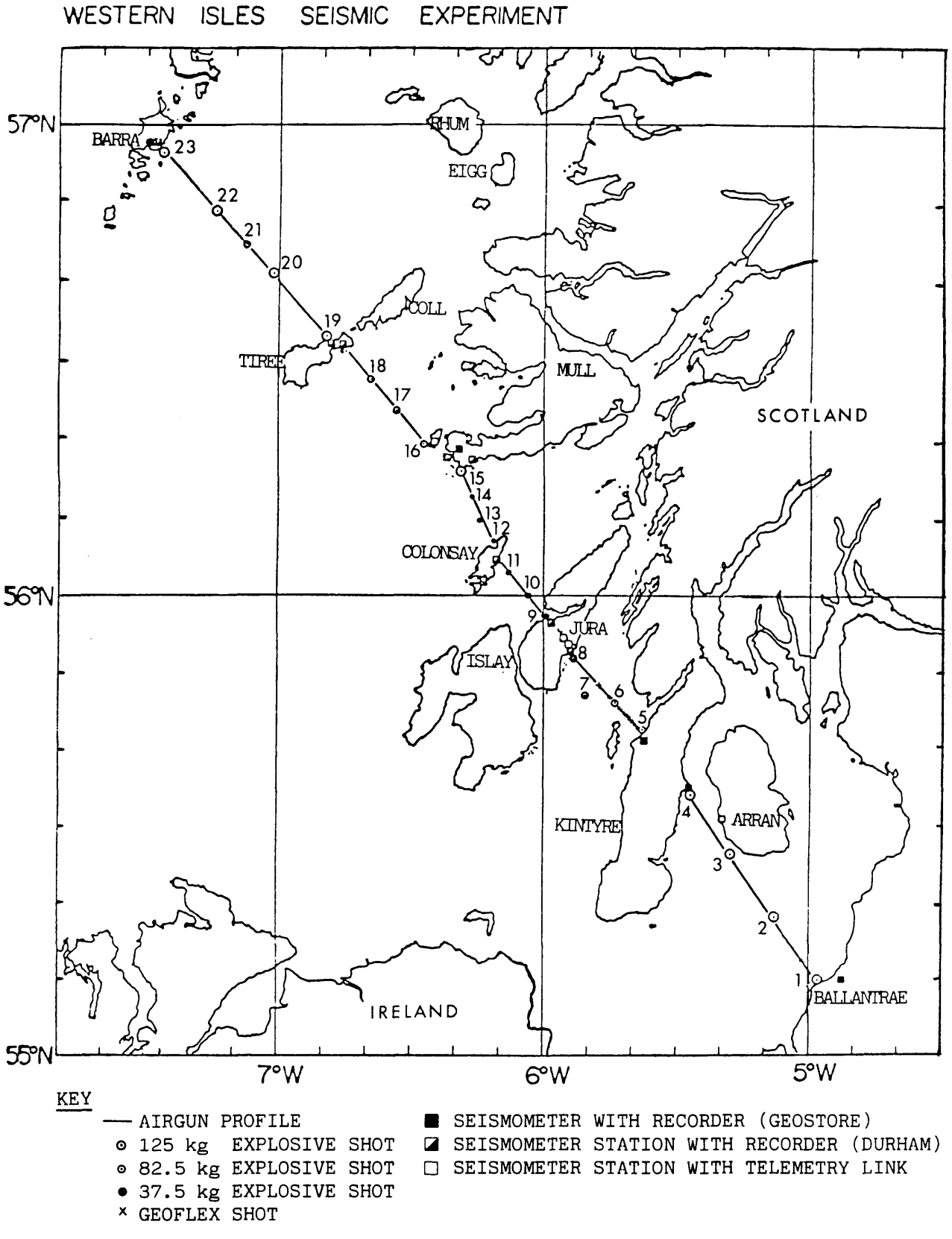

Fig. 2.1: Station locations, shot locations and line of airgun profile for WISE1. The types of recorders used and the size of the shots are also shown.

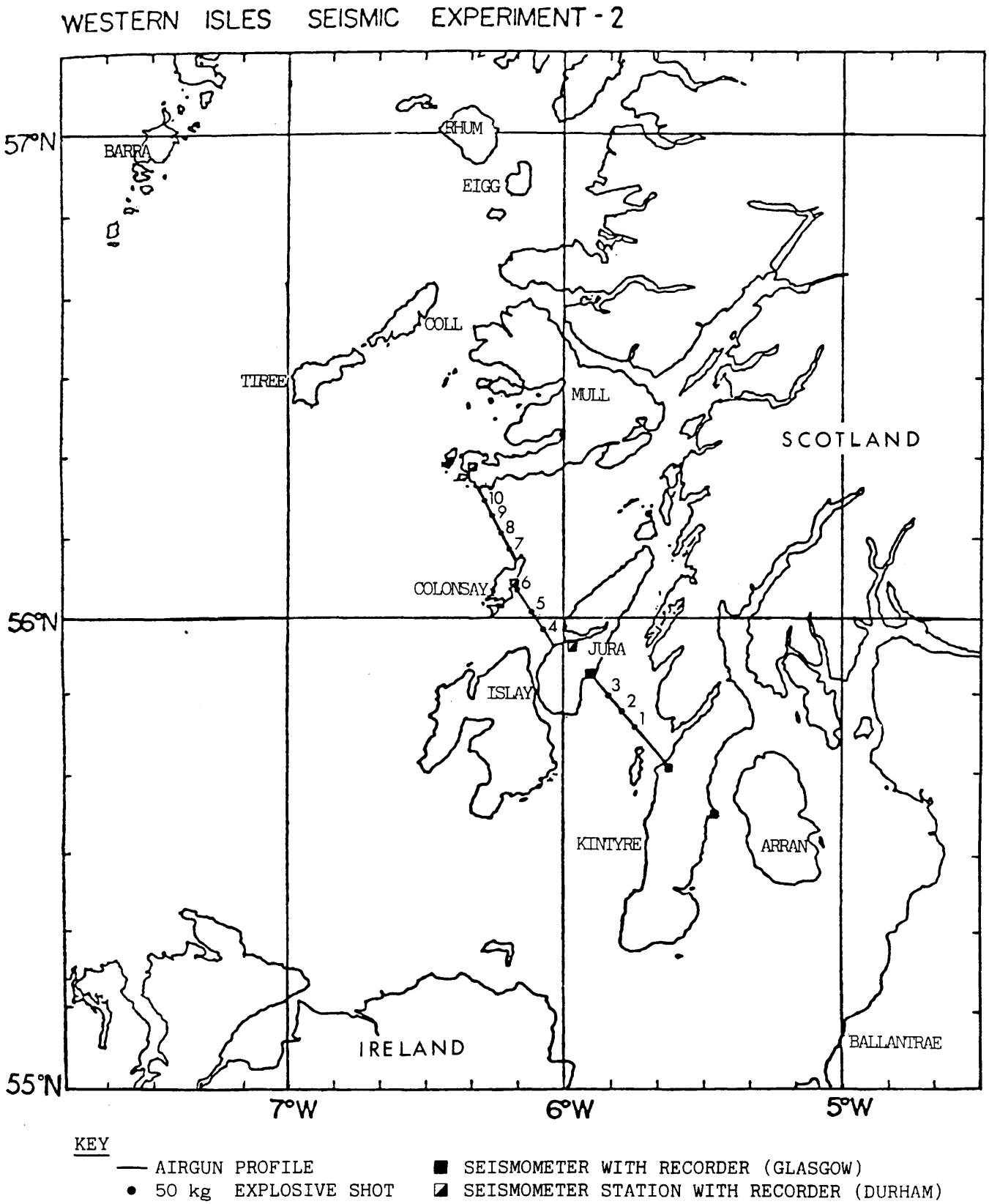

Fig. 2.2: Station locations, shot locations and line of air gun profile for WISE2. The types of recorders used and the size of the shots are also shown.

2.2.2. WISE Phase 2

Since the quality of the data from WISE1 (both explosive and airgun) was poor, mainly because of wind noise in many stations and inadequate energy output from the airguns, the second phase of WISE was executed to supplement the data of the first phase (Fig. 2.2).

This time, ten 50 kg shots were fired at sites evenly distributed amongst the WISE1 shots. One shot (shot no 8) was located as closely as possible to that of the previous phase (shot no 13), to provide a link between the two profiles in addition to the reoccupation of, approximately, the same recording stations. The airgun profile between Mull and Kintyre was re-run and this time two 1000 cu.in. Bolt PAR airguns were fired simultaneously in order to provide better signal strength. The details of the explosive shots and airgun profiles are provided in the Appendix 1 (Tables A.5 and A.6).

During this phase the stations on Mull, Iona and Colonsay operated with Willmore Mk.3 seismometers and Durham Mk.3 recorders, the station at North Jura used Willmore Mk.2 seismometer and recorder type while the stations on Kintyre and South Jura used the cassette recorder developed at Glasgow University.

2.2.3. Navigation and Bathymetry

The Decca Main Chain was used in the first phase for position fixing. The system uses one master and three slave transmitters and provides a hyperbolic pattern whose intersection points help

define the position of the ship (McQuillin and Ardus 1977). The main drawback of the system is that it suffers from sky-wave effects which produce poor reception and variable errors during twilight and darkness periods.

Although its principal use is for navigation and not for surveying, its accuracy (about 100 m in the Hebridean region in 70% of occasions during full daylight conditions and about 50 m along the rest of the line) makes it adequate for crustal refraction surveys. This accuracy, quoted by Decca, is achieved after correcting for the fixed errors using the Decca charts of fixed errors for the West Scottish region.

During the second phase, the short range Decca Trisponder system was mainly used, with resort to Decca Main Chain made only when breakdowns occurred. The Trisponder system works in range-range mode by transmitting a tone burst of known frequency from the ship to three receivers on land, which return similar signals on receipt from the master on ship. The travel times are then converted to distance and the location of the ship is identified as the triangle formed by the arc intersections. Since only two "responders" were available for WISE, the intersection point of the corresponding arcs was taken as the position of the ship, with probable errors of a few tens of metres (McQuillin and Ardus 1977).

An echosounder was used throughout the survey to record the depth to the sea floor along the line.

2.3. DESCRIPTION OF DATA

2.3.1 WISE Phase 1

The magnetic tapes with the explosive data were replayed - after being digitized - onto paper records using a jet pen oscillograph. The digitizing rates were 60 samples/sec for the Geostore recordings and 50 samples/sec for the Durham Mk.3 recordings. The vertical and the two horizontal traces of a seismometer were plotted alongside together with the corresponding MSF code to facilitate picking (Fig. 2.3).

Later, they were filtered (2-20 Hz) and displayed as reduced sections (Fig. 2.4 to 2.9).

As mentioned in section 2.2, the quality of the WISE1 explosive data was far from desirable, especially for recordings in the middle of the line. Though various steps had been taken to ensure good quality for the data, Summers (1982, Chapter 2) felt that they were not adequate. The stations on Kintyre and Arran did not function due to incorrect setting. Moreover, wind noise and (or) dirty recorder heads, were probably the main reason for the bad quality of the data recorded at stations on Tiree, Iona, Mull, Colonsay and Girvan (e.g. Fig. 2.5, 2.6 and 2.9).

The overall success rate was about 45% (114 useful recordings out of 264, excluding the Arran and Kintyre stations which did not operate at all). In contrast, the Geoflex shots near to Kintyre gave very clear arrivals at the South Jura station (Fig. 2.10).

In the case of the airgun data, since the signal to noise

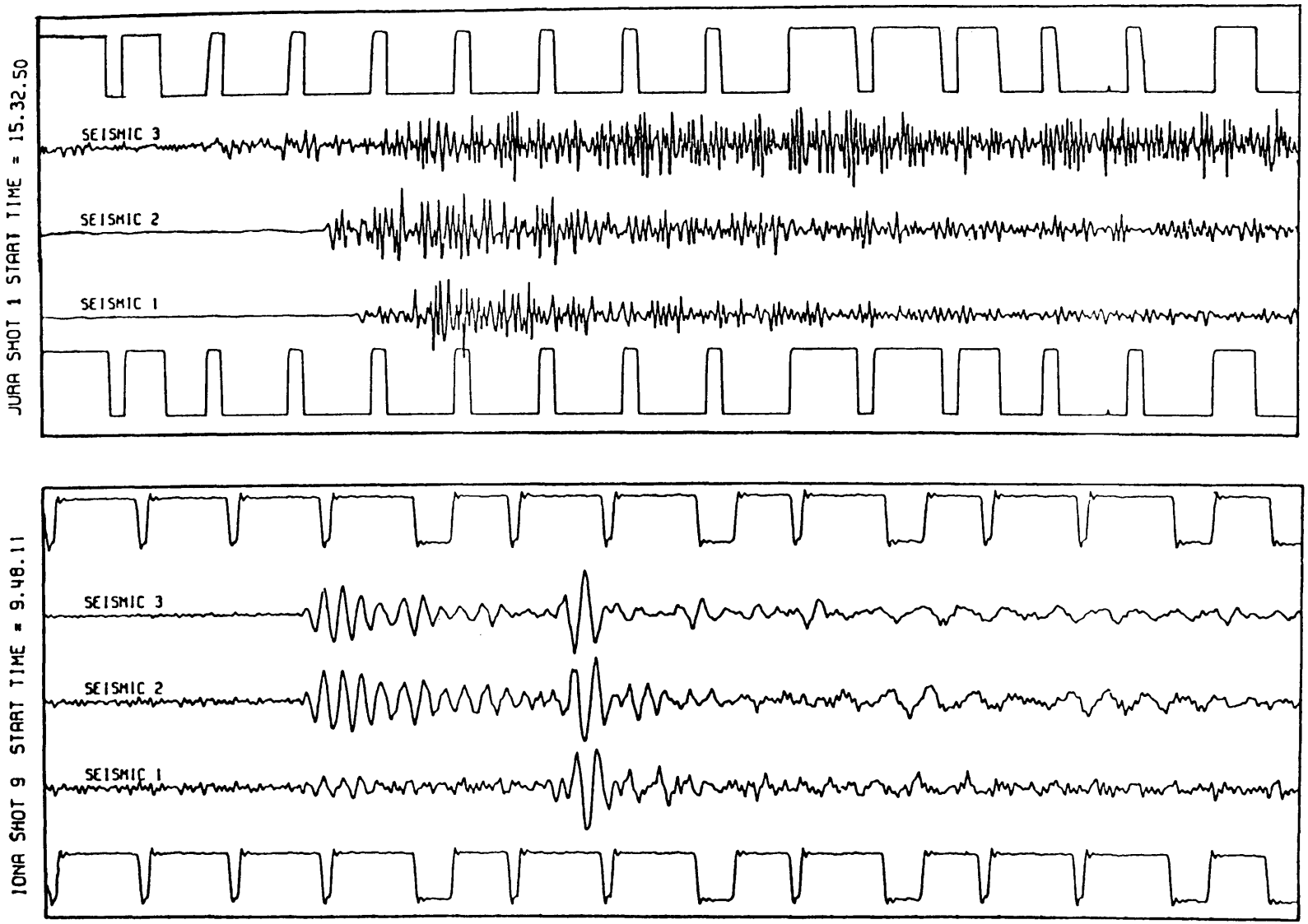

Fig. 2.3: Example of explosive shot records from both phases of WISE showing the method of display used by Summers to time the arrivals (after Summers, 1982).

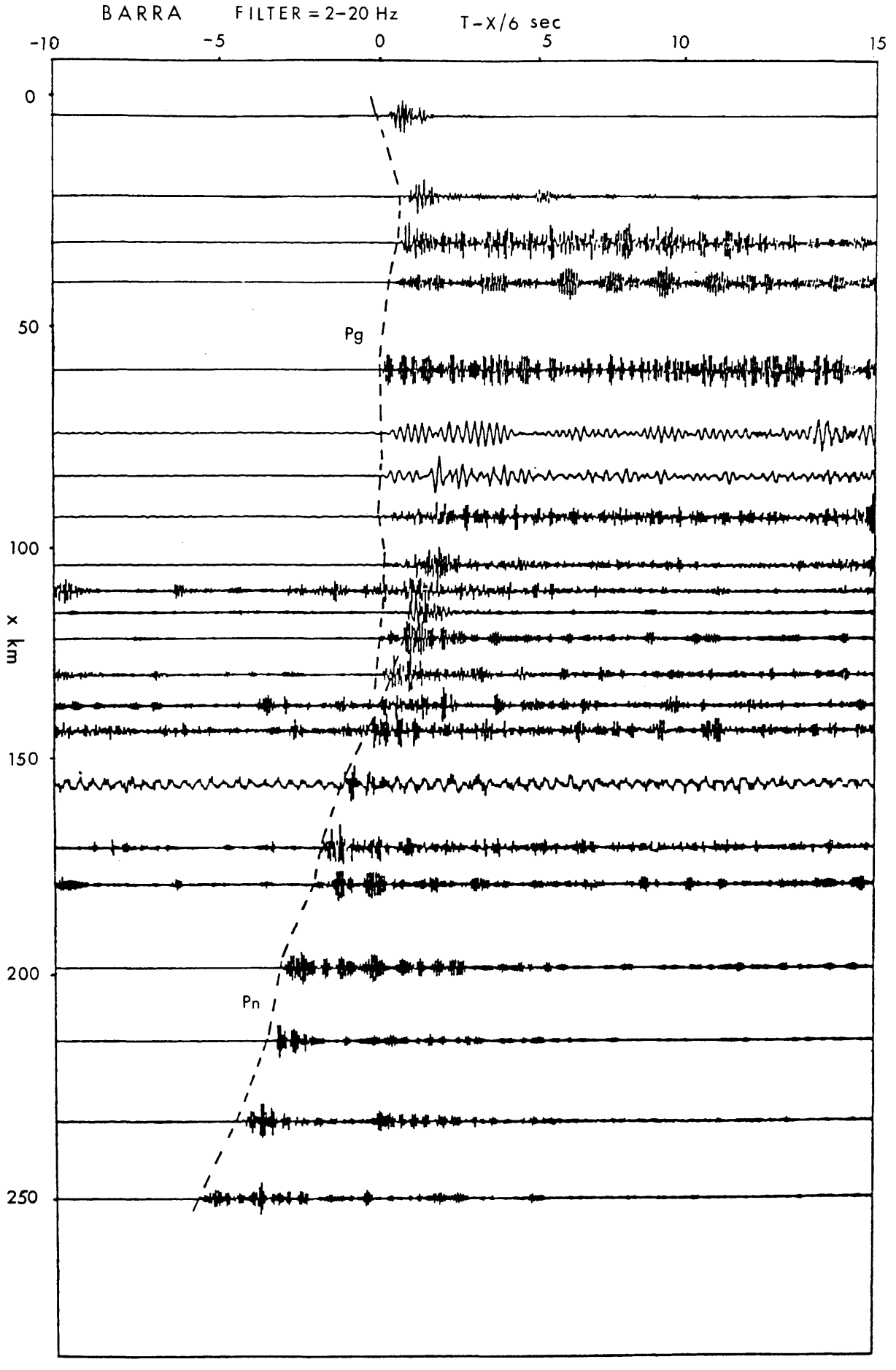

Fig. 2.4: Reduced record section for Barra station (after Summers, 1982).

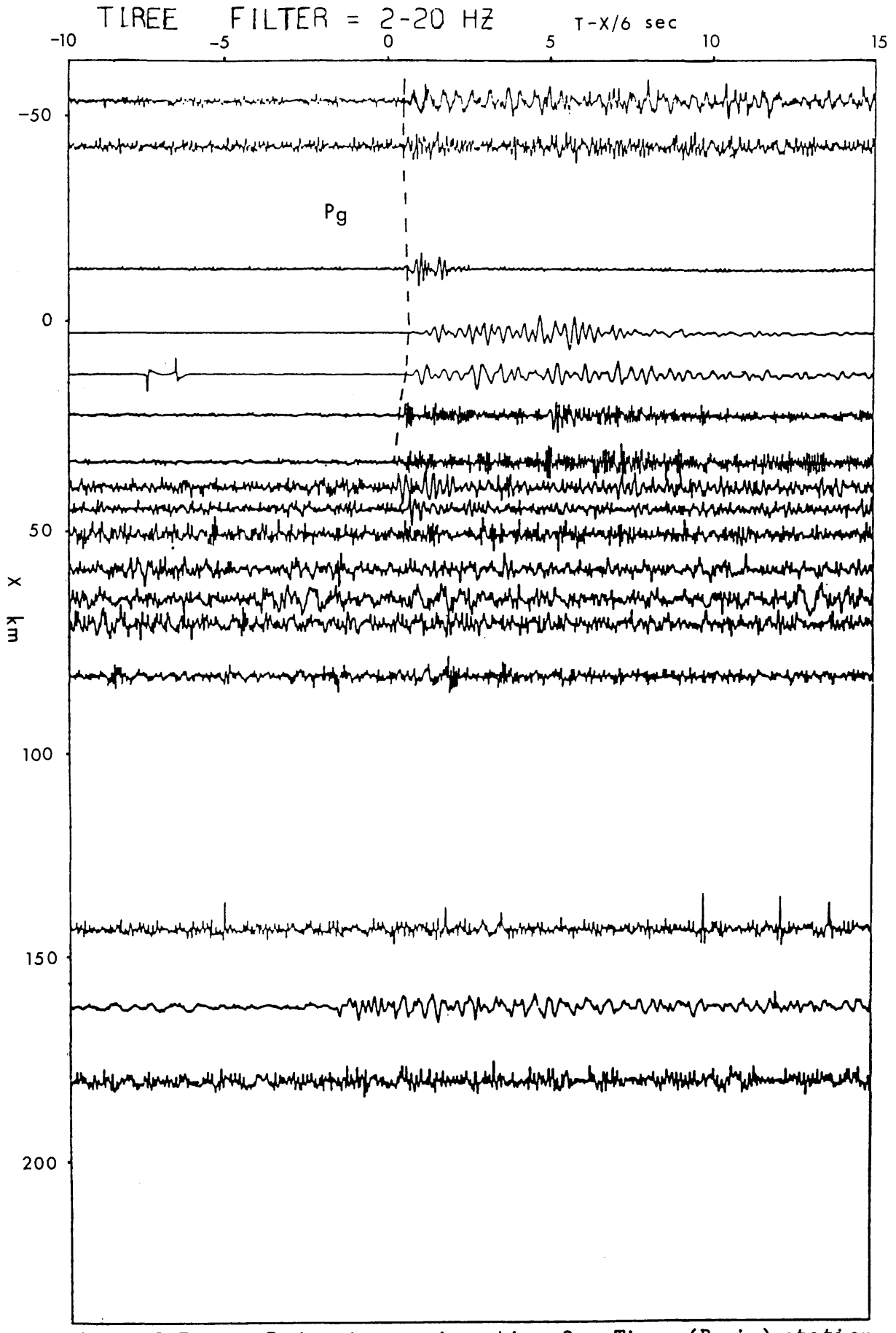

Fig. 2.5: Reduced record section for Tiree (Ruaig) station (after Summers, 1982).

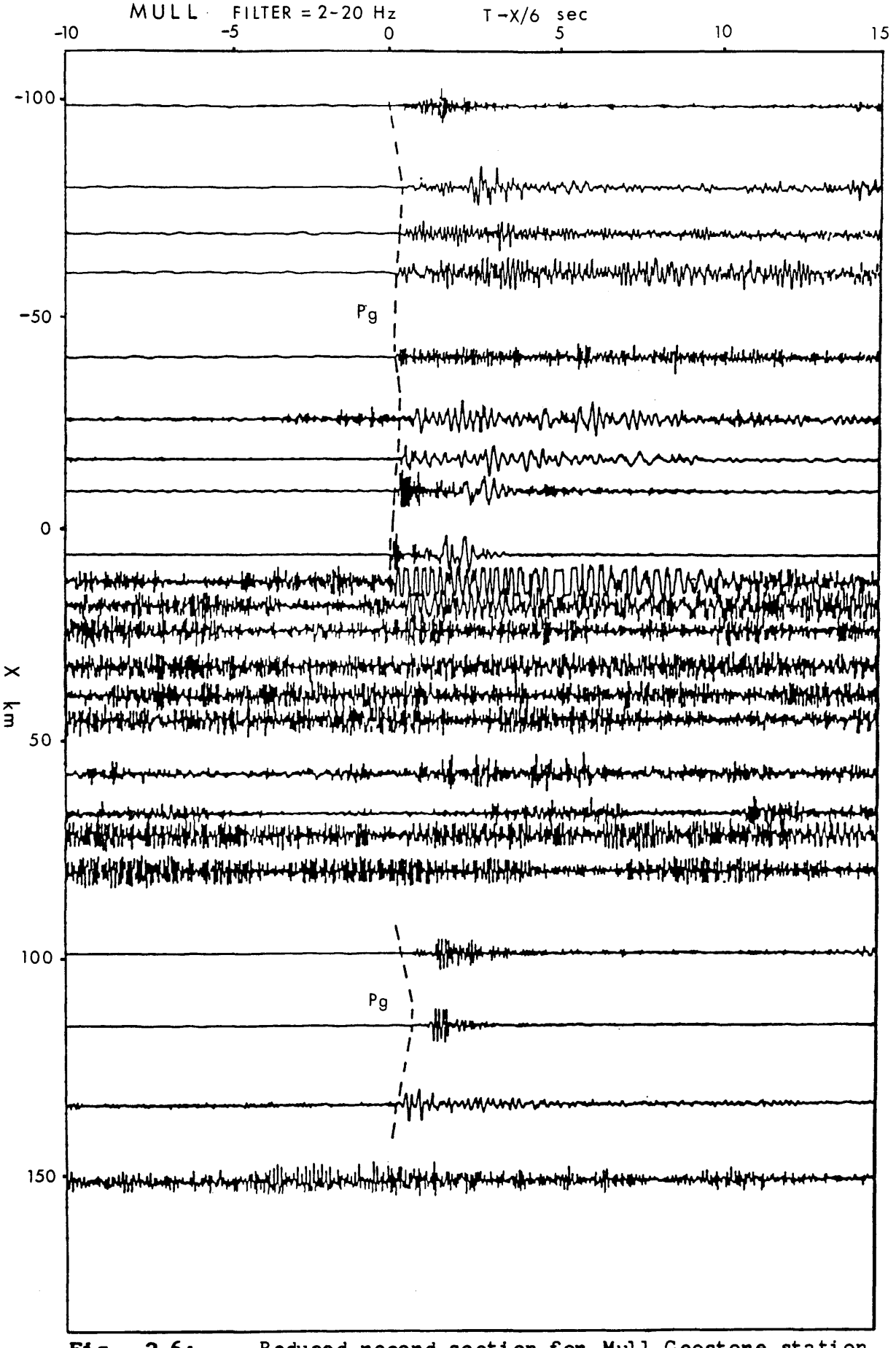

Fig. 2.6: Reduced record section for Mull Geostore station, Phase 1 (after Summers, 1982).

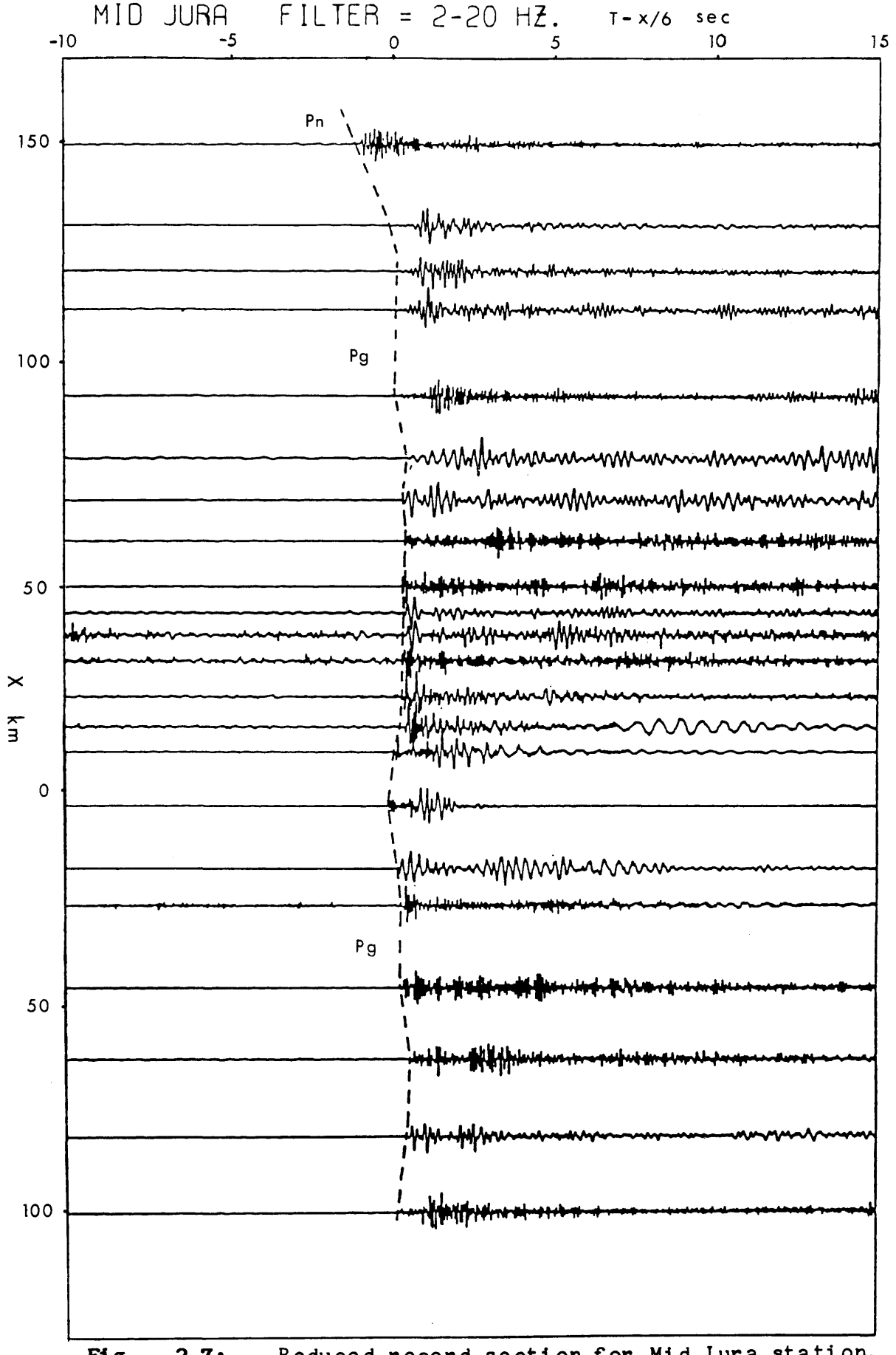

Fig. 2.7: Reduced record section for Mid Jura station, Phase 1 (after Summers, 1982).

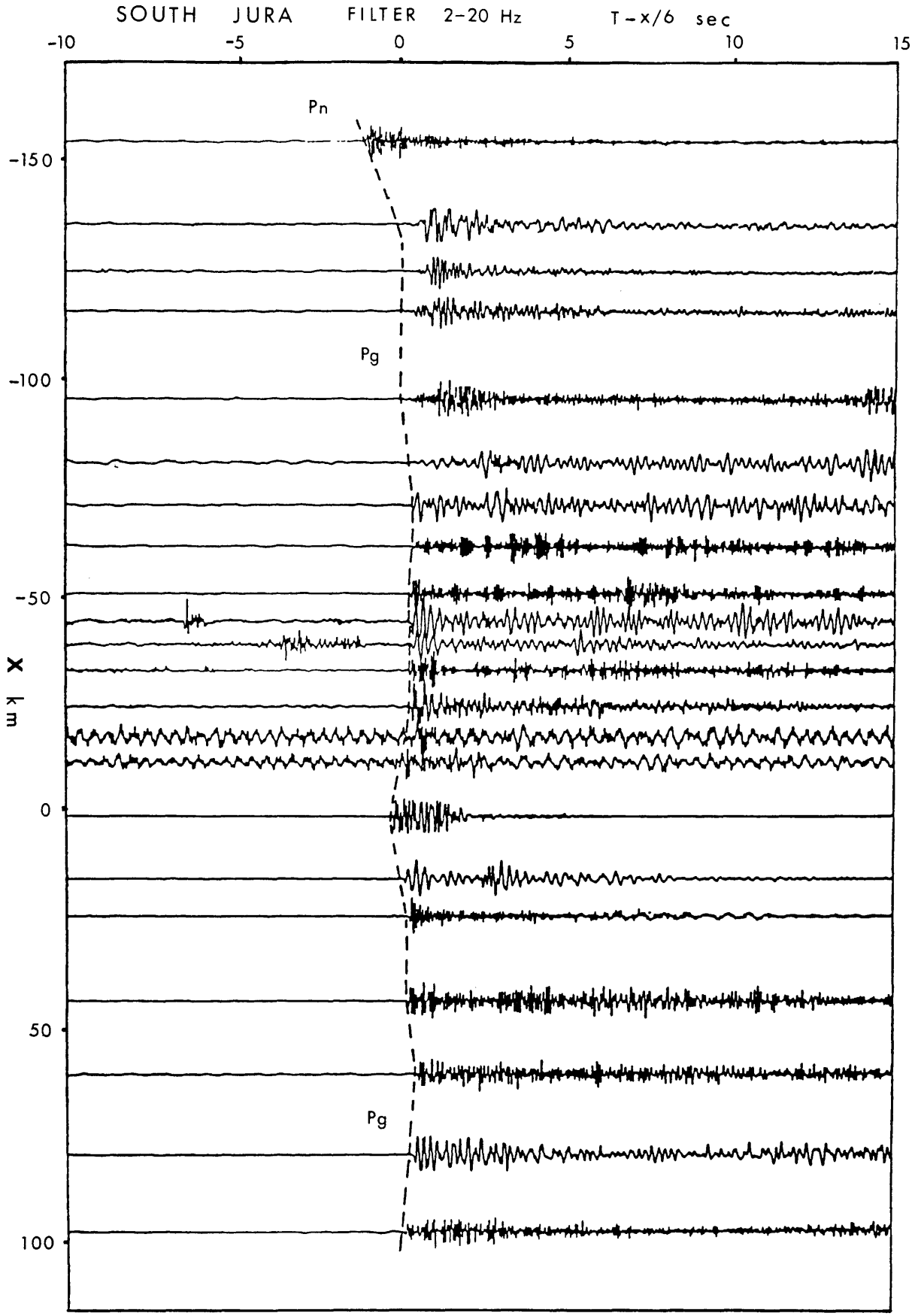

Fig. 2.8: Reduced record section for South Jura station, Phase 1 (after Summers, 1982).

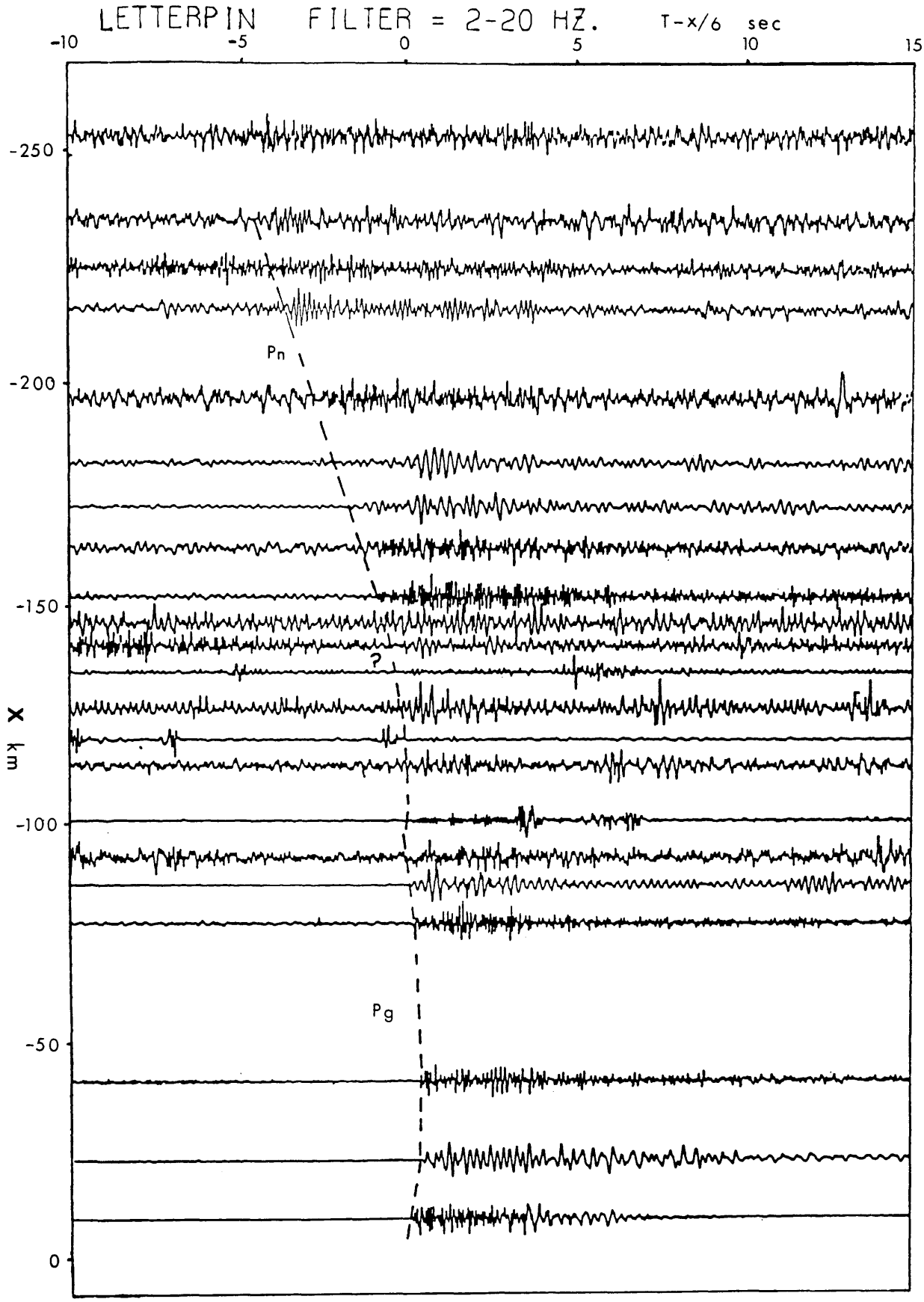

Fig. 2.9: Reduced record section for Letterpin station, Phase 1 (after Summers, 1982).

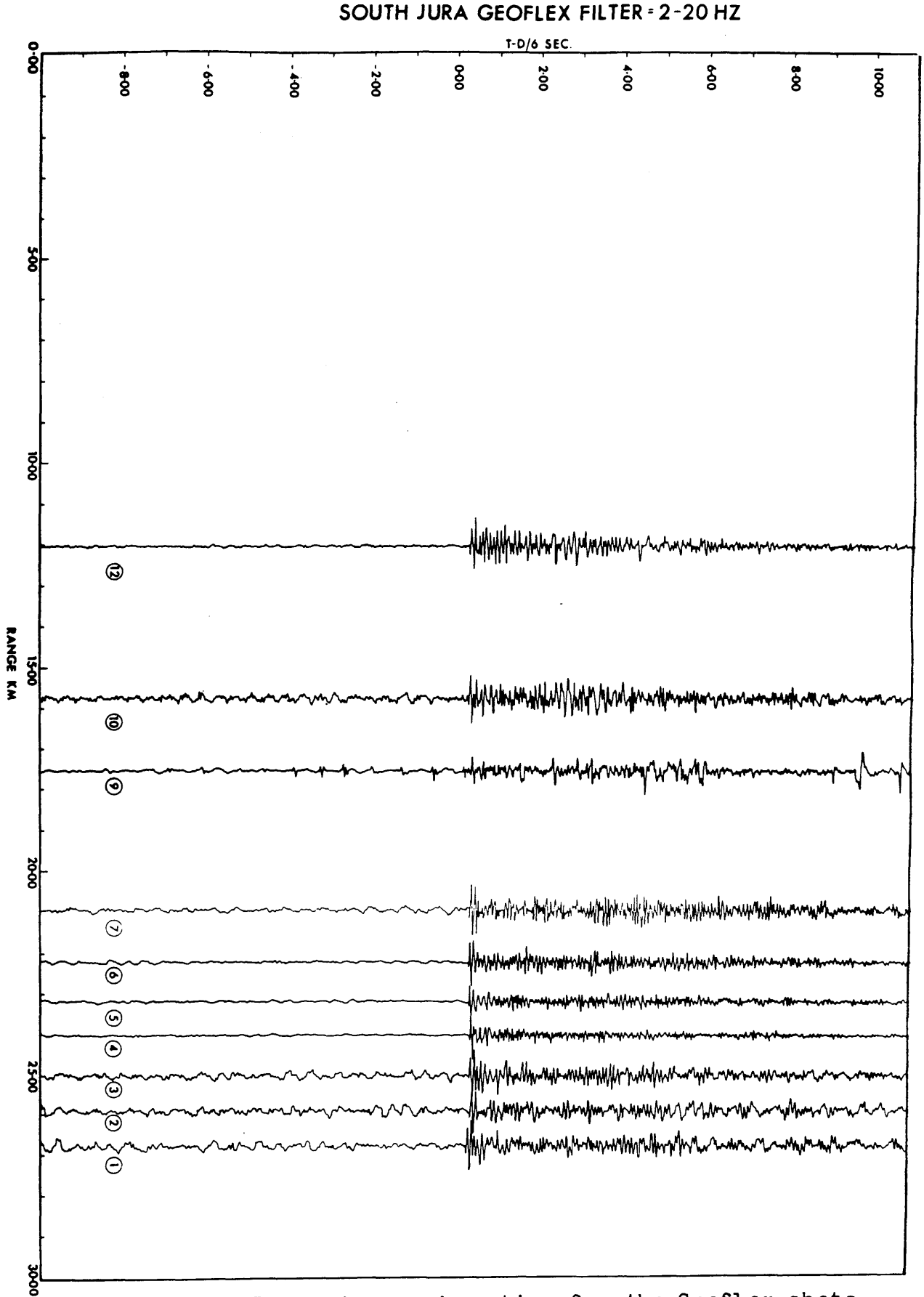

Fig. 2.10: Reduced record section for the Geoflex shots recorded at South Jura station, Phase 1.

ratio was usually too small for manual pick, even after filtering (2-30 Hz), methods for the enhancement and the automatic detection of the signals were developed. Three M.Sc. theses (Birtles 1980, Warren 1981, Smith 1982) were developed out of the efforts to detect the first arrivals in the airgun records.

A short account of the work on the automatic signal detection as applied to some airgun data is given in section 2.4.2.

2.3.2. WISE Phase 2

The same procedure of basic processing as for the WISE1 data was followed. The quality of both explosive and airgun data was greatly improved. Success rate for the explosive data was almost 100%, with all traces showing clear arrivals (Fig. 2.11 - 2.14).

The quality of the airgun data was variable. The line from Mull to Colonsay was not reversed on Colonsay and the strength of the signal falls off rapidly beyond the Great Glen fault (probably due to scattering and/or high absorption in the crush zone). The line from Colonsay to North Jura was reversed, but the signals recorded on Jura were very noisy. After filtering, the automatic picking procedure was applied and it seemed that a number of signals were retrieved (Casson 1982). The most successful line was the one from South Jura to North Kintyre, recorded on Glasgow University recorders. Most of the traces display good P and S-wave arrivals, quite adequate for picking, but they were not made into reduced sections (see next section).

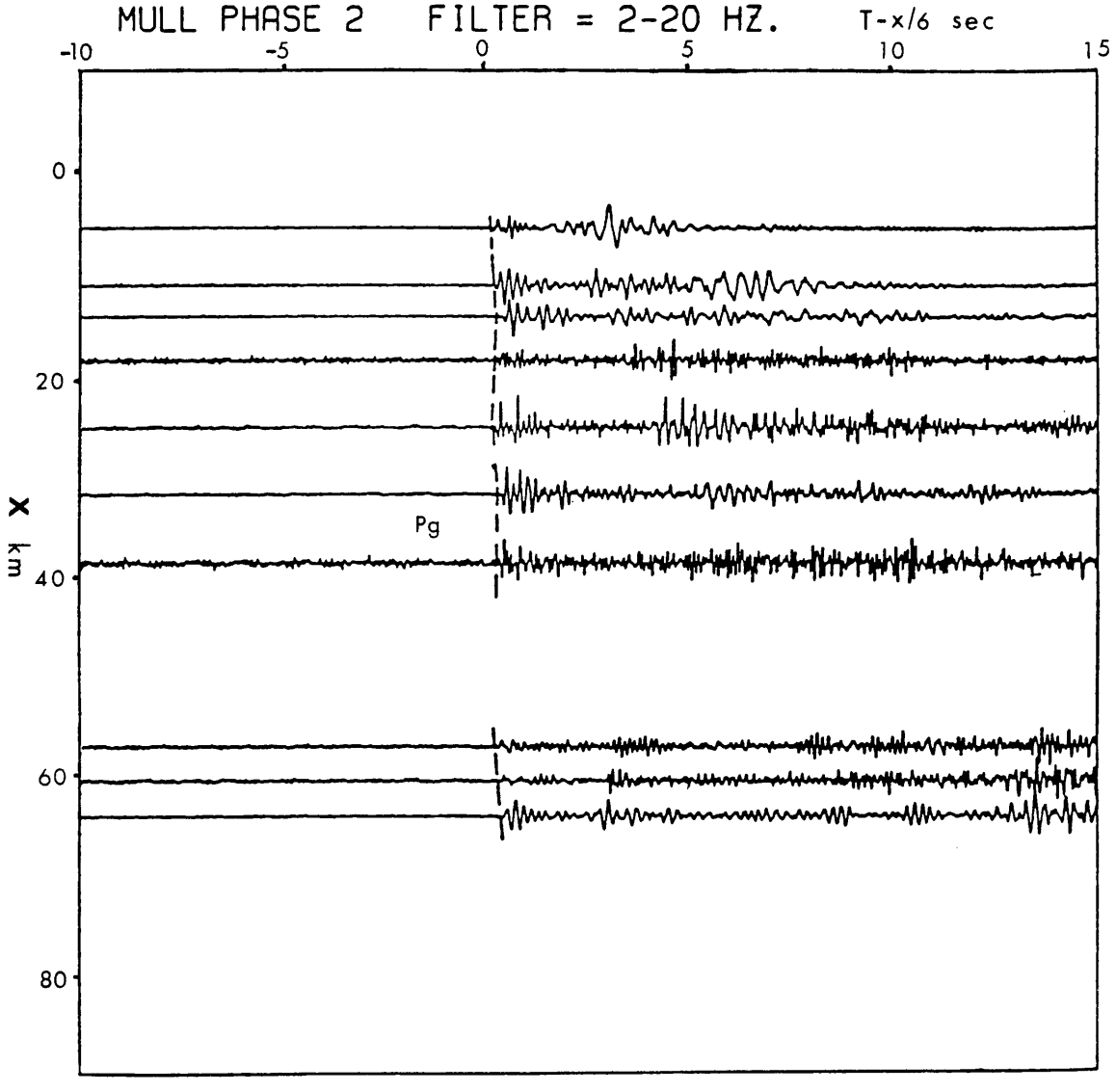

Fig. 2.11: Reduced record section for Mull station, Phase 2 (after Summers, 1982)

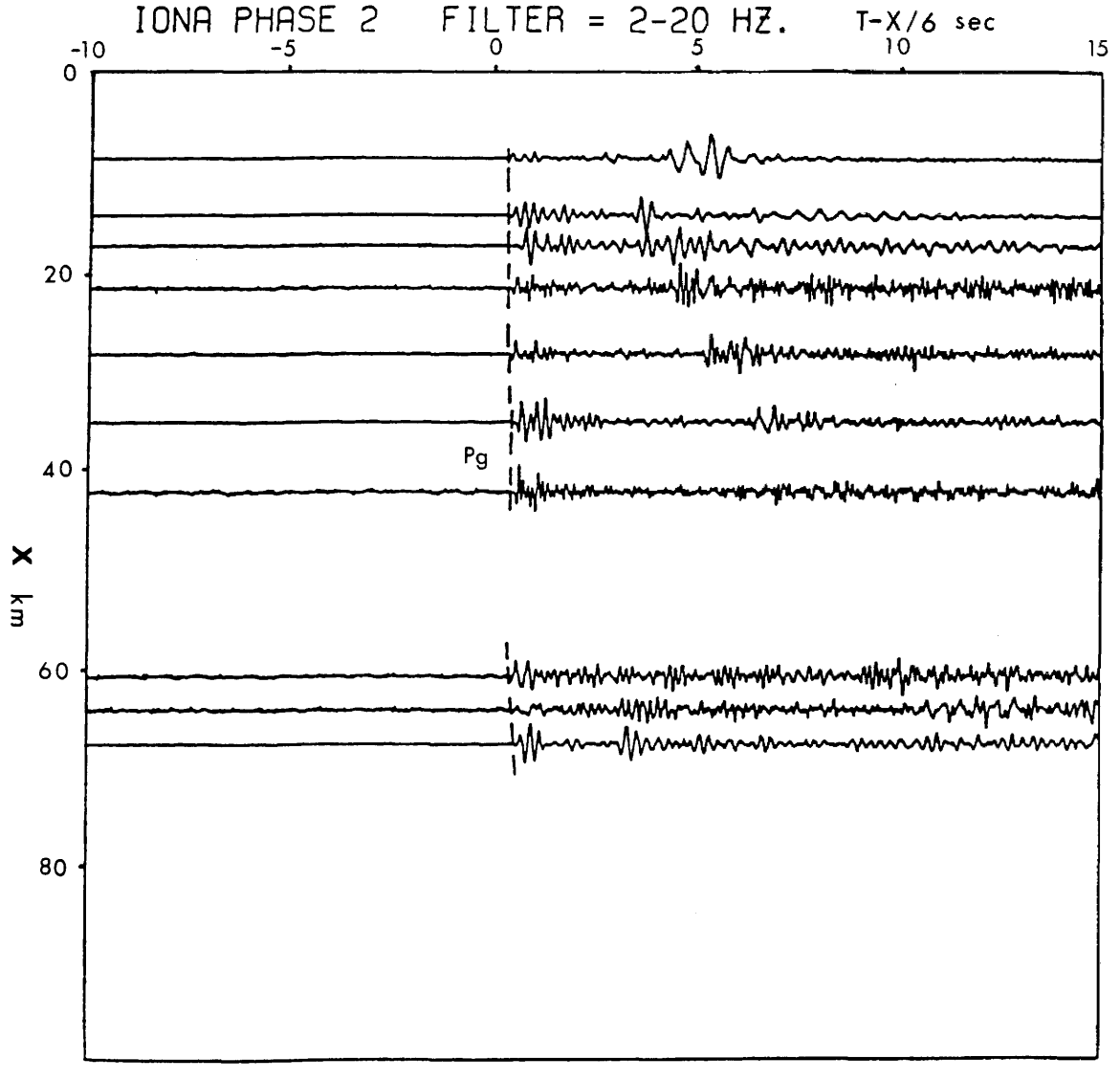

Fig. 2.12: Reduced record section for Iona station, Phase 2 (after Summers, 1982).

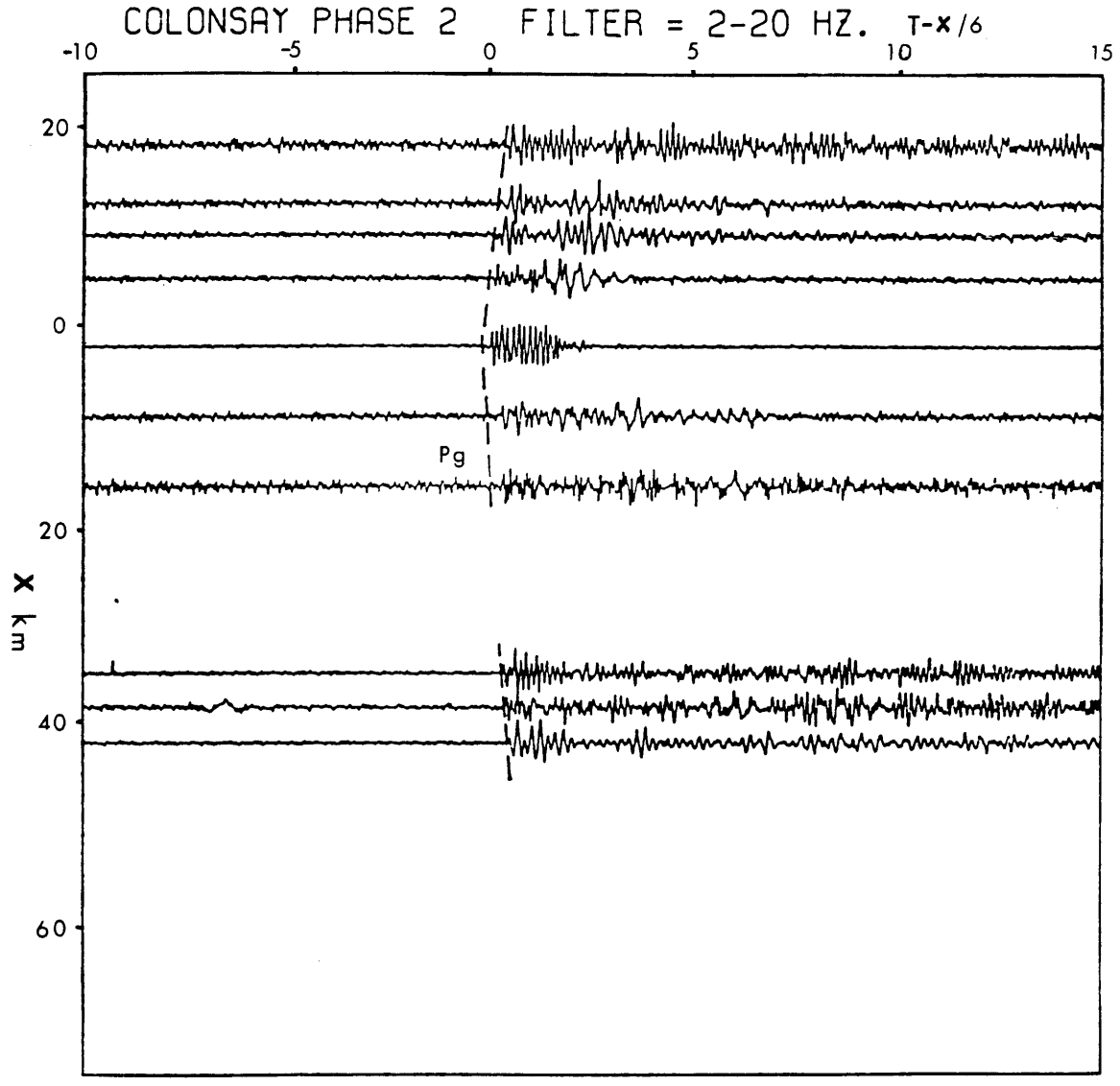

Fig. 2.13: Reduced record section for Colonsay station, Phase 2 (after Summers, 1982).

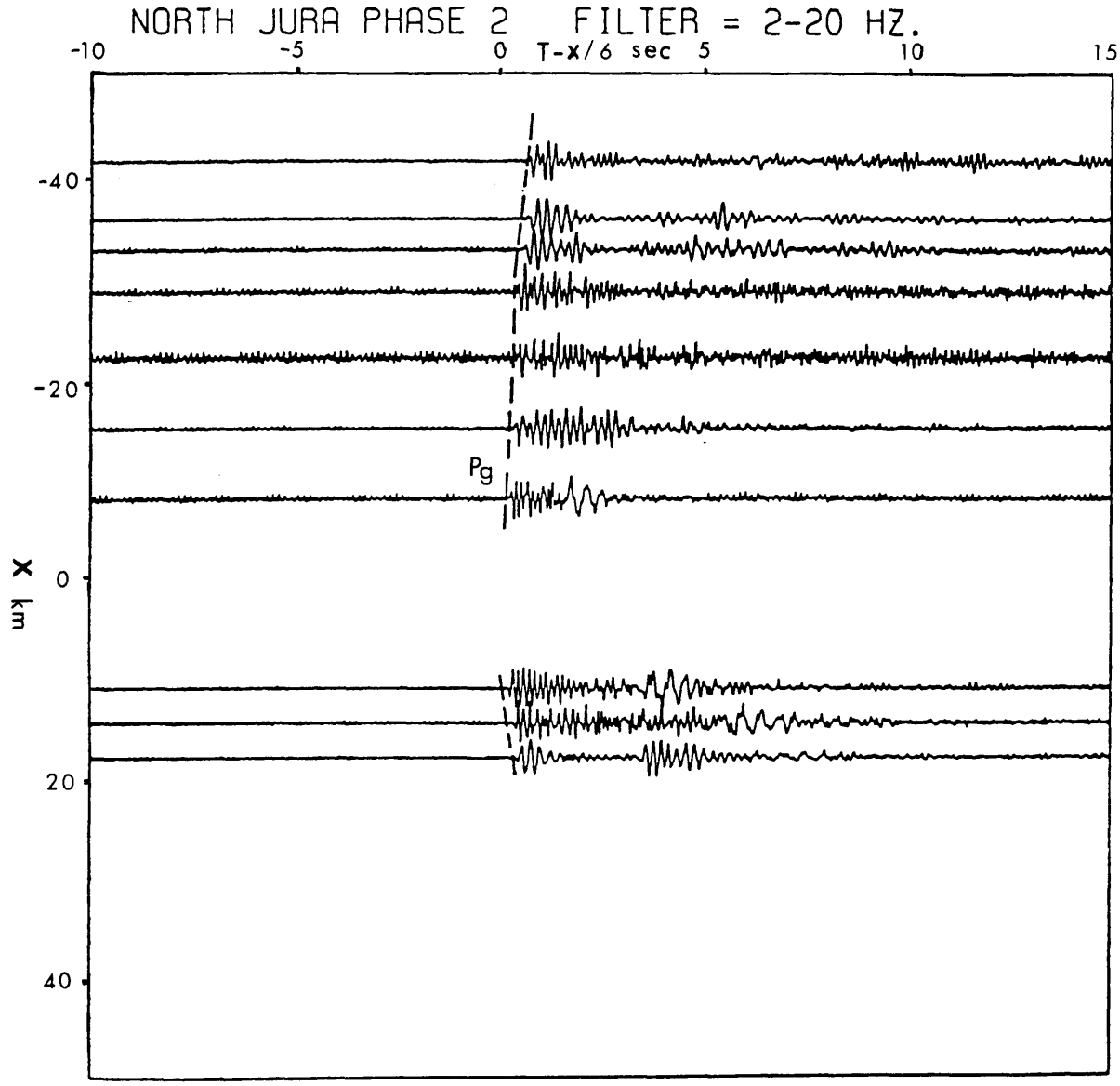

Fig. 2.14: Reduced record section for North Jura station, Phase 2 (after Summers, 1982).

2.3.3. The reduced record sections of the explosive shots

All the record sections available are shown in Figures 2.4 to 2.14. The sections shown were produced by signals recorded on the Durham Mk.3 recorders or on Geostores as these could be digitised. Paper playbacks were made at Glasgow University of the South Jura and North Kintyre stations of the second phase where the Glasgow cassette recorders were used. These could be picked quite adequately but due to high gains used during recording, the records did not always retain the shape of separate phases without clipping and were not made into reduced sections (Summers 1982).

Two groups of first arrivals are recognised in the records, direct Pg arrivals with velocity 6.0 $\pm$ 0.10 km/sec being generally observed at distances less than 130 km, and the Moho Pn arrivals with velocity 7.98 $\pm$ 0.07 km/sec at distances beyond 150 km (e.g. Fig. 2.4, 2.7 and 2.9).

No indication of a mid-crustal layer (or of a steep velocity increase) exists in the records since no P^* refractions or PiP wide-angle reflections from such a layer can be recognised as was possible for the North Scottish shelf (Smith and Bott 1975) and the Caledonian part of the LISPB profile (Bamford et al 1978). Those arrivals are usually sought at ranges 50-120 km and the records from Barra, Jura and Letterpin do not display any such arrivals (though the quality of the Letterpin data is too poor to permit any definite conclusion, Fig. 2.9).

But on the Barra record section (Fig. 2.4) a group of second arrivals can be tentatively recognised between 80-130 km grading

into Pn arrivals. They display apparent velocity of about 7 km/sec and probably represent either PmP wide-angle reflections or refractions from a relatively thin lower crustal layer. The absence of greater amplitudes in that group of arrivals could then be explained, at least partly, by the reverberant and noisy nature of the traces in the middle of the section.

Some other characteristics of the sections, include the very low frequency content of traces 17 and 18 (WISE1) as observed in most of the stations, obviously due to the "screening" effect of the Tertiary basaltic cover, the scattering of high frequencies from the Tertiary intrusions, and the intervention of the low velocity Mesozoic sediments (e.g. Trostle 1967). Low frequency content can also be observed in traces 21 and 22 due to considerable thickness of the Mesozoic sediments. The apparent absence of S-arrivals in the records of the first phase is probably due to the noisy nature of the traces. Some S-arrivals can be identified in the sections of the second phase despite the fact that only vertical geophones were used.

2.4. PICKING OF THE WISE DATA - ACCURACY ESTIMATIONS

The bulk of the picking was done by Summers (1982, Chap.2) and checked by the author using dye-line copies of most of the reduced record sections made during a visit to Durham University. A brief account will be given here with emphasis on the appreciation of the accuracy of the picks after careful visual inspection of the traces, and total errors involved in the arrival times.

2.4.1. Picking of the explosive data (WISE1 and WISE2)

The picking procedure involved the identification of the first arrivals on the reduced sections and the subsequent use of the jet-pen records for more accurate timing. The arrival times as picked by Summers are listed in Appendix 1 (Tables A.7 and A.8). A comparison can be made with the author's picks (from the dye-line copies) by plotting them on the same reduced T-X graphs (Fig. 2.15 to 2.28).

In these graphs it appears that there is usually a difference between the author's picks and Summers's picks with the former being earlier by about 0.10 sec. The pattern of the apparent velocities is usually the same for the two sets of picks and occasional "jumps" in Summers's picks were identified and accordingly corrected. A more detailed account is given in section 2.5.

Moreover, the accuracy of one sample in picking of the clear arrivals, quoted by Summers, that being 0.016 sec for Geostore recordings and 0.02 sec for Durham Mk.3 recordings, is

considered rather optimistic for most of the clear arrivals. Inspection of dye-line copies and careful examination of the character of the onset signals of the reduced sections (from most of the shots of both phases), showed that the uncertainty in the arrival times for WISE1 traces was usually about 0.05 sec or more (except for the Jura recordings) and that for the majority of the WISE2 traces it was 0.03 to 0.05 sec (Tables A.11 and A.12, Appendix 1). These estimates of the picking errors involved for individual arrivals have been incorporated in the reduced T-X graphs (Fig. 2.15 to 2.28). There, it can be seen that the errors usually increase with the offset distance, due to wave attenuation and the absorption of high frequencies. These errors exclude those due to the timing of the shots (+/- 0.03 sec at maximum) and position fixing errors (+/- 0.03 sec at max), as those will be characteristic of the particular shot with their contribution being the same in all corresponding traces and comparison between traces recorded at adjacent stations will only reveal inaccurate picking.

The maximum total errors are also listed in Appendix 1 (Tables A.11, A.12) and the reasoning behind their statistical evaluation is the following: the errors in the position fixing values obey normal probability distribution (with its variance increasing away from the Main Chain - see McQuillin and Ardus, 1977) and the same must be true for the timing of the explosions and the picking of the first arrivals (since the former involves an estimate for the advance of the ship and the latter subjective measurement of length, on a jet-ink record, up to a selected onset). The position of the selected onset will depend

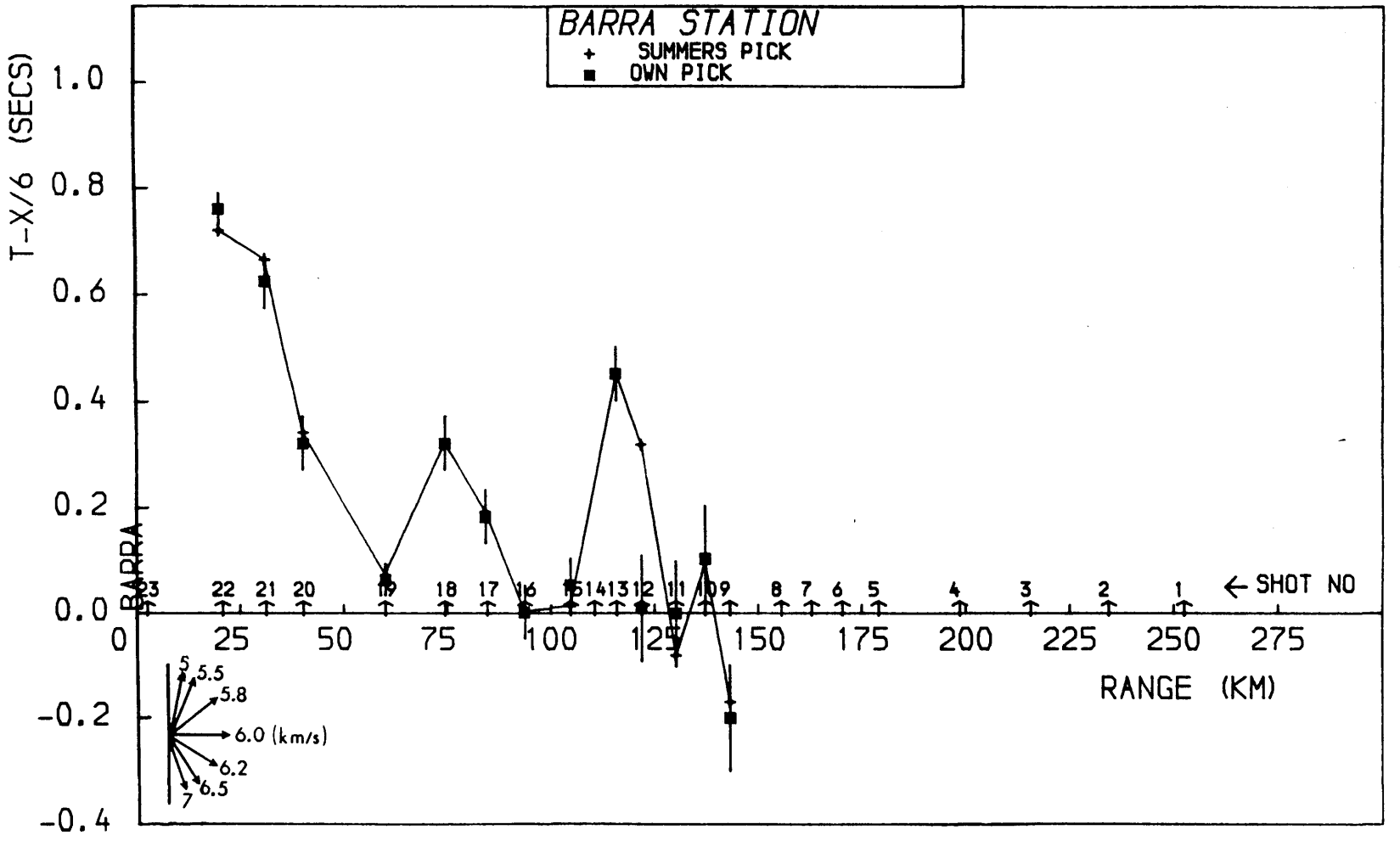

Fig. 2.15: Reduced T-X graph of Summers's picks and the author's picks with corresponding picking error bars for the Barra station (Pg arrivals).

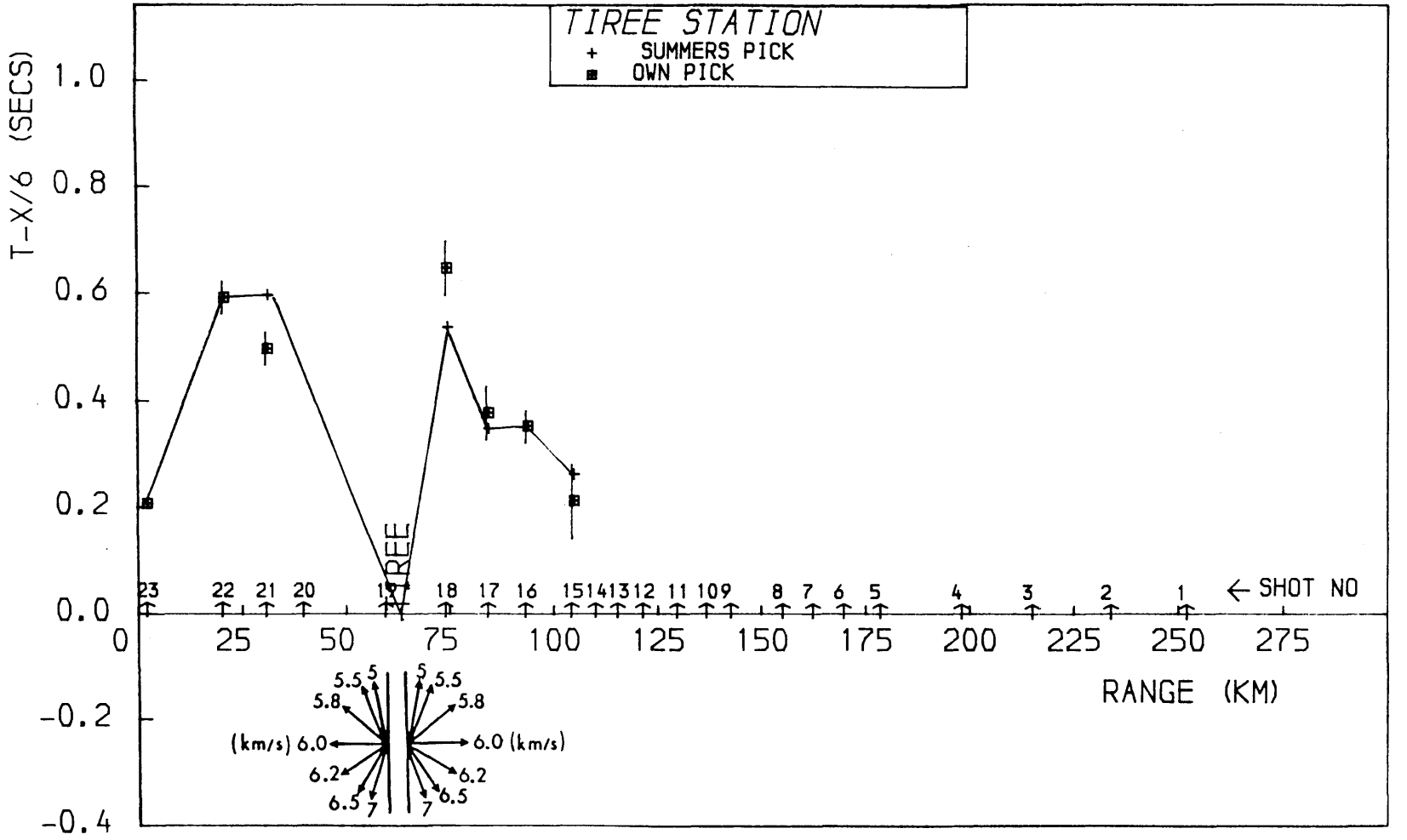

Fig. 2.16: Reduced T-X graph of Summers's picks and the author's picks with corresponding picking error bars for the Tiree (Ruaig) station.

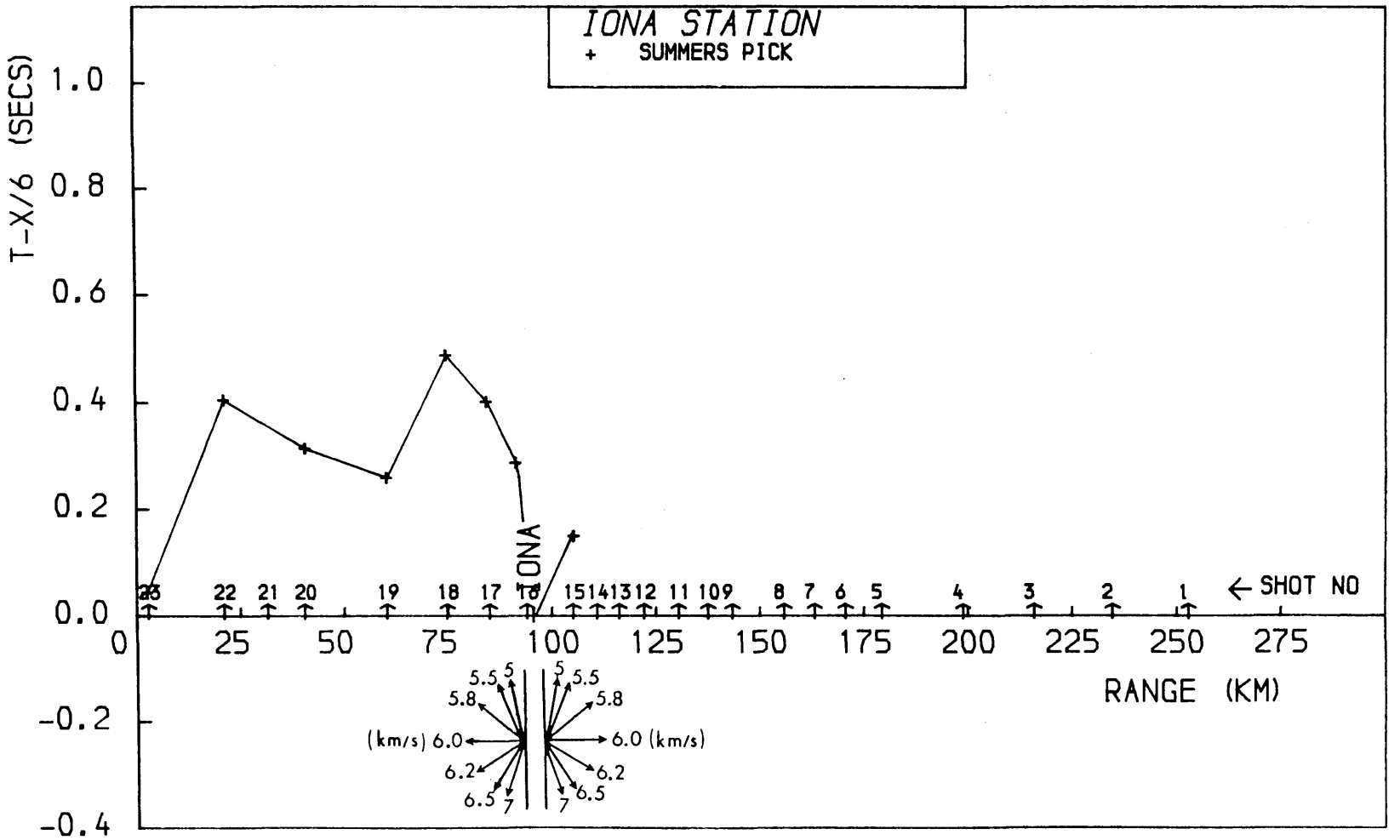

Fig. 2.17: Reduced T-X graph of Summers's picks for the Iona station (WISE1). No record sections were available for this station.

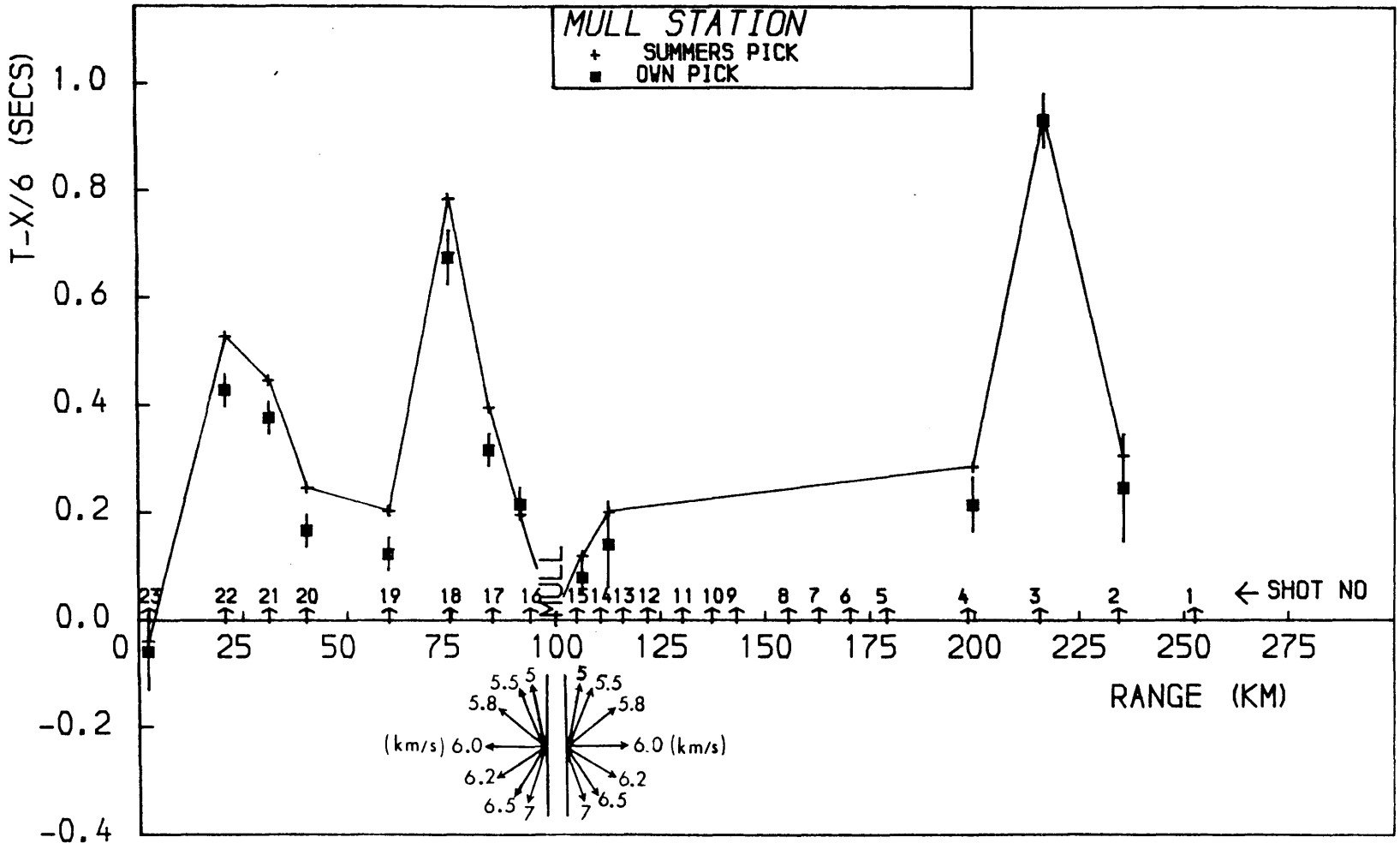

Fig. 2.18: Reduced T-X graph of Summers's picks and the author's picks with corresponding picking error bars for the Mull station (WISE1).

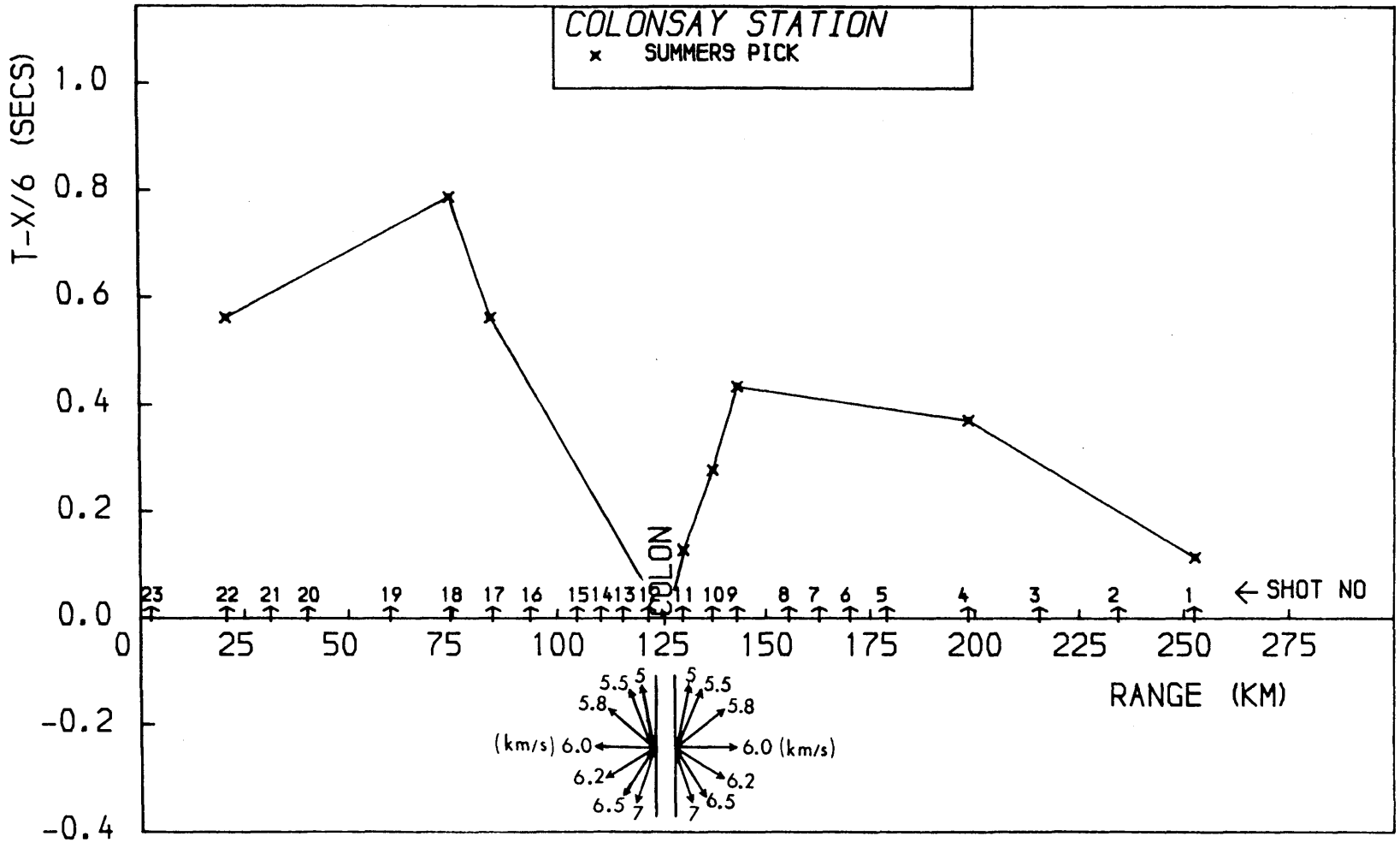

Fig. 2.19: Reduced T-X graph of Summers's picks for the Colonsay station (WISE1). No record sections were available for this station.

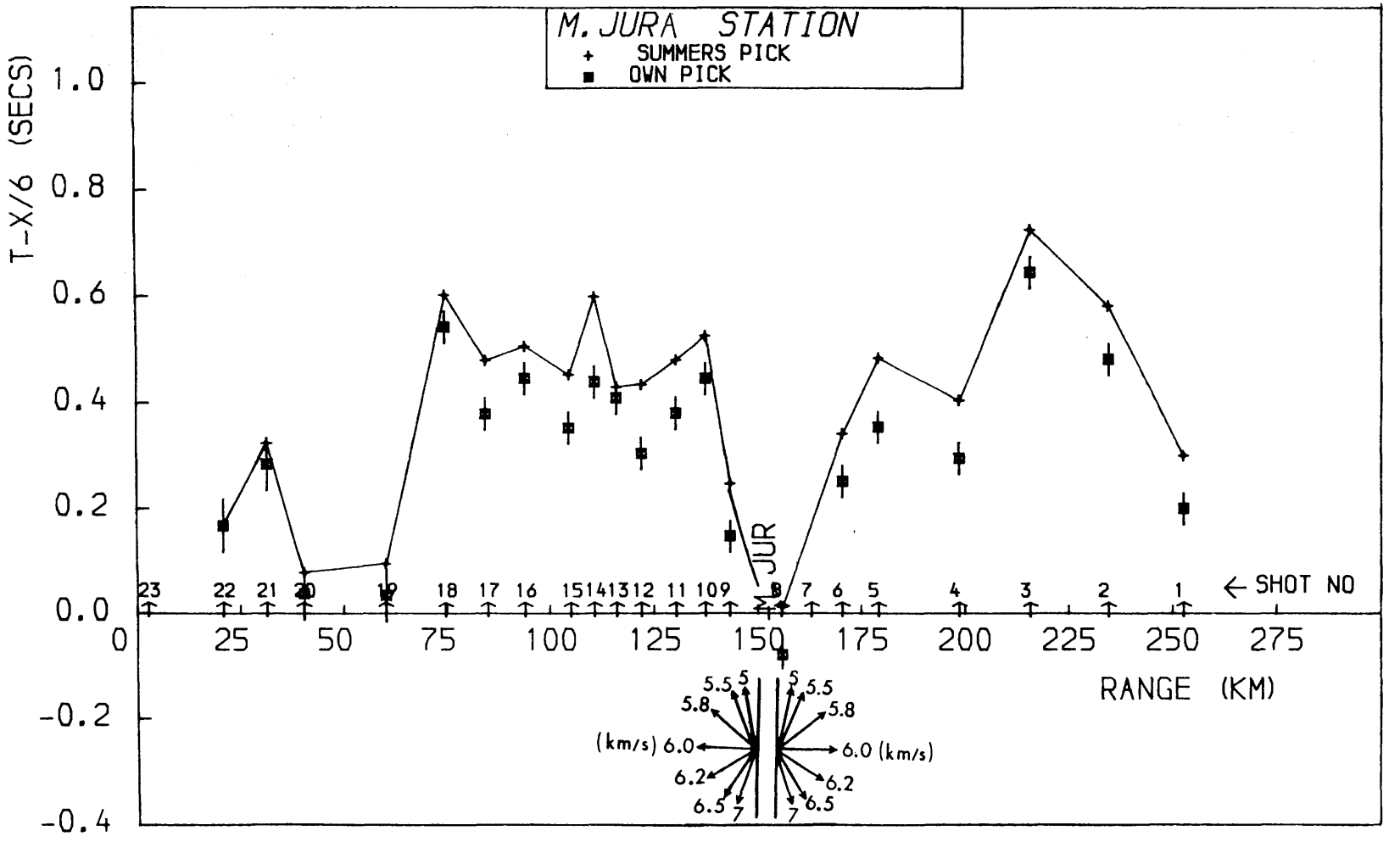

Fig. 2.20: Reduced T-X graph of Summers's picks and the author's picks with corresponding picking error bars for the Mid Jura station (WISE1).

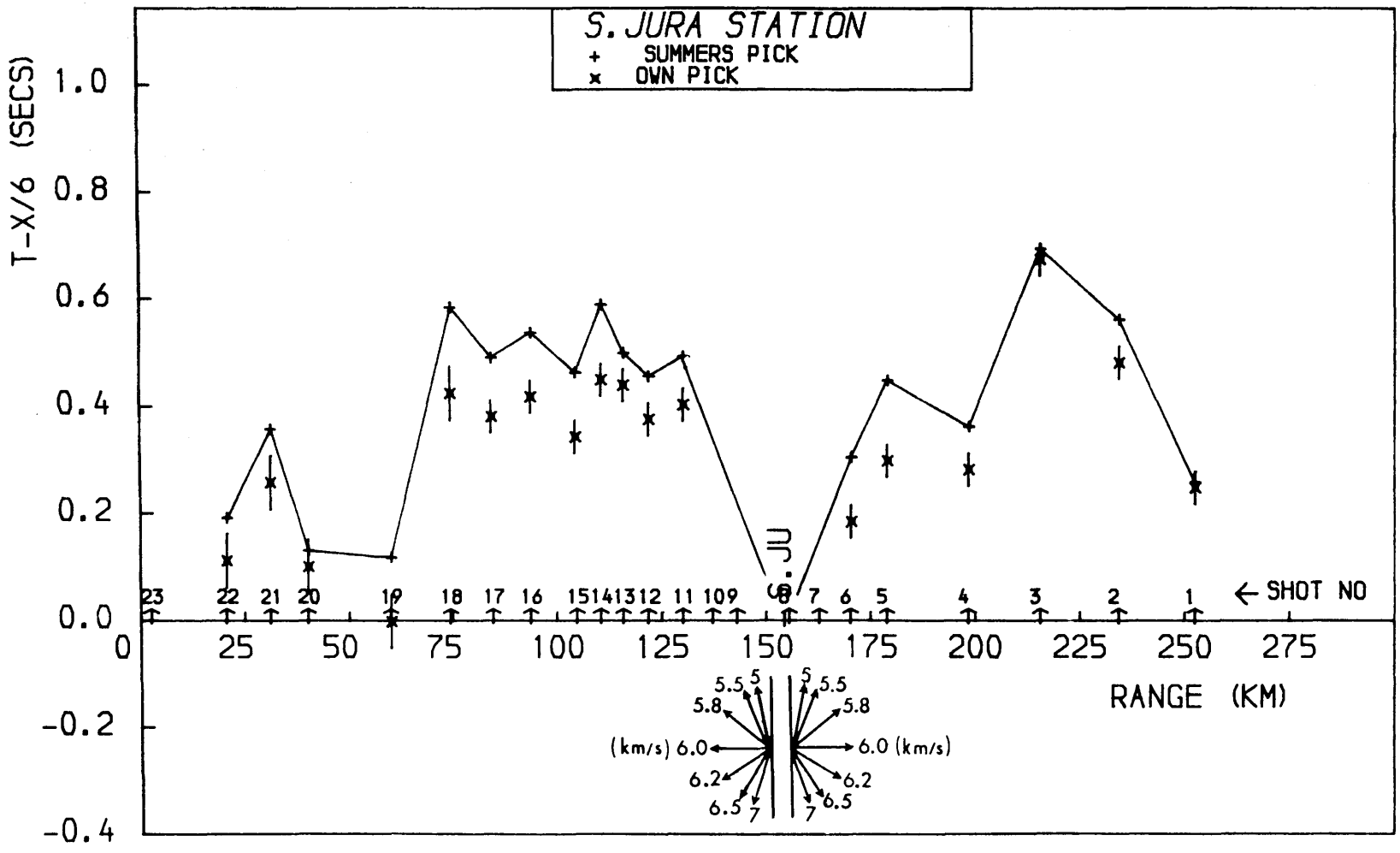

Fig. 2.21: Reduced T-X graph of Summers's picks and the author's picks with corresponding picking error bars for the South Jura station (WISE1).

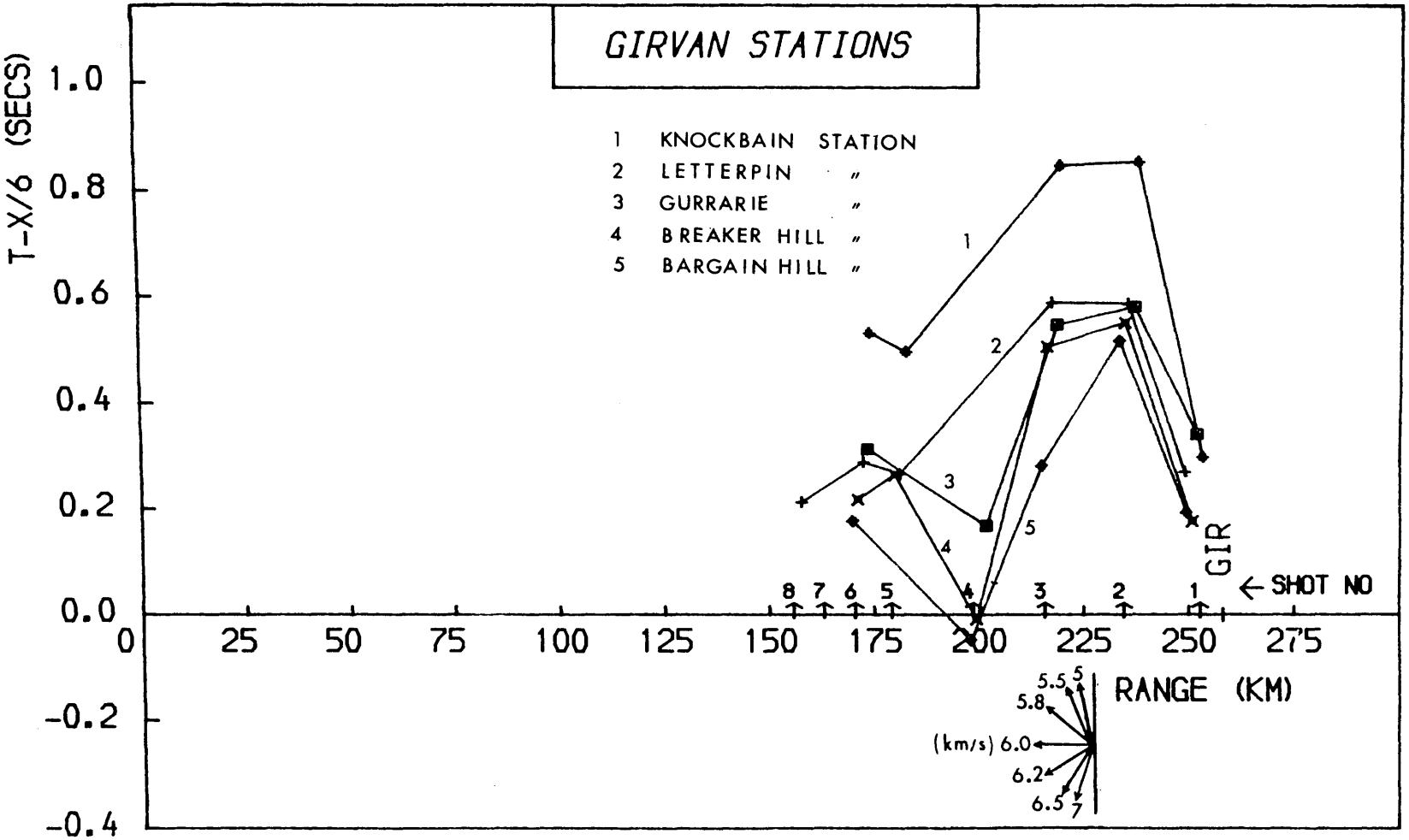

Fig. 2.22: Reduced T-X graph of Summers's picks for the Girvan station. Slight shot offsets are due to 3-dimensional distribution of stations (WISE1).

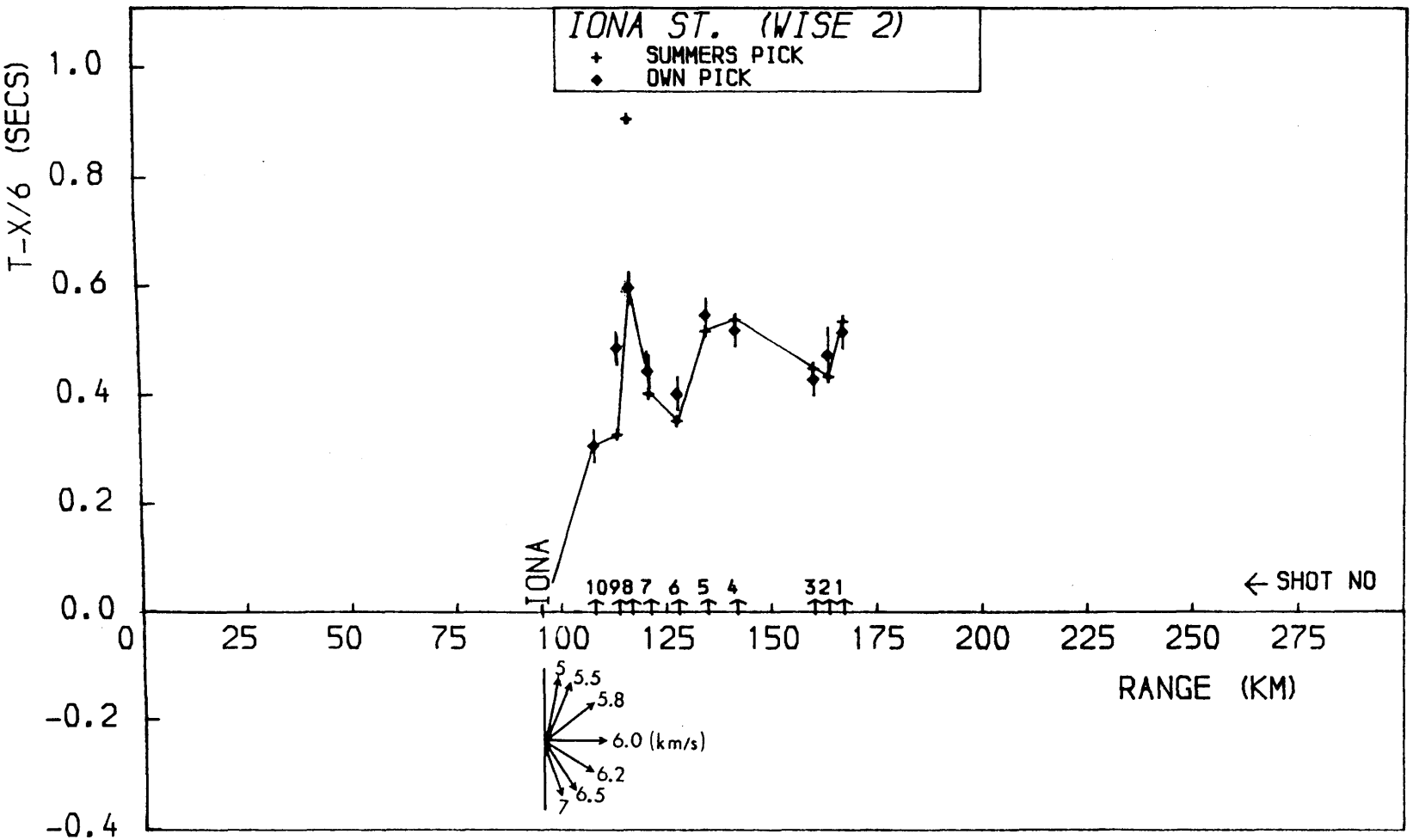

Fig. 2.23: Reduced T-X graph of Summers's picks and the author's picks with corresponding picking error bars for the Iona station (WISE2).

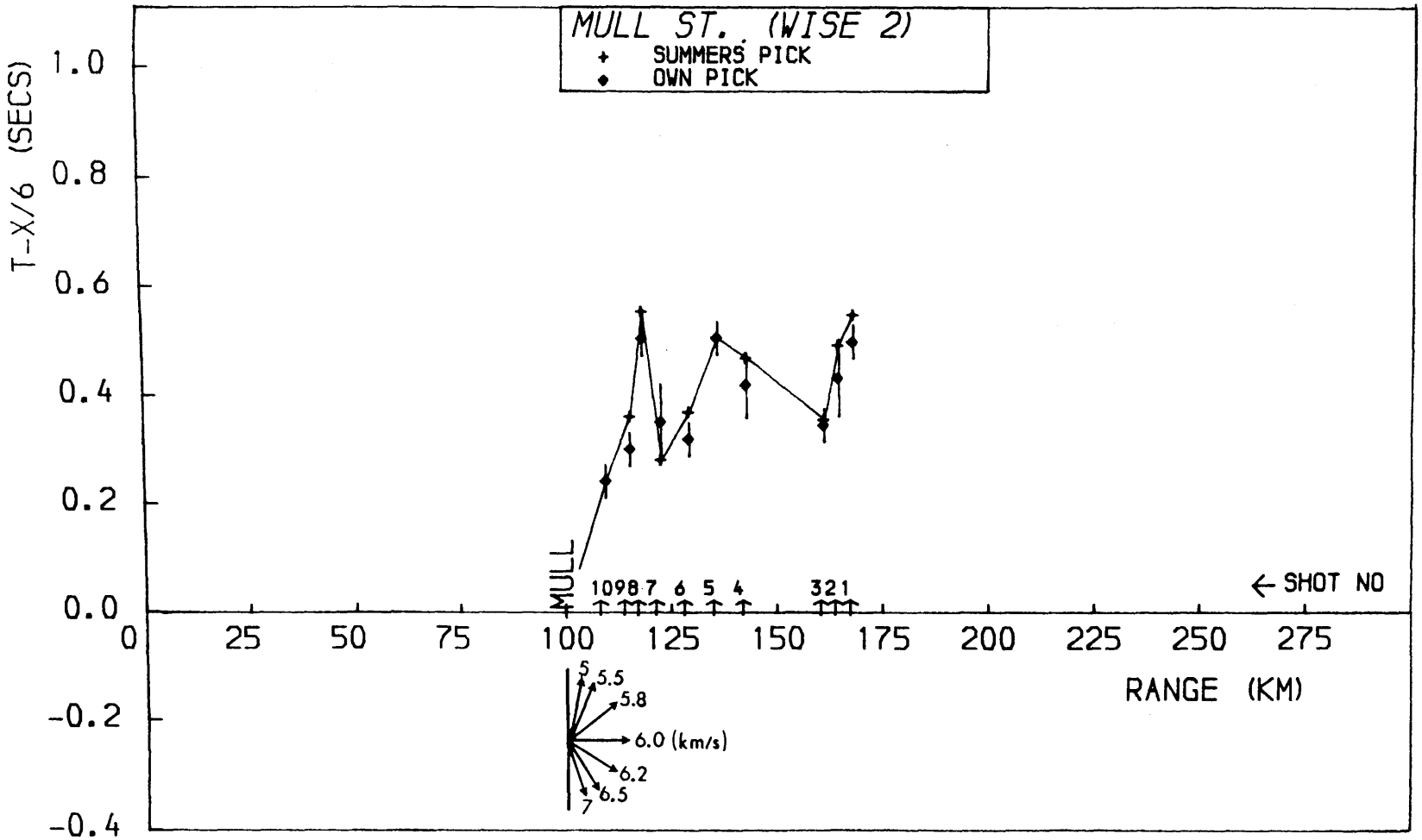

Fig. 2.24: Reduced T-X graph of Summers's picks and the author's picks with corresponding picking error bars for the Mull station (WISE2).

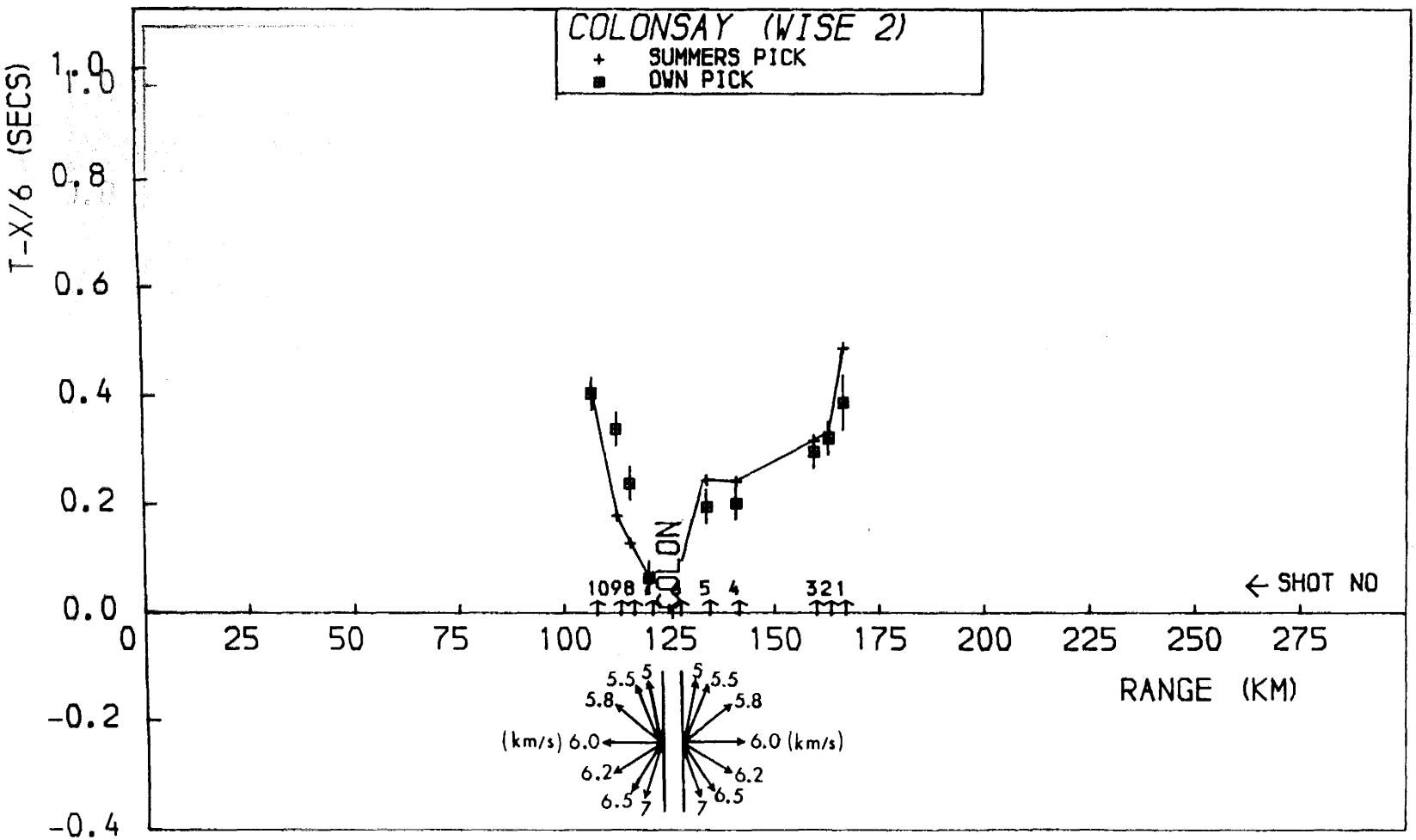

Fig. 2.25: Reduced T-X graph of Summers's picks and the author's picks with corresponding picking error bars for the Colonsay station (WISE2).

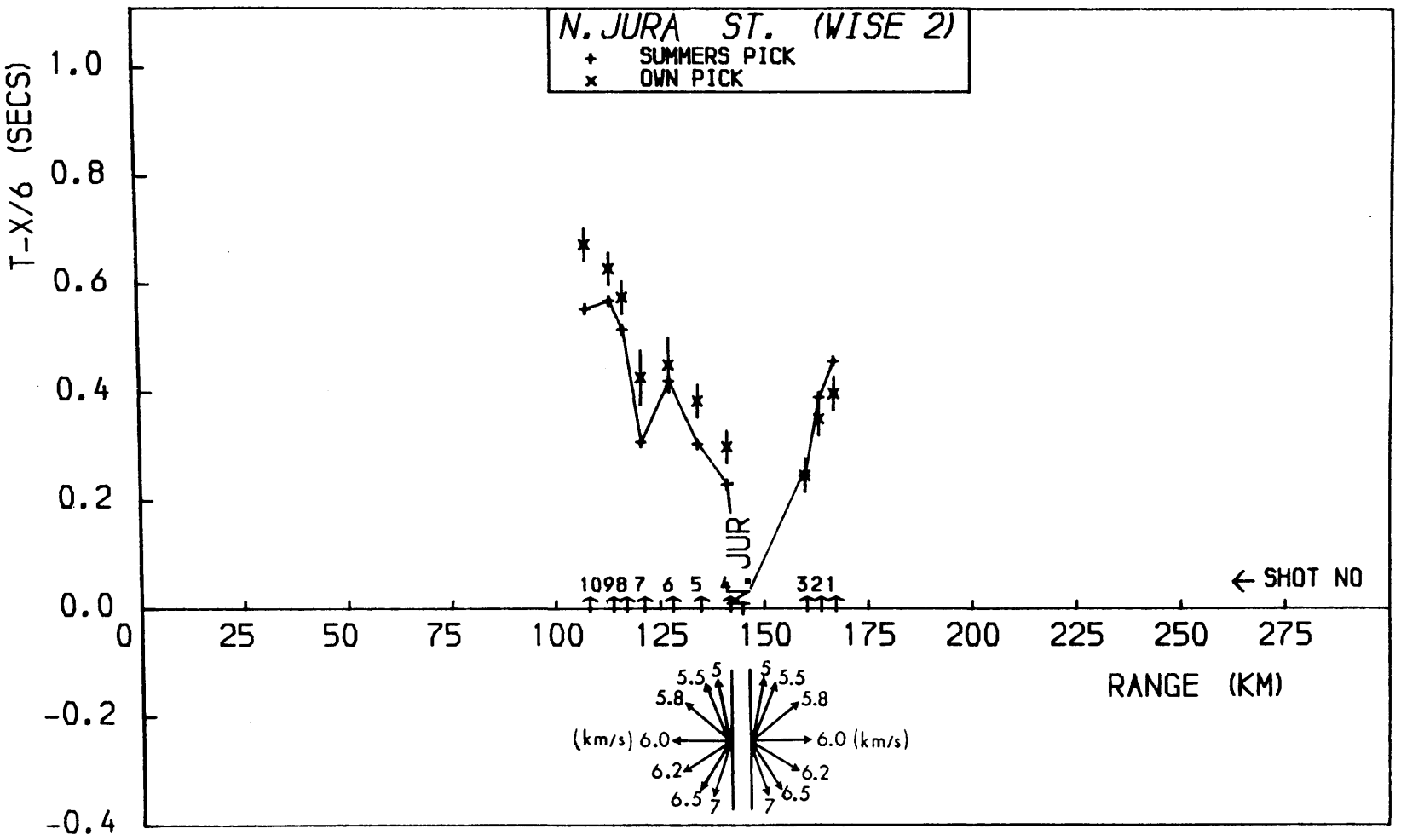

Fig. 2.26: Reduced T-X graph of Summers's picks and the author's picks with corresponding picking error bars for the North Jura station (WISE2).

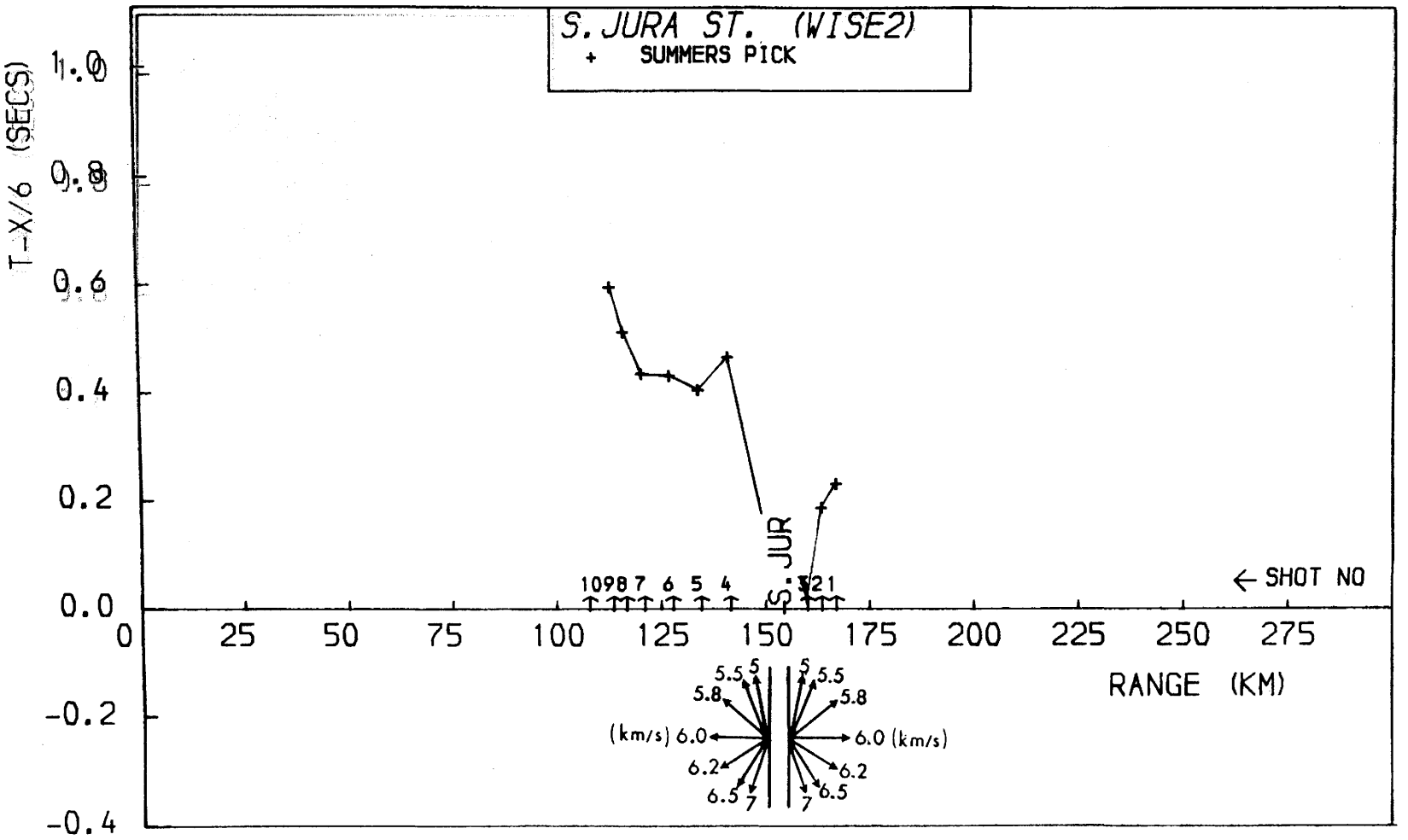

Fig. 2.27: Reduced T-X graph of Summers's picks for the South Jura station (WISE2). No record sections were available for this station.

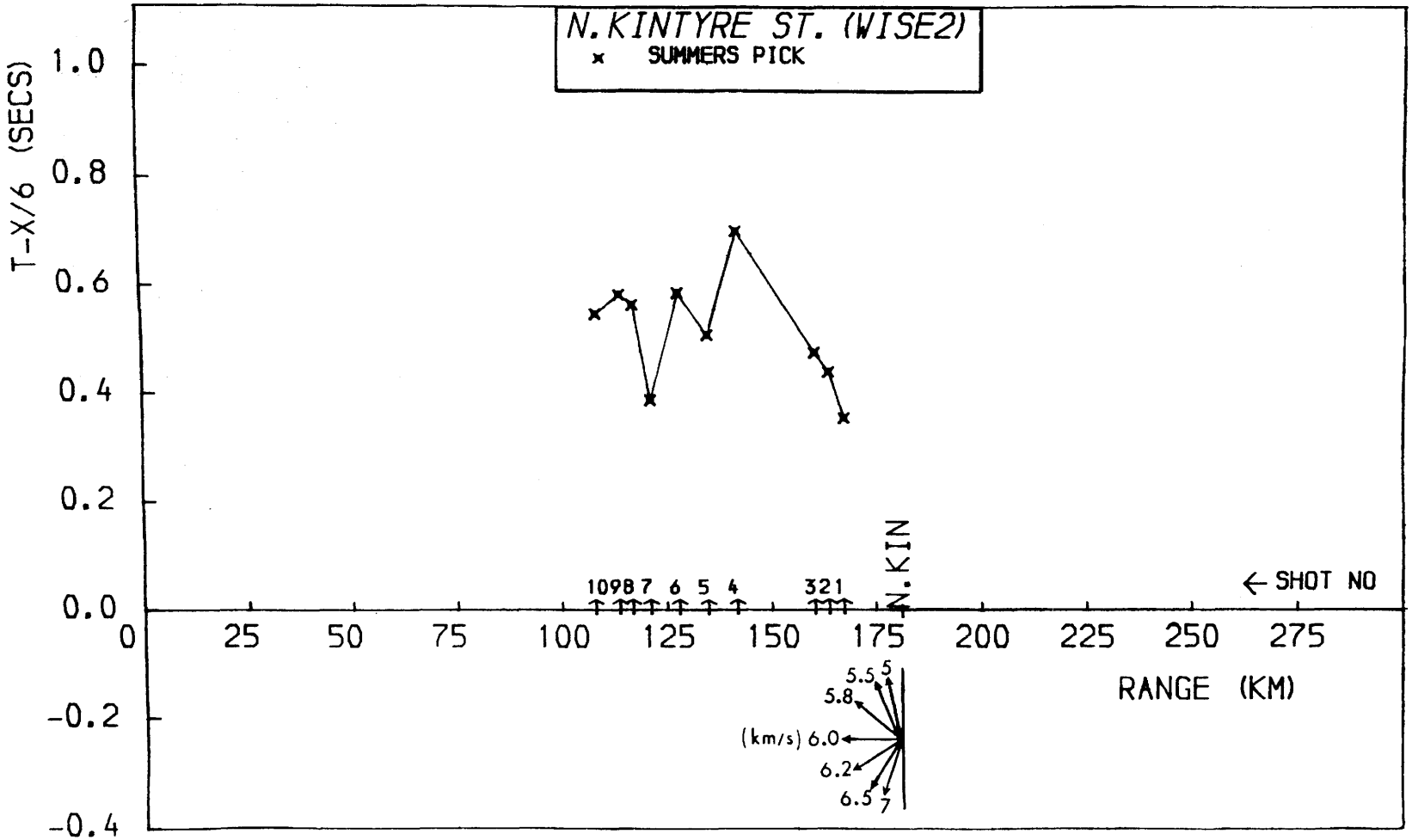

Fig. 2.28: Reduced T-X graph of Summers's picks for the North Kintyre station (WISE2). No record sections were available for this station.

on the signal to noise ratio, with late picks being more probable in high noise. The corresponding ambiguity will not usually be greater than half a cycle (e.g. 0.05 sec for 10 Hz frequency) for moderately noisy arrivals, and one cycle for the more noisy but recognisable arrivals, though in a few cases it can well exceed those values (Tables A.11 and A.12, Appendix 1). That might have happened to picks for shots 17 and 18 (Inner Hebrides basin) recorded at Mull (Fig. 2.6) and for shots 14, 13, 10 and 9 recorded at Barra (Fig. 2.4).

Since the three sources of error are independent of each other the variance of the joint distribution is equal to the sum of the variances of the individual distributions. There is a 98% probability that the joint error is less than twice the variance of the joint distribution. It is thus unlikely that the error will exceed this value, which we call, the maximum error.

2.4.2. Signal enhancement in the airgun data

Since the airgun data acquired during the first phase of the experiment were very noisy and only a small number of arrivals could be picked by eye (e.g. Fig. 2.29 to 2.32), efforts were made to enhance and detect the signals automatically (Birtles 1980, Warren 1981).

Birtles used predictive deconvolution in an attempt to increase the signal to noise ratio, but without much success due to computing problems. He also applied the cross-correlation technique by averaging five adjacent traces and cross-correlating the result with the next trace (the onset was considered to be at the position of maximum correlation).

The method appeared to work to some extent but there was no detailed review of the results and the data were reworked by Warren (1981). He emphasised the cross-correlation technique, after filtering of the data (4-32 Hz) to remove low frequency noise and after shaping the signal by using predictive deconvolution. The shaping of the signal was considered important for its easy detection by the matched filter. The cross-correlation was used in the same fashion as used by Birtles but with a decision function involved. The decision function used for updating the five adjacent signals (whose average was cross-correlated with the next signal) was the correlation coefficient, and a value of 0.7 was considered to give the optimum results. Finally, every three traces were shifted in mid-onset position and stacked together in an attempt to improve the signal to noise ratio.

An example of the above procedure and results is shown in Figures 2.33 to 2.35.

Though initially it was thought that the processing was successful, comparison between corresponding explosive shot times and the airgun times, for the Mull-Tiree line, showed significant discrepancies (of the order of 0.10 sec or more). A careful re-examination of the methods applied, by Summers (1982), demonstrated some of their weaknesses. Amongst others, the use of predictive deconvolution was thought to be inappropriate since the technique was not developed for use on non-minimum delay wavelets (as most of the airgun data seem to be) or for enhancing signals immersed in noise of equal or

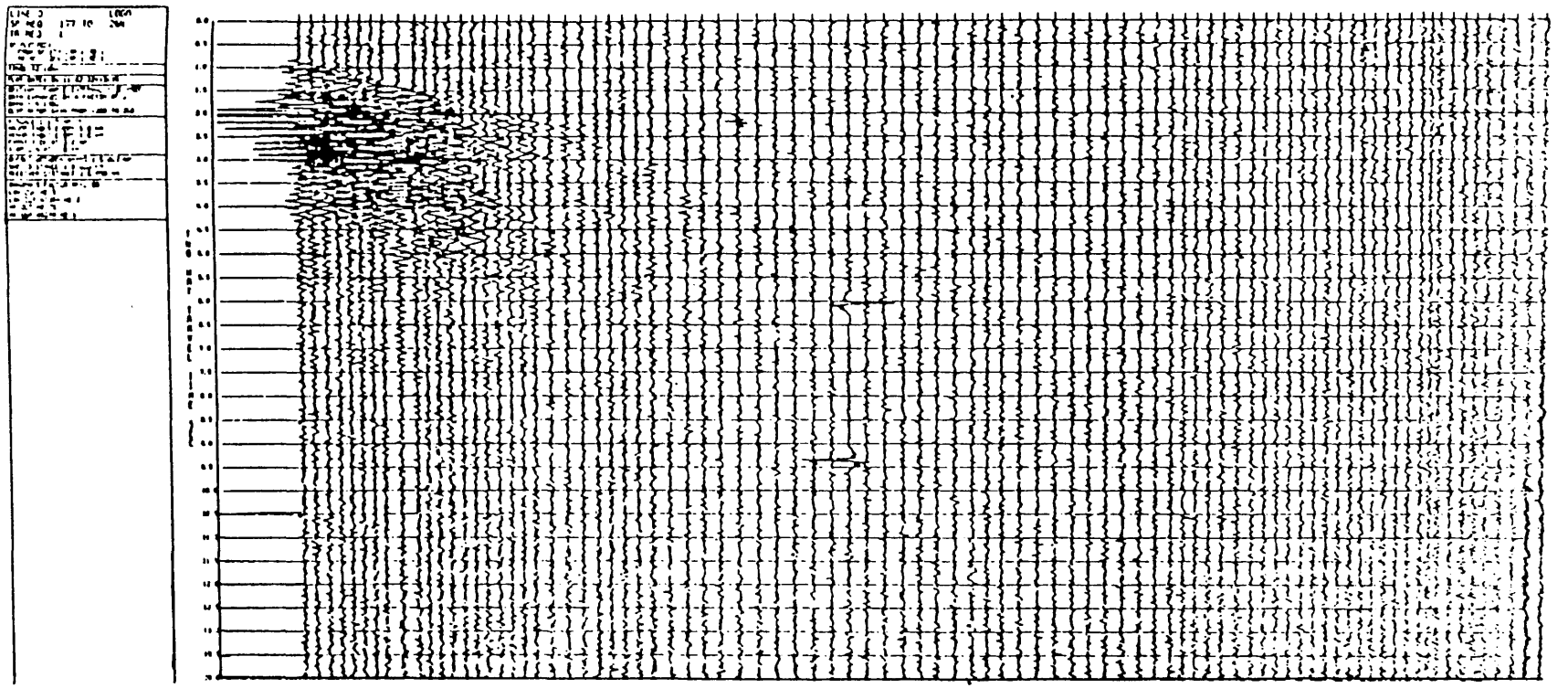

Fig. 2.29: Raw airgun data for the Mull to Tiree line recorded at the Tiree station.

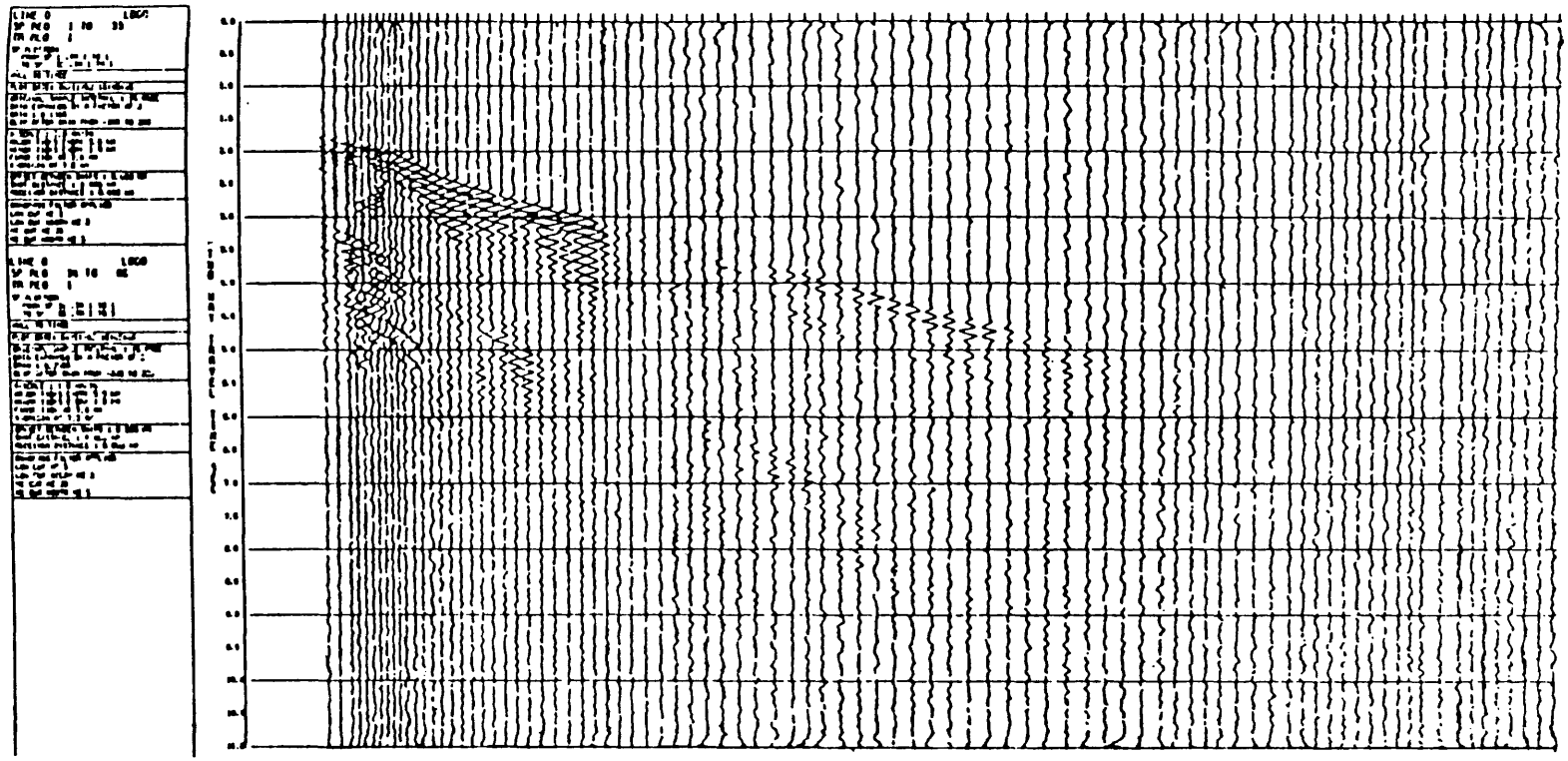

Fig. 2.30: Band passed (4-32 Hz) airgun data for the Mull to Tiree line recorded at the Mull Geostore station.

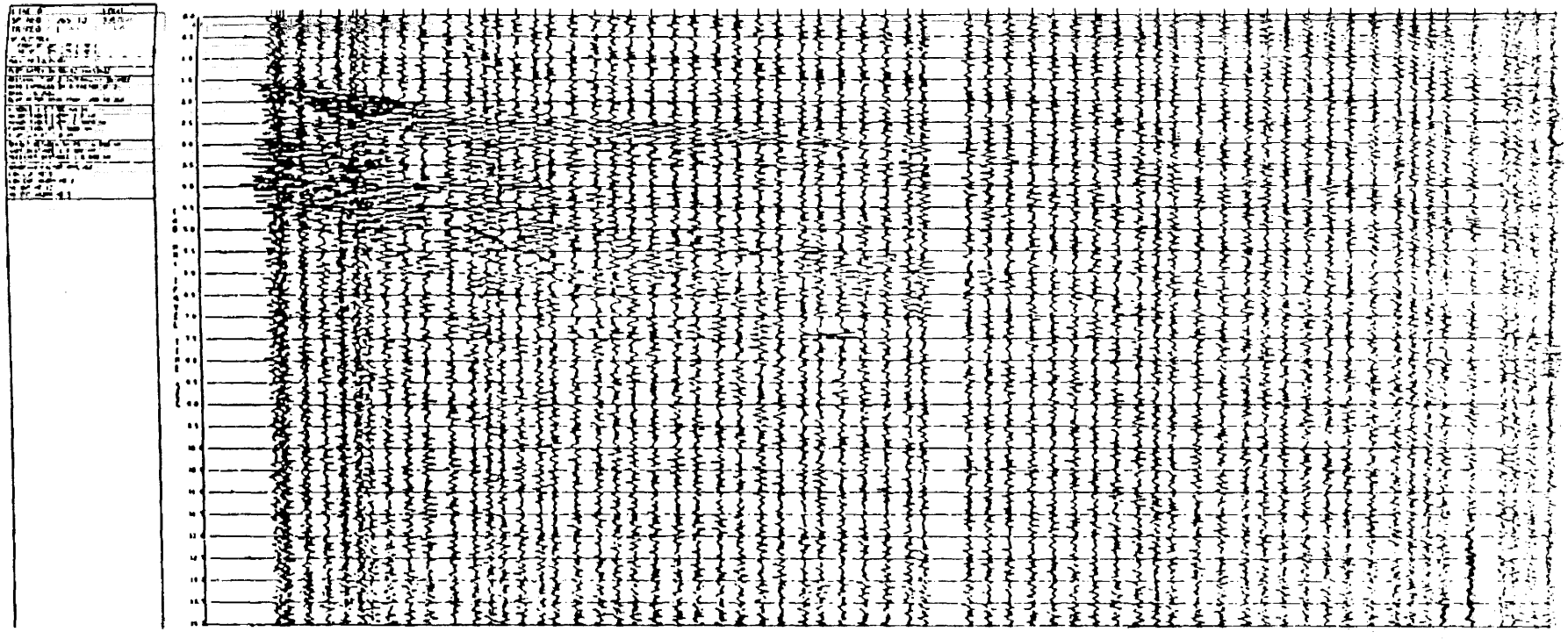

Fig. 2.31: Raw airgun data for the Mull to Colonsay line recorded at Mull.

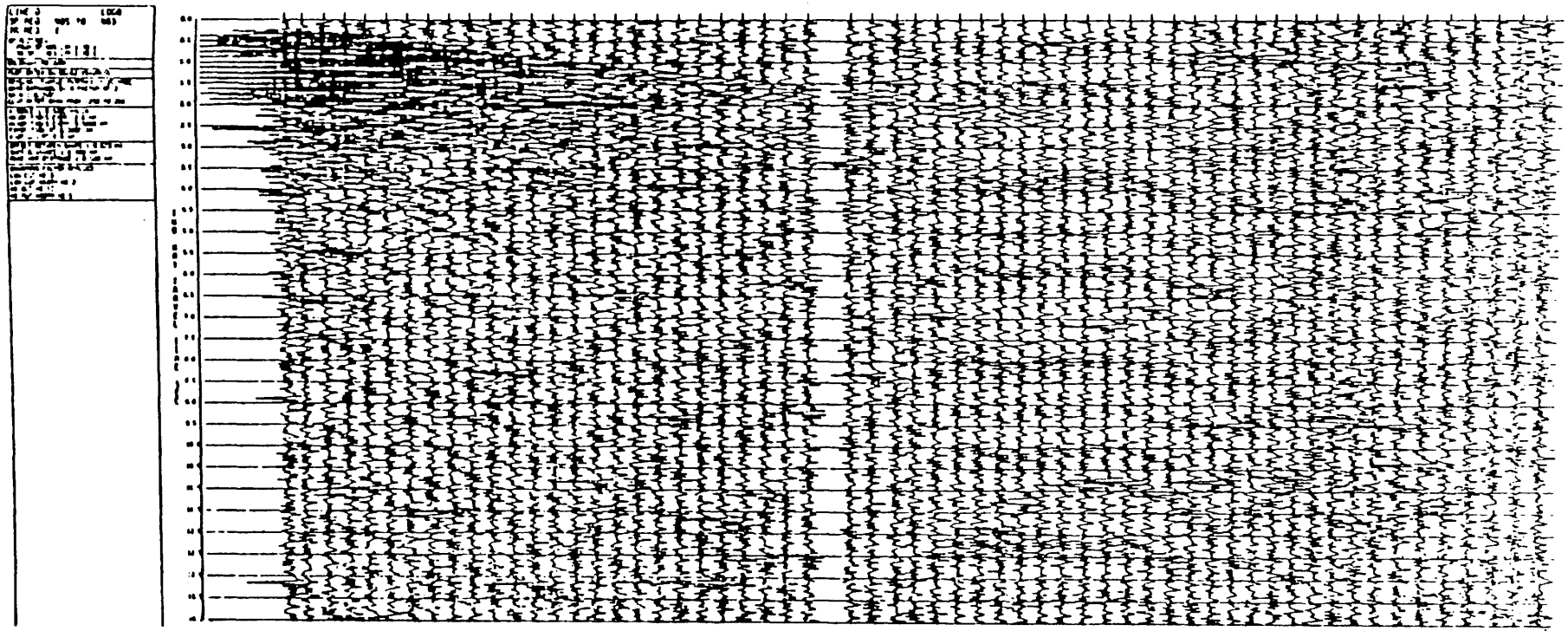

Fig. 2.32: Raw airgun data for the Colonsay to Jura line recorded at Colonsay.

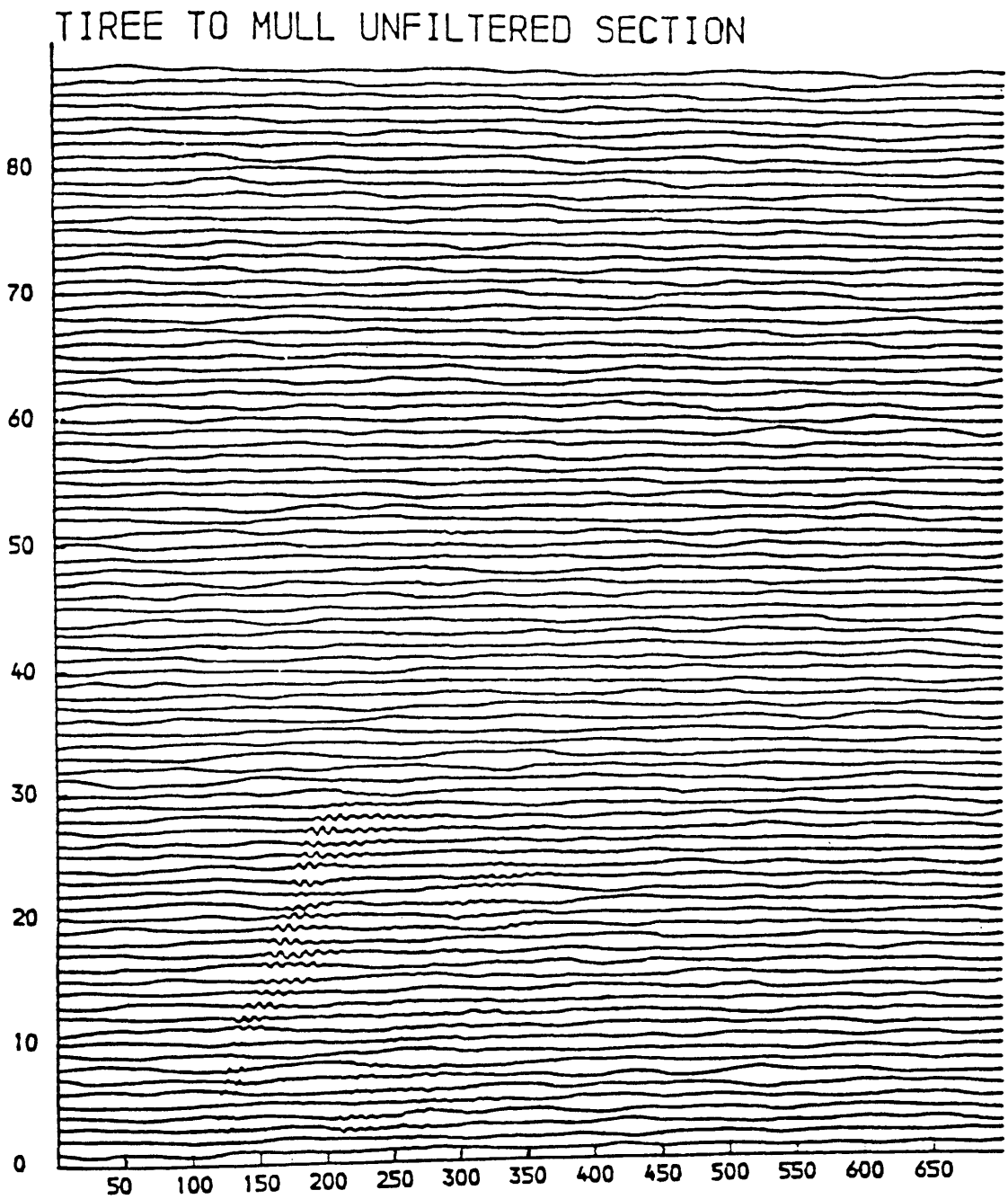

Fig. 2.33: Raw data for the Mull to Tiree airgun line recorded at Mull. Reproduced from Warren (1981).

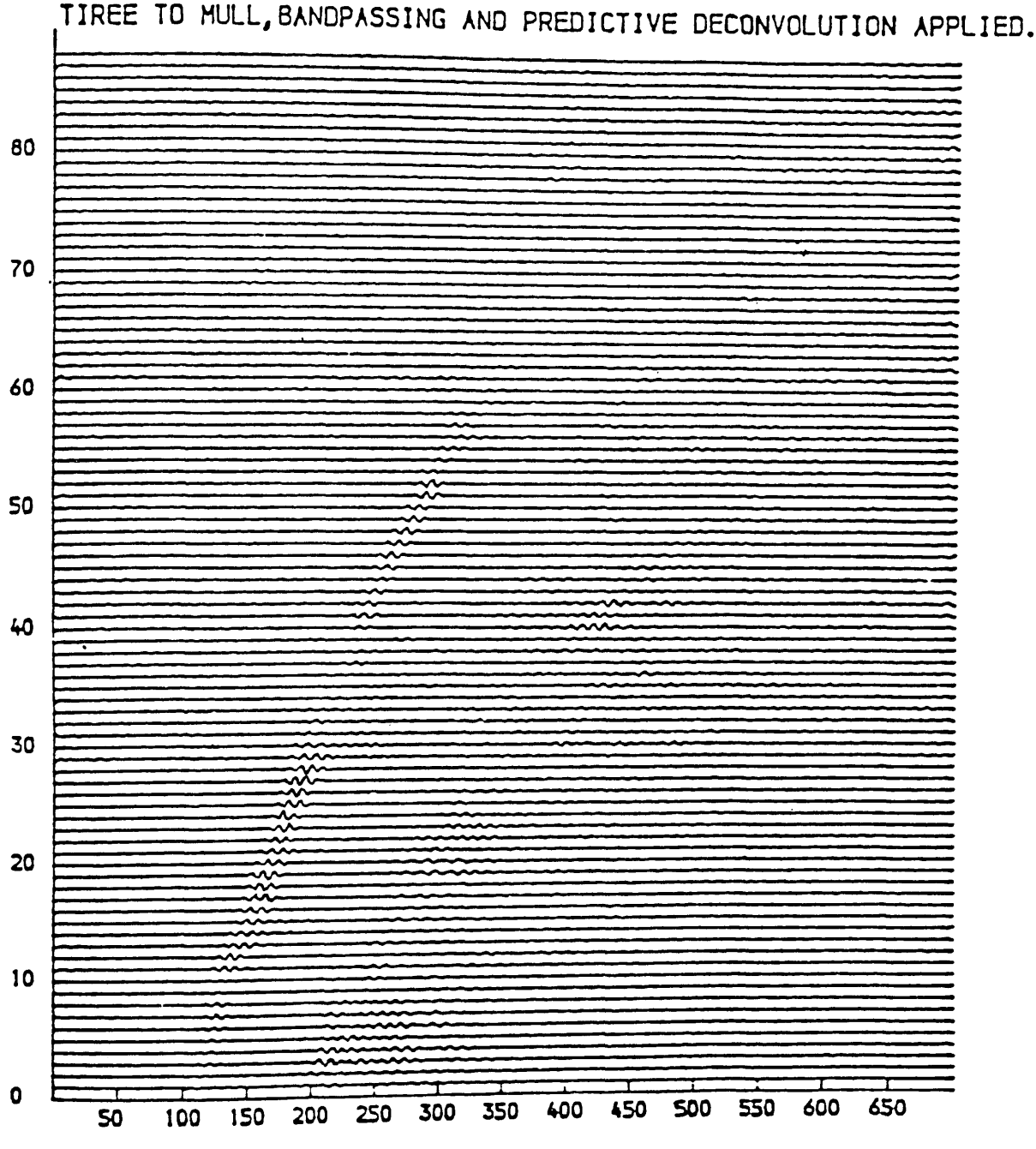

Fig. 2.34: Data from Mull after the application of predictive deconvolution. Reproduced from Warren (1981).

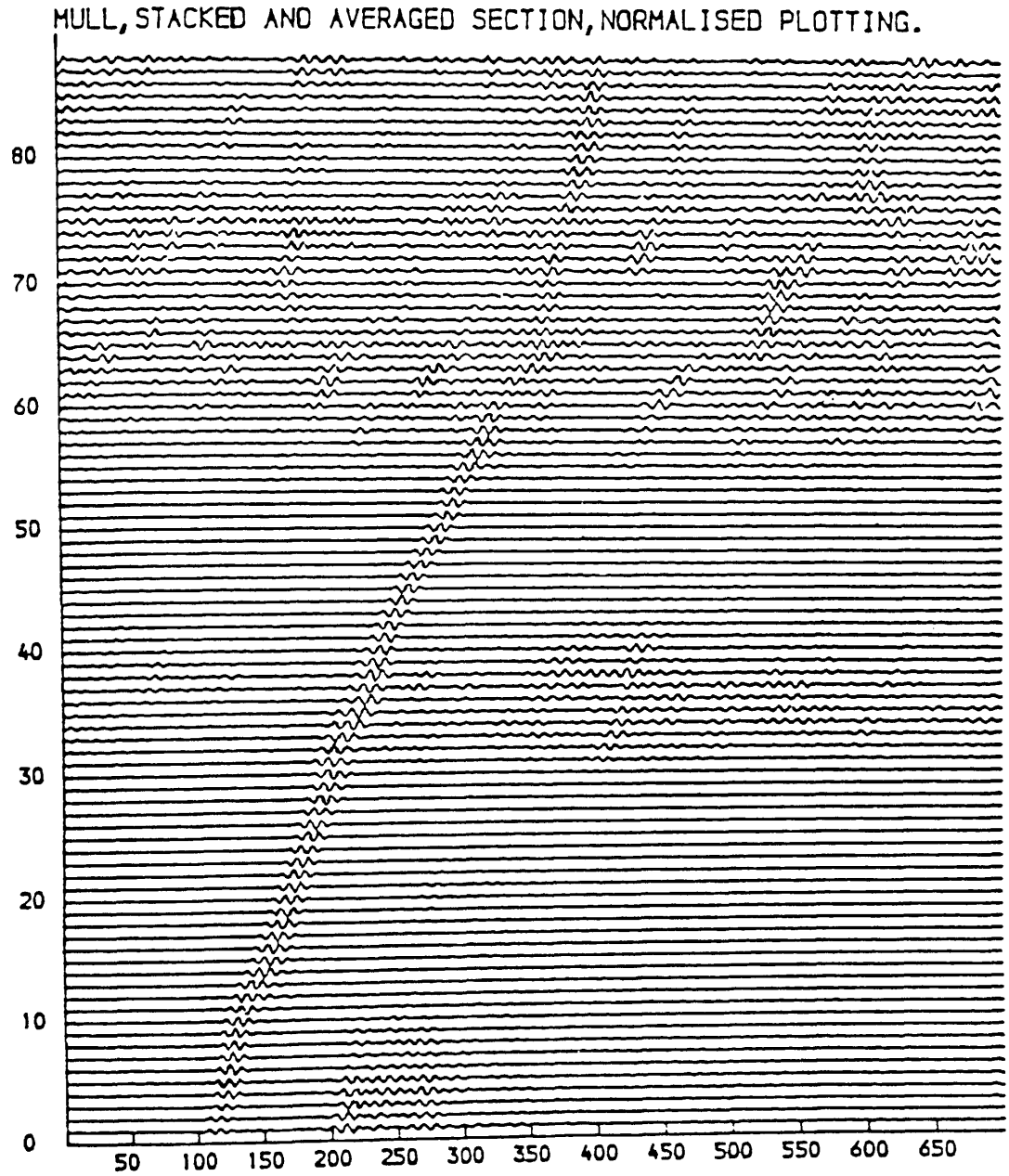

Fig. 2.35: Data from Mull after the application of the matched filter and with every five adjacent traces stacked at their position of maximum cross-correlation throughout the section. Reproduced from Warren (1981).

greater amplitude. Also, the matched filter was probably highly corrupted by noise during updating because the noise was often dominant or had the same frequency content as the signal itself.

2.4.3. Picking of the airgun data

Most of the airgun data was picked by the author during a visit to Durham University. Those were the data derived during the second phase of the experiment for the lines Tiree - Mull, Mull - Colonsay and Colonsay - North Jura. They were displayed on reduced sections in both raw and processed states, the distinction being easy as the raw data always possessed high amplitude traces near to the recording stations. The airgun data for the line Tiree - Mull from the first phase of the experiment were also picked as they represented the best airgun data of that phase.

During picking, the raw data were the first to be used and were later supplemented by the processed data in order to extend the Mull - Colonsay line beyond 15 km towards Colonsay, to reverse the Colonsay - Jura line in Jura and extend the Mull - Tiree line beyond 12 km towards Tiree.

It was found later that the picks were in good agreement with the picks of Atree and Casson, being slightly earlier (by about 0.03 sec) than theirs.

The travel times for the South Jura - North Kintyre line were initially picked by J. Hall and checked in random by the author without finding any significant differences.

The travel times and ranges of the airgun shots are listed in Appendix 1 (Table A.9).

2.5. VISUAL INSPECTION OF THE REDUCED T-X GRAPHS

The Pg first arrivals picked in ways described in the previous section are presented here on reduced T-X graphs. Direct accuracy and internal consistency evaluation of the data is now possible by comparing:

a) previous picks for the explosive data with the authors picks (sect. 2.5.1),

b) picks of arrival times for the explosive data recorded at common or near stations (sect. 2.5.1),

c) reduced arrival times for approximately reciprocal shot-station configurations (sect. 2.5.1), and

d) airgun picks (from both raw and processed record sections) with explosive shot picks recorded at the same stations (sect. 2.5.2).

2.5.1. Explosive shots

The previous picks are plotted together with current picks and their error bars (Fig. 2.15 to 2.28). Generally, whenever it is not clear which of the two picks corresponding to a particular shot is in error, Summers's picks will be preferred due to his more proper picking procedure involving use of the original jet-pen records (section 2.4; Fig.2.3, 2.4).

The Barra plot (Fig. 2.15) shows no important discrepancies between the two data sets apart from shot no 12. As its arrival appears quite clear on the reduced record section (Fig. 2.4) and is the only one deviating from the pattern of agreement, the

current pick will be used.

In the Tiree (Ruaig) graph (Fig. 2.16) the cause of the discrepancies for shots 18 and 21 of about 0.10 sec is not clear. The previous pick will be used for both shots, for shot 18 due to its closer agreement with the airgun data (Fig. 2.43).

For the WISE1 Mull, M. Jura and S. Jura stations (Fig. 2.18, 2.20 and 2.21) the current picks come earlier by about 0.10 sec. The differences, which cannot be attributed to anything else but some error in the plotting procedure of the reduced record sections or the preliminary character of these sections, fluctuate much less for the high quality records of M. Jura and S. Jura thus preserving the pattern of the apparent velocities. Again, the previous picks will be used due to their closer agreement with the WISE2 explosive data sets (Fig. 2.37 and 2.39) and the airgun data (Fig. 2.43 to 2.46). Shots recorded at Girvan stations have given arrival times (Fig. 2.22) which, though usually in agreement, occasionally disagree by about 0.20 sec. The differences can, at least partly, be explained by the diverse geology of the area and the 3-dimensional configuration of the stations (Chapter 4).

In the WISE2 plots (Fig. 2.23 to 2.28), Summers's picks appear to be more consistent with the airgun data (Fig. 2.43 to 2.46), even though both sets of picks usually preserve the apparent velocity pattern (Fig. 2.23 to 2.26). Summers's pick for shot 8 recorded at Iona (Fig. 2.23) is obviously in error (Fig. 2.23, 2.24 and 2.40) and current pick is preferred, but his pick for shot 9 is adopted due to its closer agreement with the similar

picks from the Mull station (Fig. 2.24).

The sets of picks for the Colonsay and N.Jura stations display systematic differences of opposite sign, of the order of 0.07 sec, on either side of each station (Fig. 2.25 and 2.26). Due to closer agreement of the previous picks to the airgun data (Fig. 2.44 and 2.45), those picks are preferred.

No reduced record sections were available for the WISE2 S. Jura and N. Kintyre stations (section 2.3.3) and the existing picks (Fig. 2.27 and 2.28) can only be compared with the airgun data (section 2.5.2).

Another way of checking the internal consistency of a small part of the data, is by comparing reduced arrival times for (approx.) reciprocal shot-station configurations. Since all the stations were situated on land basement and the nearest shots on low-velocity sea-bottom sediments, it is obvious that small delays were introduced for particular traces. The ray-paths corresponding to these shot-station configurations, will then sample the same intra-basement velocity variations and small differences will be due to near-surface basement velocity variations and errors in positioning / timing of the shots and picking of the first arrivals. Table 2.1 shows the shot-station pairs for which a comparison was possible. It can be seen that the travel times are usually compatible apart from those in groups B and C. The differences there, can be partly explained by higher velocities under shot 19 than under the Tiree station and (or) propagation of rays from Iona to Tiree through the Torridonian rocks of the Inner Hebrides basin.

TABLE 2.1

	Shot no	Station	T-X/6 (sec)
A.	16	Barra	0.00
	23	Iona	0.04
	{ 23	Mull	-0.04 }
B.	19	Barra	0.07
	23	Tiree(R)	0.21
C.	16	Tiree(R)	0.35
	19	Iona	0.26
	{ 19	Mull	0.20 }
D.	8	Barra	-1.13
	23	M.Jura	-1.09
	23	S.Jura	-1.07
E.	6 (WISE2)	N.Jura	0.42
	9	Colonsay	0.43

Remarks: 1) All shots from WISE1 unless otherwise stated
2) Shot 16 at 4.00 km from Iona
" 23 " 2.70 km " Barra
" 19 " 4.15 km " Tiree (Ruaig)
" 8 " 1.50 km " S.Jura
" 9 " 1.20 km " N.Jura
" 6W2 " 1.50 km " Colonsay

The arrival times for both phases recorded at the same stations have been plotted in Figures 2.36 to 2.39 in order to provide more complete T-X graphs for the evaluation of the apparent velocities and the inspection of the consistency of the data. In the S. Jura plot (Fig. 2.39), it can be seen that the shot 8 (WISE2) pick shows no significant difference to shot 13 (WISE1) pick, thus confirming the successful link between the two phases of the experiment (section 2.2.2).

The arrival times from a particular phase recorded at near or same stations are shown in Figures 2.40 to 2.42.

It can be seen that though the agreement is usually good, occasional discrepancies of about 0.10 sec suggest that the

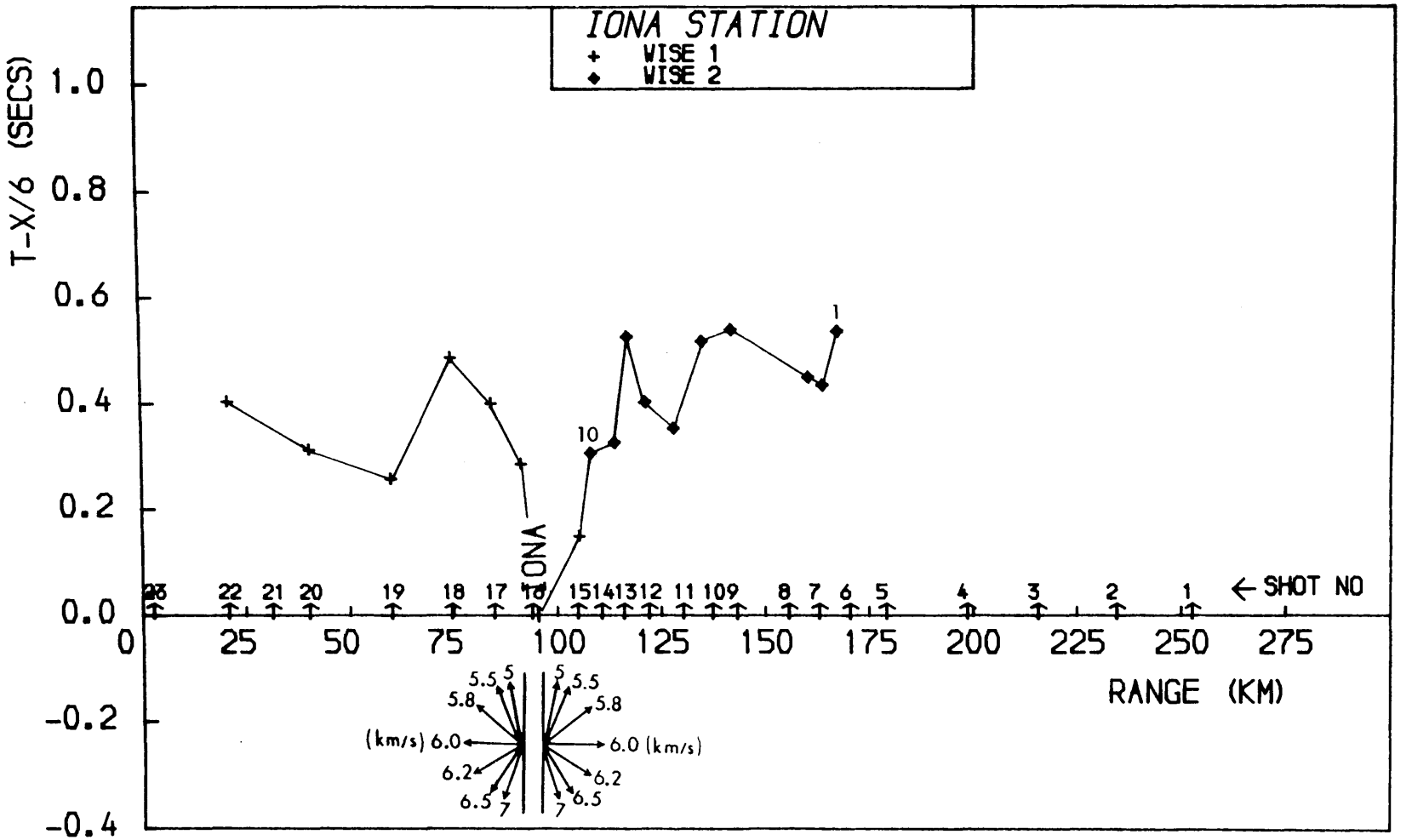

Fig. 2.36: Reduced T-X graph for the WISE1 and WISE2 explosive shots recorded at Iona.

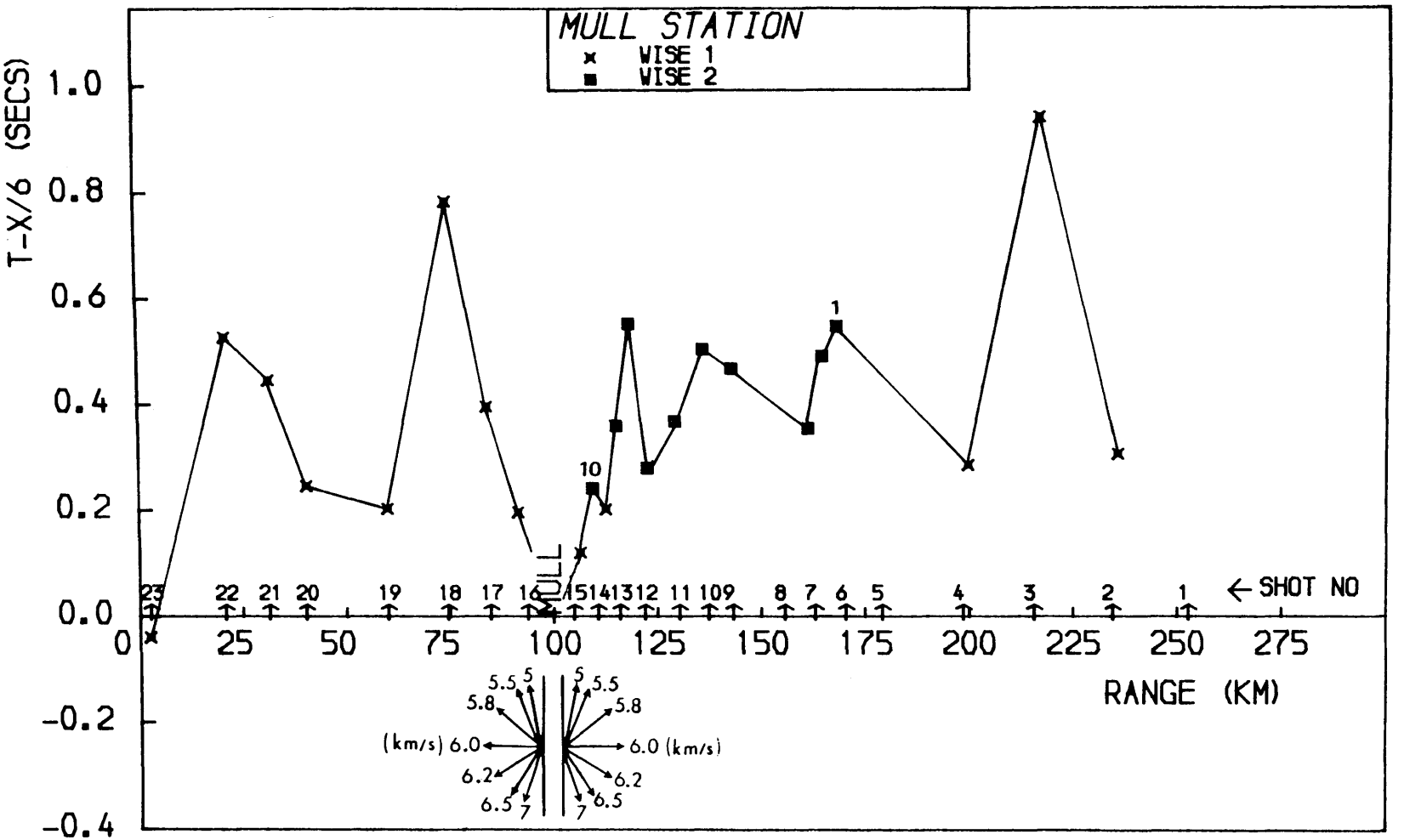

Fig. 2.37: Reduced T-X graph for the WISE1 and WISE2 explosive shots recorded at Mull.

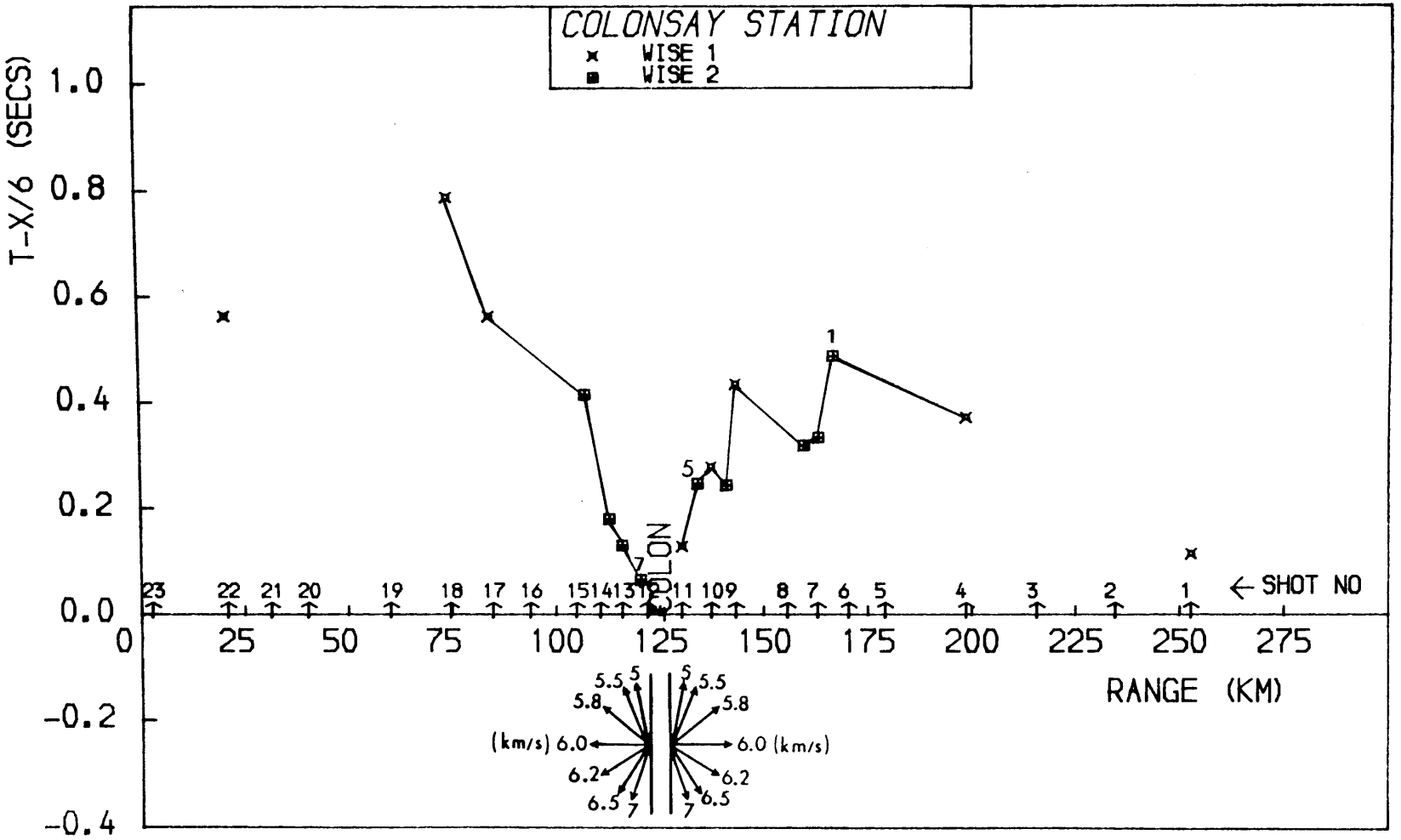

Fig. 2.38: Reduced T-X graph for the WISE1 and WISE2 explosive shots recorded at Colonsay.

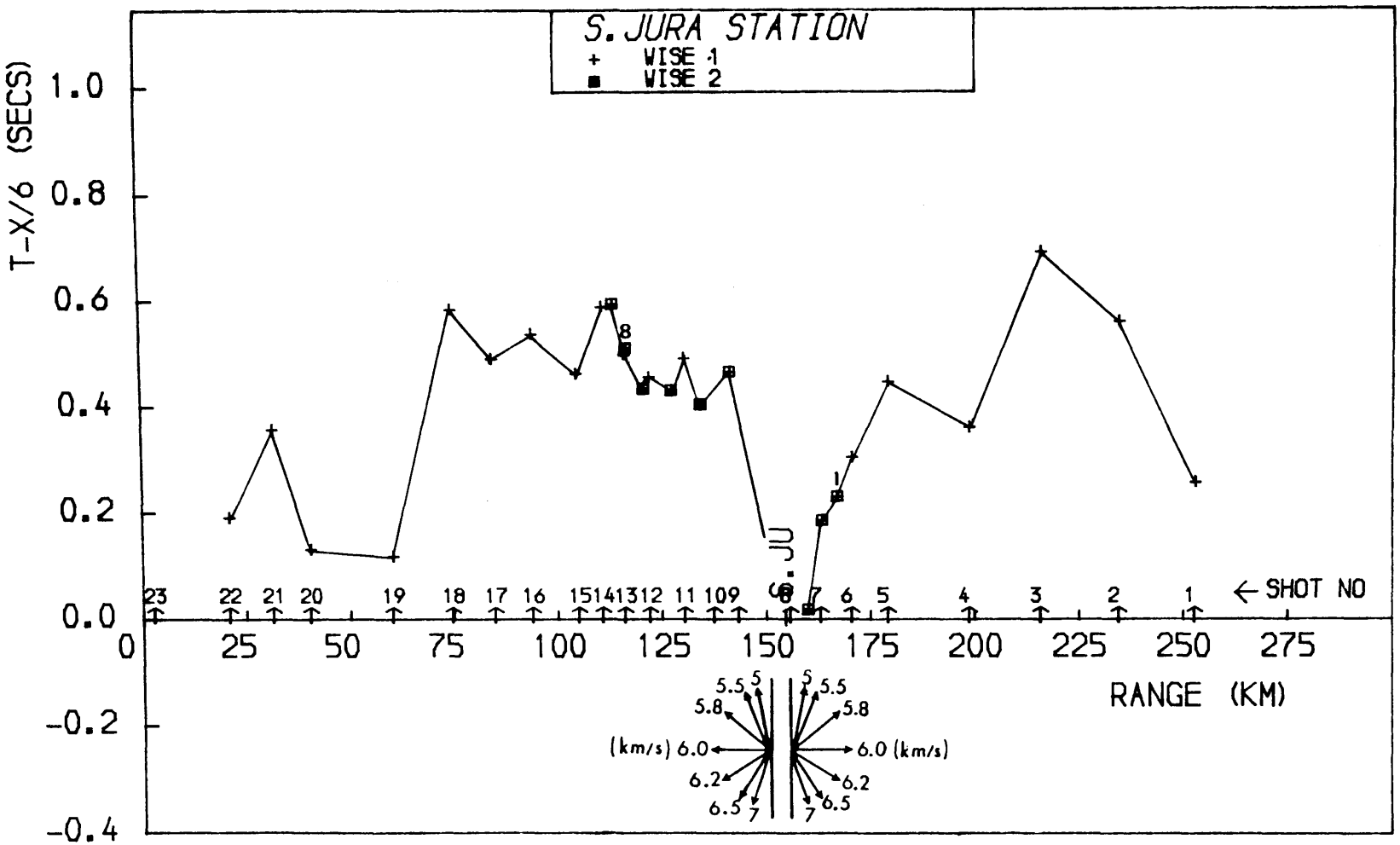

Fig. 2.39: Reduced T-X graph for the WISE1 and WISE2 explosive shots recorded at South Jura.

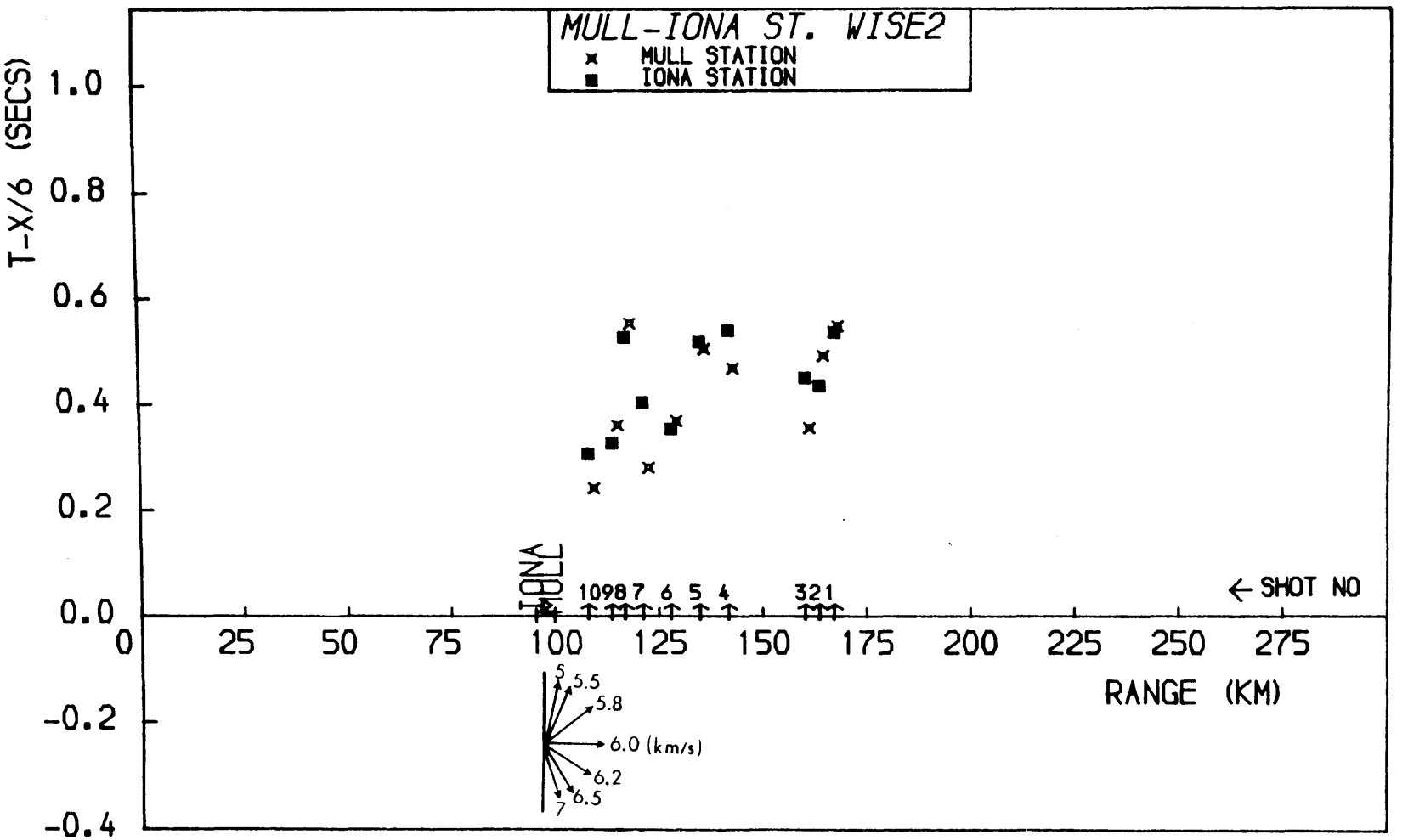

Fig. 2.40: Reduced T-X graph of the WISE2 explosive shots recorded at Mull and Iona.

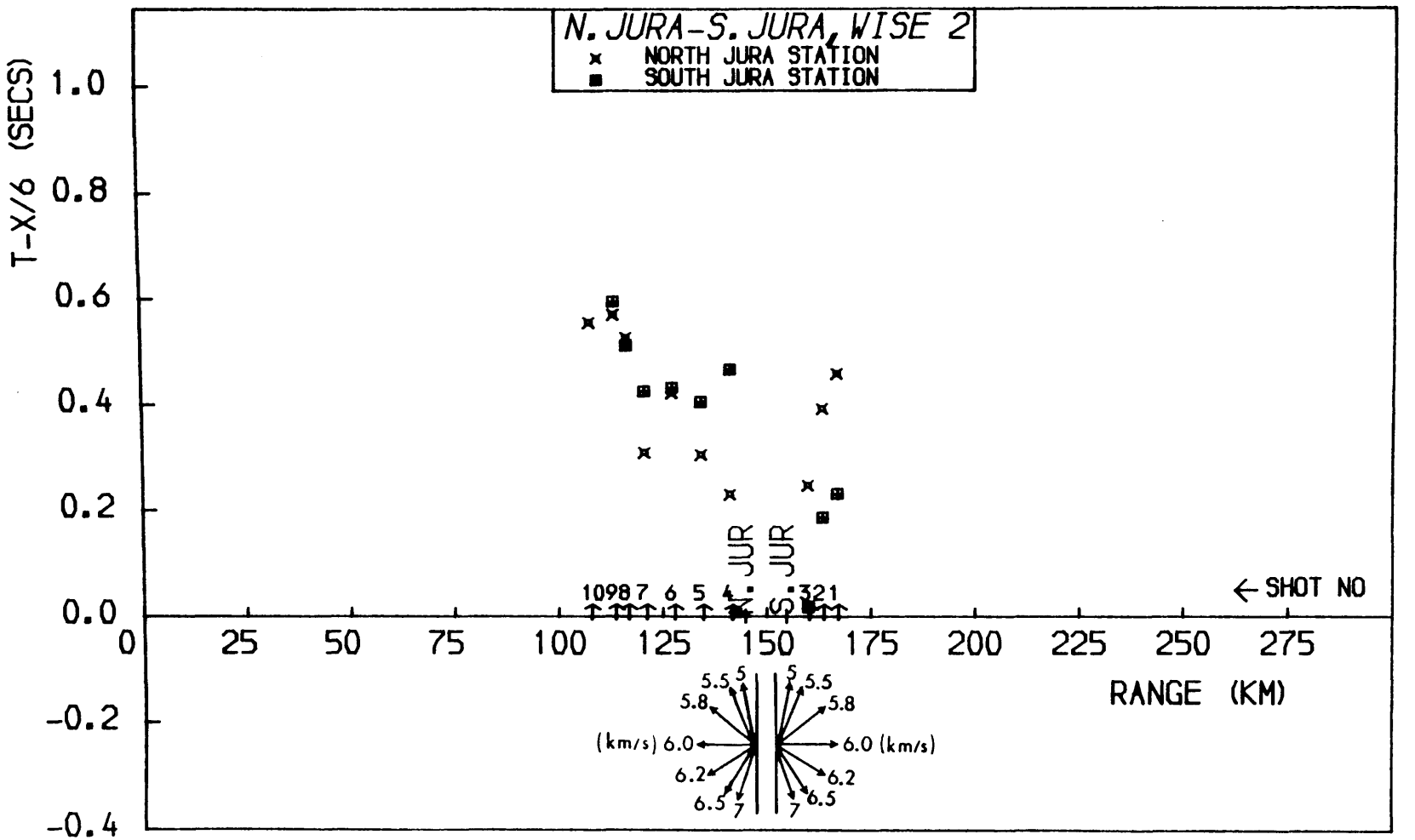

Fig. 2.41: Reduced T-X graph of the WISE2 explosive shots recorded at North Jura and South Jura.

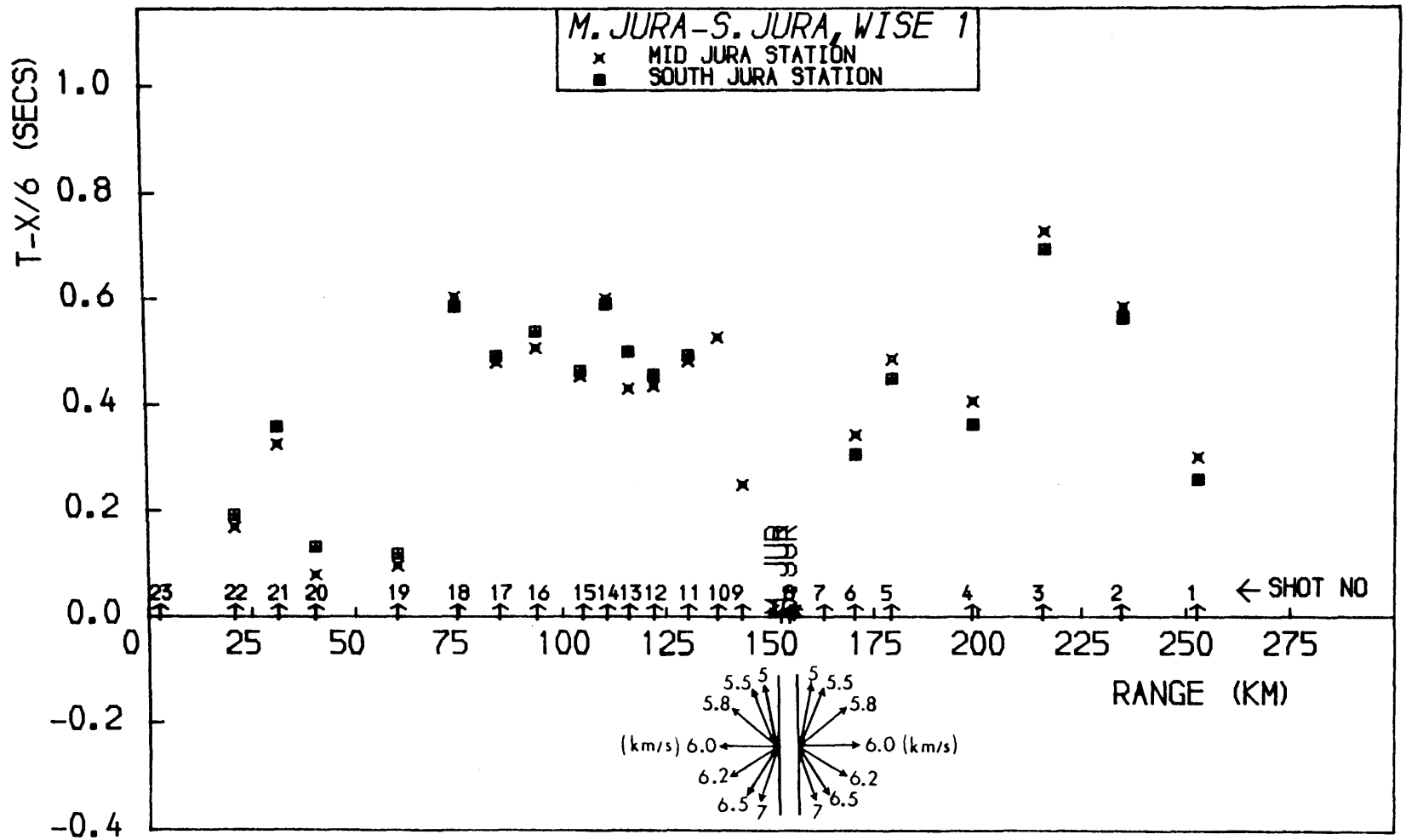

Fig. 2.42: Reduced T-X graph of the WISE1 explosive shots recorded at Mid Jura and South Jura.

final models will not probably satisfy a small part of the data.

2.5.2. Airgun and Geoflex shots in conjuction with the short-range explosive shots

The most significant doubts about the quality of the airgun data come after comparing the airgun arrival times with the explosive shots times, corrected for shot depth differences (Fig. 2.43 to 2.46). Usually, the airgun times lag behind the explosive shot times by 0.04 to 0.20 sec.

The Tiree-Mull line (Fig. 2.43) as recorded at Mull and Iona is the most problematical. The shot 16 pick (at Iona) appears delayed by 0.10 sec in comparison to the clear airgun arrivals from that part of the line, probably due to erratic selection of the onset. Moreover, the airgun data recorded at Iona and Mull appear to be delayed by 0.20 sec in comparison to the shot 17 time at the same stations. Since the automatic picking procedure was used in this part of the line (sect. 2.4.3) and the arrivals for the explosive shot are fairly clear, the airgun recordings of this part of the line towards Tiree will only be used tentatively for modelling. The numerous Tertiary dyke intrusions together with the increasing thickness of the Mesozoic sediments and the cover of Tertiary basalts in the area (Binns et al 1974), might have been responsible for the dissipation of the airgun energy and the failure of the auto-picking methods.

The Mull-Colonsay line shot during WISE2 (Fig. 2.44), though not reversed, presents fewer problems. There appears to be an average lag of about 0.05 sec for the air-gun data with the

deviations from that average falling within the expected error range (see Appendix 1). The line is supplemented with the auto-picked data beyond the range of 15 km and despite the good agreement with shot 8, shot 7's time (probably a little too early, Fig. 2.24) shows that the auto-pick subroutines have been probably led astray and the airgun picks beyond 20 km, the south margin of the Great Glen fault zone, should not be trusted.

The Colonsay-North Jura line (Fig. 2.45), shot during Phase 2, was extended beyond 10 km towards Jura and reversed using auto-picked data. Again, the airgun data lag behind the explosive data by an average of about 0.06 sec for both recording stations and the deviations from that average are compatible with the total errors of Appendix 1.

The best quality airgun data come from the S.Jura-N.Kintyre line, shot during Phase 2 (Fig. 2.46). They all represent clear arrivals and so do the explosive data from both phases and the Geoflex data from Phase 1. Despite that, the arrival times of the shots 1, 2 and 3 appear to be earlier (by about 0.08 sec) than the airgun data when recorded at Jura, and later (by a slightly smaller amount) when recorded at Kintyre. This kind of pattern implies either a position fixing error or an error during the calculation of the shot-receiver ranges. The error appears to be common either to the large explosive shots of both phases or to the airgun and Geoflex data which again were acquired at different phases. Despite all efforts no such an error could be found in the shot-receiver range calculation and the remaining posibility is a shot position fixing error of about 400 m.

After that, in order to minimize the impact of the velocity model of this line on the rest of the WISE model during their integration (Chapters 3,4), it is decided to model the line along the airguns arrival pattern but shifted midway between its actual position and the corresponding explosive shots arrivals. Such a compromise will mainly influence the thickness of the near-surface low velocity layer by a few hundred metres and its effect will be negligible in the central part of the line (5-20 km).

Another discrepancy is due to the arrival times of G1 (Geoflex 1) shot and the 5W1 shot, the 5W1 time being compatible with the time recorded at M.Jura (Fig. 2.46). They will both be ignored during the modelling of this line as they bear no significant effect in the models.

The small differences between Geoflex and airgun arrival times will be discussed in the next section.

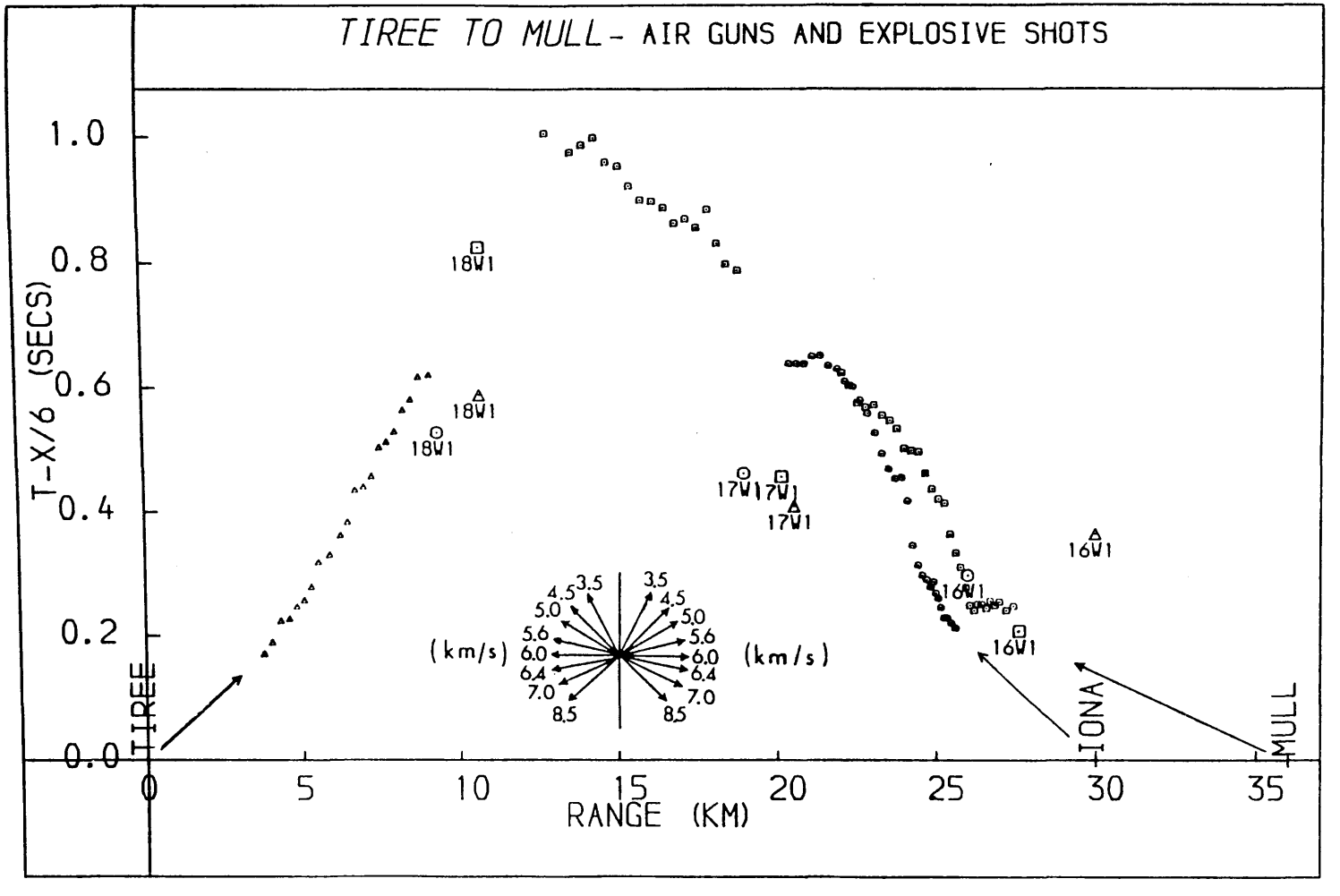

Fig. 2.43: Reduced T-X graph of the airgun and explosive data recorded on the Tiree, Iona and Mull stations. The same marks (of different sizes) have been used for shots recorded at a particular station.

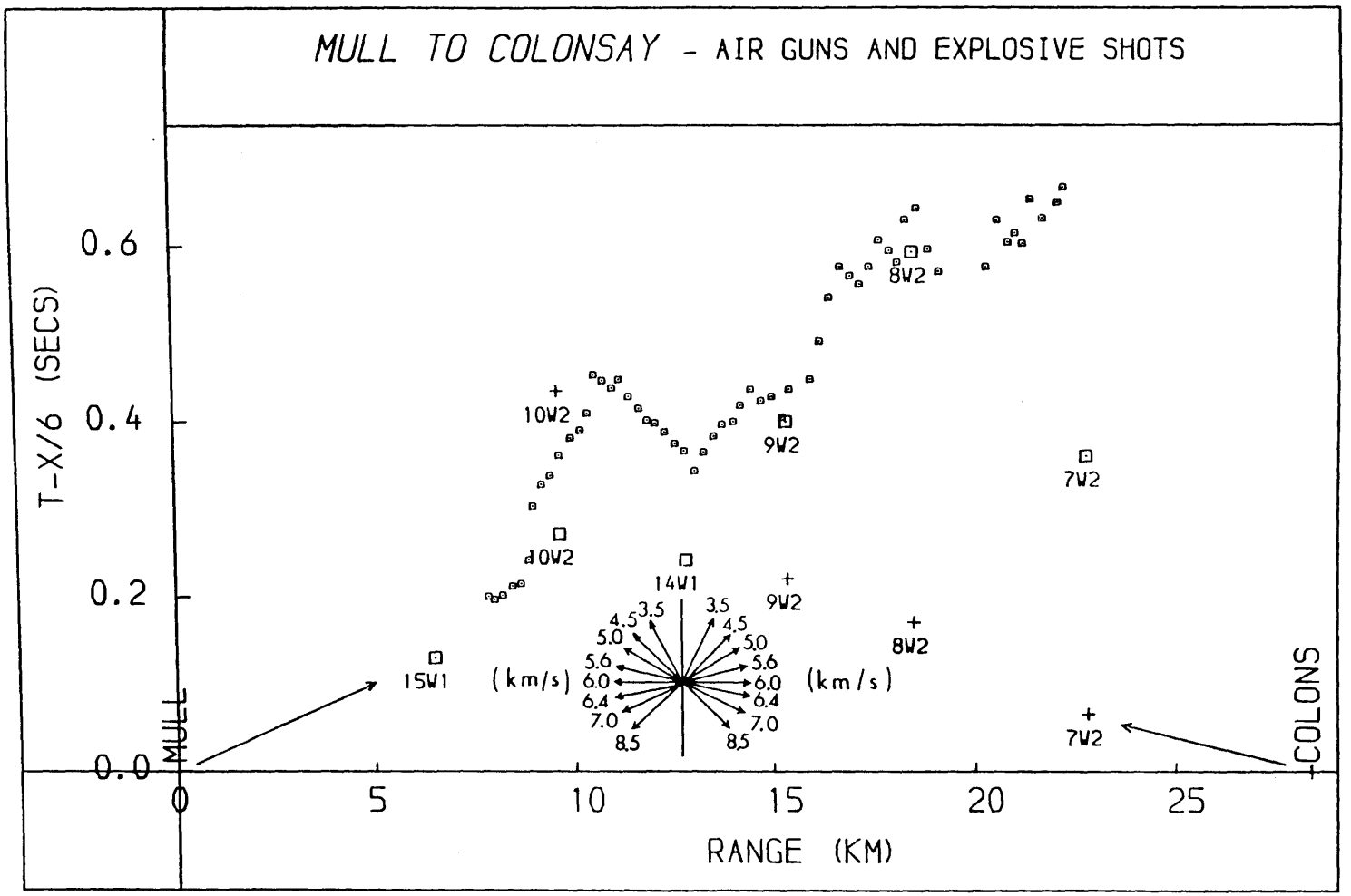

Fig. 2.44: Reduced T-X graph of the airgun and explosive data recorded at the Mull and Colonsay stations. The same marks (of different sizes) have been used for shots recorded at a particular station.

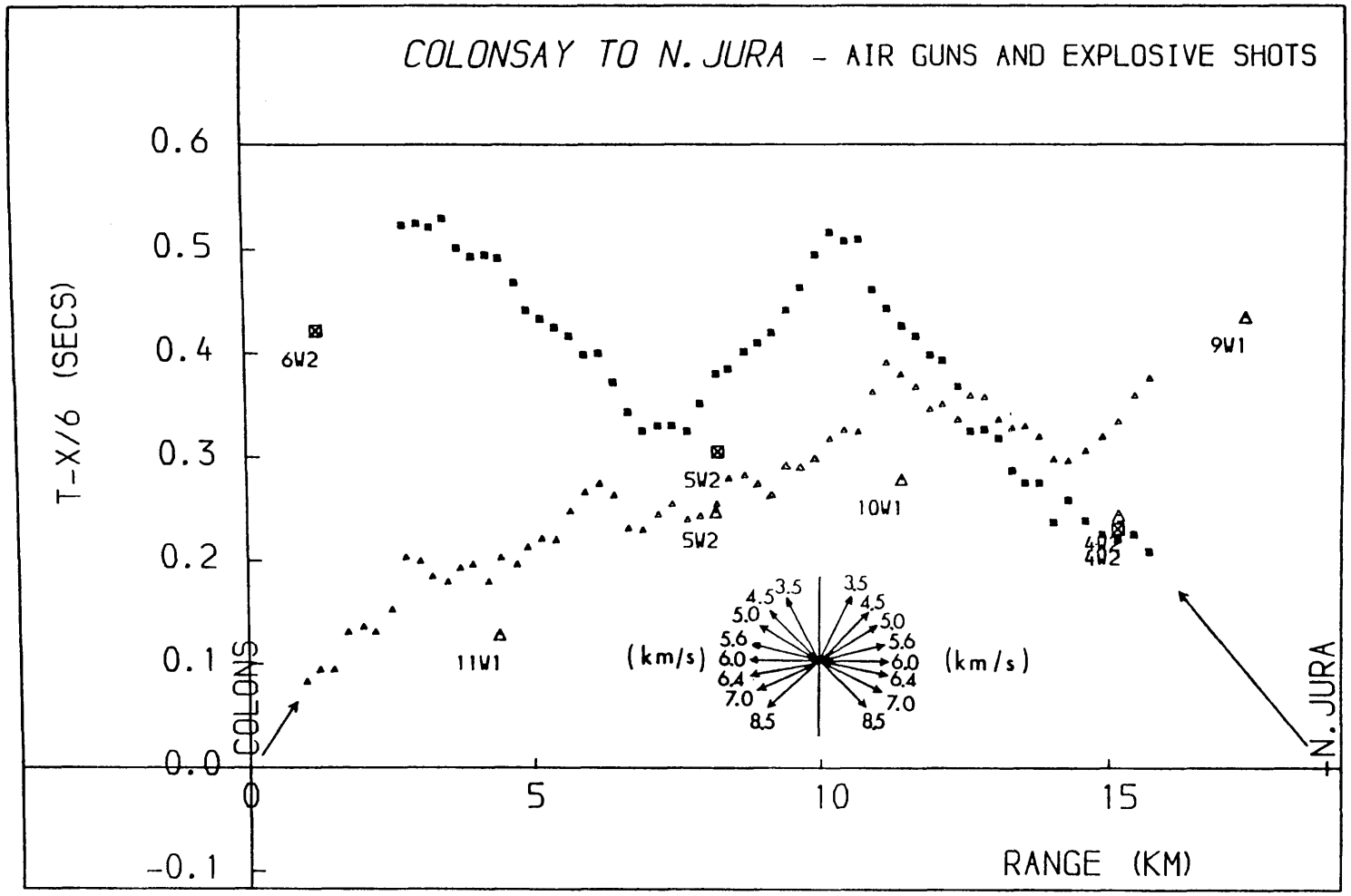

Fig. 2.45: Reduced T-X graph of the airgun and explosive data recorded at the Colonsay and North Jura stations. The same marks (of different sizes) have been used for shots recorded at a particular station.

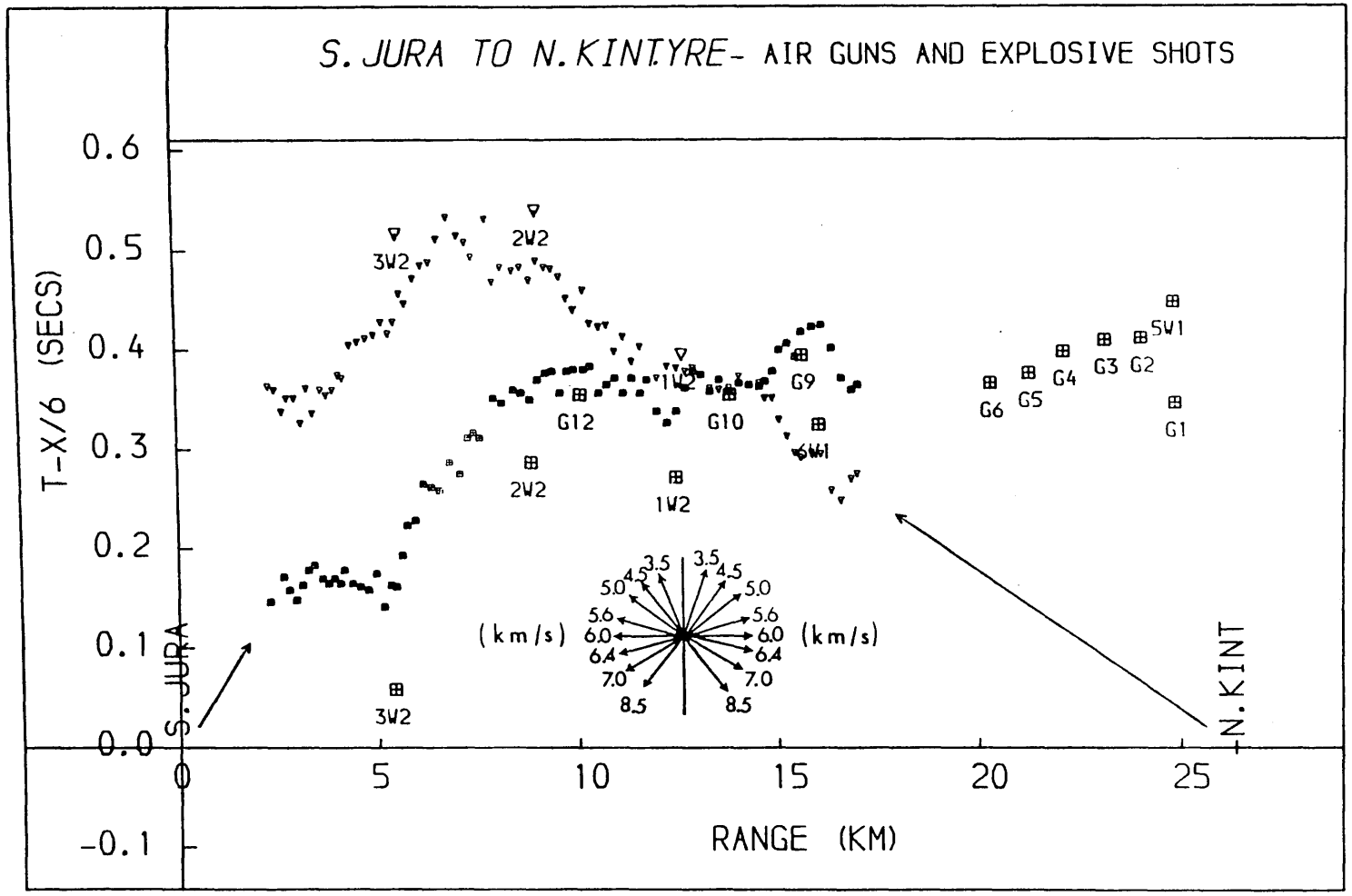

Fig. 2.46: Reduced T-X graph of the airgun and explosive data recorded at the South Jura and North Kintyre stations. The same marks have been used for shots recorded at a particular station. The shots denoted by G are the Geoflex shots.

2.5.3. Probable causes of the misfits between the airgun and the explosive data

The differences between the airgun data and the explosive data discussed in the previous section can, at least partly, be explained by a number of factors. The most obvious one are errors in the explosive data due to picking, positioning and timing of the shots (Appendix 1).

But the systematic nature of the differences (apart from the Jura-Kintyre line, see previous section), suggests an underlying cause common to all airgun data. This could be incorrect timing of the shots, but the Jura-Kintyre line (Fig. 2.46) shows good agreement between the airgun and Geoflex shots thus rendering the above possibility remote, for that particular line. In spite of that, the systematic delay of 0.02 sec, which the airgun data show in comparison to the Geoflex data, provides the first indication that it might be caused by different shot characteristics. Indeed, the shock-pulse rise-time for a 1000 cu.in. Bolt PAR airgun operating at 2000 psi is about 0.01 sec, with the pulse width being about 0.03 sec at its far-field signature (Bolt PAR airgun manual). In contrast, the pulse rise-time for a dynamite explosion is a few hundreds of microseconds thus resulting in much greater high frequency content and a much narrower pulse width at similar distances of the far field signature (Kramer et al 1968). That, in conjuction with a 5-7 times greater energy output of the larger Geoflex shots (Appendix 1, Table A.4; a 1000 cu.in. airgun is equivalent in

energy output to 0.7 lb of 60% dynamite /Rayleigh-Willis curves, Kramer et al 1968, Sheriff and Geldart 1982) and despite high frequency absorption, can create a steeper onset signal which will cause earlier picks. The local geology, with the metamorphosed Dalradian rocks (low attenuation of high frequencies / Dobrin 1976) and the probable absence of Mesozoic or earlier rocks, should have contributed to that result. The difference will be doubled if the timing of the shots coincides with the onset of sufficient firing current to the airgun valve, the delay being typically about 0.015 sec. Moreover, low firing voltage can cause firing delays of up to 0.03 sec (BOLT Tech. Corp., pers. comm.).

The above described effect should be more prominent for the big explosive shots in the area which deliver 60-130 times more energy than that of the airguns.

Other effects were also considered, such as the interaction between primary and reflected pulse from the sea surface, and the influence of the secondary pulse. The first one might have exerted some influence, especially during automatic picking, by magnifying the amplitude of the negative part of the pulse and thus affecting the maximum cross-correlation position (see below). The second one is unlikely to have played any role at all, as the secondary pulse has about 3 times smaller amplitude than the primary one and occurs, for a 1000 cu.in. airgun, about 0.15 sec later (Bolt airguns manual, Rayleigh-Willis curves).

Moreover, the increase of the airgun-explosive shots difference with increasing distance from a particular recorder (Fig. 2.43 to 2.46), can be explained by a partial failure of

the cross-correlation process under conditions of high noise (sect. 2.4.2) with the maximum values of the correlation coefficient resulting at mid-onset positions (Summers 1982, Chap. 3). A similar effect takes place, in the presence of high noise, during manual picking when the selected picks come later than the ones selected from high signal / noise ratio.

From the above, it can be seen that a correction of -0.02 sec for the airgun data is well justified and necessary. Similar differences have also been observed in other refraction experiments (G. Westbrook, pers. communication). A further shift of -0.02 sec due to noise effects etc. (not applicable to Jura-Kintyre line) will make up for most of the observed average difference.

2.6. COMPUTER PROGRAMS USED FOR THE PRESENTATION OF THE DATA

All the reduced T-X graphs for both the explosive and the airgun data were plotted using programs TXWISE and TXAIRGUN (Appendix 2). The programs were developed specifically for the presentation needs of this project and using GHOST routines can allow for a number of plotting options (reduced / unreduced T-X graphs, error plotting, superposition of different data sets, etc.) all of which are well explained within the program listings.

CHAPTER 3

INTERPRETATION TECHNIQUES AND PROCEDURE

3.1. INTRODUCTION

This chapter examines the interpretation techniques used, their limitations and general procedure followed. In order to appreciate the usefulness of the main technique used in the current interpretation, the ray-tracing method, a critical review of the previous techniques employed by Summers (1982, Chapter 6) and results produced will firstly be offered.

3.2. PREVIOUS INTERPRETATION TECHNIQUES AND RESULTS

The previous techniques used for the interpretation of the explosive data were the time-term and the plus-minus methods.

The time-term method (Scheidegger and Willmore 1957, Willmore and Bancroft 1960, Berry and West 1966, O'Brien 1968, Bamford 1973), is based on the concept of delay times, first introduced by Gardner (1939) and like other methods based on the same concept (e.g. Wyrobek 1956, Gardner 1967, Barry 1967), it involves the separation of a wave travel-time into three components. The first component is the hypothetical time for the wave to travel the offset distance along a refractor, and the other two (shot and station delay times) are the hypothetical times which are required to be added to the first component due to the depths of the refractor below the shot point and the geophone respectively (e.g. Berry and West 1966, Bamford 1973). The separation problem in the time-term method is solved

statistically in a way that would best fit the observed travel times since their number is usually much greater than the number of the time-terms. The time-terms are usually assumed to be characteristic of the particular shot or geophone. The least squares criterion is applied to minimize (with respect to each time-term) the sum of the squares of the residuals between the observed and the calculated travel times, and the final calculation of the time-terms and refractor velocity involves the inversion of a set of simultaneous linear algebraic equations in matrix form usually achieved by a computer (Berry and West 1966).

The main advantage of the method is its effectiveness in handling large amounts of data derived from shots and recorders with an areal spread (i.e. not on the line).

But the method fails (Berry and West 1966, O'Brien 1968, Bamford 1973), if the assumptions behind the delay time concept are violated. The assumptions commonly violated are:

1) the velocity of the overburden varies only with depth within the critically refracted ray cone under the shot or station,
2) the refractor velocity is constant, and
3) the slope and curvature of the refractor are small, (slope $< 10^{o}$).

Along the WISE profile, the existing evidence and the pattern of the apparent velocities (from explosive and airgun data, see Chapter 2) suggest that all the above assumptions are violated. The overburden velocity to the refractor varies laterally (Mesozoic to Torridonian transition, intra-Dalradian velocity

contrasts); the refractor velocity is not constant and probably varies both laterally (low velocity Great Glen fault zone) and with depth due to compaction effects and variable degree of metamorphism (Hall 1978a, Hall and Simmons 1979, Hall and Al-Haddad 1979). Finally, the slope of the refractor might occasionally be considerably greater than 10° (Inner Hebrides basin, Lewisian-Dalradian interface).

The above points will be clarified in Chapters 4 and 5, but it was felt by Summers that it was due to those limitations together with the lack of control on the shallow velocity variations and the absence of more data from important stations, like those of Tiree and Kintyre, that the calculated travel times deviated considerably from the observed ones during a final check with a ray-tracing program (Summers 1982, Chap. 6 and 7). The final model included the results of an effort to determine lateral velocity variations in the basement by using the plus-minus method (Hagedoorn 1959). Though some broad variations were established by that method, it was obvious that the model had oversimplified both the geophysical and geological aspects of the interpretation (Summers 1982, Chap. 7).

It is finally thought, that the least-squares criterion (or L2 norm) used in the time term method is probably inappropriate for data containing a number of suspected erratic picks (Chap. 2), as the large weight of the squares of those picks during the minimization process in conjuction with the data gaps from key stations, will probably unbalance the final solution considerably.

A more appropriate norm would have been the L1 norm ie. the minimization of the sums of the absolute values of the residuals ("robust" modelling e.g. Claerbout and Muir 1973, Menke 1984), which will be effectively used during the present modelling.

3.3. CURRENT INTERPRETATION TECHNIQUE

3.3.1 Method and Program - Introduction

A ray-tracing program based on the method of Cerveny et al (1974) was used for the inversion of the WISE data.

Briefly, the method involves the computation of the ray diagram and the geometric spreading of seismic body waves in laterally inhomogeneous 2-D media with curved interfaces. The rays and the geometric spreading are described by a system of ordinary differential equations which can be integrated numerically through the interfaces, by successively calculating the initial conditions necessary for determining the discontinuous changes in the refracted and/or reflected rays after their encounter with an interface.

Two versions of a program employing the above method were used. The first one (RAY), was used only for preliminary interpretation before the acquisition of the second program. Modelling with it proved to be very cumbersome and time consuming mainly because the program was not designed for work on complicated models like those of WISE, and a bundle of rays emerging at points around the receiver, had to be generated for the travel time to be successfully interpolated (initial value ray-tracing). Continuous velocity variation within each layer

was achieved by linear interpolation of velocity values specified at the corners of a rectangular grid system.

The second program (SEIS81) employed the same algorithm and integration routines, but general re-structuring and a number of new routines greatly improved its flexibility. The model can be laterally inhomogeneous with curved interfaces, block structures, isolated bodies and vanishing interfaces. The source can be situated anywhere in the medium and the receivers can be irregularly distributed along the surface. A time-saving improvement was the iterative generation of rays with their emergence points getting progressively closer to the receiver position (two-point or source-to-receiver ray-tracing). Special care is also given to the calculation of rays in certain singular regions of the wave field, such as the critical region and the boundaries of shadow zones.

Since the program SEIS81 was mainly used for modelling, that program will be implied in any relevant reference.

3.3.2 Velocity interpolation

The velocity function for a particular layer was originally interpolated by fitting bicubic splines at the nodes of the rectangular velocity grid corresponding to that layer (routine VELOC), but it was soon realised that the interpolation method, though generally ideal for producing a smooth velocity function for quick ray-tracing, was responsible for the widely different results (calculated arrival times) compared to those obtained by using linear interpolation (RAY program).

The main reason for that lies in the high velocity gradients, necessary for the modelling of features like the Great Glen fault zone and intra-Dalradian contrasts, which the splines inherently cannot cope with; instead they produce wild oscillations between the grid points so creating nonsensical velocity values (Fig. 3.1).

Since a large number of closely spaced grid points would have been needed to control the oscillations of the splines, thus rendering the modelling very cumbersome, a bi-linearly interpolating routine was fitted (VELOC1) and the SEIS81 program was modified to permit selective use of the two interpolating routines for a particular layer through routine VCHECK.

The only problem with the bi-linear interpolation (2-D Taylor expansion of first order), is that it creates second order interfaces across the grid lines if the velocity gradient is not constant (Fig. 3.2, 3.3). For that reason, rays just entering a rectangle can have the directions of their propagation considerably changed, thus creating secondary shadow regions.

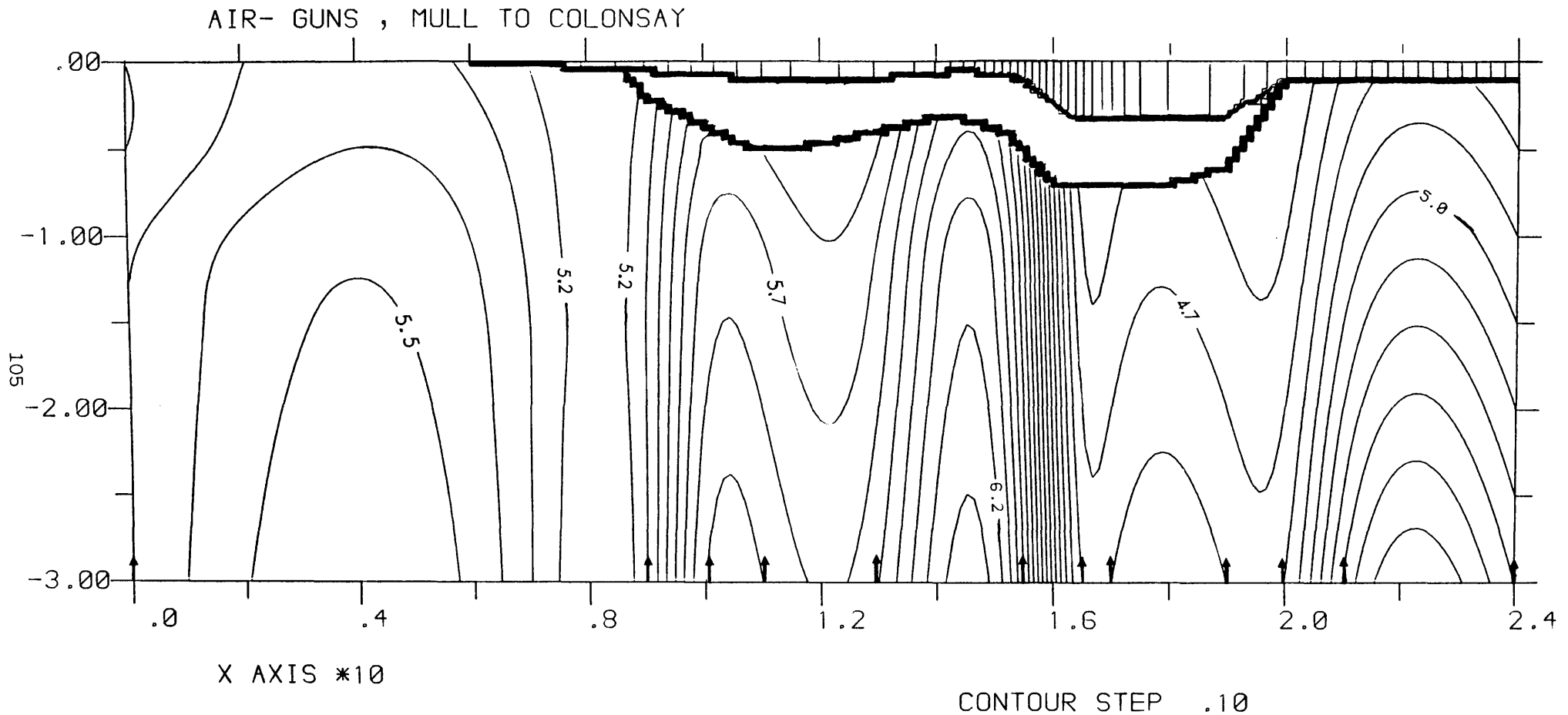

Fig. 3.1: Model illustrating the velocity interpolation using bicubic splines and the unpredictable behaviour of the splines when the model contains sudden high velocity gradients. The velocity interpolation matrix had dimensions of 200 X 100. To be compared with Fig. 3.2.

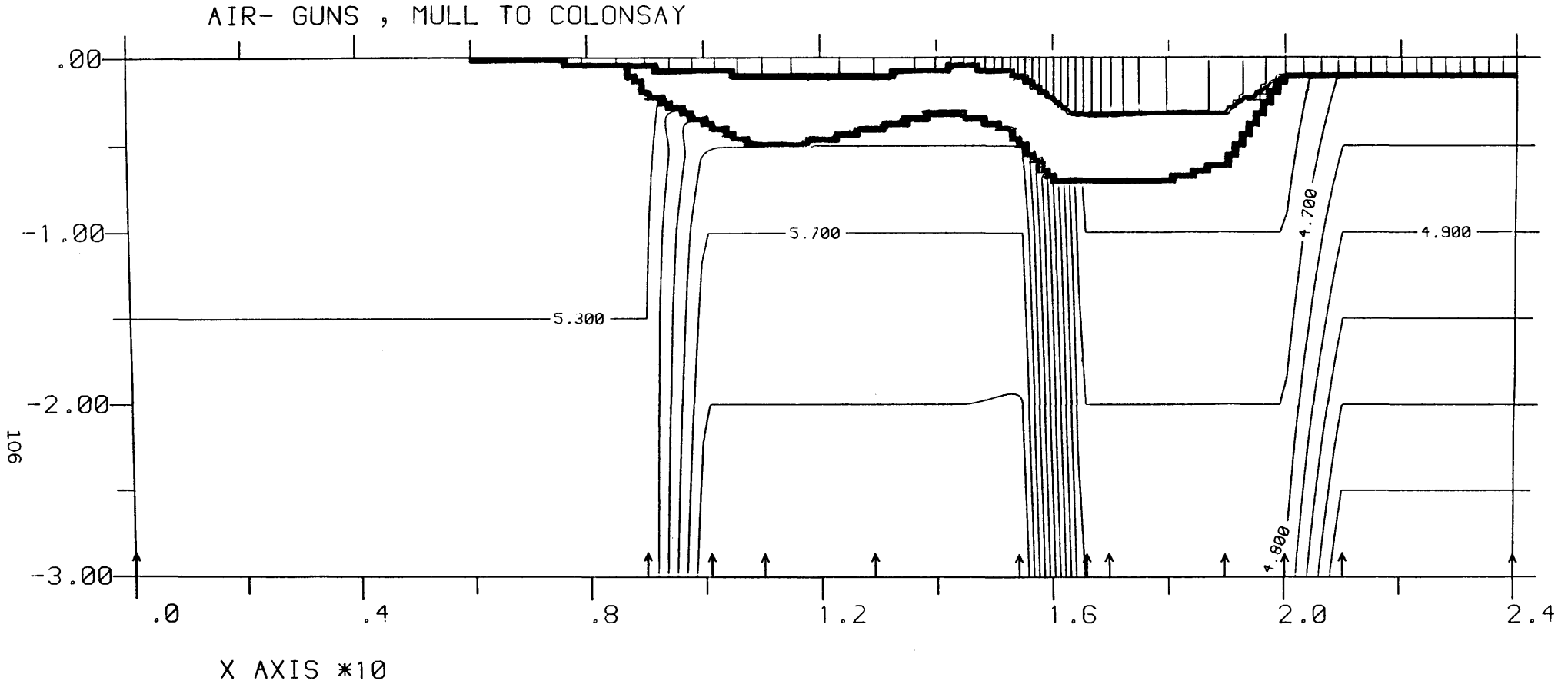

Fig. 3.2: Illustration of linear interpolation for the model of Figure 3.1. The velocity control lines are the same as in that model. The velocity interpolation matrix had dimensions 200 X 100.

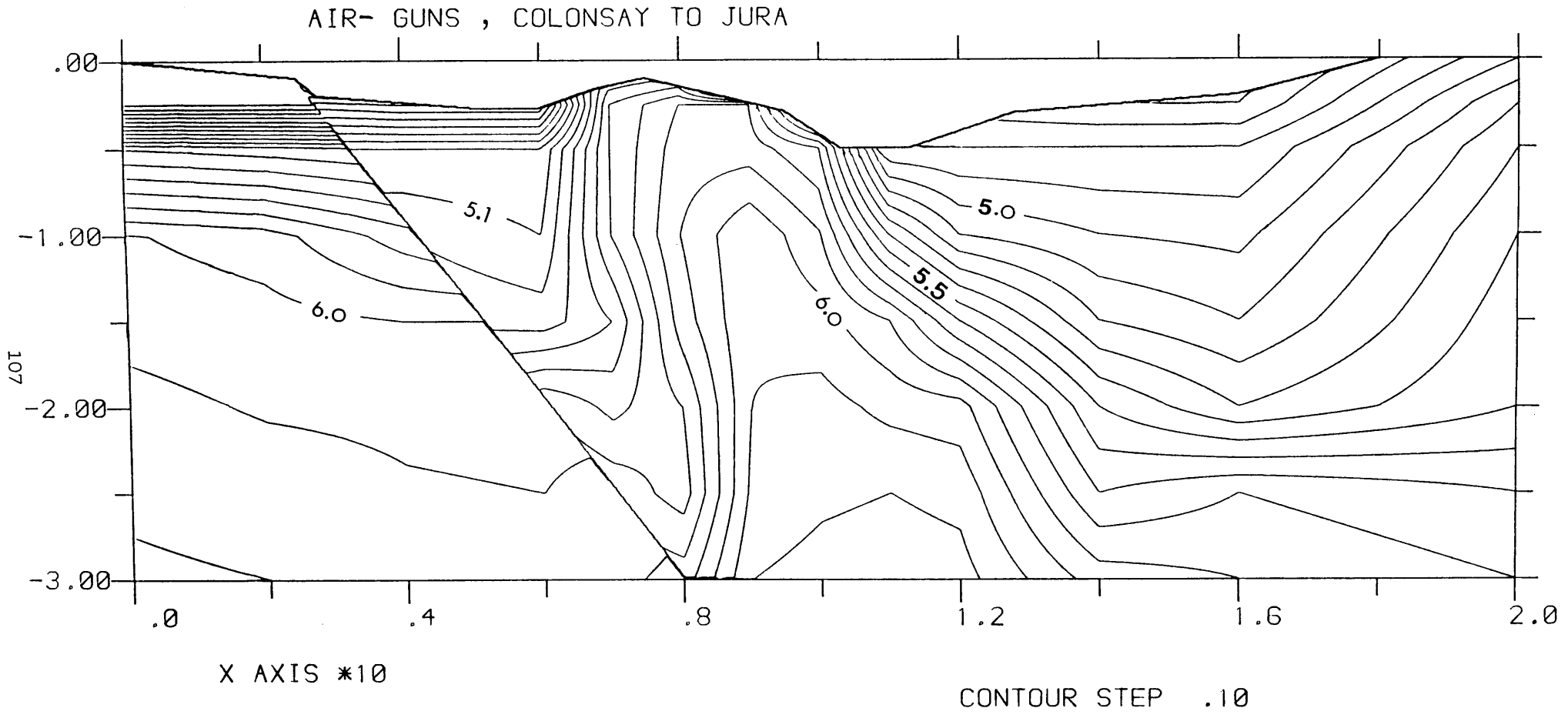

Fig. 3.3: Linearly interpolated velocity model illustrating the simulation of interfaces through the interpolation of a velocity matrix of dimensions 1000 x 500. The corners along contours ("second order" interfaces, section 3.3.2) usually define the initial velocity grid.

This effect can be greatly reduced by spreading the gradient over a wider area and/or by increasing the number of grid points (usually much less than the increase needed to control spline interpolation), but it still does not make the calculation of amplitudes particularly attractive (section 3.3.4).

An optional by-product of the velocity interpolation routines is the transformation of the P-wave velocity matrix to shear velocity or density matrices by using published or locally-known relationships.

3.3.3 Other aspects or extensions of the program package

A novel feature of the program was the use of subroutines for the manual, semi-automatic or automatic generation of numerical codes relating to complex refraction-reflection sequences. Thus, later arrivals can be modelled with ray-tracing and the contributions of different wavefields can be explicitly shown during synthetic seismogram production in order to appreciate their joint effects.

A serious drawback of the program was found to be its inability to define interfaces with more than one depth corresponding to the same range e.g. recumbent or salt-dome like interfaces, thus necessitating the use of continuous velocity change as the alternative available means of representation.

Amongst the useful extensions and changes to the program, was the use of the velocity interpolating routines (VELOC and VELOC1) and the modified subroutine MODEL in order to produce velocity matrices sufficiently large for the correct representa-

tion of the models. The close approximation of the interfaces, in relation to the model's physical size, primarily dictated the size of the velocity matrices (ie. the interpolation step) usually being 200-400 in range (X) and 100-200 in depth (Y). Finally, a subroutine containing GINOSURF routines was constructed for the contouring of the velocity sections (subroutine GRIDCONT), the interfaces being defined by the step-like accumulation of contours (Fig. 3.1 to 3.3).

Typical CPU contouring times (using an ICL 2980 computer) for the above velocity matrix dimensions, were in the range 150-500 sec, and high resolution interface imaging needed matrix dimensions of 1000 X 500 and about 1800 sec CPU time (Fig. 3.3).

The ray diagrams were produced by program RAYPLOT originally written by B. Doody and later corrected and enhanced by the author.

Program SEIS81 containing (amongst others) the above quoted subroutines MODEL, VELOC, VELOC1, GRIDCONT, VCHECK is listed in Appendix 2.

3.3.4 Overall evaluation of the method

The main advantage of the ray-tracing method against other interpretation techniques used in refraction seismology, is its ability to simulate "real earth" conditions, ie. complicated layered structures with both vertical and lateral velocity gradients within each layer. Moreover the method permits the use of geological or geophysical information, acquired through other geophysical methods, to constrain and reduce the range of the

final models.

The main assumptions behind the ray method are the isotropy of the model and the absence of phenomena like diffractions and edge waves. The later automatically imposes a smoothness requirement for the propagating medium according to which the dimensions of all inhomogeneities are considerably greater than the wavelength of the dominant frequency (eg. Cerveny 1985). That requirement, together with the inherent low accuracy of the ray method during the calculation of amplitudes in singular regions (caustic region, critical region, edges of shadow regions), and the sensitivity of the ray amplitudes to the small details of the velocity model (section 3.3.3), restrict the use of the ray method to that particular class of models.

Though new methods and programs have been developed in the last few years (for a review see Cerveny 1983), they are mainly concerned with more accurate evaluations of the wave-field for synthetic seismogram construction, by tackling the above cited weaknesses of the ray method.

3.4. INTERPRETATIONAL ASSUMPTIONS AND PROCEDURE

Apart from the general assumptions concerning ray-tracing stated above, the most obvious one is the validity of the 2-dimensional interpretation. That assumption is believed to be valid here, because of the nearly linear layout of shots and receivers and the approximately perpendicular direction of the profile in relation to the main known structures. The only part of the profile where 3-D effects become significant, is the Iona-Mull area where the increased offset of the Mull station from the rest of the profile is accompanied by a slight change in the direction of the profile for shots between Mull and Colonsay (Fig. 2.1, Chap. 2).

Generally, since not all stations lie exactly on the same line or the same line segments, for interpretational purposes, a straight line profile was "constructed" by preserving the shot-station distances for a particular station and adjusting the station-station distances in a way that would place the station and the recorded shots in the right position in respect to the known lithological boundaries in the area. This method still results in maximum residual offsets along the line of the order of 100 m, due to projection of a 3-D shot-station configuration to two dimensions, corresponding to time differences of about 0.02 sec, which were individually corrected during modelling.

In the same way, the Mull station was effectively offset towards Iona by variable distances of few km, depending on the particular shot or group of shots, which are believed to have

introduced small errors (0.01-0.02 sec) due to small lateral velocity contrasts in the Ross of Mull granite and variable near surface delays. The sketch map of Figure 3.4 ilustrates the above described situation.

Modelling started as usual (e.g. Miller and Gebrande 1976), by testing crude models derived by direct inversion techniques. Crude basement velocity-depth functions for a number of points along the WISE profile were derived by applying Wiechert inversion (Summers 1982, Chap.6). Calculation of the arrival times and iterative fit to the observed explosive shot times started from the foreland area (Sea of the Hebrides), and progressively propagated along the rest of the profile. Though an optimum interpretation procedure (as far as modelling time is concerned) should generally start at that part of the profile where the most of the constraints are available, that usually being the middle part, at the time modelling started it was felt that the foreland area offered a good starting point for the acquaintance of the author with the ray-tracing method and the local geology, the known geology being simpler than that of the rest of the line (Chap. 1).

As modelling propagated along the line it was realised, as it had been by Summers (Chap. 7), that knowledge of the shallow structure was indispensible for the interpretation of the basement structure, therefore the airgun data together with gravity and other geophysical and geological data were used in an effort to constrain the models.

Since the distances between stations and the nearest shots were of the order of 5-10 km and no information on the thickness

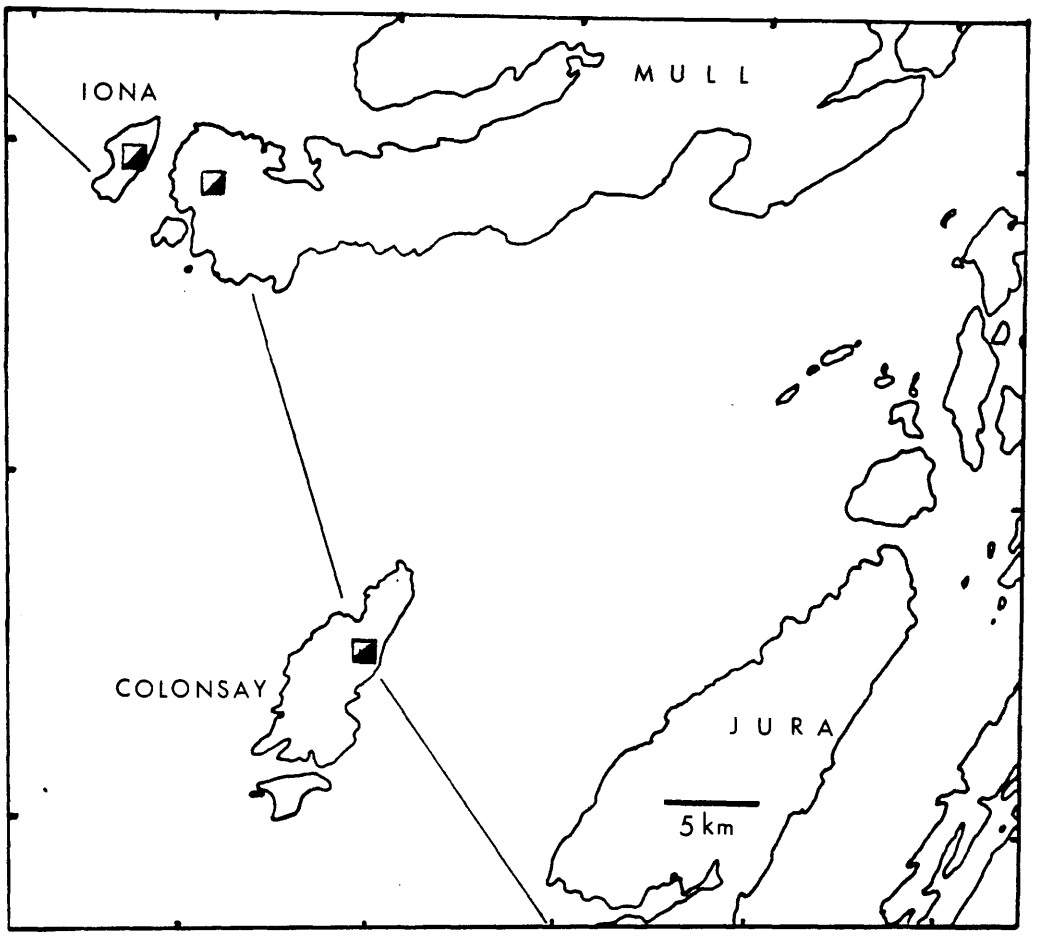

Fig. 3.4: Sketch map of the Mull-Colonsay area with the 3-D configuration of shots and stations. During modelling (in two dimensions) the Mull and Iona stations were effectively displaced along arcs of radii equal to the corresponding shot-station ranges, thus creating the "modelling line" of the profile where distances between successive stations are variable in order to preserve the actual positions of the shots (section 3.4).

of the bottom sediments or the upper basement structure could then be extracted from the data, all the available information was used on the velocity-depth distribution of the first few hundred metres under shots or stations. Sometimes reasonable assumptions had to be made.

No simple rules were found in order to reduce the number of model iterations. Naturally, the number of iterations increases with the complexity of the model and availability of data and it was usually found that small changes during an iteration, produce the quickest results.

3.5. MODEL ACCURACY CONSIDERATIONS

All the interpretation methods employed in refraction seismology, including ray-tracing, are bound by the limitations and ambiguities inherent to refraction shooting.

Apart from problems and uncertainties due to the quality of the data, already discussed in Chapter 2 for the WISE profile, the limitations of the method involve incorrect assumptions related to low-velocity layers, hidden layers and the problem of distinguishing between velocity layers and high velocity gradients (e.g. Northwood 1967). To some extent, these problems can be solved by modelling the amplitudes of particular phases during synthetic seismogram production, the models usually involving fairly high velocity contrasts amongst horizontal or sub-horizontal crustal layers and being derived from closely spaced (2-3 km) high quality recordings, recorded at both ends of the line (e.g. Muller and Fuchs 1976).

In the WISE profile, the layout of shots and stations

was designed for upper crustal investigation optimised for the central part of the profile (typically Iona to Kintyre), where the availability of data and other constraints was highest (Chapters 2 and 4). Due to that particular layout of shots and stations, with their corresponding ray paths -or Fresnel zones- forming a dense mesh, the modelling could be treated as a tomographic problem and the existence of regions within the basement, with higher or lower than average velocity, could then be investigated. The "accuracy" of particular geophysical models (or parts of models) could then be judged in a semi-empirical basis, by deciding whether the number of ray-nodes in a particular region, the velocity contrast obtained, the size of the region and the certainty of other constraints, outweigh the uncertainties in the data quality, sedimentary delays and velocity averaging effects during ray refraction propagation. If that does not happen for some regions within the velocity-depth section, then -strictly speaking- the problem becomes underdetermined in a statistical sense and assumptions have to be made in order to get a solution. Obviously, least-squares techniques cannot be used in underdetermined problems, and this applies to the WISE explosive data set towards the ends of the profile (Sea of the Hebrides, Arran basin).

Therefore, the failure of the time-term analysis done by Summers (1982, Chap. 6) should have been expected.

3.6 GRAVITY INTERPRETATION

When considerable density contrasts occurred amongst different rock units, gravity modelling was used in conjunction with the seismic models in order to further constrain the geophysical and geolocical interpretation.

Since the program used was appropriate for 2-dimensional interpretation, the gravity profiles had to be chosen as perpendicular as possible to the gravity contours in order to increase the validity of the interpretation, and thus slight offsets from the seismic line were allowed.

The program used (G2DPLOT) employs the method of Talwani et al (1959) for the calculation of the gravity effect of 2-dimensional bodies with specified density contrasts. A linear regional field can be subtracted from the observed gravity field and the shapes and density contrasts of the bodies can be changed interactively in order to get a better fit between the observed and calculated gravity field. Finally a plot of the last model can be produced on a VDU in order to inspect the goodness-of-fit and the whole procedure can start from the beginning within the same program running session.

The program was originally developed at Leeds University and was only slightly modified in order to increase the quality of its graphical output.

CHAPTER 4

GEOPHYSICAL AND GEOLOGICAL INTERPRETATION: SHALLOW STRUCTURE

4.1 INTRODUCTION

This chapter consists of the presentation and discussion of the geophysical models of the shallow structure (typically down to 2-3 km depth) constructed during the present work and their geological interpretation.

The models for the shallow structure are mainly derived by modelling the airgun data while the models for the deep structure (Chapter 5) were derived by using the explosive data.

It is emphasized that the separation to shallow and to deep structure is somewhat arbritrary and is only made in order to facilitate the presentation and discussion of the results.

A review of the existing knowledge on the physical properties of the rocks in the area will firstly be offered (section 4.2).

4.2 PHYSICAL PROPERTIES OF THE ROCKS

4.2.1 Introduction

Published figures for seismic velocities, densities and magnetizations of the main known rock units present in the area were used during modelling and interpretation.

Usually, the values for a specific property of a rock show considerable spread and a reasonable estimate for the adopted value had to be made, but occasionally, the proximity of the sampled areas to the WISE profile added more weight to the related values.

4.2.2 Seismic Velocities

a) Lewisian

The extensive differentiation and variability in the metamorphic grade of the Lewisian rocks of north-west Scotland and the Outer Hebrides (Chapter 1) have resulted in a wide range of velocities as measured using first-arrival data or laboratory (ultrasonic) techniques.

Velocities ranging for 5.75 to 6.15 km/sec have been measured from unreversed refraction profiles in the area west of Shetland (Browitt 1972), while first-arrival data from a commercial reflection line in the west of the Hebrides produced velocities ranging up to 6.2 km/sec (Blundell, 1981). In the same area, about 10 km west of Barra a reversed refraction line of a few km length produced velocity of 5.5 km/sec whereas other short profiles in an area between the Outer Hebrides and the continental slope produced velocities ranging from 5.5 to 6.35 km/sec which were considered characteristic of Lewisian rocks subjected to variable degree of weathering and metamorphic reworking (Scourian to Laxfordian; Jones 1978, 1981).

The (basement) velocity differences between the Laxfordian and the Scourian Lewisian rocks have been more conclusively established with the NASP (Smith and Bott 1975) and LUST (Hall 1978a) seismic refraction profiles. The Laxfordian rocks were attributed velocities of 6.0 to 6.1 km/sec and the Scourian rocks velocities of 6.4 to 6.5 km/sec (at depths of burial of about 1 km or more). Moreover, the velocity increase with

depth, for both Laxfordian and Scourian rocks, due to compaction effects and the closure of microcracks in the rocks were established from both the LUST profile and measurements of ultrasonic velocities in hand specimens under pressures up to 8 kbars (Hall and Simmons 1979).

Since the refraction velocities for near-surface Lewisian rocks of about 5.5 km/sec quoted earlier are in good agreement with the ultrasonic velocity measurements from Laxfordian samples (under low pressures), similar velocities will be considered possible for Laxfordian rocks.

b) Torridonian

Torridonian rocks overlying the Lewisian foreland west of Shetland have been investigated by unreversed refraction profiles and velocities of 4.6 to 4.8 km/sec have been calculated (Browitt 1972).

Similar velocities have been measured for the rocks underlying the Permo-Triassic succesions in the Sea of the Hebrides, which were interpreted by most authors as Torridonian. Velocities of 4.8 km/sec from IGS refraction lines (reversed) shot west of Skye have been reported by Smythe et al (1972), and a velocity of 5.0 km/sec by Armour (1977) for the part of the HMSP profile shot between the Isle of Lewis and the Scottish mainland.

c) Dalradian

Despite the importance of the Dalradian basin in the Caledonian orogeny (Chapter 1) little seismic work has been done in order to investigate its internal structure or define the

seismic properties of Dalradian rocks belonging to different groups.

A number of short refraction profiles (a few hundred metres in length) on the Dalradian schists of South Kintyre, produced velocities in the range 4.5 to 5.5 km/sec (Wilson 1978). The lower values characterized highly weathered or fractured rocks and they will not probably be representative of the velocities at deeper levels.

A site of Dalradian schists in west Arran (about 4 km east of Kintyre and WISE profile) was investigated by Hall (1969) employing hammer lines of a few tens of metres long. A velocity of 4.0 km/sec was calculated, but for Carboniferous rocks where comparison was possible, hammer derived velocities were about 1 km/sec lower than refraction velocities derived from small explosive shots over distances of few kilometres. Despite the possibility that the velocity-depth gradient might be higher for the Carboniferous rocks than for the metamorphosed Dalradian rocks it is quite probable that a difference in velocity of similar magnitude will also be valid for refraction velocities of Dalradian schists.

Finally, it is worth mentioning that interval velocities of about 5.1 km/sec (at a depth of 2 km) were established from the WINCH profile which crosses the southwestward extension of the Dalradian outcrops of Islay and Jura at a distance of 10 km SW of Islay (Hall et al 1984).

d) Permian to present

Velocities for Permo-Triassic and younger Mesozoic rocks usually lie in the range 2.5 - 3.5 km/sec.

Browitt (1972) calculated values of 2.7 - 3.6 km/sec from unreversed profiles west of Shetlands. Two IGS refraction lines shot west of Skye (Smythe et al 1972) produced velocities of 3.0 km/sec and 3.9 km/sec which were interpreted as Permian / Mesozoic. Similar velocities come from the interpretation of first-arrival data from the WINCH profile (Hall et al 1984) as it crosses the previously established Mesozoic basins to the south of Islay and Kintyre.

Tertiary sediments are characterised by velocities (interval or refraction) in the range of 2.0 - 2.5 km/sec and Quaternary by 1.5 - 2.0 km/sec (e.g. Smythe and Kenolty 1975, Hall et al 1984).

Tertiary basaltic lavas at the south of Skye show refraction velocities of 4.0 - 4.5 km/sec (Lunn 1984) and interval velocities of about 4.2 km/sec from within the Colonsay basin have been interpreted as Tertiary lavas (Hall et al 1984).

4.2.3 Densities and magnetizations

a) Lewisian

The Lewisian rocks comprise the most dense structural units in the area.

The most widespread Lewisian type of rock along the WISE profile, the grey gneiss (amphibolite facies), shows a fairly uniform density of about 2.80 $Mg\,m^{-3}$. McQuillin and Watson (1973) have measured 2.77 $Mg\,m^{-3}$ from the Outer Hebrides, Durrance (1976) 2.79 $Mg\,m^{-3}$ from the Lewisian of Islay and Bott and Tuson (1973) measured 2.80 $Mg\,m^{-3}$ during a gravity survey of the Skye, Mull and Ardamurchan Tertiary igneous centres.

No densities have been measured from Tiree or Iona but petrologically the gneiss there is similar to that at Islay and Outer Hebrides (e.g. Westbrook 1972).

Rocks in the Outer Hebrides containing remnants of granulite facies mineral assemblages show densities of about 3.0 $Mg\,m^{-3}$ (McQuillin and Watson 1973). In contrast, Bott et al (1972) and Hall (1978a) have reported a density of 2.69 $Mg\,m^{-3}$ for the biotite gneisses and about 2.80 $Mg\,m^{-3}$ for the granulites near the Ben Stack line in Sutherland.

Magnetization contrasts are quite high amongst Lewisian rocks around the Sea of the Hebrides giving rise to large variations in the magnetic field (e.g. Aeromagnetic Map of Great Britain, IGS, 1968). Contrasts of 5 - 10 times between granulites and amphibolites are quite common (Powell 1970, 1978).

b) Torridonian

From an area to the east of Skye, Nettleton regression densities averaging 2.72 $Mg\,m^{-3}$ have been reported by Hipkin and Hussain (1983).

Similar densities have been found for the Torridonian of Islay (Durrance 1976). Sandstones produced mean densities of 2.70 $Mg\,m^{-3}$ and phyllites of 2.72 $Mg\,m^{-3}$.

The Torridonian rocks are generally very weakly magnetized (Powell 1970).

c) Dalradian

Dalradian rocks exhibit a wide range of densities depending on their lithology and the sampled area.

Densities of 2.82 $Mg\,m^{-3}$ for Dalradian slates and 2.73 $Mg\,m^{-3}$ for grits and phyllites in Cowall have been reported by Qureshi (1970), while Tuson (1959) measured lower densities for phyllites (2.70 $Mg\,m^{-3}$) and schistose grits (2.66 $Mg\,m^{-3}$) in North Arran.

Durrance (1976), from his gravity survey of Islay, has reported densities of 2.61 $Mg\,m^{-3}$ for limestones, 2.66 $Mg\,m^{-3}$ for the quartzites and 2.72 $Mg\,m^{-3}$ for the phyllites while 150 samples from the schists of South Kintyre produced a mean density of 2.65 $Mg\,m^{-3}$ (Wilson 1978).

In contrast, Nettleton regression densities from Kintyre averaged 2.78 gr/cc (Hipkin and Hussain 1983) a value which is significantly greater than the sample densities quoted so far for Dalradian schists, and also greater than the densities of

2.70 $Mg\,m^{-3}$ (Bullerwell 1961) and 2.74 $Mg\,m^{-3}$ (Cook and Murphy 1952) reported for the Dalradian of Northern Ireland.

The Dalradian rocks are usually weakly magnetized (Powell 1970) apart from the Tayvallich volcanics (e.g. Westbrook and Borradaile 1978).

d) Permo-Triassic and younger Mesozoic

Densities of 2.33 $Mg\,m^{-3}$ for Permo-Triassic rocks have been measured in Ireland (Cook and Murphy 1952) and similar densities averaging 2.30 $Mg\,m^{-3}$ have been measured in southern Scotland (Bott and Mason Smith 1960) and Ayrshire (McLean and Wren 1978).

Also, Tuson (1959) determined a density of 2.30 $Mg\,m^{-3}$ for the Triassic rocks of east Arran and a density of 2.43 $Mg\,m^{-3}$ for the similar rocks of west Arran.

In contrast, deep-borehole density information from a great number of North Sea commercial wells produced average density for Triassic rocks of 2.53 $Mg\,m^{-3}$ and density of 2.40 $Mg\,m^{-3}$ for Jurassic and Cretaceous rocks (Zervos 1986) with high standard deviations of about 0.1 $Mg\,m^{-3}$ or more. The high standard deviations mainly reflect the effect of different depths of burial on the porosities (and hence the densities). Thus surface samples of sedimentary rocks are bound to provide underestimates of the average formation density. That is probably the reason why most workers choose slightly higher densities (2.35 - 2.45 $Mg\,m^{-3}$) for the Permo-Triassic and younger Mesozoic rocks.

4.3 BARRA TO MULL

4.3.1 Barra to Tiree

No airgun data were recorded at this part of the profile and the explosive shots 19 to 23, having an average spacing of more than 10 km, cannot provide any information on the velocity structure of the Sea of the Hebrides basin or the depth to the Lewisian basement. For that reason, a brief summary will be offered of the existing geophysical controls in the area which were used to constrain the model of all explosive shots from WISE.

The work of Binns et al (1973) in the Sea of the Hebrides has helped define the major geological structures (Fig. 4.1), mainly by collecting gravity data, shallow seismic, deep seismic data and core samples. Features of the Minch fault and the Camasunary - Skerryvore fault were clearly imaged and the areal distribution of Mesozoic, Torridonian and Lewisian rocks was adequately mapped.

The cross-sectional shape of the Mesozoic basin was also determined along certain reflection profiles, one of them being profile CC' (Fig. 4.1) which is situated very near to the WISE profile and clearly shows the Permian / Mesozoic strata reaching a maximum thickness of about 2.1 km (Fig. 4.3, assuming uniform P-velocity of 3.0 km/sec). The extensional origin of the Mesozoic basin, showing a fault-bounded half-graben shape, is further supported by the existence of two small extensional Mesozoic basins (of a few hundred metres depth) situated near to the margin of the Sea of the Hebrides basin and overlying

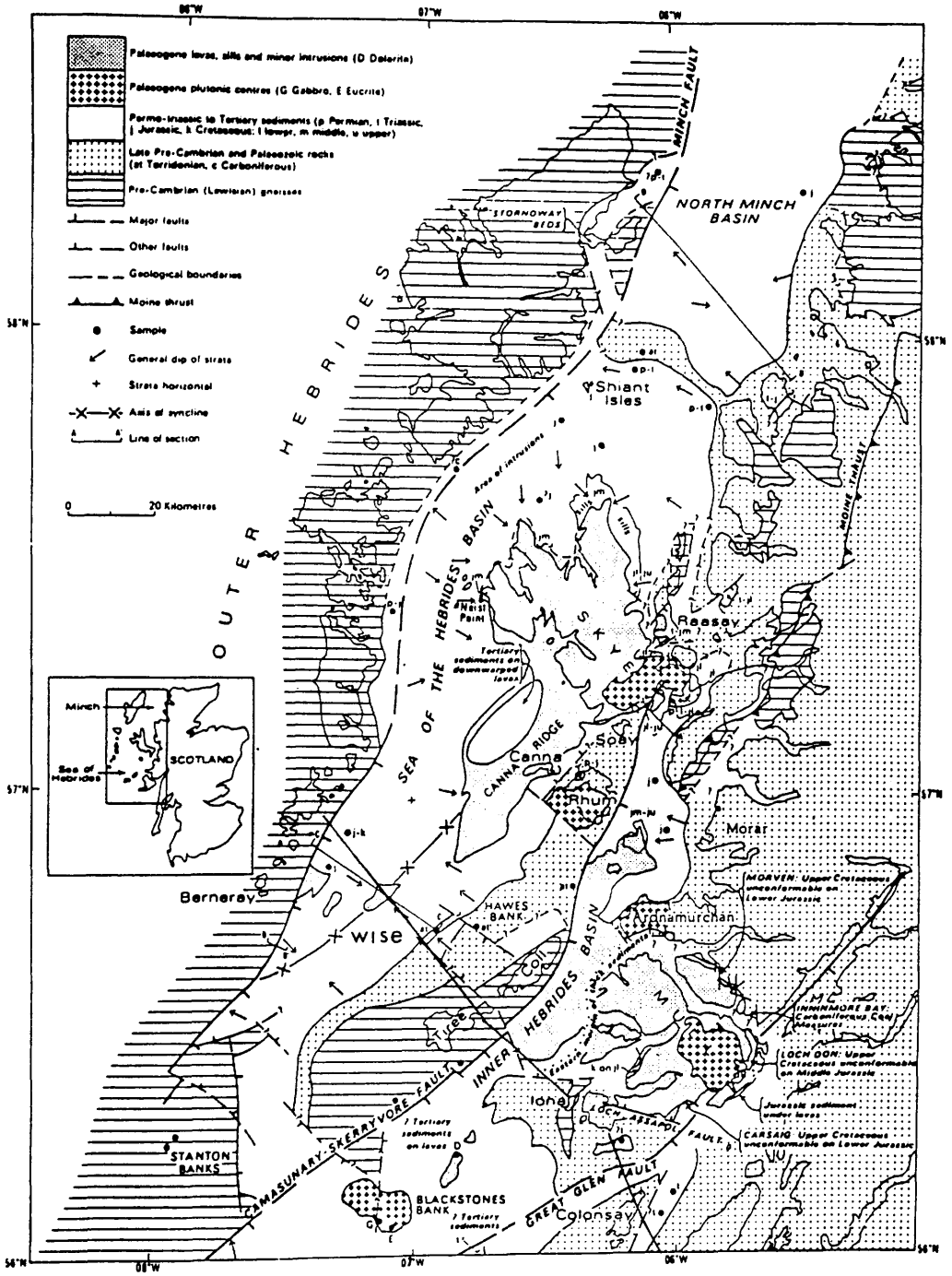

Fig. 4.1: General geology of the Hebridean region and position of the WISE profile (after Binns et al 1975).

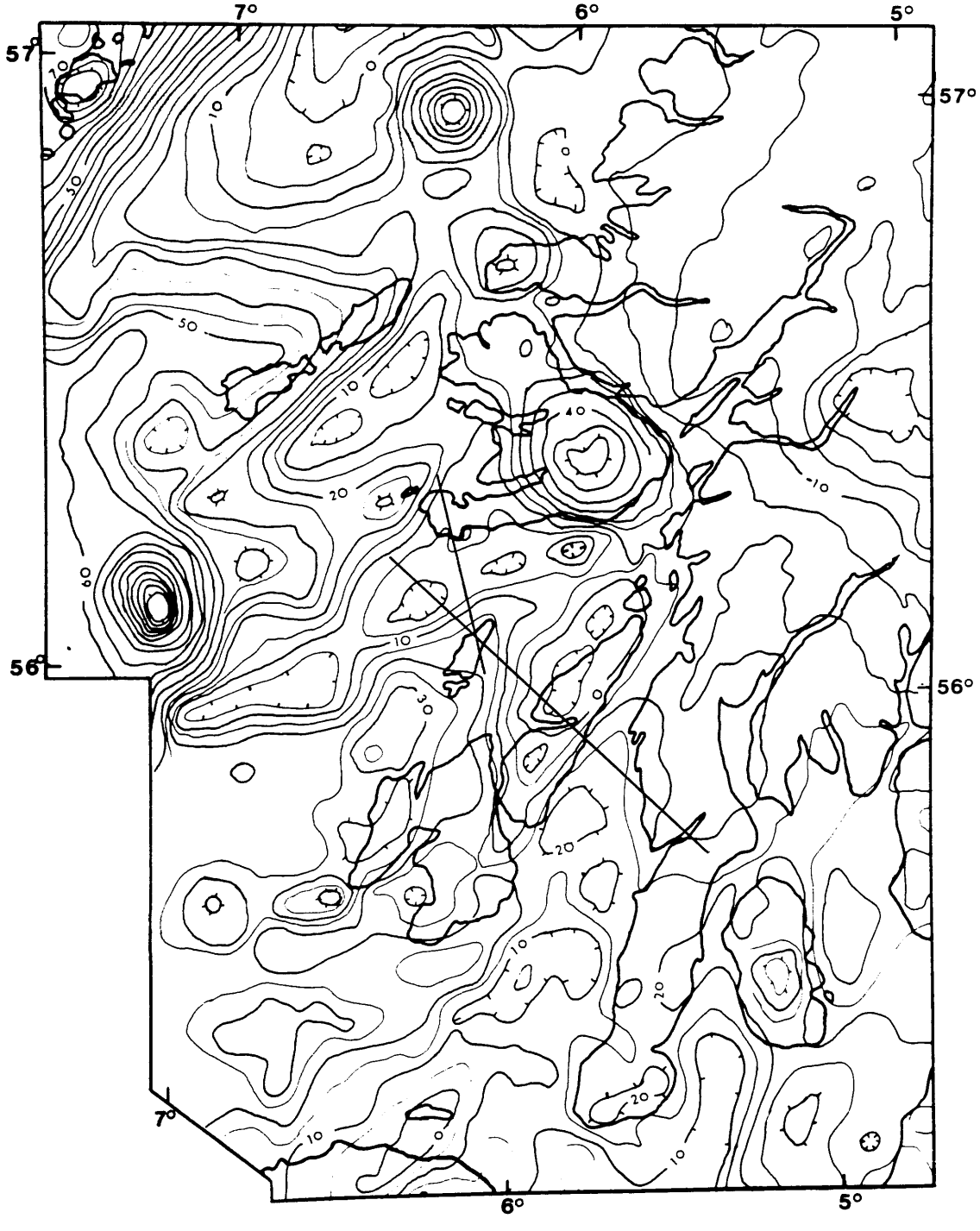

Fig. 4.2: Gravity field map for the WISE area and locations of the profiles used for interpretation (after Hipkin and Hussain 1982).

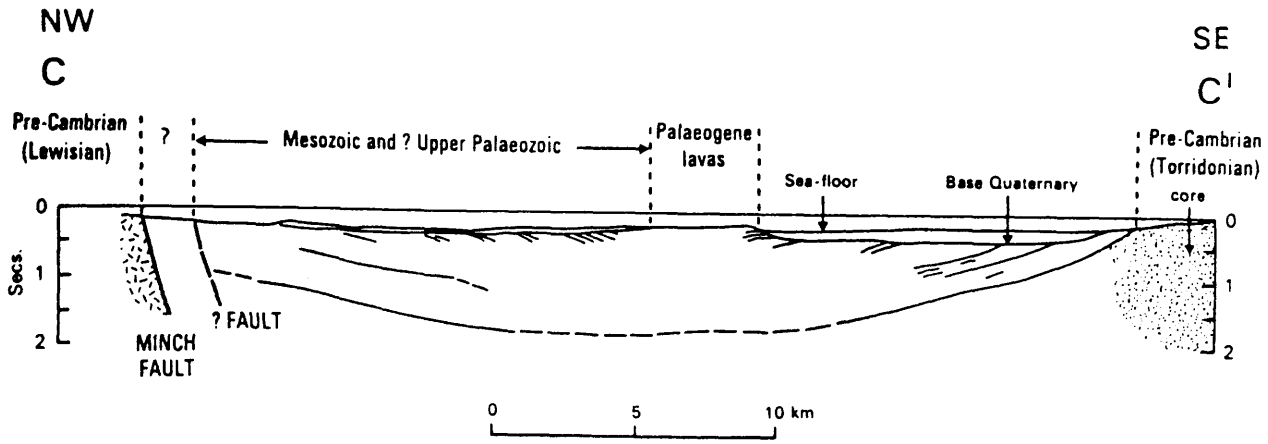

Fig. 4.3: Section C - C' across the Sea of the Hebrides Basin from deep and shallow seismic profiles. For location see Fig. 4.1 (after Binns et al 1975).

Torridonian and Lewisian rocks (Fig. 4.4, Uruski 1982).

Further deep seismic work in the area and the execution of a seismic reflection profile along the WISE profile (Hobbs 1985), tentatively concluded that the maximum thickness of the Mesozoic rocks was about 2.5 km (at the centre of the basin) and the maximum thickness of the Torridonian rocks (about 4 km) took place below the southern margin of the basin, as the Outer Isles Thrust was interpreted as being a reactivated fault surface between Torridonian and Scourian rocks (Fig. 4.5).

The gravity and magnetic fields usually correlate quite well (Fig. 4.2, 4.6), the major discrepancies being due to irregular high amplitude / short wavelength magnetic anomalies from the Tertiary lavas or the Tertiary igneous centres (Fig. 4.1).

The positive, high amplitude / long wavelength magnetic anomaly extending over a long strip to the east of Barra is probably due to an extensive tract of Scourian granulites

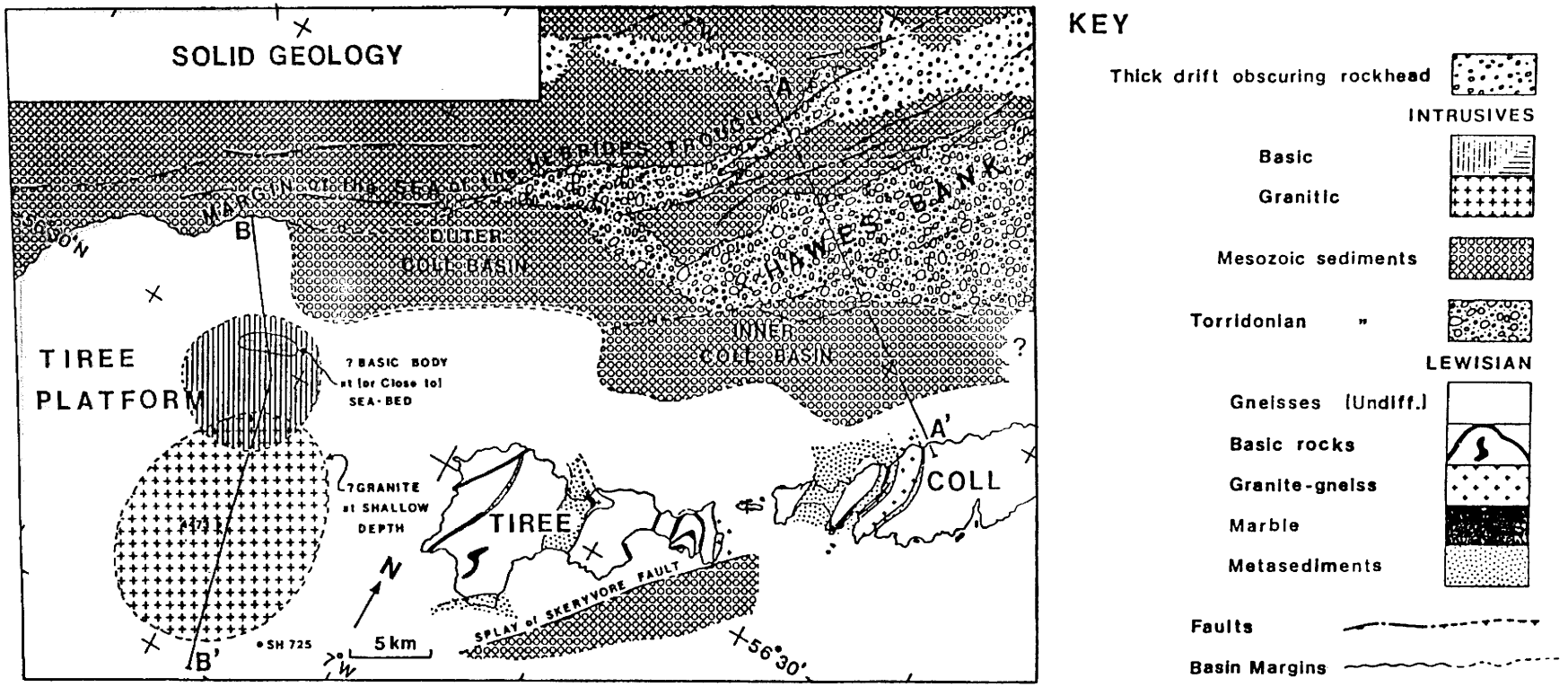

Fig. 4.4: Detailed geological map of the area around Tiree and Coll showing the exact position of the Inner and Outer Coll basins (after Uruski 1982).

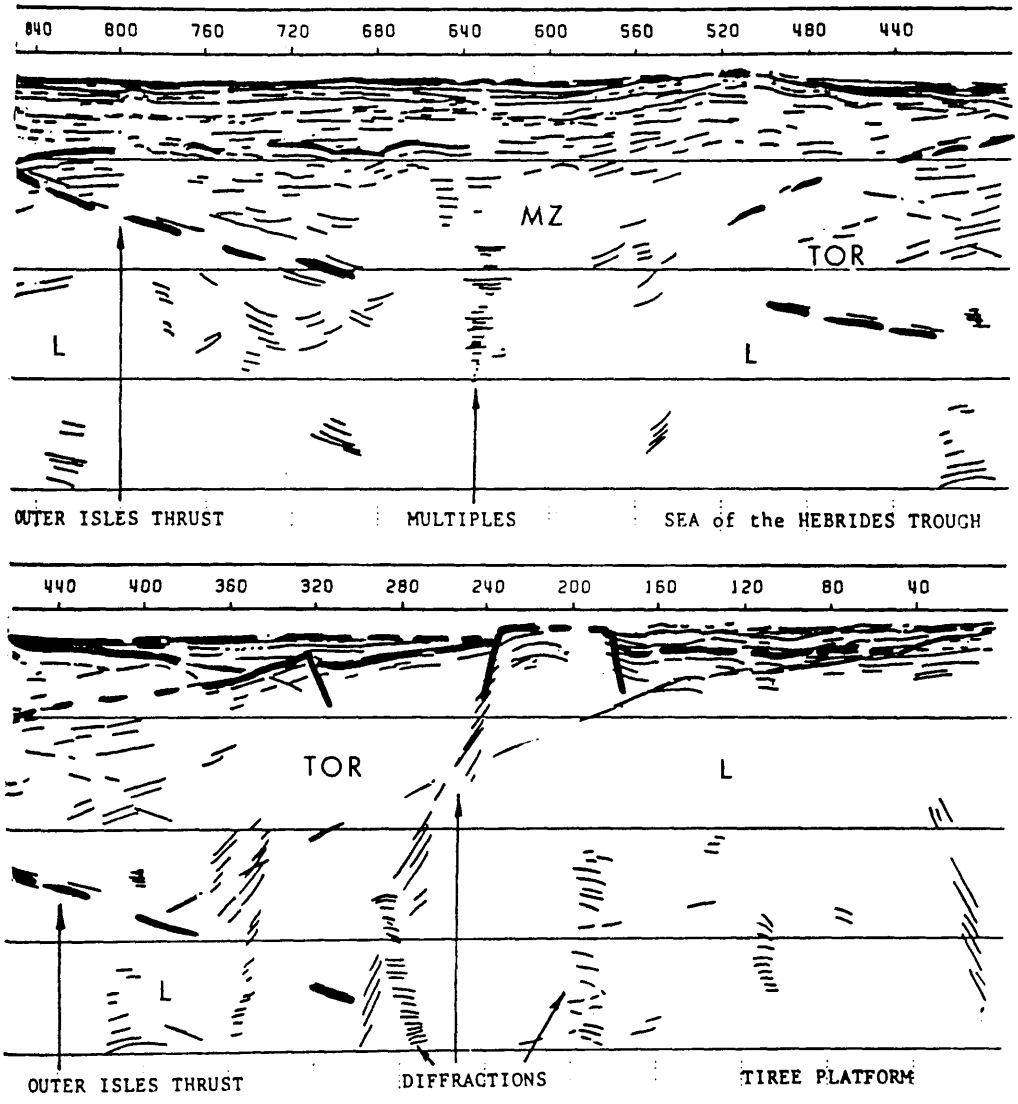

Fig. 4.5: Reflection profile along the WISE profile and interpretation (after Hobbs 1985).

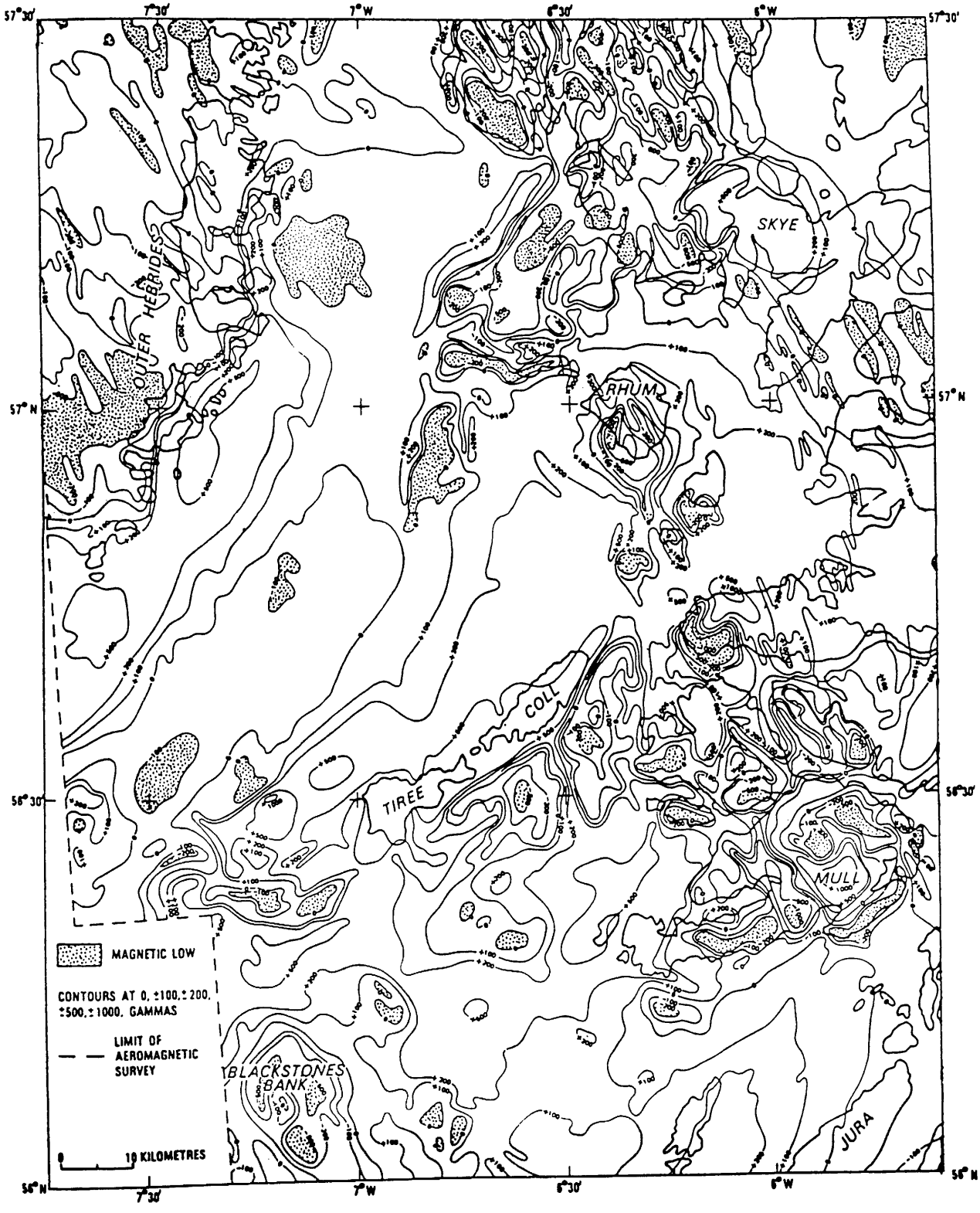

Fig. 4.6: Aeromagnetic map of the Hebridean region.

occuring at shallow depth and above the Outer Isles Thrust (Powell 1970), though granulites are also locally present to the west of the Thrust and their high pyroxene content gives rise to the high gravity values over northeastern Barra (McQuillin and Watson 1973). The Minch fault then probably marks the eastern limit of the shallow granulites (Powell 1970, Binns 1973).

The only positive information that comes from the explosive shots in the area concerns the average basement velocity under the basin. The travel times of shots 19 and 23 (recorded at Barra and Tiree respectively) imply an average velocity of 5.95 km/sec. Thus, Scourian granulites cannot form a major component of the Lewisian basement under the basin.

4.3.2 Tiree to Mull

The airgun data in this part of the profile will be used only tentatively due to their large discrepancies with the explosive shot data (section 2.5.2).

A preliminary inspection of the pattern of the apparent velocities of the data recorded at Tiree shows two segments with velocities about 4.3 and 3.75 km/sec (Fig. 4.7).

These apparent velocities can be simply interpreted in terms of the known geology. The updated solid geology map of the Sea of the Hebrides (British Geological Survey, 1984) provided by D. Evans, which combined the data used by Binns et al (1973) with recently acquired data by BGS and University of Aberystwyth workers, shows, in contrast with the map of Binns et al, the Camasunary-Skerryvore fault passing very near (2-3 km) to the south coast of Tiree (Fig. 4.8). Thus, as a first

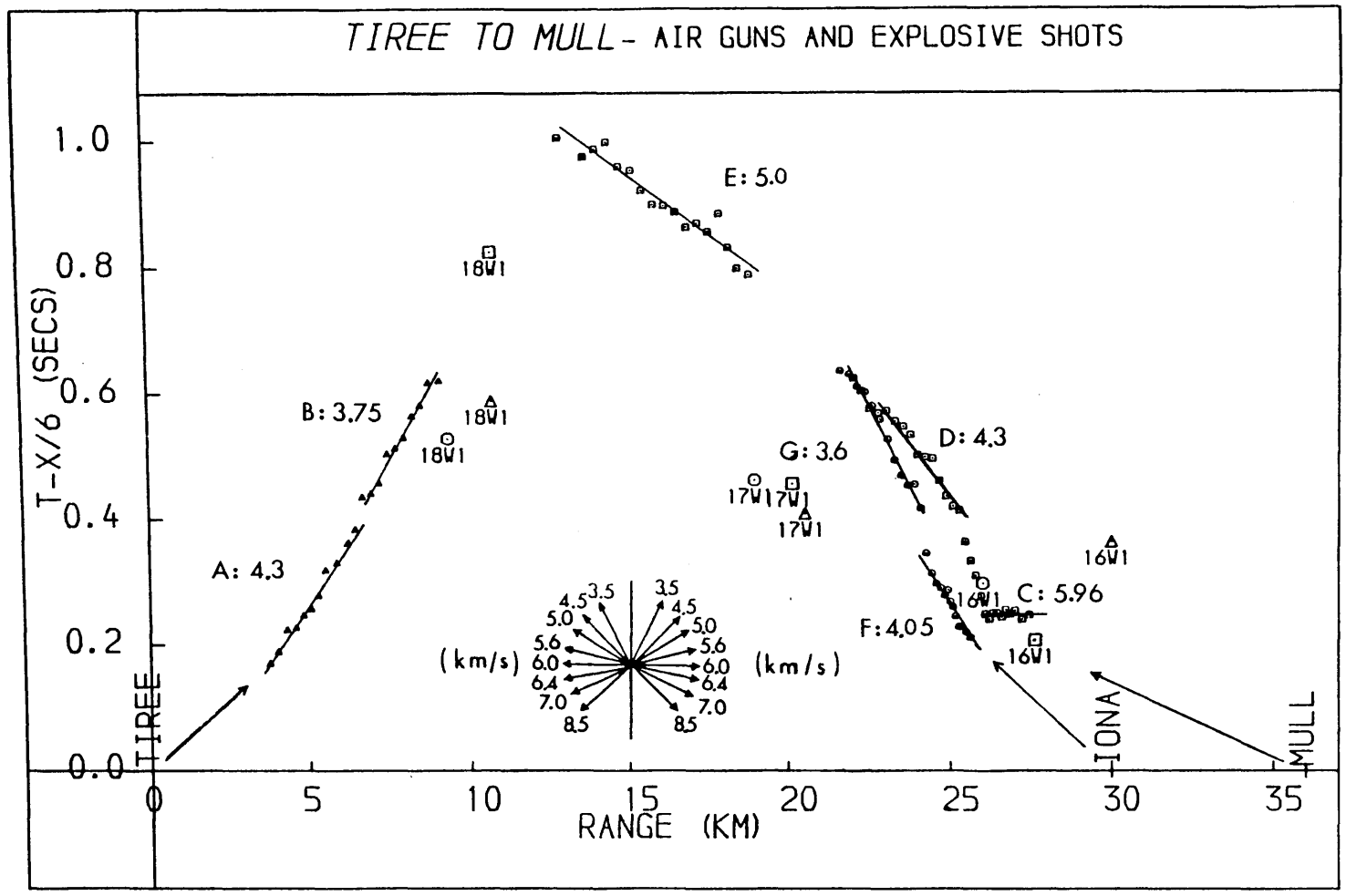

Fig. 4.7: Apparent velocities (in km/sec) for the airgun data of the Inner Hebrides basin. Shot groups D and G or C and F correspond to the same shots recorded at Mull and Iona but appear displaced relatively to each other due to the 3 - D configuration of shots and stations.

approximation, the above apparent velocities could represent velocities from the Lewisian rocks of the Tiree platform overlain by Mesozoic sediments of increasing thickness.

Using the known formula:

$$V_{d\downarrow(u\rightarrow)} = V1/\sin(O \pm o) \qquad (4.1)$$

where: $V_{d,(u)}$ = observed downdip (or updip) velocity

$V1$ = top layer velocity

O = critical angle of head-wave refraction

o = angle of dip

and assuming velocities of 6.0 km/sec for the Lewisian rocks and 3.0 km/sec for the Mesozoic sediments we get dips for their interface of 15° and 23° for segments A and B respectively (Fig. 4.7).

These dips will then represent either a continuous interface or (more probably) a step-like interface arising from a number of fault splays at that part of the Camasunary fault, and the above quoted dips will reflect the average dips across the interface as the step-edge diffractions and the stacking process of the automatic signal detection for the airgun data will tend to smooth out the refracted arrivals. Consequently, the actual fault planes will be much steeper than the calculated dips imply.

The existence of the fault splays is supported by the solid geology map of the area (Fig. 4.8) and by the linear shape of the negative magnetic anomaly at a distance of about 3 km SE of Ruaig station at East Tiree (Fig. 4.6). Though the geology map only shows Mesozoic sediments in that area, the examination of

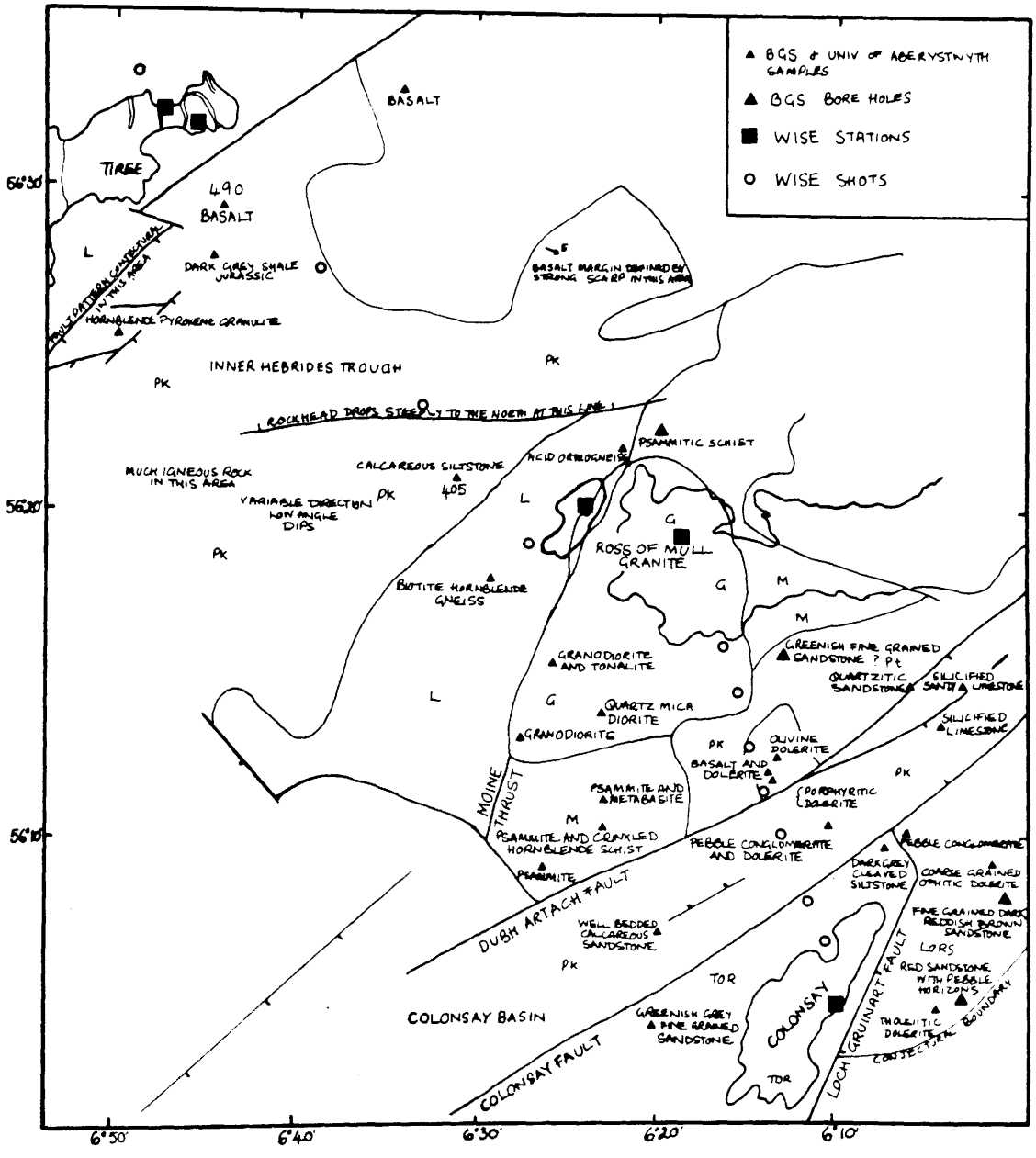

Fig. 4.8: Sketch map of the solid geology (and sample information) of the area between Tiree and Colonsay as interpreted from surveys of the British Geological Survey and the University of Aberystwyth (information provided by D. Evans. BGS).

the preliminary map with the shallow seismics information showed no sign of any penetration and stratification of the strata, which was typical of the basaltic cover of the basin to the NE. Also, recovered sample No 490 was a basalt.

The introduction of the basalt then, the SE margin of which, as shown by the magnetic anomaly, roughly coincides with the change in the pattern of the apparent velocities (5 - 6 km from Tiree), together with the fact that the apparent velocity of 4.3 km/sec for segment A falls within the expected range of velocities for lavas (section 4.2.2), will imply that the shot waves propagated laterally through vertical pile of lavas and the fault plane to the Lewisian rocks of Tiree. Some Mesozoic rocks are probably preserved under the lavas whose thick ness is similar to that of the lavas at the SE of Coll as the magnitudes of the associated magnetic anomalies suggest.

The airgun data recorded at Mull and Iona show a general pattern of apparent velocities which is compatible with the known geology, though some important discrepancies do occur for the two data sets.

The Mull data show apparent velocities for segment C (8.5 to 10 km from station) of 5.96 km/sec compatible with Lewisian (Laxfordian) velocities. Unfortunately, the same group of airguns produced arrivals at Iona (Group F) with apparent velocity of 4.05 km/sec which is much lower than any reported Lewisian velocity (section 4.2.2) and can only be attributed to some error during the preliminary processing of the data.

A sudden delay of about 0.10 sec in the arrival times can be

observed at a distance of 10 km from the Mull station and at the corresponding distance of 5.8 km from the Iona station, implying a probable down-faulted structure and the end of Lewisian outcrops, in agreement with the solid geology map of Fig. 4.8.

Since there is not any significant change of the depth to bedrock at this point, the greatest part of that delay (about 0.07 sec) is interpreted as arising from a thick sedimentary sequence overlying the Lewisian rocks of the Iona Platform. Since the sample No 405 (Fig. 4.8) was not an arkose (typical of Torridonian strata) the sequence has been interpreted as Mesozoic though Binns et al (1973) had envisaged Torridonian strata (Fig. 4.1).

The apparent velocities of segments D and G, that correspond to the same group of shots, are 4.3 km/sec and 3.6 km/sec respectively, and their difference can be explained considering the smaller distance of the shots to the Iona station (which thus samples shallower structure than the Mull station). The average value of these velocities (3.95 km/sec) is compatible with Torridonian strata (assumed P-wave velocity of 3.0 km/sec) which start with a combined thickness of 0.6 km, dip towards Tiree at an angle of about 20^{o} and attain thickness of 1.7 km after 3 km distance (at the point where the rockhead lowers to the NW, Fig. 4.8). This interpretation is not unique if Mesozoic rocks overlie the Torridonian and another possible interpretation is that the 3.6 km/sec segment represent Mesozoic rocks overlying Torridonian rocks of velocity 4.3 km/sec.

Finally, the segment E with apparent velocity of 5 km/sec probably reflects an increasing thickness of Mesozoic and

Torridonian rocks (overlying Lewisian basement) and / or Tertiary rocks which were postulated by Smythe and Kenolty (1975) but have not been sampled in the area.

The above described interpretation is shown in Fig. 4.9 but the great differences between airgun and explosive data make the interpretation suspect mainly as far as actual thicknesses of formations are concerned, or at best the possible velocity contrasts are loosely compatible with the known geology.

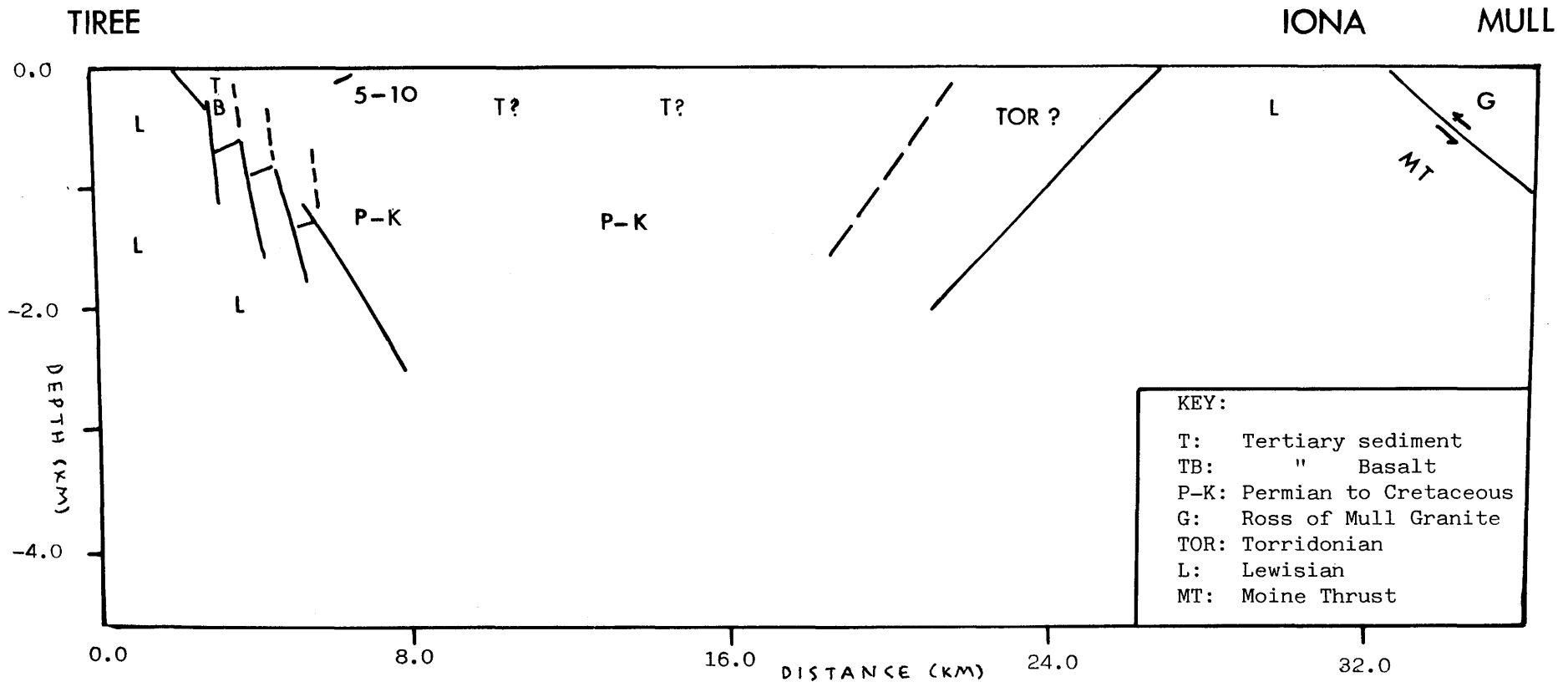

Fig. 4.9: Interpretation of the airgun data recorded at Tiree, Iona and Mull.

4.4 MULL TO COLONSAY

4.4.1 Introduction

This airgun line was not reversed at Colonsay and since the recorders were located on basement no velocities can be calculated from the data alone or any depth-to-bedrock information can be obtained. For that reason, the data will be interpreted according to the known geological and geophysical information produced by the surveys of Rashid (1977), Barber et al (1979) and Wilson (1979).

Since the density of the shallow seismic lines was much greater in the Glasgow University survey interpreted by Wilson and Rashid, their interpretation of the solid geology will be preferred against that of Barber et al when occasional discrepancies occur.

4.4.2 Seismic Interpretation

The solid geology of the area together with the existing sample information in the BGS map (Fig. 4.8), which is effectively the same as that of Barber et al (1979), is dominated by the Ross of Mull granite and the Great Glen fault zone with Moinian rocks in between covered in places by Mesozoic strata.

The pattern of the apparent velocities (Fig. 4.11) shows a velocity of about 5.30 km/sec for segment A which corresponds to shots on the Ross of Mull granite.

Segment B with an apparent velocity of about 4.0 km/sec and its high delay (relatively to segment A) signifies the end of the

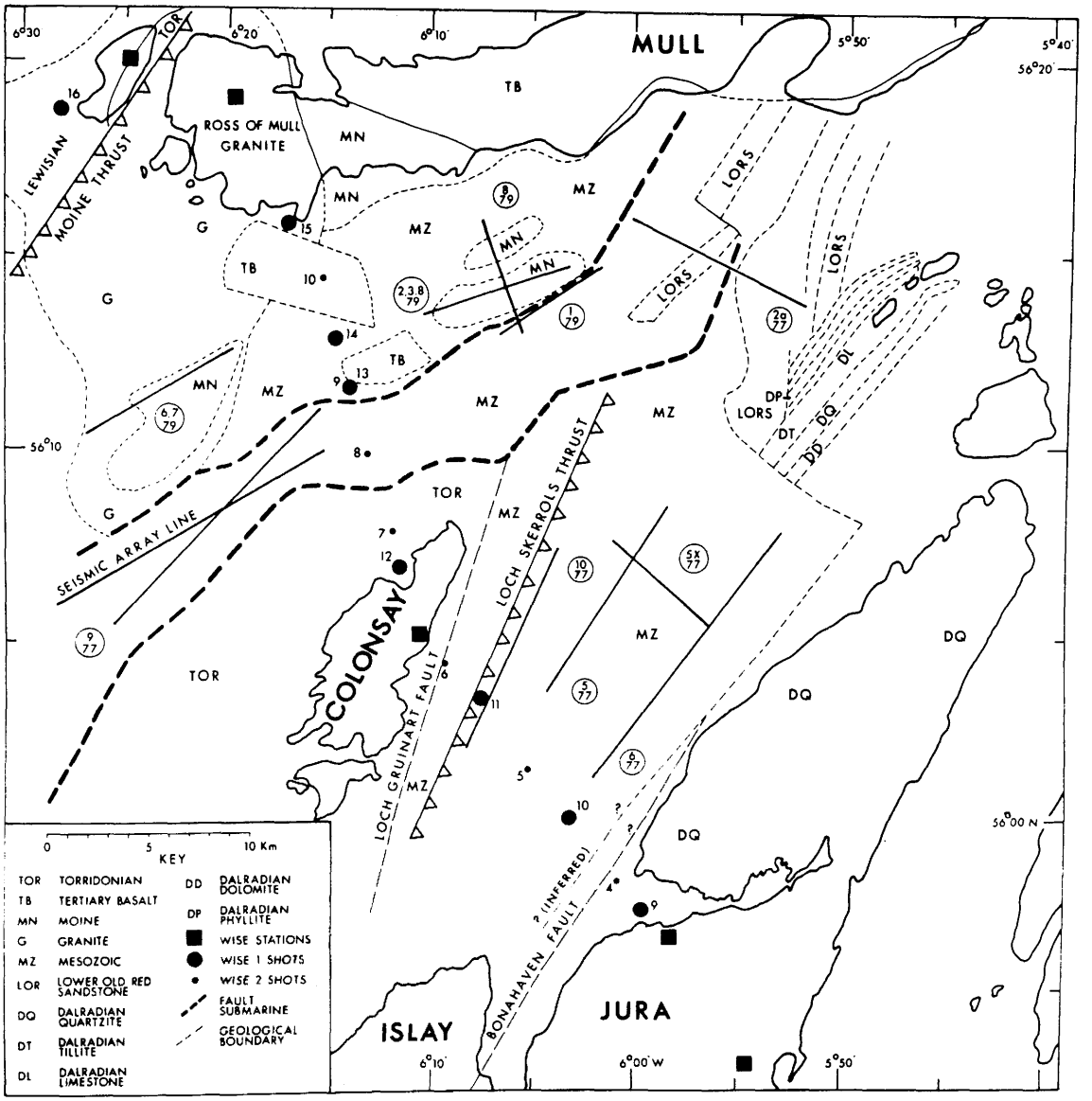

Fig. 4.10: Solid Geology map of the area between Mull and Jura with Wilson's refraction profiles and WISE shot and station locations (after Wilson 1979).

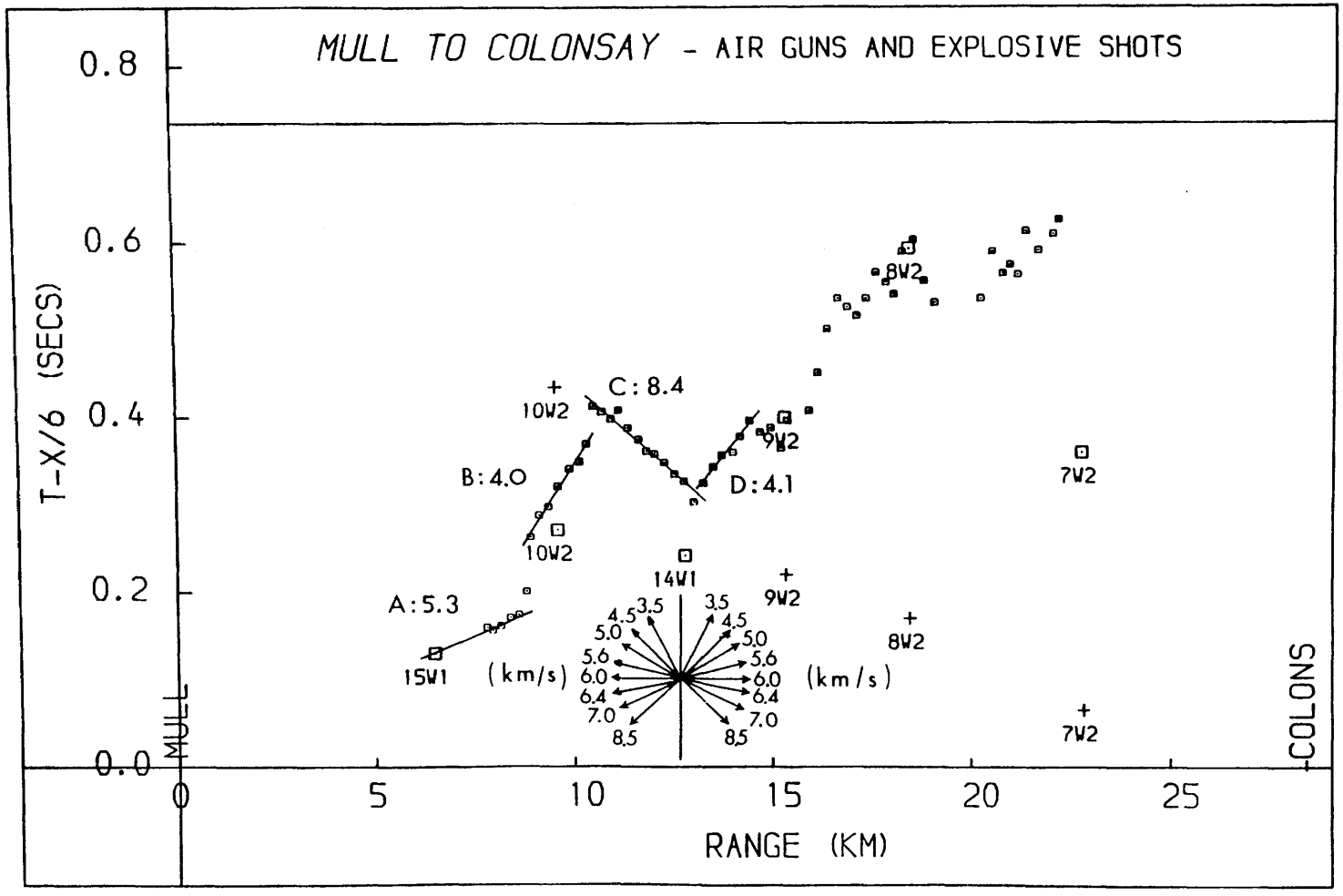

Fig. 4.11: Apparent velocities for the Mull - Colonsay airgun line.

surface outcrop of the granite and an increase in the thickness of the sedimentary cover, which, supposing a P-wave velocity of 3.0 km/sec, should be dipping at about 15° towards Colonsay (Formula 4.1) if the basement velocity is 5.5 km/sec.

In the same way, the velocities of segments C and D (8.4 and 4.0 km/sec) can be interpreted as arising from oppositely thickening low velocity rocks (3 km/sec) at angles of 13° towards Mull and 15° towards Colonsay respectively, (which overlie high velocity (5.5 km/sec) basement).

The rest of the airgun shots and the explosive shots recorded at Colonsay are considered in the ray-traced model due to the many variables entering the apparent velocity values.

Ray-tracing

The ray-traced model is shown in Figure 4.12 and is mainly constrained by the following:

1) The depth-to-bedrock information along the profile according to Wilson, modelled as a layer of uniform velocity of 1.5 km/sec.

2) The short refraction profiles of Wilson numbered 1,2,3,8,6,7 and 9 (Fig. 4.10). Profiles 6 and 7 showed average basement velocity of 5.4 km/sec, indicating Moinian rocks, and similar velocities were calculated from profiles 1,2,3 and 8 (Table 4.1). Profile 9 was shot on the Great Glen fault zone (Colonsay basin) and showed the existence of 300 m of low velocity sediments (2.0 km/sec probably Quaternary in age) and 270 m of Mesozoic strata (velocity 3.55 km/sec).

The main features of the model are the low velocity layer with velocity of 3.5 km/sec interpreted as Mesozoic in age, the Moine

rocks and the granite being indistinguishable from each other and the vertical low velocity zone representing the Great Glen fault crush zone.

The edge of the basin, at 8.5 km from the Mull station, exactly corresponds to the Mesozoic subcrop projected under the basaltic cover as mapped by Wilson (Fig. 4.10). The sudden thickening of the sediments to about 500 m is rather unexpected since the short refraction lines to the NE and SW (lines 1,2,3,8,6 and 7) only show Mesozoic strata which are thinner by one order of magnitude.

But the preservation of a considerable thickness of Tertiary lavas, probably of the order of 200-300 m, as shown by Wilson's map and the negative aeromagnetic anomaly (Fig. 4.6), suggest the existence of a basement hollow where an underlying sequence of low velocity sediments can explain the pattern of the first arrivals. The lavas do not probably have any considerable effect on the thickness of the sediments since velocities as low as 4.0 km/sec have been attributed to them (section 4.2), but there still remains the possibility that at least some of the delay is due to a screening effect of the basalts.

The previous interpretation implies that a probable fault continues to the NNE from the southernmost border of the granite with the Mesozoic rocks of the fault zone along the SE surface limit of the granite (Fig. 4.10). The fault downthrows Mesozoic and Moinian rocks to the SE and it might have originated due to the Mesozoic tension the direction of which was perpendicular to the granite / Lewisian contact.

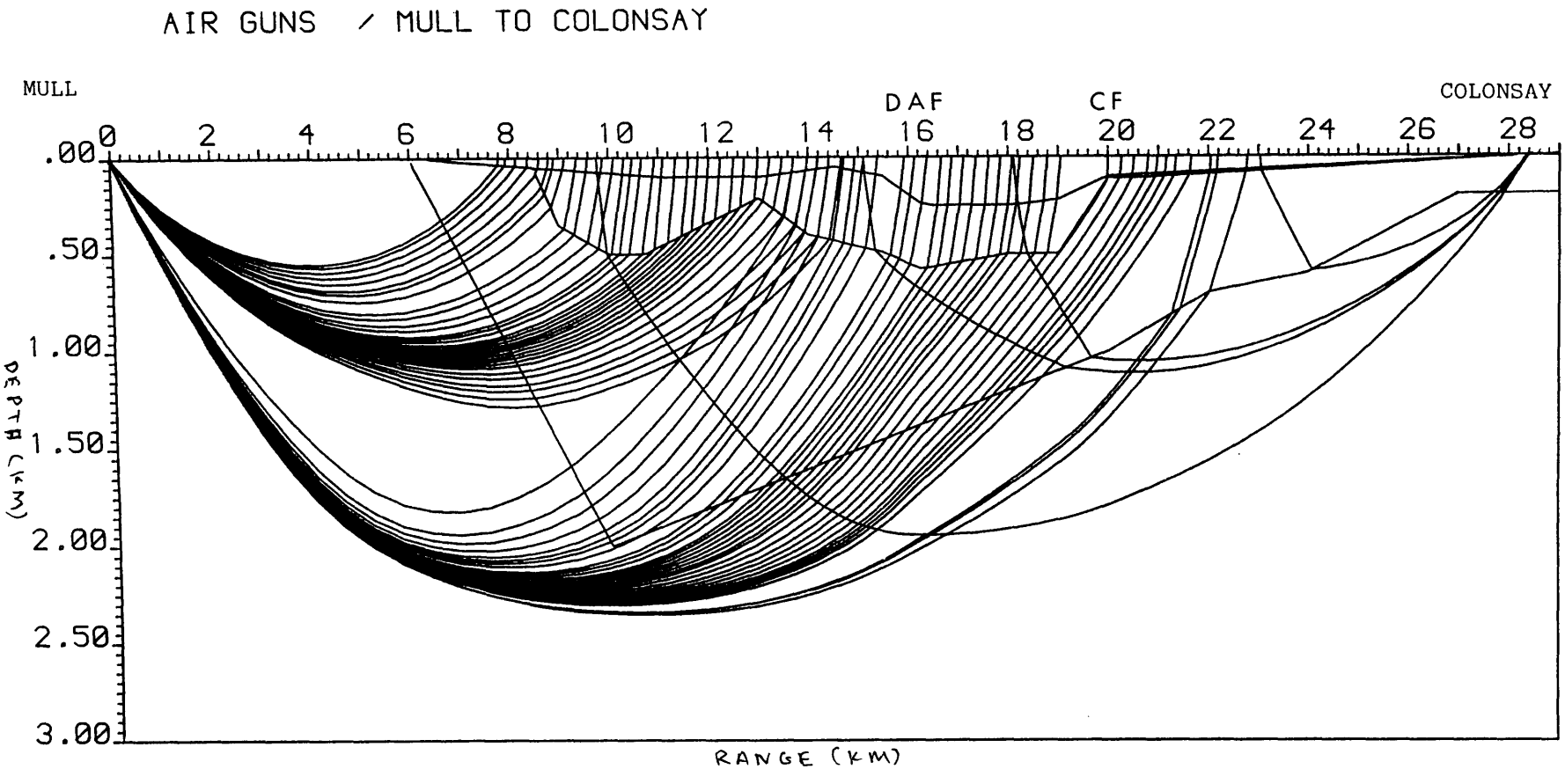

Fig. 4.12: Ray-tracing diagram for the Mull - Colonsay airgun data.

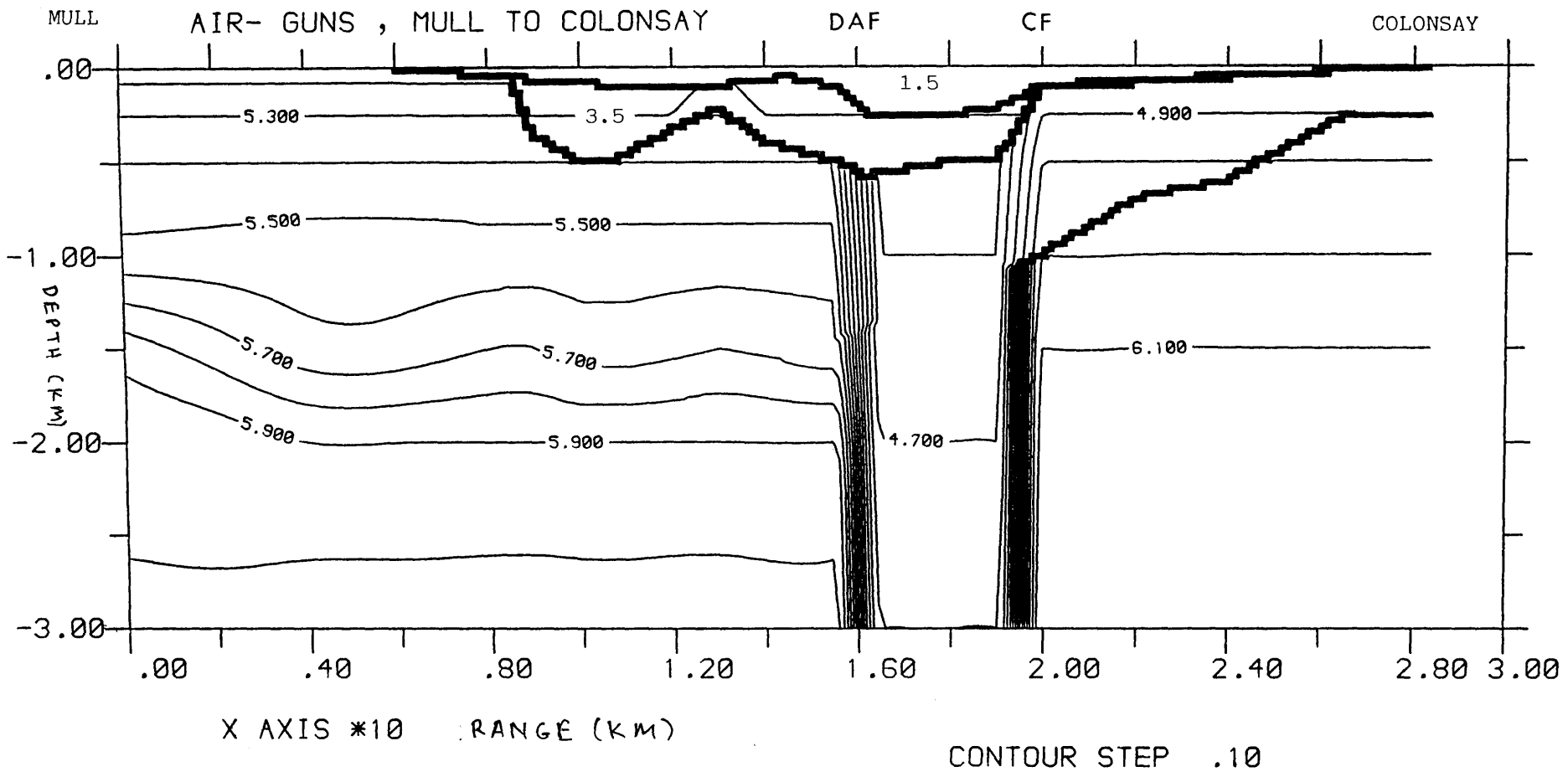

Fig. 4.13: Velocity-depth distribution for the Mull - Colonsay area. Basement velocity interpolation matrix has dimensions 23 x 8.

The basement high then, at 10 - 14 km from the Mull station, that corresponds to the magnetic anomaly and helped explain the apparent velocities, probably has not such a relief as in Figure 4.13 and partly reflects the existence of the lavas.

The basaltic cover probably extends to the SE margin of the GGF zone as shown by the dolerite samples recovered (Fig. 4.8) but it must be very thin as it is undetectable in the aeromagnetic map.

The Dubh Artach fault, at 16 km distance from the Mull station, is clearly seen on the composite bathymetric and depth-to-bedrock profile (Fig. 4.13) but it does not seem to form a steep boundary to the Mesozoic basin as happens at the southwestward extension of the fault (Evans et al 1980, Hall et al 1984). This might not necessarily be true if the basement velocity has been underestimated. Some Lower Old Red Sandstone rocks probably underlie the basin (e.g. Barber et al 1979, Seismic Array Line / Table 4.1) but profile 9 (Fig. 4.10) showed a wide range of velocities for the basement rocks (Wilson 1979), probably suggesting that the lower velocities might arise from shattered basement and the higher velocities from less shattered basement which could be Lewisian, Moinian, Torridonian or LORS. Also, the Tertiary sediments believed by Smythe and Kenolty (1975) and Hall et al (1984) to overlie the basin should be very thin or absent (profile 9). The thickness of about 400 m of Mesozoic sediments then, shown in Fig. 4.13, is only a minimum estimate.

Despite the fact that the vertical low velocity zone probably shows underestimated velocities down to 1.5 km depth or so, a

reasonable fit for the explosive data recorded at nearby stations requires a delay of 0.15 - 0.20 sec situated roughly below the GGF zone which is then most simply interpreted as being confined between the Dubh Artach and Colonsay faults and representing the cataclastic rocks of the crush belt which on land appear to be confined to a zone of 2 - 3 km wide (Eyles and McGregor 1952). This problem will be investigated further in Chapter 5, as it cannot be entirely separated from other aspects of the composite model of all the explosive shots (like the shape of the Dalradian basin, the near-surface delays, etc.)

The goodness-of-fit plot for the shots 7, 8 and 9 at Colonsay (Fig. 4.14), implies very high velocities (6.5 - 6.7 km/sec) for the Lewisian basement of Colonsay which are obviously unrealistic, since the Torridonian thickens to the NW as shown in the gravity model of the next section, and the exposed Lewisian rocks of Islay appear to be more like Laxfordian than Scourian (e.g. Westbrook and Borradaile) as the high velocities suggest. Also, shot 7 recorded at Mull was probably picked too early as the Iona pick satisfies the model very closely (Chapter 5).

The granite / Moine interface could not be imaged probably due to low velocity contrast, relatively small thickness of the Moine rocks and the lack of more controls on the other aspects of the model. The granite / Lewisian interface is also seismically indistinguisable from the WISE data, as the delay times for explosive shots recorded on Mull and Iona (e.g. Fig. 2.40) do not show any systematic difference implying a

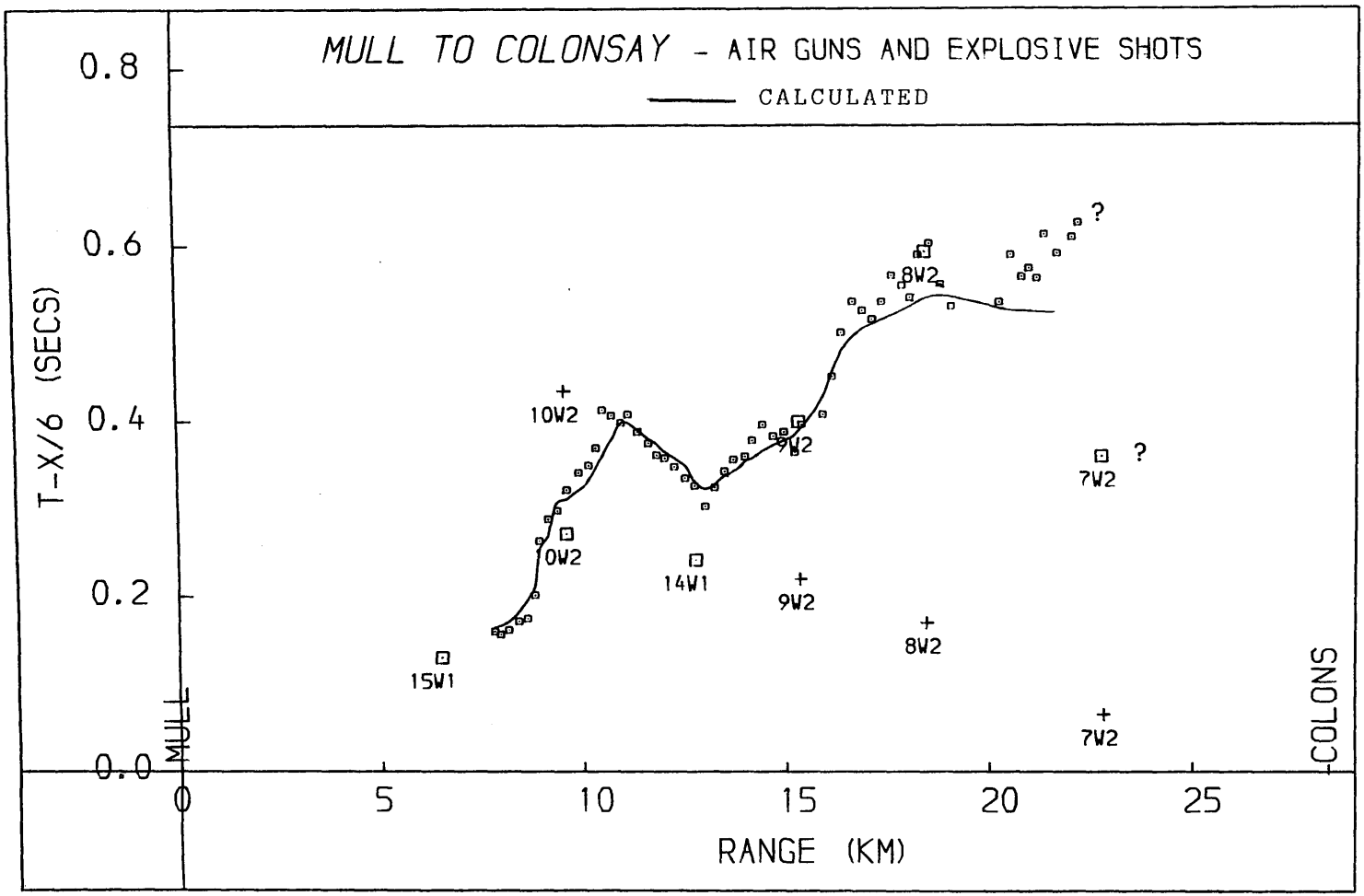

Fig. 4.14: Goodness-of-fit plot for the Mull - Colonsay airgun data. A smooth curve has been fitted to the calculated travel times of the airgun data.

significant velocity change across the Moine Thrust.

That is supported by published figures on granite velocities (e.g. Telford et al 1976, Bott 1982) and of Caledonian granites (Dimitropoulos 1981), all showing velocities around 6.0 km/sec at depths of 1 - 2 km.

4.4.3 Gravity Interpretation

Some of the above uncertainties, as the lateral extent of the granite and the shape of the granite / Lewisian interface, can be partly resolved with the interpretation of the gravity field.

The final model (Fig. 4.15), produced by program G2DPLOT, is constrained by the known surface geology and densities of the rocks and by the seismic model. The most characteristic feature of the gravity field, which is reduced by a regional of 20 mgal (since the calculations concern density contrasts), is that its lowest value does not mark the Colonsay basin (16 - 20 km from Mull station) but instead takes place at a distance of 14 - 15 km from the station. That suggests that low density rocks with similar thickness as those at the Colonsay basin, exist to the NW of the Dubh Artach fault.

The Lewisian / granite interface can be seen dipping at 20° - 25° to the SE where it flattens out and the granite (density 2.65 $Mg\,m^{-3}$) attains its maximum thickness of about 3 km under the sedimentary cover (density 2.44 $Mg\,m^{-3}$). Some Moinian rocks (density 2.70 $Mg\,m^{-3}$; Hipkin and Hussain 1983) are probably preserved under the basin but their low density contrast with the granite renders their thickness uncertain.

The above are in agreement with the ideas of Beckinsale and

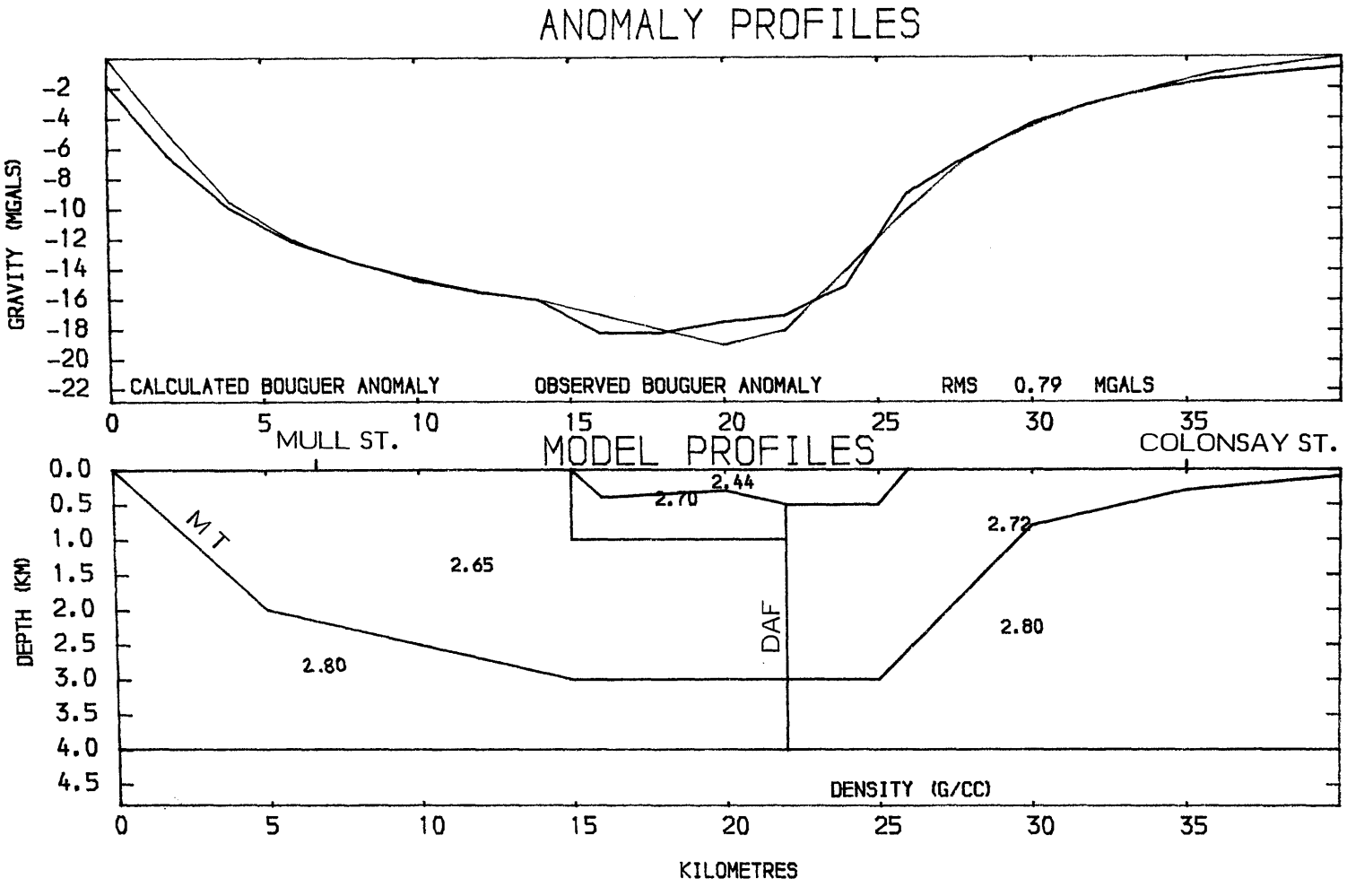

Fig. 4.15: Gravity model for the Mull - Colonsay area. For location see Fig. 4.2.
(DAF: Dubh Artach Fault, MT: Moine Thrust)

Obradovich (1973) who concluded that the intrusion of the granite postdated the Moine thrusting and it was probably controlled at deep levels by the GGF crush zone and at shallow levels by the Moine Thrust zone.

The model also shows the GGF zone forming the SE boundary of the granite and the Lewisian rocks of the Islay - Colonsay platform rise under the Torridonian cover to a depth of less than 0.5 km under Colonsay.

4.4.4 Conclusions

1) A probable Mesozoic basin with maximum thickness of about 500 m lies to the NW of the Colonsay basin.

2) Lewisian (Laxfordian amphibolites), Moine and granite rocks cannot be seismically distinguished.

3) An extensive granite sheet probably underlies the area to the NW of the Great Glen fault zone and wedges upwards at about 20° under the Ross of Mull to form the estern boundary of the Moine Thrust.

4) The Lewisian basement at the SE rises under the Torridonian from about 1.5 km near the fault zone to less than 0.5 km under the Colonsay.

5) The fault zone coincides with a low velocity zone whose structure is uncertain at shallow depth.

The geological interpretation is shown in Figure 4.16.

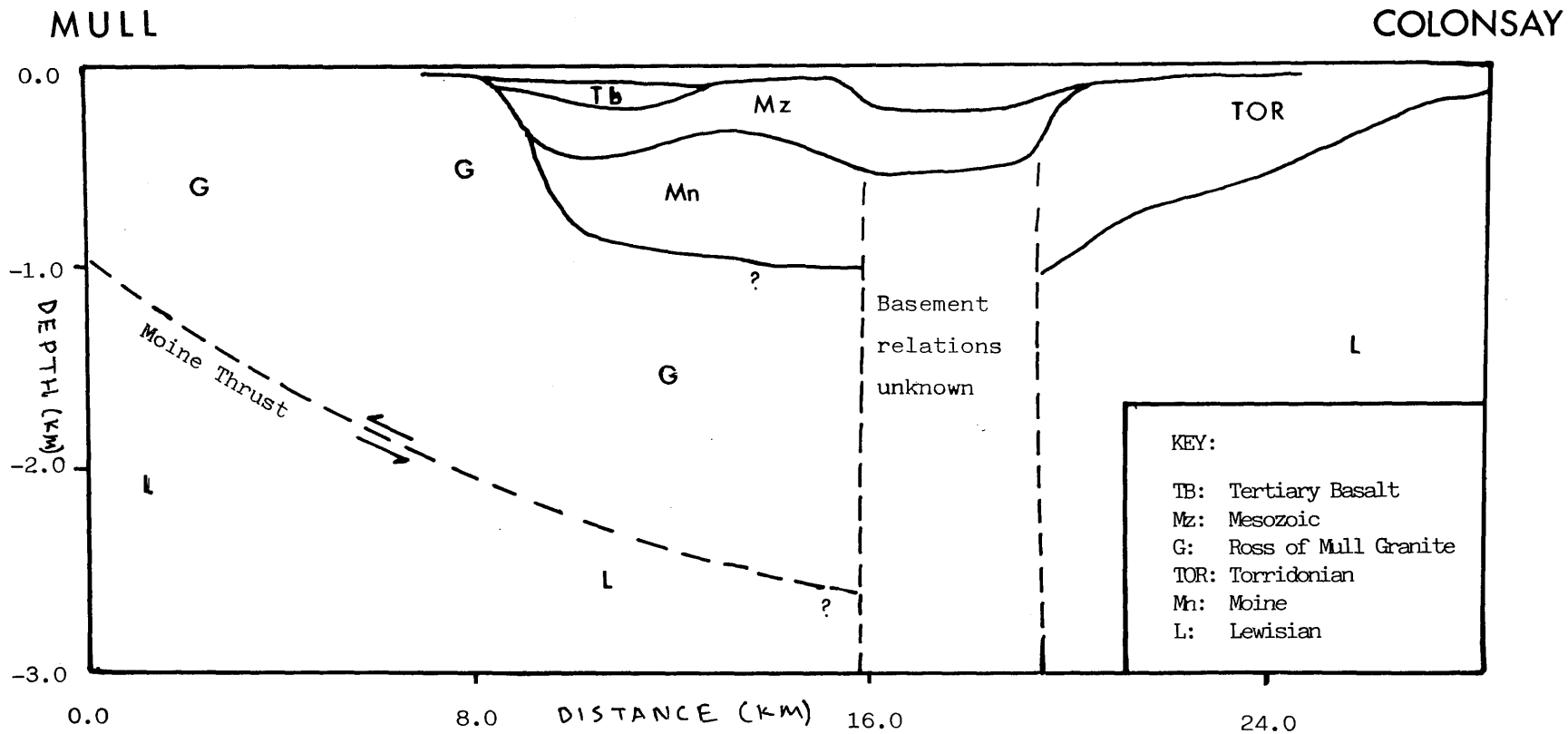

Fig. 4.16: Geological interpretation for the Mull - Colonsay area.

TABLE 4.1

Interpretation of the short refraction profiles between Mull and Jura used as controls in current project. For locations see Fig. 4.10. After Wilson (1979).

Profiles of 1977	
5/77	280 m Mesozoic limestone 3.5 km/sec
5x/77	Inconclusive
6/77 (150)*	56 m sediment 2.5 km/sec 425 m Mesozoic 3.4 km/sec Dalradian phyllite 4.9 km/sec
6/77 (40)*	30 m sediment 2.0 km/sec 145 m Mesozoic sandstone 2.7 km/sec 300 m Mesozoic limestone 3.3 km/sec Dalradian phyllite 4.7 km/sec
9/77 (40)*	300 m sediment 2.0 km/sec 270 m Mesozoic 3.55 km/sec Moine ? 5.8 km/sec Torridonian ? 4.9 km/sec
9/77 (150)*	280 m sediment Mesozoic 3.5 km/sec
10/77	200 m Mesozoic limestone 3.55 km/sec Dalradian phyllite 5.05 km/sec

Seismic Aray line usually observed Mesozoic velocities but two velocities > 4.0 km/sec were considered as indicating probable LORS strata.

Profiles of 1979	
1/79	Mesozoic 3.7 km/sec Moine 4.8 km/sec
2/79	Thin sediment 2 km/sec Moine 5.5 km/sec
3/79	Inconclusive
6/79	Mesozoic 2.8 km/sec
7/79	Thin sediment 2.2 km/sec Mesozoic 3.1 km/sec
8a/79	Thin recent 1.95 km/sec Moine 5.3 km/sec
8b/79	Thin recent 1.8 km/sec Moine ? 4.4 km/sec and thin recent 2.0 km/sec Moine 5.6 km/sec

* Volumes of airguns used (in cu. in.)

4.5 COLONSAY TO JURA

4.5.1 Introduction

The quality of these airgun data was ambiguous and the data recorded at North Jura were picked using the automatic signal detection programs (section 2.4.2) but they will be used here due to their relative agreement, after a fixed correction of 0.04 sec (section 2.5.3), with the explosive data of the second Phase recorded at N. Jura (Fig. 4.17).

4.5.2 Seismic Interpretation

The sedimentary cover in the area has been assigned to Mesozoic age on the evidence of the apparent velocities and the clear stratification shown in the shallow seismic profiles (Wilson 1979). The pattern of the apparent velocities (Fig. 4.17) can be partly explained by the known geology according to Wilson and Rashid (Fig. 4.10).

Segment A for the data recorded at Colonsay shows a velocity of 4.5 km/sec which is compatible with Torridonian velocities (section 4.2) overlying the Lewisian basement and (or) through an increasing thickness of Dalradian rocks overlain by some Mesozoic rocks. The data here appear to be scattered and show rapid changes in their delays over distances of few hundreds of metres probably due to the characteristically irregular Dalradian topography.

The data recorded at North Jura usually show a much smoother arrival pattern due to their automatic picking, and display three segments with apparent velocities of 4.4, 8.7 and 4.6

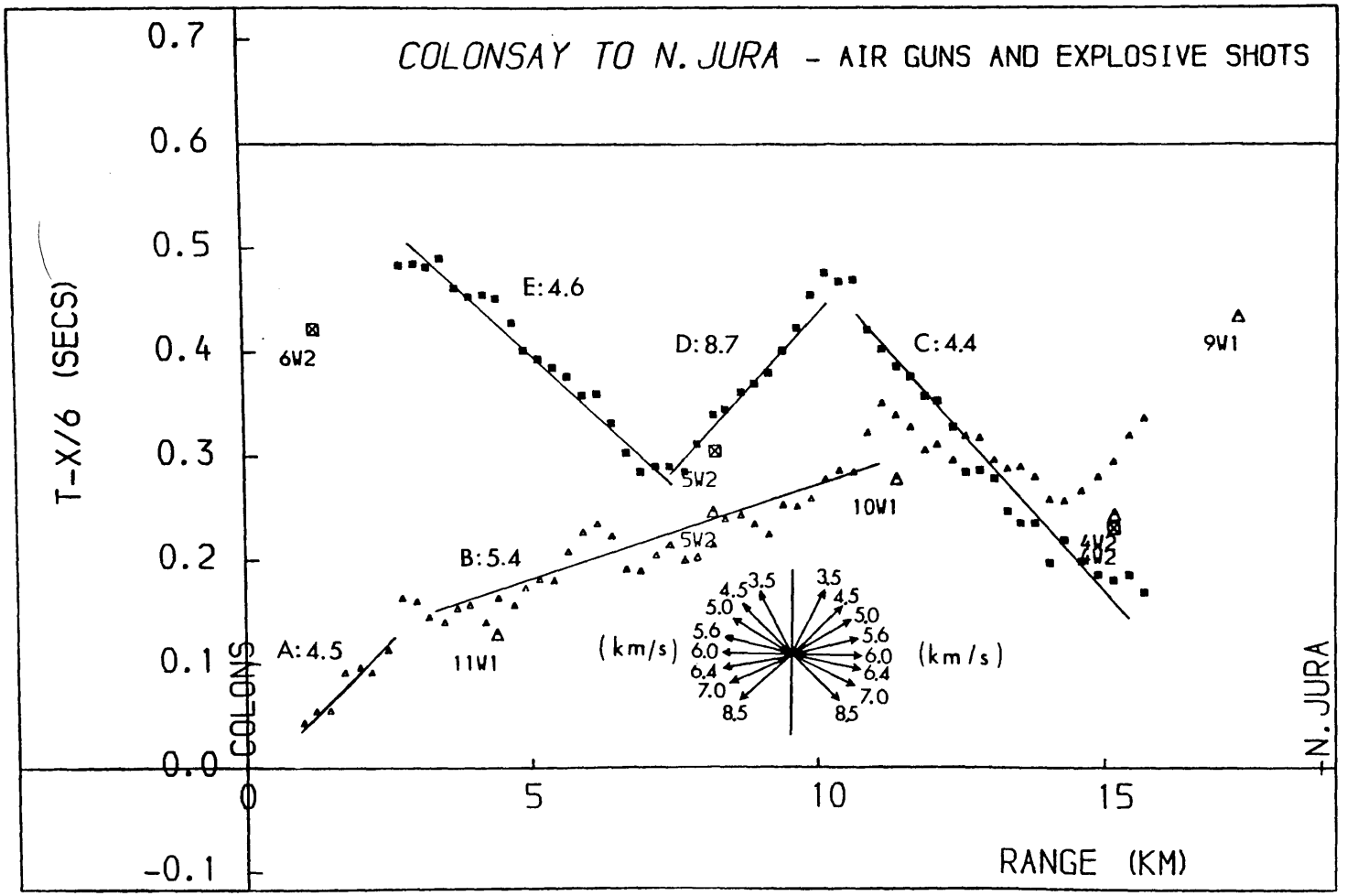

Fig. 4.17: Apparent velocities for the Colonsay - North Jura line.

km/sec. Since the Dalradian structure in the area is probably sub-vertical and these data do not clearly correlate with the Colonsay data, they will be considered in the ray-tracing model.

Ray-tracing

The ray-traced model is shown in Figure 4.18, and is mainly constrained by the following:

1) The thickness and velocity of the Mesozoic cover and the basement as determined at the NE of the line by Wilson's (1979) refraction profiles 5,6 and 10 (Fig. 4.10) which showed a thickness for the Mesozoic of 200 - 400 m (Table 4.1). Only profile 10 can be used as an absolute control, as it crosses the WISE profile at a distance of about 5 km from the Colonsay station and profiles 5 and 6, which show a thickening of the Mesozoic cover towards Jura, since they are situated 3 - 5 km to the NE of the line can only suggest the order of magnitude for the thickness of the Mesozoic rocks.

2) The position of the Loch Gruinart fault determined by Evans et al (1980) and Wilson (1979) as being about 2-3 km from the Colonsay station and the depth-to-bedrock profile as determined by Wilson.

The most important feature of the model is the high velocity zone situated under a thin Mesozoic cover between 6 and 10 km from the Colonsay station. It almost entirely stems from the need to obtain a reasonable fit for the delayed and early groups of arrivals at the N. Jura station at distances of about 10 km and 7 km respectively from the Colonsay station, even though some support for the delayed group comes also from the arrivals

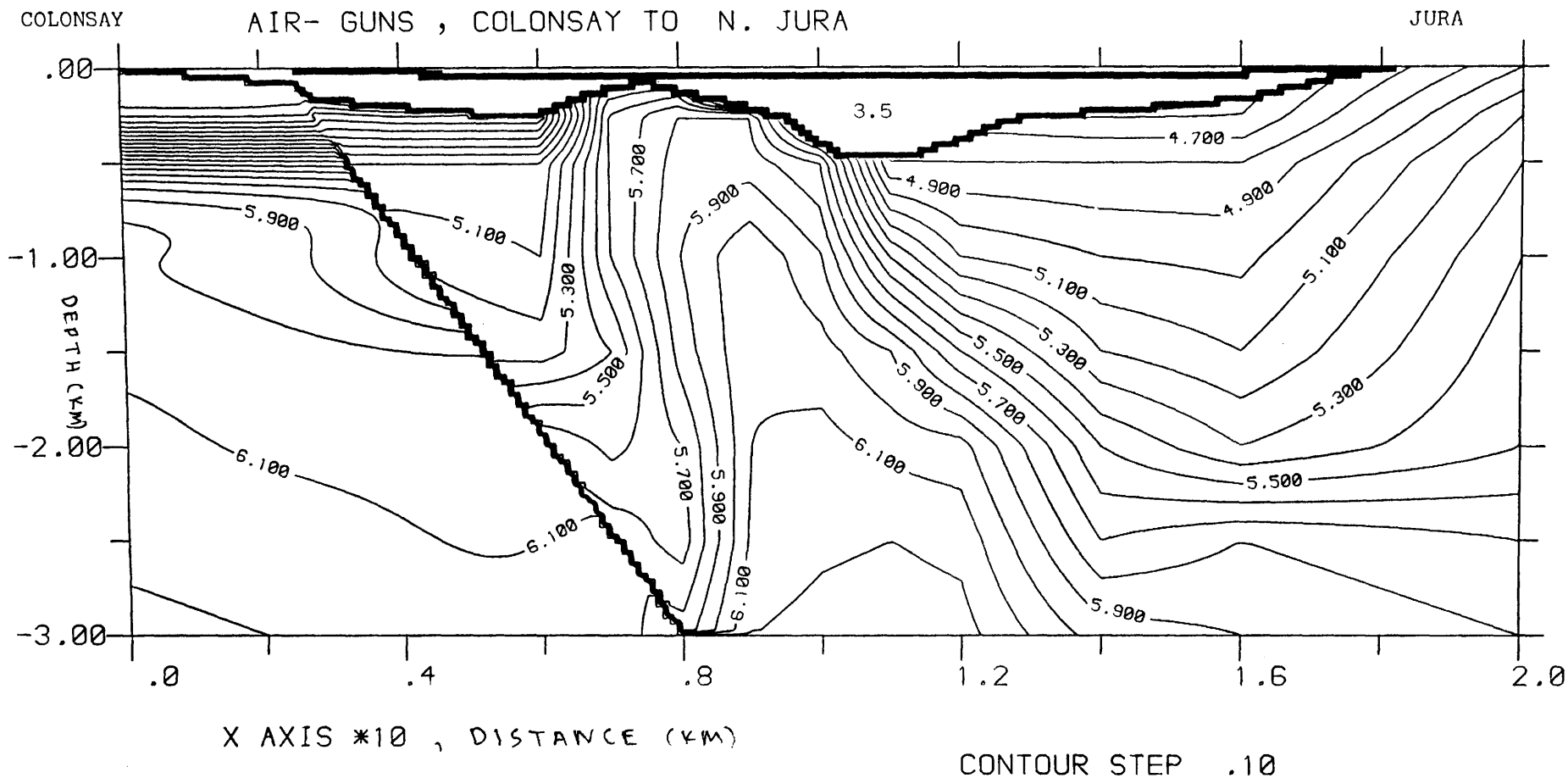

Fig. 4.18: Velocity - depth distribution for the Colonsay - North Jura area. Basement velocity interpolation matrix has dimensions 13 x 8.

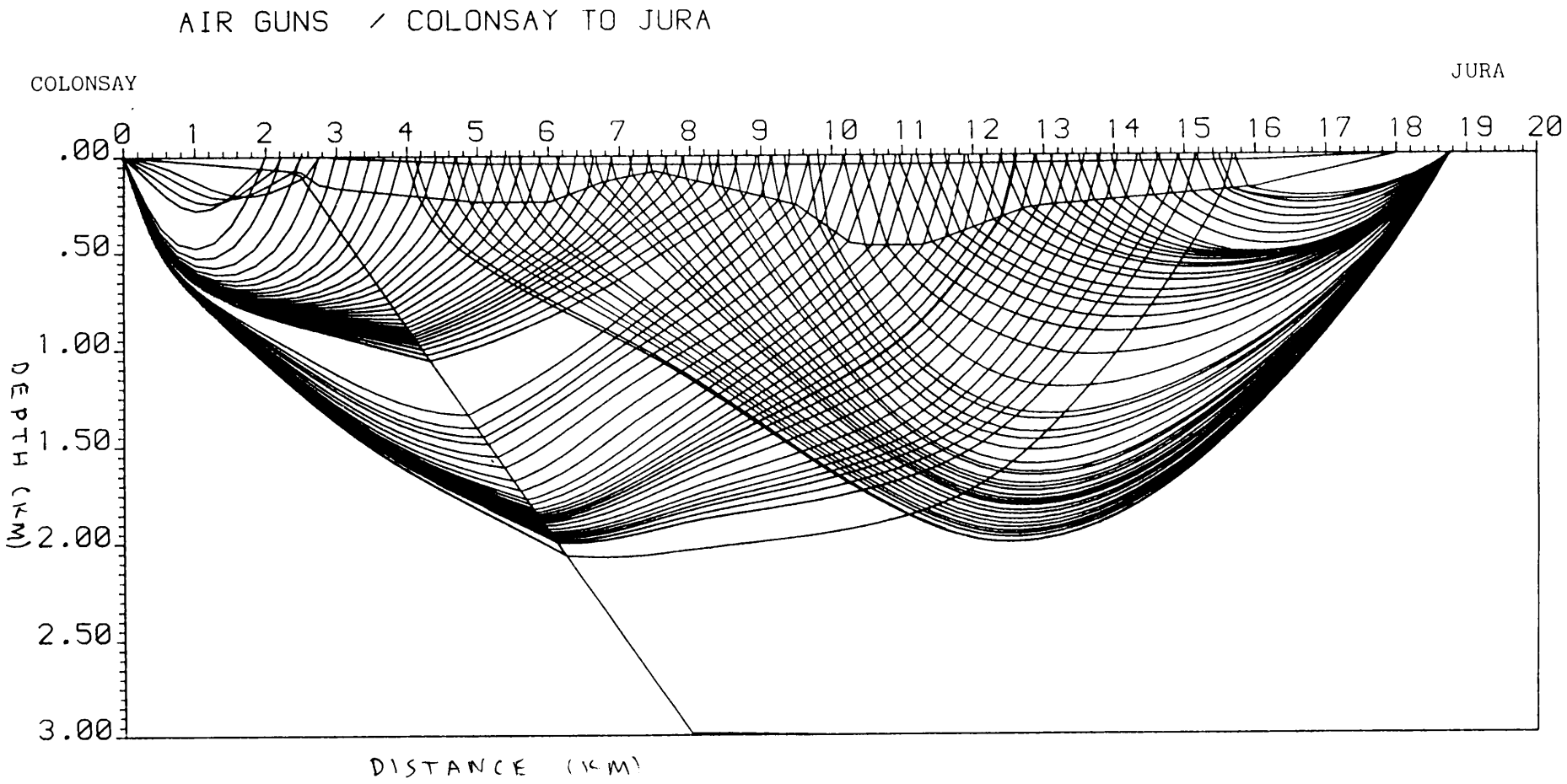

Fig. 4.19: Ray-tracing diagram for the Colonsay - North Jura airgun data.

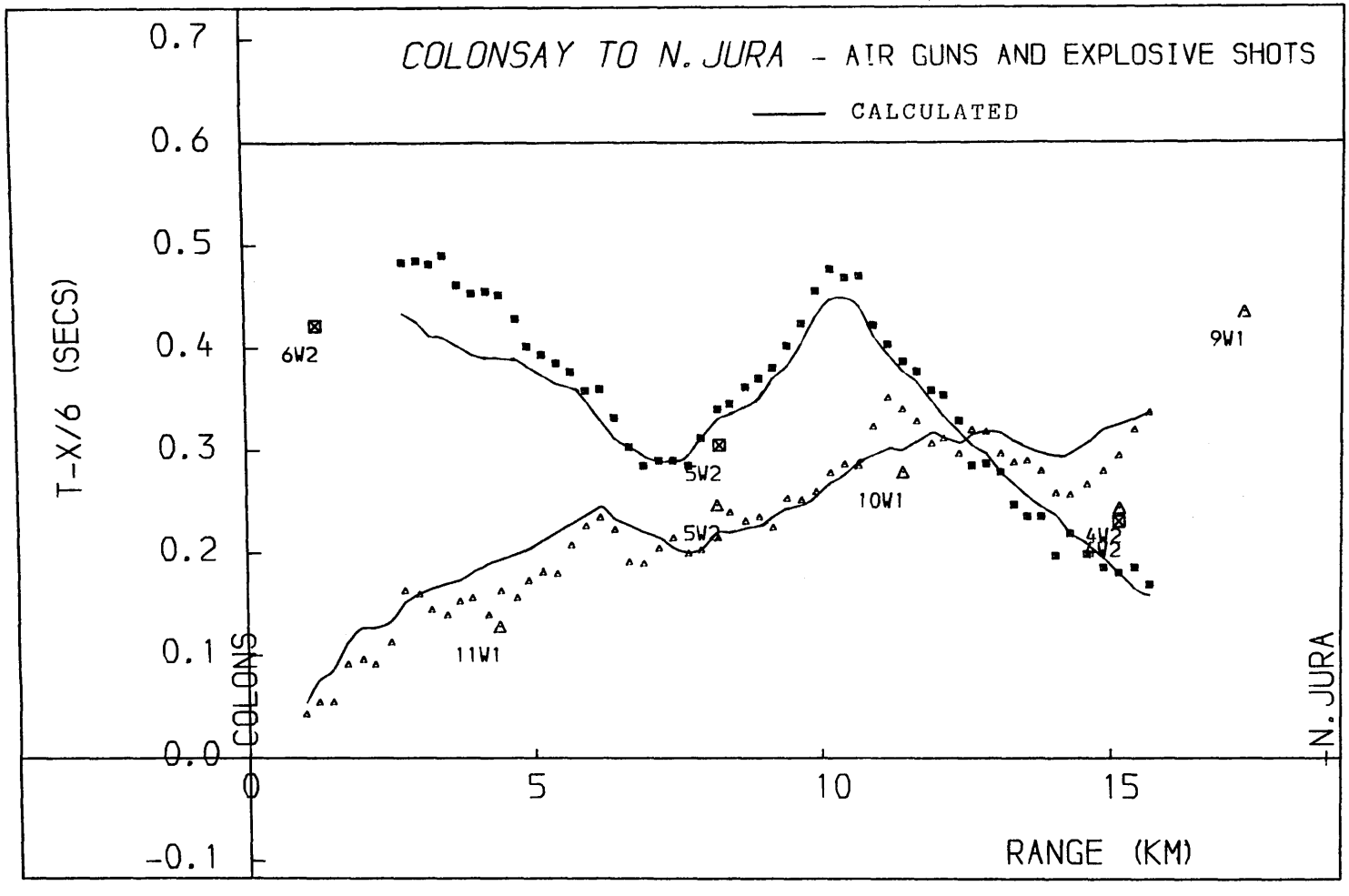

Fig. 4.20: Goodness-of-fit plot for the Colonsay - North Jura airgun data. A smooth curve has been fitted to the calculated travel times.

at Colonsay (Fig. 4.17).

The ray-diagram then (Fig. 4.19) can show that rays propagating along the axis of the high velocity zone give rise at N. Jura to arrival times much higher than those arising from rays delayed by the low velocity basement rocks on either side of the feature and by the Mesozoic cover of variable thickness. In contrast, rays towards the Colonsay station propagate through oblique zones of alternating high and low velocities and as a result they display apparent velocities of intermediate values.

The Mesozoic layer has been assigned velocity of 3.5 km/sec (Table 4.1) and the sudden variation in thickness between 9 km and 11 km, necessary for a better fit of the data there, is probably the single most important unconstrained feature of the model, apart from a reliable calculation of the velocity along the strike of the high velocity zone, due to the distance - about 3 km - of profiles 5 and 6 at the NE (though the variation is loosely supported by the profiles). Alternatively, if the Mesozoic cover there has similar thickness as at the NW and SE, in order to get a reasonable fit for the data recorded at N. Jura, the velocity in the high velocity zone should increase to about 6.4 - 6.5 km/sec at the centre of the zone.

At the southeastern end of the line the Mesozoic / basement interface has been placed to a depth of about 200 m in order to produce a better fit for the data there recorded at N. Jura, while keeping quartzite velocities within reasonable limits. That would imply that the fault off the NW coast of Jura (inferred by Wilson) closely follows the coast line in a curved rather than linear trend (Fig. 4.10), thus being interpreted as

the seaward extension of the Bonahaven fault which on Islay exhibits a small downthrow to the NW (Durrance 1976).

The second interface starting at 3 km distance from Colonsay and dipping at about 30° to the SE represents the Loch Gruinart fault which separates Lewisian from Dalradian rocks (and the Bowmore sandstones in Islay) and is most probably just another splay of the Great Glen fault of moderate sinistral displacement and a small downthrow of Mesozoic rocks to the SE and a much greater one (about 4 km) of Dalradian rocks and Bowmore sandstones (e.g. Dobson et al 1975, Durrance 1976, Westbrook and Borradaile, 1979, Evans et al 1980 / Fig. 4.8).

The Lewisian basement at Colonsay, overlain by the Torridonian sediments, is fairly shallow (about 300 - 500 m, as the onset of segment B suggests in Fig. 4.17) and has been assigned Laxfordian velocities (section 4.2.1) in agreement with the gravity models (Fig. 4.15 and 4.21), the magnetic interpretation of Westbrook and Borradaile and the existence of Lewisian gneisses at the NE tip of Colonsay.

The quartzite basement has been assigned a velocity of about 5.0 km/sec at the surface increasing to about 5.5 km/sec at 2 km depth in order to match the nearby airgun and explosive shot times and in accordance with the basement velocities found by the relevant profiles of Table 4.1. Rashid (1979) measured ultrasonic velocities of about 5.3 km/sec for Dalradian quartzite and an average velocity of about 5.3 - 5.5 km/sec is also implied from the travel times of shots 9 and 10 (WISE1) recorded at the M. Jura and S. Jura stations.

The high velocity zone could represent an uplifted piece of Lewisian basement but the absence of any pronounced gravity (Fig. 4.2) or magnetic anomaly (Fig. 4.6) renders that possibility remote. Alternatively, an extrapolation of the known geology at Islay to the north along the strike of the outcropping Dalradian formations would place the extension of the Islay anticline at about the right distance from Colonsay and then the high velocities could be attributed to a zone within the anticline, most probably the Dolomitic group of the Dalradian, of the Islay Quartzite group, which crops out about 10 km to the SW at the northeastern tip of Islay (Fig. 4.23).

The highly metamorphic nature of these rocks would probably justify the high velocities at that part of the model while velocity anisotropy effects due to the phyllite minerals and the quartzite grains within the anticline rocks being strongly oriented along the axis of the structure (in responce to the orogenic stress system, Chapter 1), might have increased considerably the velocities "felt" at the Jura station thus creating the characteristic pattern of the arrival times.

The low velocity rocks sitting on the Loch Gruinart fault interface could then represent the north-eastward continuation of the Bowmore sandstones which can be seen on Islay (Fig. 4.23) overlain by an undetermined thickness of quartzite. The downward extension of this zone becomes obscure below a depth of about 2 km due to the velocity averaging effects on the refracted rays. It is quite possible though that it continues to about 4 km depth where, as in Islay, the Loch Gruinart fault probably passes onto the Loch Skerrols Thrust.

4.5.3. Gravity Interpretation

The gravity model (Fig. 4.21) includes also the area between Jura and Kintyre which will be examined in section 4.6. The profile is taken perpendicular to the gravity trend under examination, to improve the validity of the model, and thus slightly offsets the WISE profile.

The main feature of the model is the gravity low above the Jura Quartzite which was assigned density of 2.65 $Mg\,m^{-3}$ (Durrance 1976). The limit of the formation towards Kintyre is constrained by the surface geology while the limit towards Colonsay is the SE side of the anticlinal structure imaged in the seismic model. A density of 2.70 $Mg\,m^{-3}$ has been assumed for the combined body of anticlinal phyllites, dolomites, limestone and the probable Bowmore Sandstones (Durrance 1976, Westbrook and Borradaile 1978). The model shows the inclined contact of the anticline and the Jura Quartzite and also that the Jura Quartzite reaches a maximum depth of about 6 km. Its shape is triangular rather than that of an inclined wedge (if constant density is assumed for the formation) which means that the strata change their dip at a shallow depth from 25° - 40° to the SE (Anderton 1977) to about 20° to the NW. This suggests that the Jura Quartzite contact with the Easdale group rocks (Fig. 1.6, 1.9, 4.23) also dips to the NW.

Alternatively, if the shape of an inclined wedge is adopted for the Quartzite formation then a lateral increase of density of about 0.15 $Mg\,m^{-3}$ has to be assumed in order to produce the

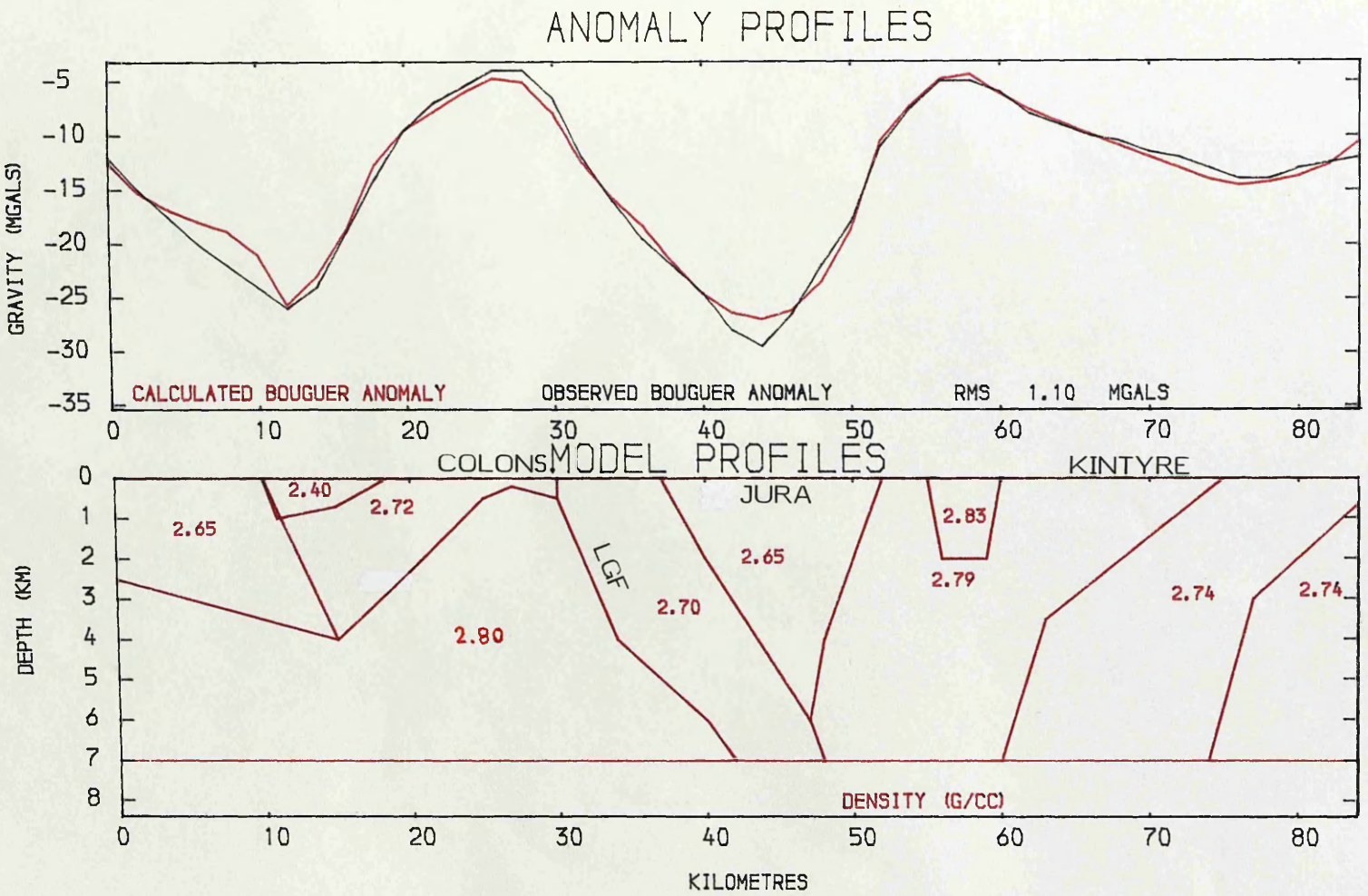

Fig. 4.21: Gravity model for the area between Colonsay and Kintyre. For location see Fig. 4.2. (LGF: Loch Gruinart Fault)

triangular shape of the gravity anomaly. That possibility exists considering the abundance of dense and weakly magnetized epidiorite sills (Powell 1970, Durrance 1976) within the Easdale group rocks and Jura Quartzites which at depth might further increase their volume as they intrude quartzite rocks but they do not advance along the bedding planes up to the surface due to their increased inclination near the surface and the existence of the Ardrishaig phyllites. The phyllites provide a more convenient intrusion medium due to their vertical disposition and higher schistosity.

The epidiorite intrusions were the result of NE - SW tension and thus they are parallel to the Dalradian strike (Borradaile 1979).

4.5.4 Conclusions

a) The pattern of the apparent velocities of the airgun data recorded at N. Jura can be best explained with the introduction of a high velocity zone (> 6 km/sec) interpreted as the core of the Islay anticline, dipping parallel to the Lewisian interface at an angle of about 30° - 50° at a distance of about 6 - 10 km from the Colonsay station.

b) The Bowmore sandstones of Islay most probably continue to the NE and form a substantial part of the low velocity rocks (5.0 - 5.5 km/sec) trapped between the Loch Gruinart fault and the anticline (overlaid by some quartzites).

c) The Jura Quartzite shows refraction velocities of 5.0 - 5.5 km/sec and a geologically plausible 2 - dimensional gravity interpretation shows that its southeastern part increases its density considerably with increasing depth, probably due to Dalradian epidiorite sills.

The geological interpretation is shown in Figure 4.22.

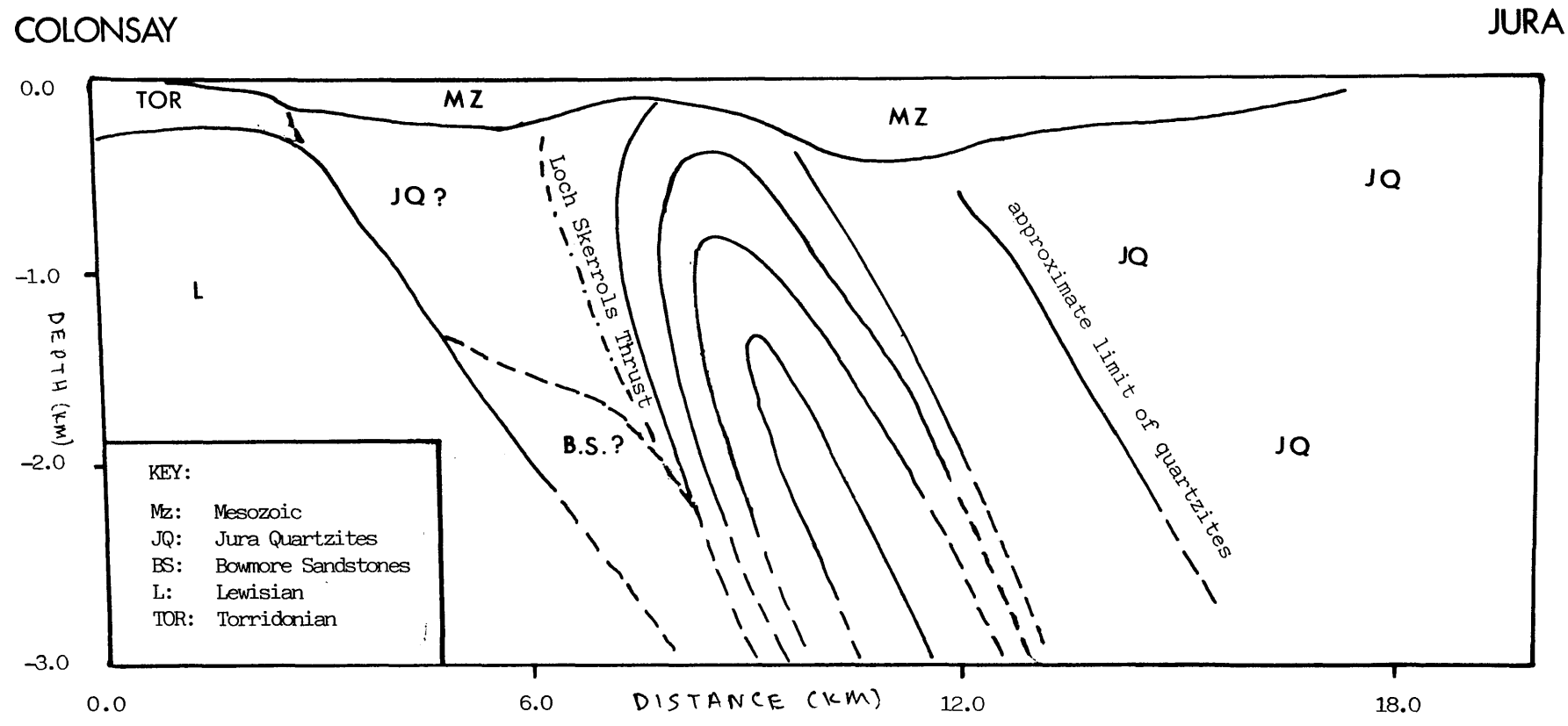

Fig. 4.22: Geological interpretation for the Colonsay to North Jura area.

4.6 JURA TO KINTYRE

4.6.1 Introduction

The airgun and Geoflex data of this line, though believed to be accurate in their apparent velocities pattern, were corrected in the manner described in section 2.5.2 in order to minimize their difference with the good quality explosive data of both phases from this area.

4.6.2 Seismic Interpretation

The pattern of the apparent velocities, uncorrected for water depth, is shown in Fig. 4.2 4.

Segment A with apparent velocity of 6.0 km/sec is considered to represent the Port Ellen phyllites (Fig. 4.23) heavily intruded by the epidiorite sills (section 4.5.3)

The water depth increases between 5.5 and 6.5 km (from Jura station) from about 50 m to over 200 m and then it changes as it is shown in Fig. 4.26 (Layer 1), and most of the data delays shown in that part of the line are due to the water layer.

Ray Tracing

No detailed depth-to-bedrock information was available for the profile but the soft sediments were found to be very thin or absent apart from the central trough where they reach a maximum thickness of about 100 m (McLean and Deegan 1978).

After that it was decided to vary the thickness of the soft sediment layer between 0 and 100 m in the central trough (6.5 - 12 km from Jura) in a way that would improve the fit of the

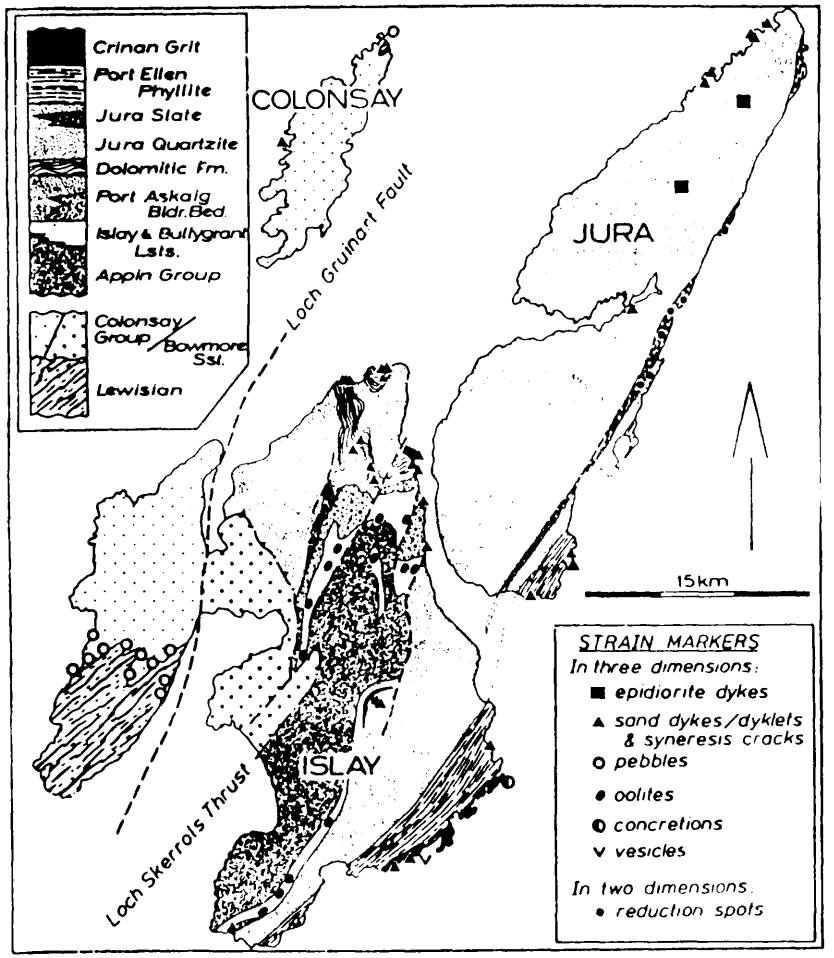

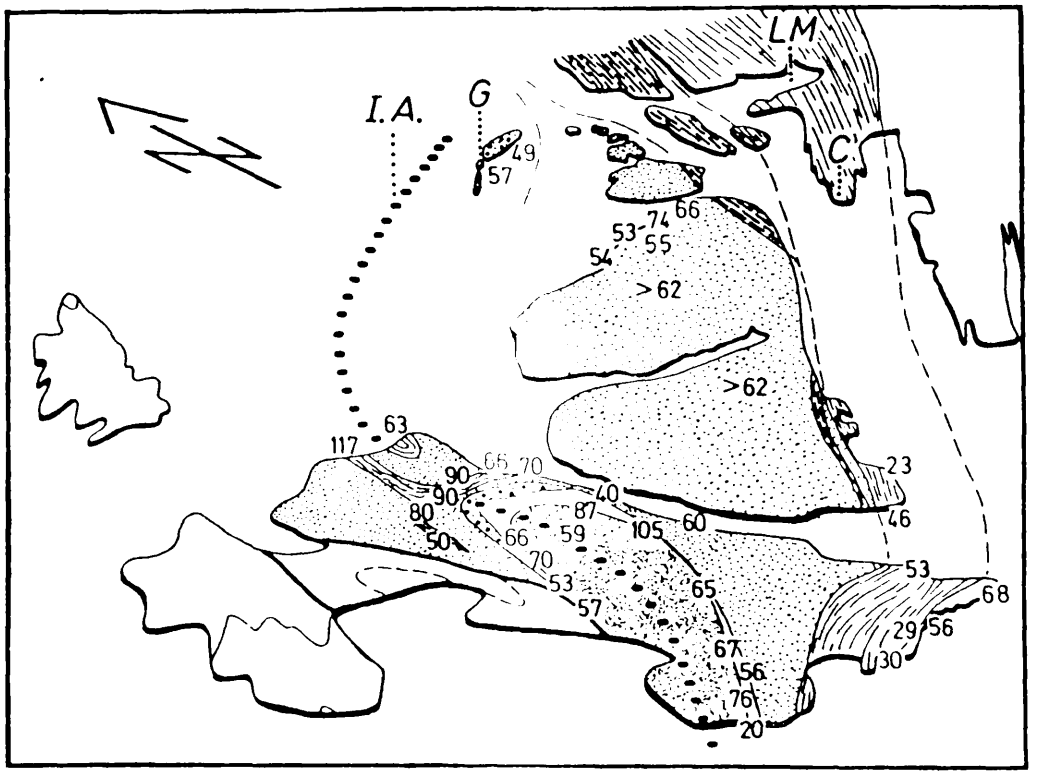

Fig. 4.23: Geology of Islay and Jura (after Borradaile 1979).

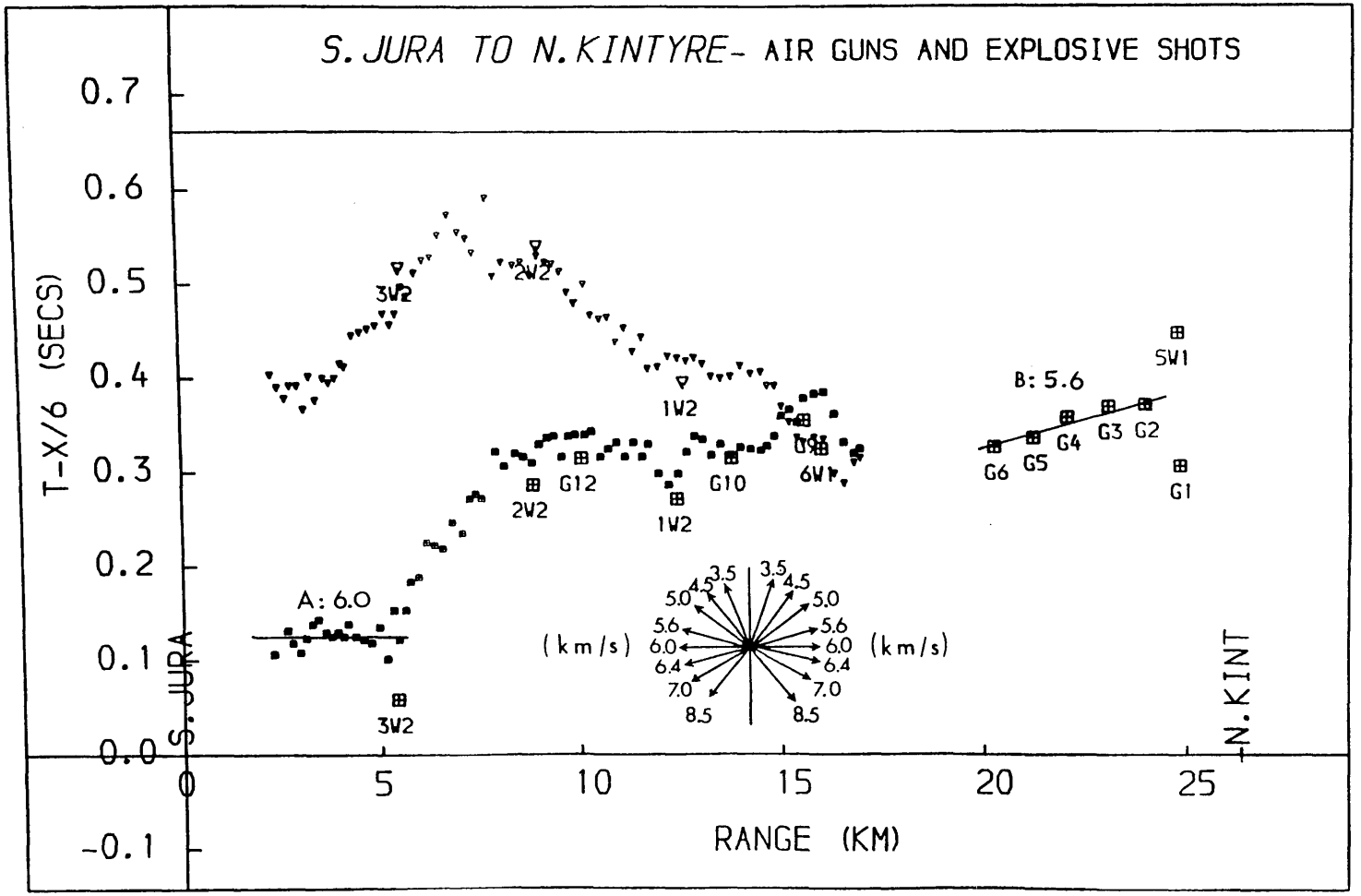

Fig. 4.24: Apparent velocities for the South Jura - North Kintyre airgun data.

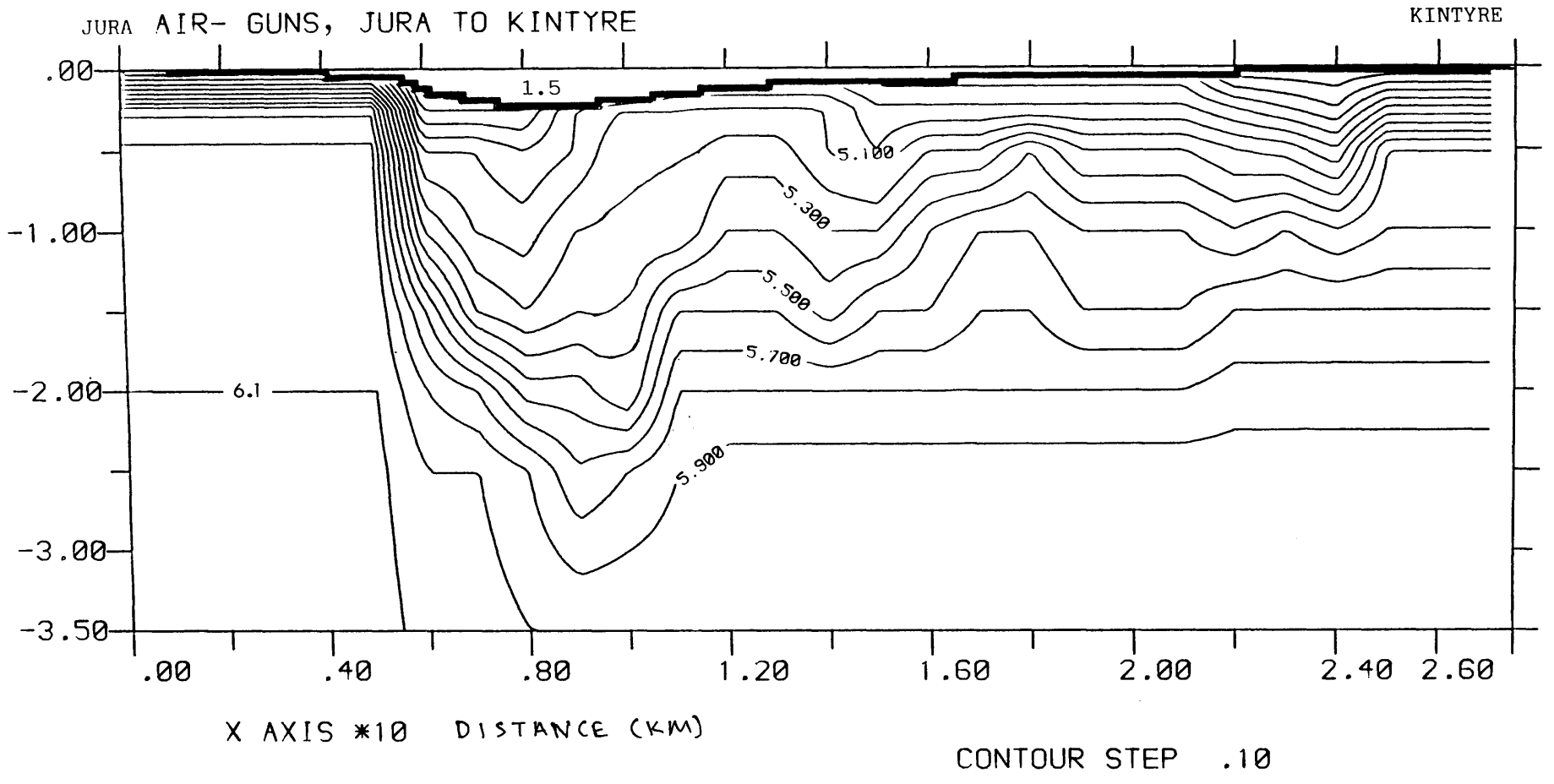

Fig. 4.25: Velocity - depth distribution for the South Jura - North Kintyre area.

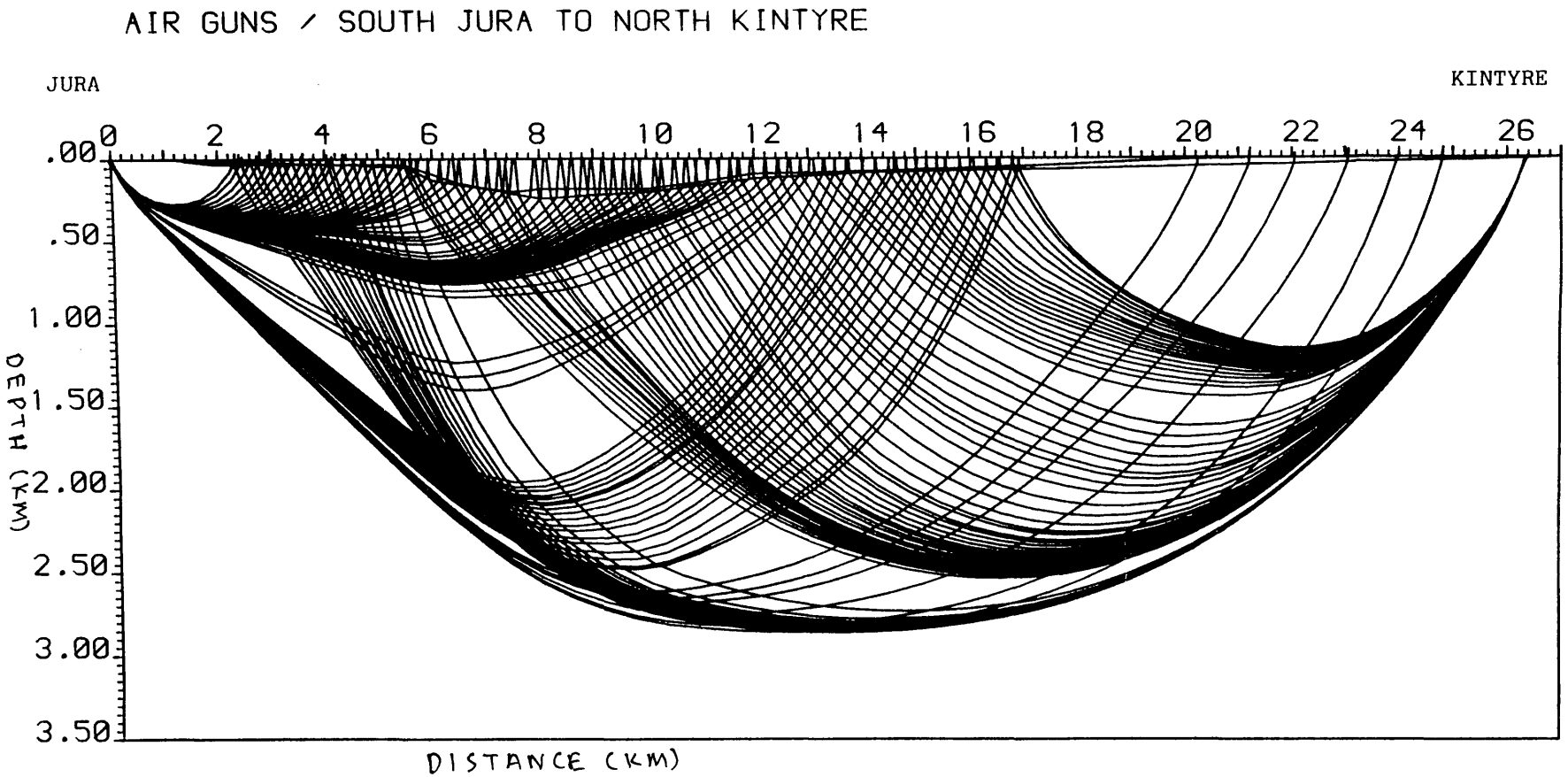

Fig. 4.26: Ray-tracing diagram for the South Jura - North Kintyre airgun data.

calculated times with the observed ones. (Fig. 4.26, Layer 2).

The final model is shown in Fig. 4.25 and its main feature is a marked velocity contrast between high velocity basement towards Jura and a low velocity basement towards Kintyre (5 - 25 km). The velocity drops sharply from about 6 km/sec to about 5.2 km/sc along a lateral transition (at a depth of 1 km) from the high to the low velocity zone.

This part of the model is mainly dictated by the need to model the data recorded at Kintyre whose delays between 4 and 10 km do not correlate with the bathymetric trough (6.8 - 10 km) or the similar data of Jura (where delay of about 0.2 sec between data at 5 and 10 km can be explained by the intervention of 200 m of water and 100 m of soft sediments of velocity 1.5 km/sec).

In particular the increase in delay times (by about o.07 sec) between 4 km and 5.5 km is not justified by the bathymetry and can only be modelled if a low velocity zone is assumed under the bathymetric trough. That is supported by the fact that the highest delays take place at the NW edge of the trough and they decrease towards Kintyre for the same water depth (6.5 - 10 km).

No other significant velocity contrasts can be supported by the data. The velocities under the bathymetric trough are believed to arise from the highly magnetic rocks which are responsible for the 300 nT aeromagnetic anomaly (Fig. 4.28) and have been interpreted (Westbrook and Borradaile 1979) as the continuation of the tholeiitic Tayvallich lavas which crop out in a series of plunge depressions along the strike of the Loch Awe Syncline through Argyllshire and Northern Ireland.

Overall, the basement is believed to consist solely of

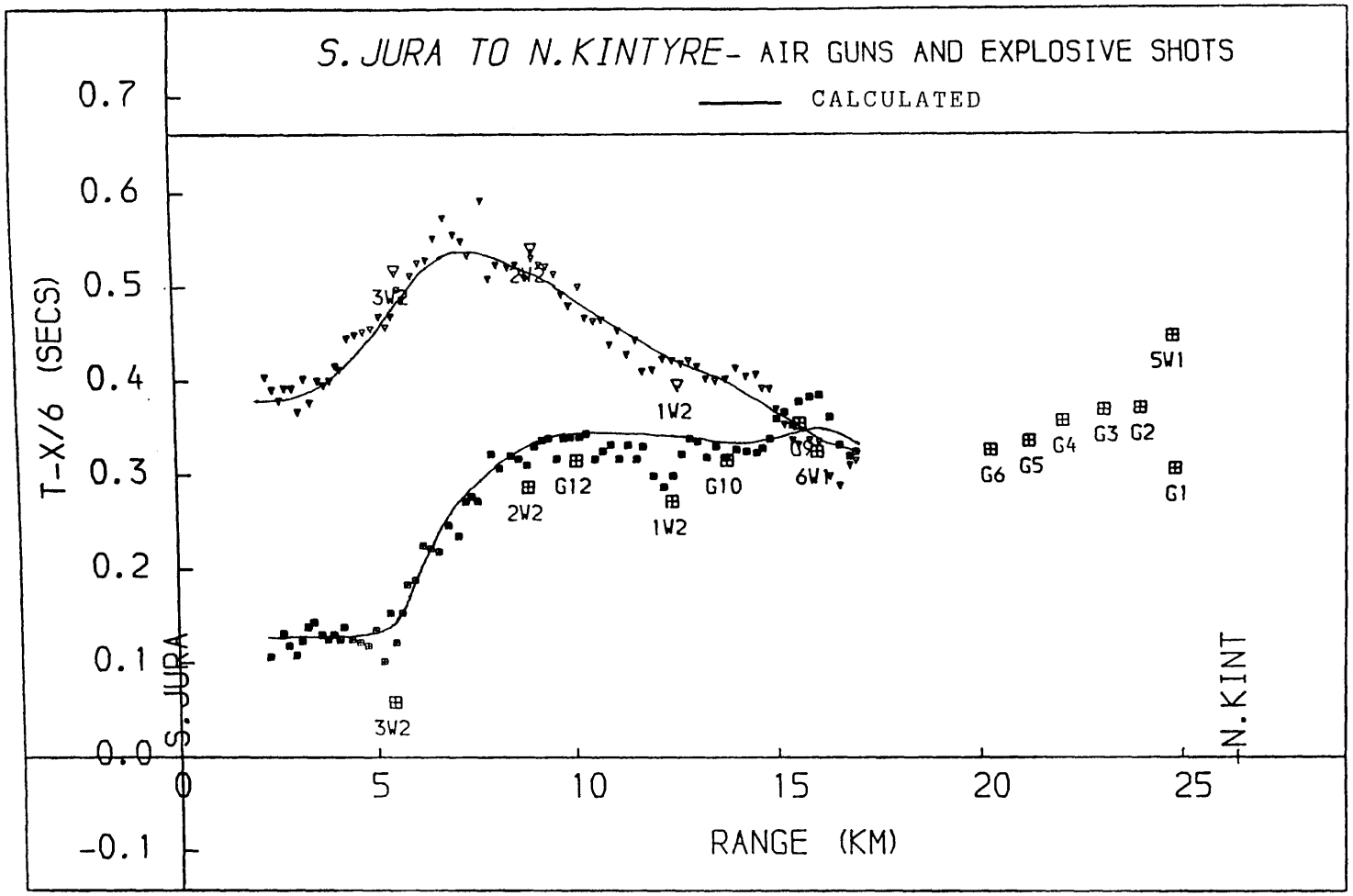

Fig. 4.27: Goodness-of-fit plot for the South Jura - North Kintyre airgun data. A smooth curve has been fitted to the calculated travel times.

Fig. 4.28: Aeromagnetic map of the area around Kintyre (after McLean and Deegan 1978).

Dalradian rocks which show characteristic irregular morphology in the shallow seismics (McLean and Deegan 1978). No Lower Old Red Sandstone or New Red Sandstone rocks are believed to overlie the Dalradian rocks and that is supported by the model.

4.6.3 Gravity Interpretation

The gravity model for this area is shown in Fig. 4.21 and the position of the gravity profile is shown in Fig. 4.10. The line crosses the Knapdale area where it is known that a thickness of about 1.5 - 2 km of Tayvallich volcanic rocks is preserved (Borradaile 1973) and the small gravity anomaly at a distance of 55 - 60 km over the volcanics clearly correlates with these rocks. The volcanics occupy the trough of the Loch Awe syncline and they are surrounded by the less dense material of the Easdale group rocks with which they show a density contrast of about 0.06 Mgm^{-3}. The slight fall of the gravity field to the southeast is then explicable considering the current ideas on the structures in the area, i.e. the erosion of the Easdale group rocks and the flattening to the southeast of the Tay Nappe (Fig. 1.7).

4.6.4 Conclusions

a) A high velocity contrast has been shown with the seismic interpretation as taking place between the Easdale phyllites / Crinan grits and the Tayvallich volcanics. No other significant velocity contrast exists within the Dalradian in this area.

b) The velocity contrast is accompanied by high magnetic and considerable gravity contrasts and interpretation of the potential fields has shown the Tayvallich volcanics increasing their thickness to the southwest to probably about 5 km across the WISE line.

The geological interpretation is shown in Fig. 4.29.

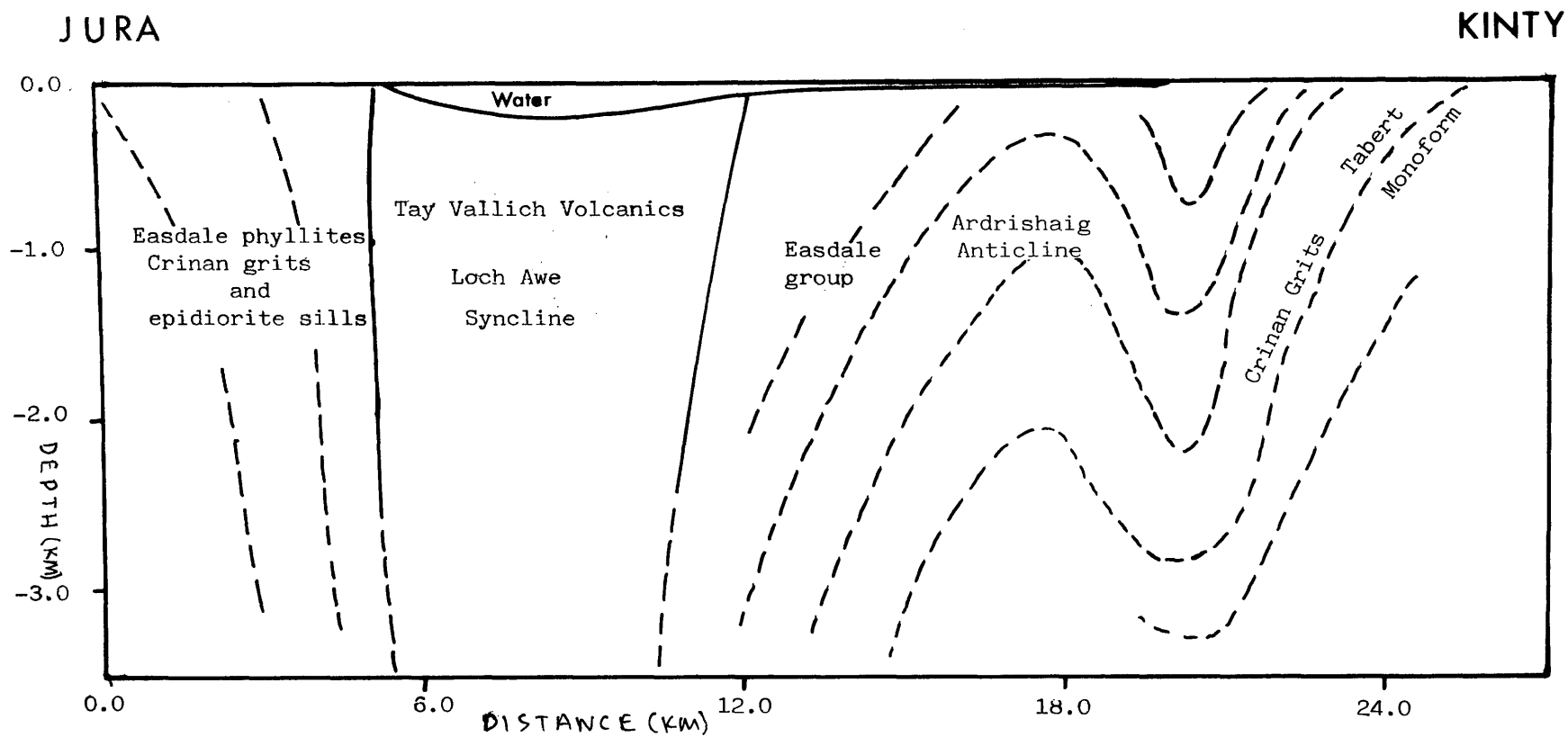

Fig. 4.29: Geological interpretation for the South Jura - North Kintyre area.

4.7 KINTYRE TO GIRVAN

4.7.1 Introduction

No airgun data were available for this part of the line and thus the present discussion will be confined to a summary of the existing information along the profile, mainly as determined by McLean and Deegan (1978), that allows for reasonable estimates of the shot sedimentary delays.

4.7.2 Geological and Geophysical controls

The pattern of the sedimentary delays for the shots 1,2,3 and 4 recorded at Girvan (Fig. 2.22) and S. Jura (Fig. 2.21) can be explained considering the expected variation in the thicknesses of the dominant rock formations in the area i.e. the Lower and Upper Old Red Sandstone, Carboniferous and New Red Sandstone strata.

The shots 4 and 1 lie directly on Dalradian and Lower Palaeozoic basement respectively and are associated with small delays, while shots 3 and 2 lie on probable Triassic and Permian rocks respectively and show larger delays.

Since no deep reflection profile exists along the WISE line, the estimates on the sedimentary cover thickness are based on structural considerations and on 3 - dimensional gravity stripping to the base Permo-Triassic after correcting for the effect of the Tertiary igneous intrusion of the Arran / Ailsa Craig line (in McLean and Deegan 1978, Fig. 12.6 and 12.7). The gravity interpretation (assumed density contrast of -0.3 $Mg\,m^{-3}$) shows about 800 m of Permo- Triassic rocks under shot 3 and 100

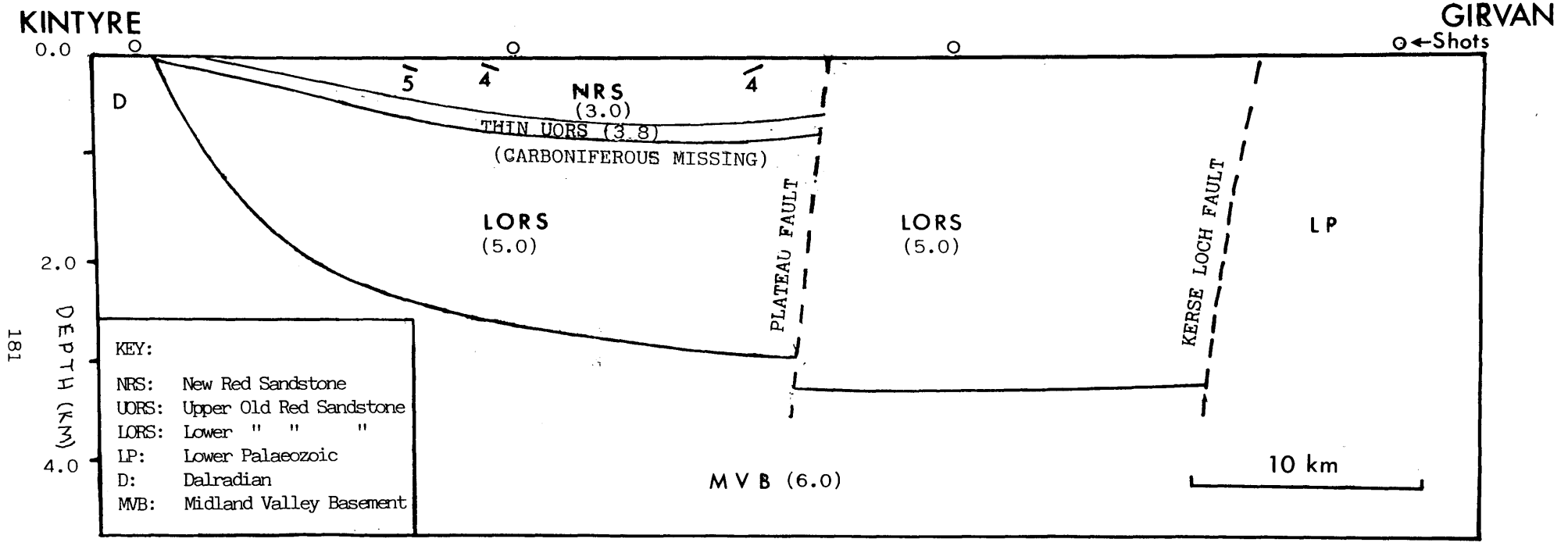

Fig. 4.30: Approximate structure along the WISE profile between Kintyre and Girvan. Positions of WISE shots are also shown. Numbers in parentheses indicate approximate P-wave velocities. Based mainly on McLean and Deegan (1978).

- 200 m under shot 2.

The Carboniferous rocks are probably very attenuated or missing while under shot 3 about 2.0 - 2.5 km of Lower ORS rocks are probably preserved and under shot 2, east of the Plateau fault, about 2.5 - 3.5 km of similar rocks are preserved (section 1.7).

The Upper ORS strata are only a few hundred metres thick on Arran (Richey et al 1930) and the seismic interpretation of McLean and Deegan shows that their thickness increases to about 800 m at the SE of Mull of Kintyre (SW Arran trough).

These rocks probably overlie the Midland Valley upper crustal refractor (velocity 6.0 - 6.2 km/sec, e.g. Davidson et al 1984) as the above quoted stratal thicknesses give delays of about 0.20 - 0.25 sec (shot 3) and 0.07 - 0.10 sec (shot 2) higher than those of shots 1 and 4, which are compatible with the observed ones.

The cross-section with the above quoted information and estimates that approximately satisfy the data is shown in Figure 4.30. The assumed formation velocities for the ORS strata are based on Davidson et al (1984). A closer fit with the data will be sought during the modelling of the deep structure.

CHAPTER 5

GEOPHYSICAL AND GEOLOGICAL INTERPRETATION: DEEP STRUCTURE

5.1 INTRODUCTION

The shallow structure, as described in Chapter 4, was continued downwards by modelling the explosive shot data from both Phases. The initial velocity gradients for the basement, at a depth greater than about 3 km, which was the limit of the airgun models, were based on WHB inversion results (Summers 1982).

5.2 GENERAL ASPECTS OF THE SEISMIC MODEL

The ray-tracing diagrams for Phases 1 and 2, and the velocity-depth distribution are shown in Figures 5.1, 5.2 and 5.3 respectively (Back pocket).

A general increase of the velocity with depth can be observed for both Lewisian and Dalradian basements obviously due to decreasing weathering and the closure of microcracks under increasing confining pressure (e.g. Kern 1978, Hall and Al-Haddad 1979, Hall and Simmons 1979).

The near-surface basement delays are difficult to be accurately quantified in the Hebridean region due to sparse shot / station coverage in that area, but shot 19 recorded at Tiree (Vaul station) and shot 16 recorded at Iona, suggest near-surface velocities of about 4.50 km/sec. This value is similar to that calculated for the gneisses to the north of the Ben Stack line in Sutherland where the interpretation of the LUST profile has shown that the near-surface delays could be as high

as 0.15 sec.

Generally, the basement gradient is controlled by the need to attribute correctly the "true" station delays under the stations and the need to obtain refracted arrivals from the shots that sit on top of the Hebridean basins. The basement velocity gradients have to be high enough at a depth of 0.5 - 2.5 km in order to get refracted arrivals at the stations.

Moreover, some uncertainty remains on the velocity structure under the Barra station. Though Lewisian granulites occur to the east of the Outer Hebrides Thrust, usually charaterised by their high density, magnetization and velocity (e.g. McQuillin and Watson 1973, Powell 1978, section 4.2), it is quite probable that their velocity is reduced as the existence of cataclastically deformed rocks observed around the Outer Hebrides Thrust zone (e.g. Sibson 1977) suggests. The Minch fault system might have also contributed to the station delay and as the Outer Isles Thrust zone its velocity structure is not controlled with the experiment.

The Hebridean region, overall, shows basement velocities ranging from 4.5 km/sec at the surface to about 6.20 km/sec at 4 - 6 km depth. The basement here underlies the Mesozoic (assumed velocities of 2.8 km/sec at the surface increasing linearly to 3.3 km/sec at 2 km depth) and Torridonian rocks (velocity of 4.8 km/sec at the surface rising to 5.2 km/sec at 4 km depth, Armour (1977) and section 4.2) whose lower interfaces have been slightly modified within the constraints described in section 4.3 to improve the fit between the observed and the calculated

arrivals. These gradients average to 3.1 km/sec, for the Mesozoic and 5.0 km/sec for the Torridonian rocks. Since first-arrival data from other Mesozoic basins in the area (e.g. Hall et al 1984 and section 4.2.1) can be effectively averaged to 2.8 - 3.3 km/sec, the assumed average velocity of 3.1 km/sec will not probably create greater uncertainty than 0.06 sec (equivalent to about 200 m for an isotropic layer) while the Torridonian layer should not create greater uncertainty than 0.02 sec for the above quoted range of velocities.

The basement velocities around Tiree appear to be higher by 0.1 - 0.2 km/sec than those around Iona suggesting higher grade metamorphism and/or probable increased proportion of basic material for the former area and/or attenuated basement structure for the latter area probably due to the Moine Thrust. Velocities at Iona are thus comparable to those on the Ross of Mull granite as the agreement between the travel times of the WISE 2 shots recorded at these stations would suggest.

A delay of about 0.20 sec for ray paths crossing the Great Glen fault zone has been attributed to the downward continuation of the low velocity crush zone which was tentatively observed on the model of the shallow structure (section 4.4). The zone can be traced with a fair degree of certainty down to about 5-6 km depth, mainly by considering the ray paths of Phase 2 - and their travel times - recorded at Iona and Mull, as shown in Fig. 5.2. For depths greater than those, the zone's seismic structure becomes ambiguous due to the uncertainties in the sedimentary delays (quoted above) for rays originating on the Hebridean basins and recorded at the South Jura and Mid Jura

stations, but mainly due to the large distances and velocity averaging effects involved in the propagation of these rays.

The substantial velocity contrast (about 0.5 km/sec), already shown between Lewisian and Dalradian rocks (Colonsay - Jura) during the modelling of the shallow structure (section 4.5), continues to a depth of at least 6 km and probably 8 - 9 km, the downward extension of the low velocity rocks being obscured by velocity averaging effects.

Towards Colonsay, the Lewisian / Dalradian interface is overlain by the high velocity Dalradian rocks, interpreted as the possible core of the Islay Anticline (Chapter 4), which are seismically indistinguishable from the Lewisian rocks and can be seen dipping at about 20^{o} to the SE.

The vertical high velocity zone at 155 - 160 km also continues downwards though its thickness becomes uncertain at depth greater than 4 km. This zone has been interpreted as the formation of Port Ellen phyllites and Crinan conglomerates heavily intruded by epidiorite sills.

Finally the low velocity basement rocks between Jura and Kintyre continue to depths of about 5-6 km and terminate against the higher velocity basement of the Midland Valley. The exact shape of the boundary between the two basements there cannot be modelled accurately due to the lack of sufficient number of recordings in the area, and thus the contours in the velocity-depth section there only suggest one possible interpretation.

5.3 HEBRIDEAN REGION: BARRA TO MULL

Modelling in this area proved to be rather problematic mainly because of a lack of accurate information on the velocity structure of the basins and the ambiguous quality of the data (Chapter 2). A further complication proved to be that the initial model had been constructed using data from the Hebridean stations and it was later found to be irreconcilable with the model of the central part of the profile (Colonsay - Kintyre) constructed by using the airgun and the WISE 2 explosive shots, producing large misfits for the calculated travel times of the high quality records of Mid Jura and South Jura stations (WISE1).

It then become clear that the explosive shot data recorded at the Hebridean stations could not support a stable model of their own, even after the introduction of the general constraints on the shallow and basement structures.

Thus, the composite model of Fig. 5.3 does not satisfy a small part of the data. These are the arrival times from shots 17 and 18 recorded at Mull and Colonsay and shot 17 recorded at Iona.

A careful examination of the relevant traces from the Mull record-section shows that the corresponding picks are quite ambiguous due to high noise or very low frequency content (section 2.4.1). The rest of the data recorded at the Hebridean stations are consistent with the model shown. The record section of Tiree also appears to possess some problematic traces (as the one of shot 16) probably due to the complicated down-faulted structure of the Inner Hebrides basin (Fig. 4.8).

The rest of the calculated arrival times usually fit the observed times (Fig. 5.4 to 5.17) to within 0.05 sec, which is considered acceptable when taking into account the quality of the data and the accuracy of the picks (Appendix 1, Table A.12), their areal coverage and the uncertainties in the shallow velocity structure quoted in the previous section.

Moreover, this part of the model satisfies the early - by about 0.20 sec - arrivals (with increasing range) at S. Jura and M. Jura stations from the Sea of the Hebrides. This can be achieved in, at least, two ways. Either by the introduction of higher velocities at a depth of 6 - 7 km or by cutting off the low velocity GGF zone at depth greater than 5 - 6 km. The ray diagram of Fig. 5.1 shows that a velocity contrast of about 0.15 km/sec at the former depth over a distance of about 50 km (50 - 100 km from Barra), produces the required effect. The former case is shown in Figure 5.3 but it must be emphasized that any intermediate model between those two extremes would satisfy the data.

Unfortunately, the shots between the GGF zone and Jura (115 - 150 km) recorded at Barra, whose rays, according to Fig. 5.1, should sample the above quoted probable features of the model, cannot help resolve the ambiguity since the traces of shots 14, 13 and 12 - at about 110, 116 and 122 km from Barra - appear to be very noisy and the attempted picks for shots 13 and 12 are probably too late by about 0.20 secs according to the calculated times (Fig. 5.4). The shots 11, 10 and 9 give calculated arrival times which fit the observed ones to within 0.10 sec which is

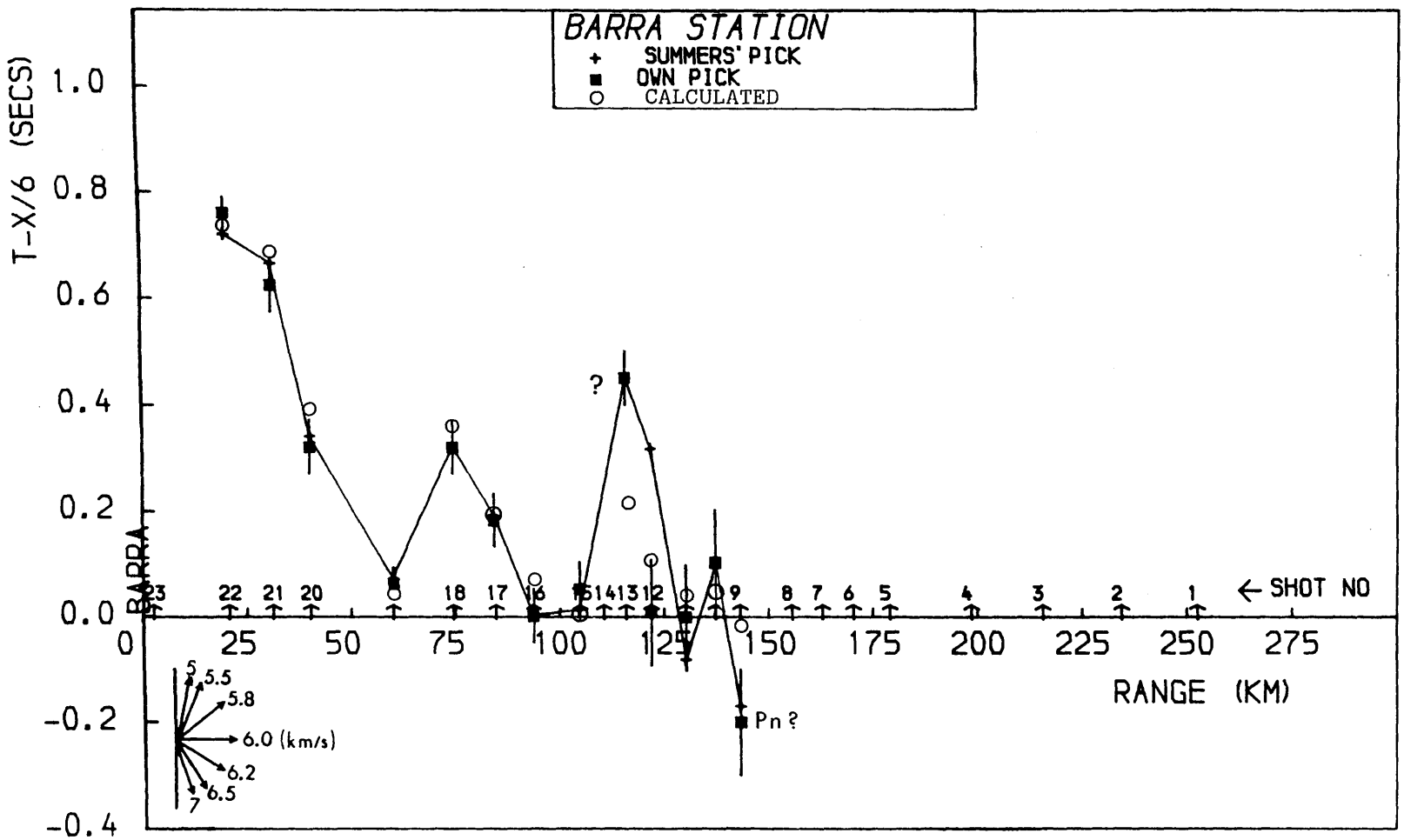

Fig. 5.4: Goodness-of-fit plot for the explosive data recorded at Barra station (Pg arrivals).

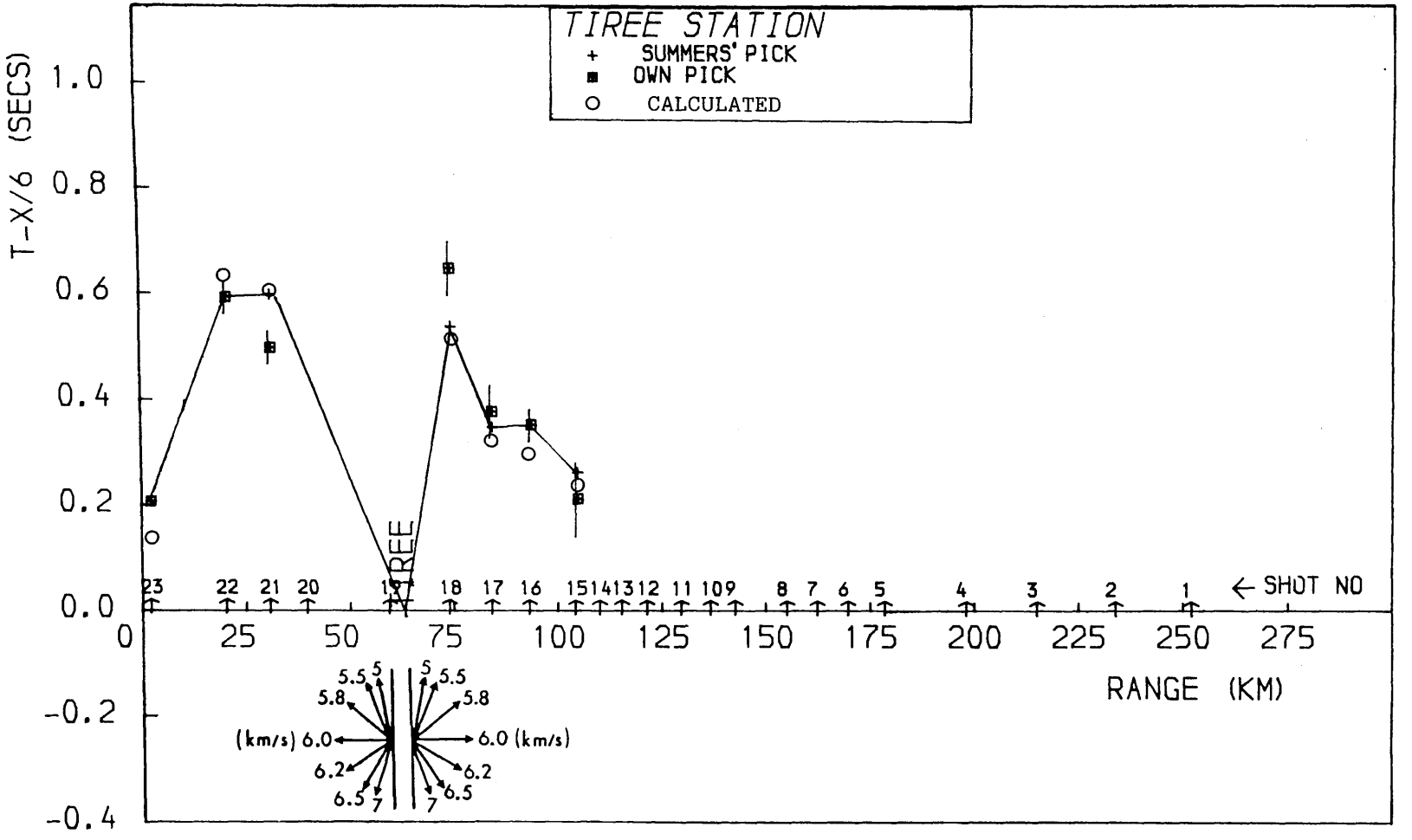

Fig. 5.5: Goodness-of-fit plot for the explosive data recorded at Tiree station.

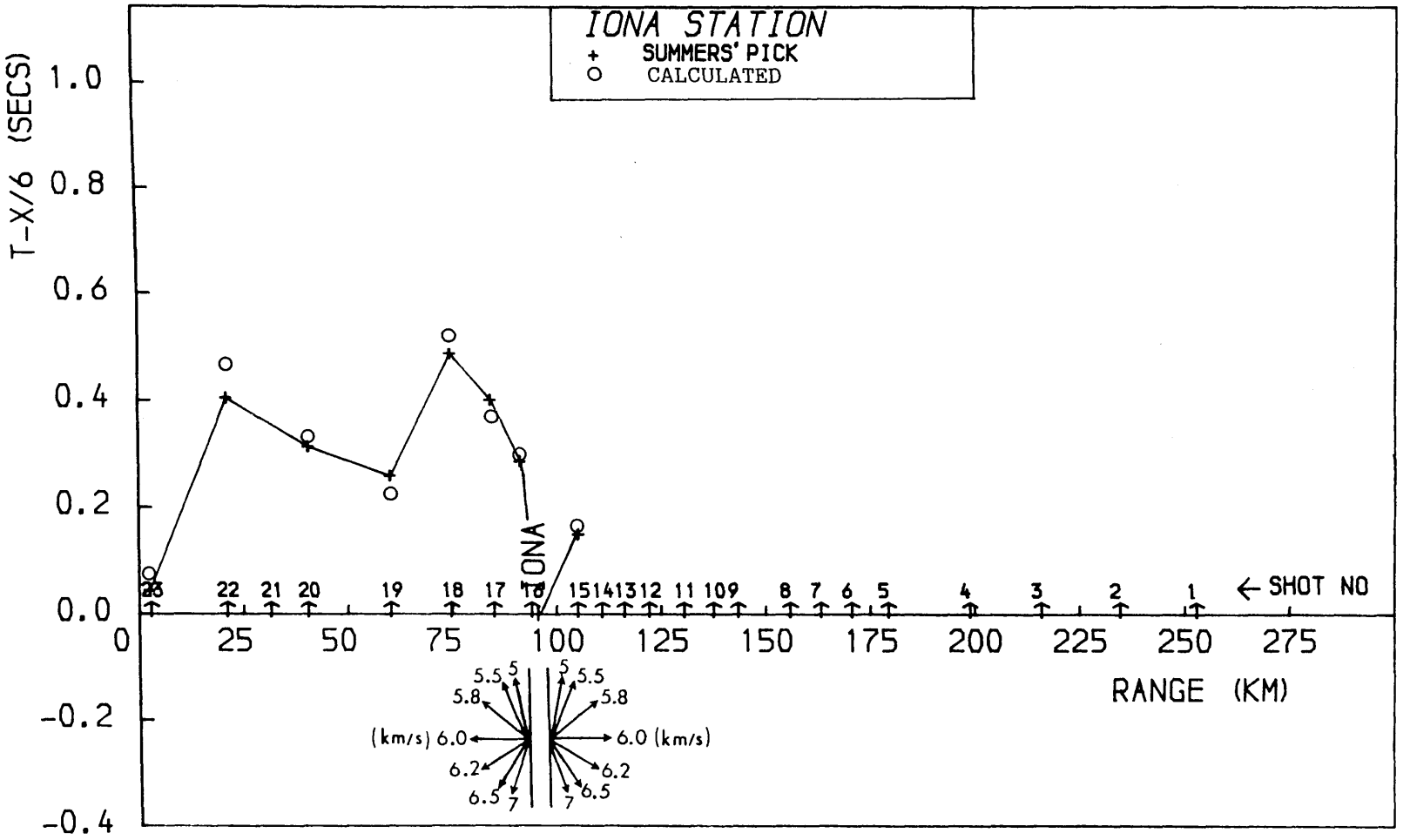

Fig. 5.6: Goodness-of-fit plot for the explosive data recorded at Iona station, (Phase 1).

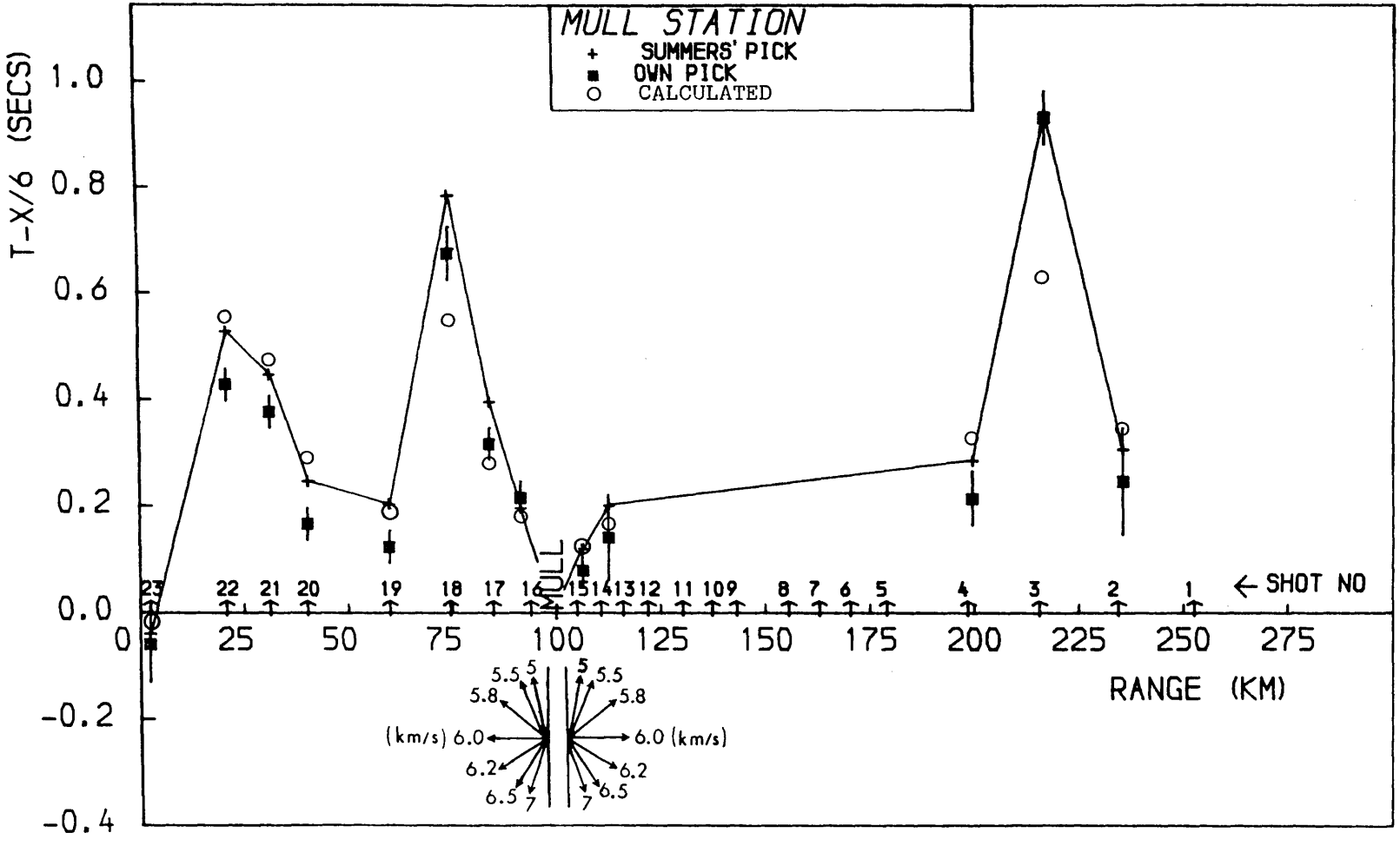

Fig. 5.7: Goodness-of-fit plot for the explosive data recorded at Mull station (Phase 1).

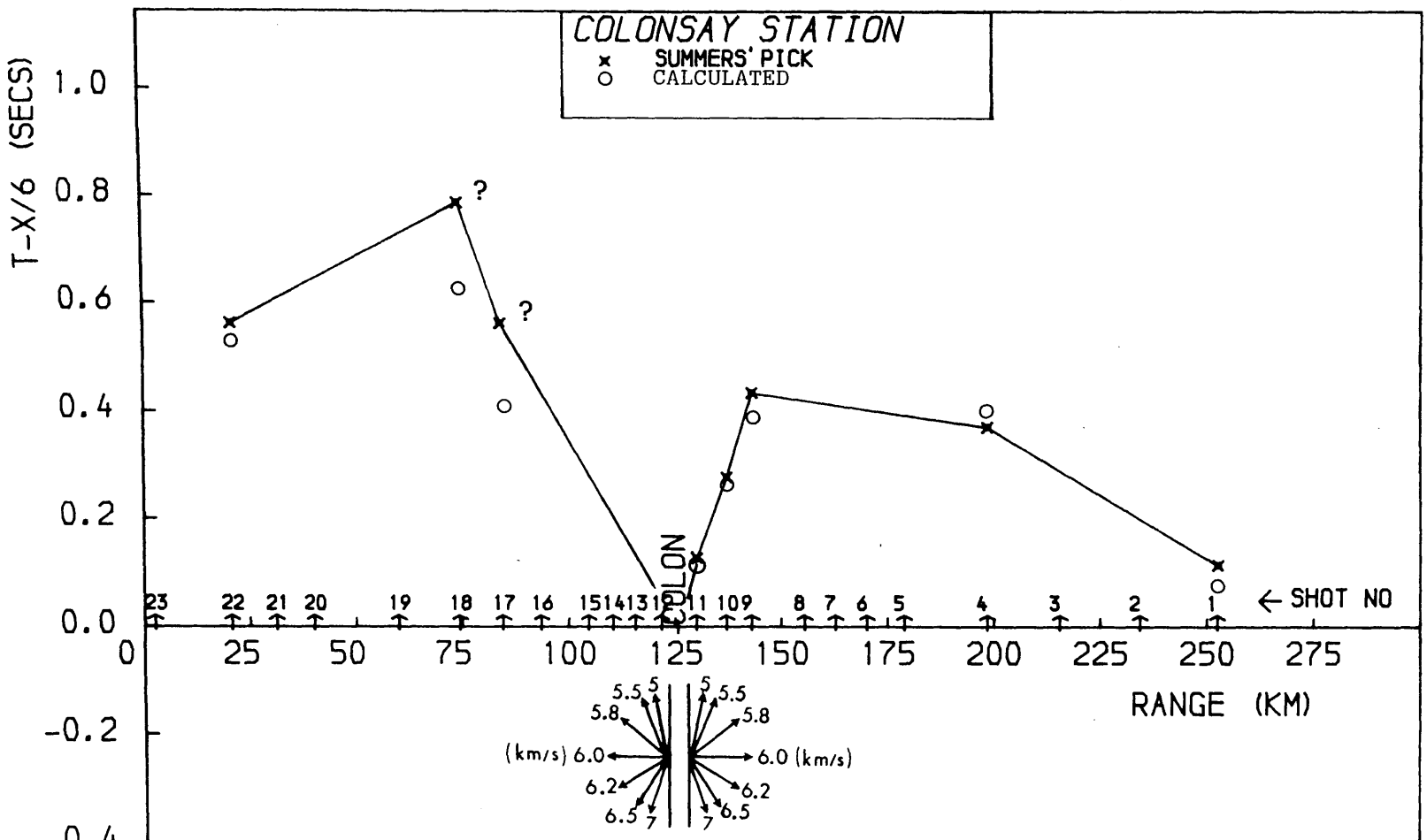

Fig. 5.8: Goodness-of-fit plot for the explosive data recorded at Colonsay station (Phase 1).

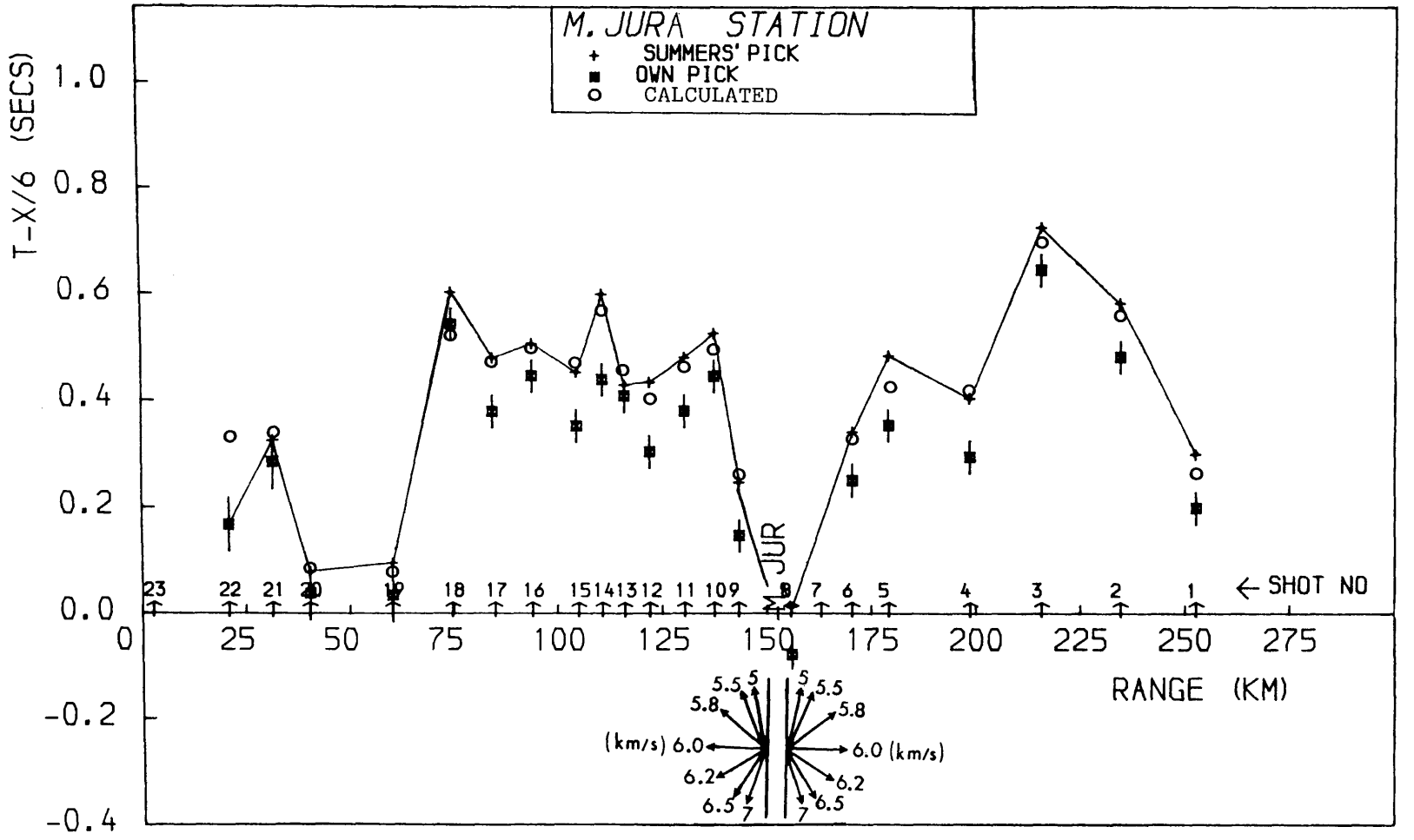

Fig. 5.9: Goodness-of-fit plot for the explosive data recorded at Mid Jura station (Phase 1).

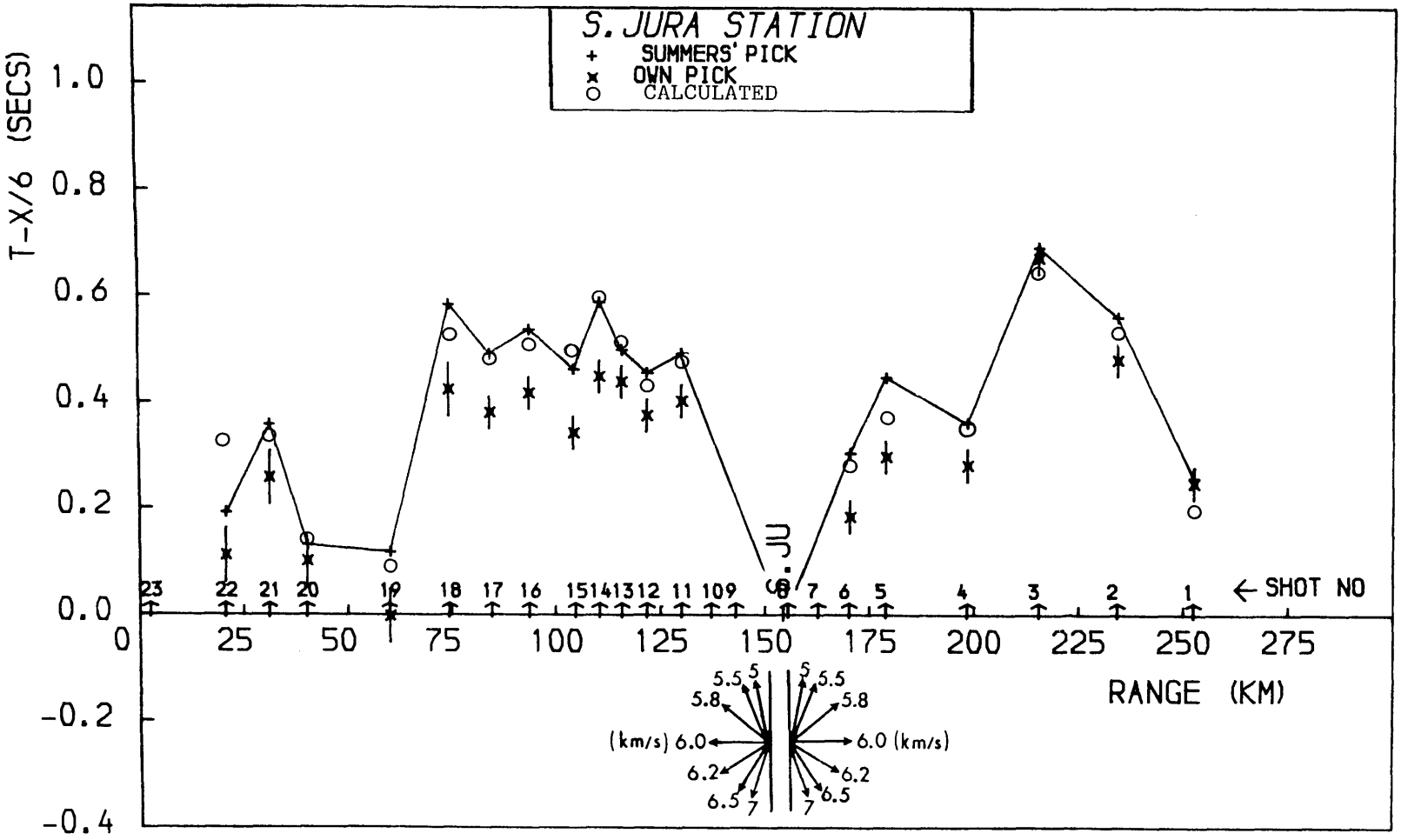

Fig. 5.10: Goodness-of-fit plot for the explosive data recorded at South Jura station (Phase 1).

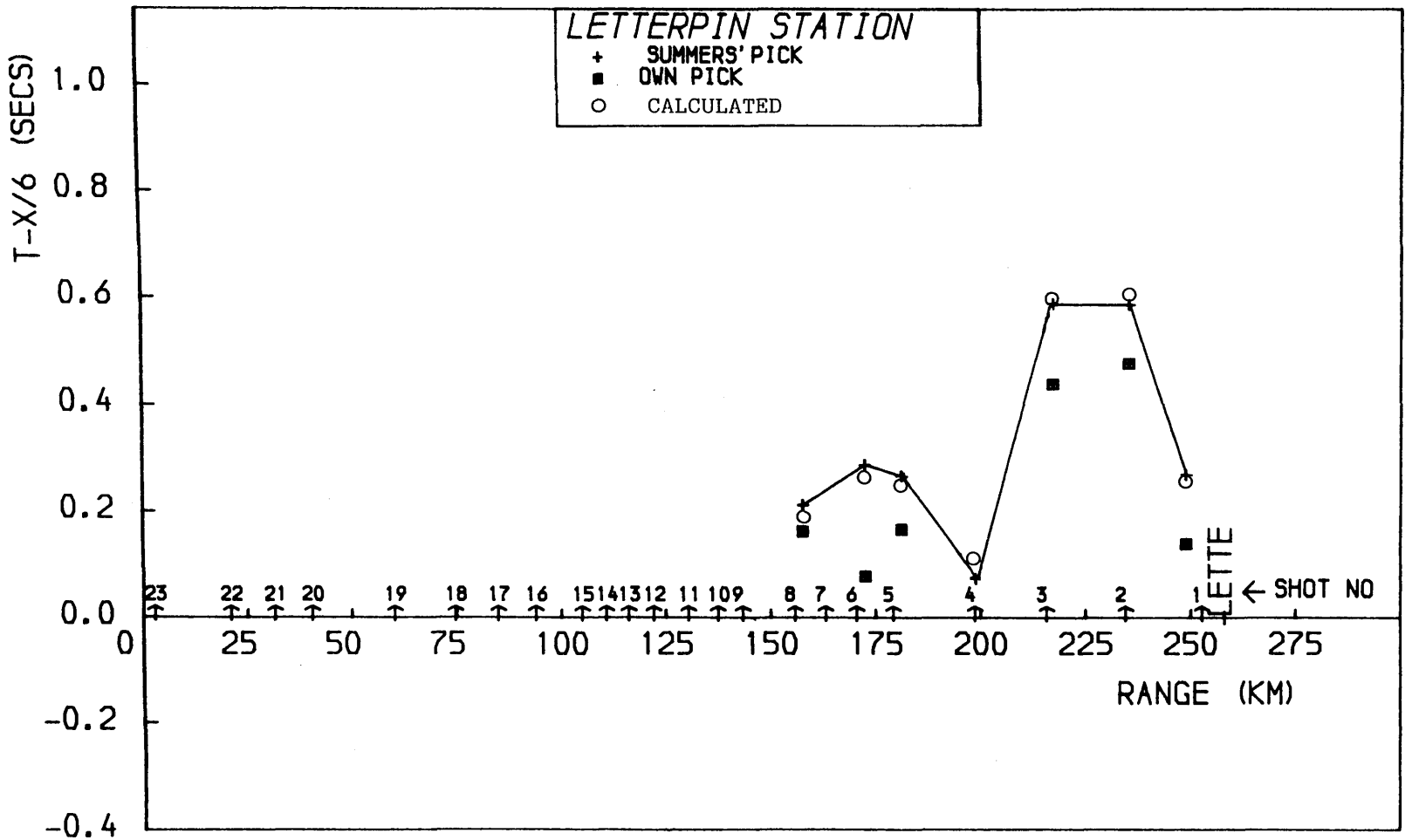

Fig. 5.11: Goodness-of-fit plot for the explosive data recorded at Letterpin station

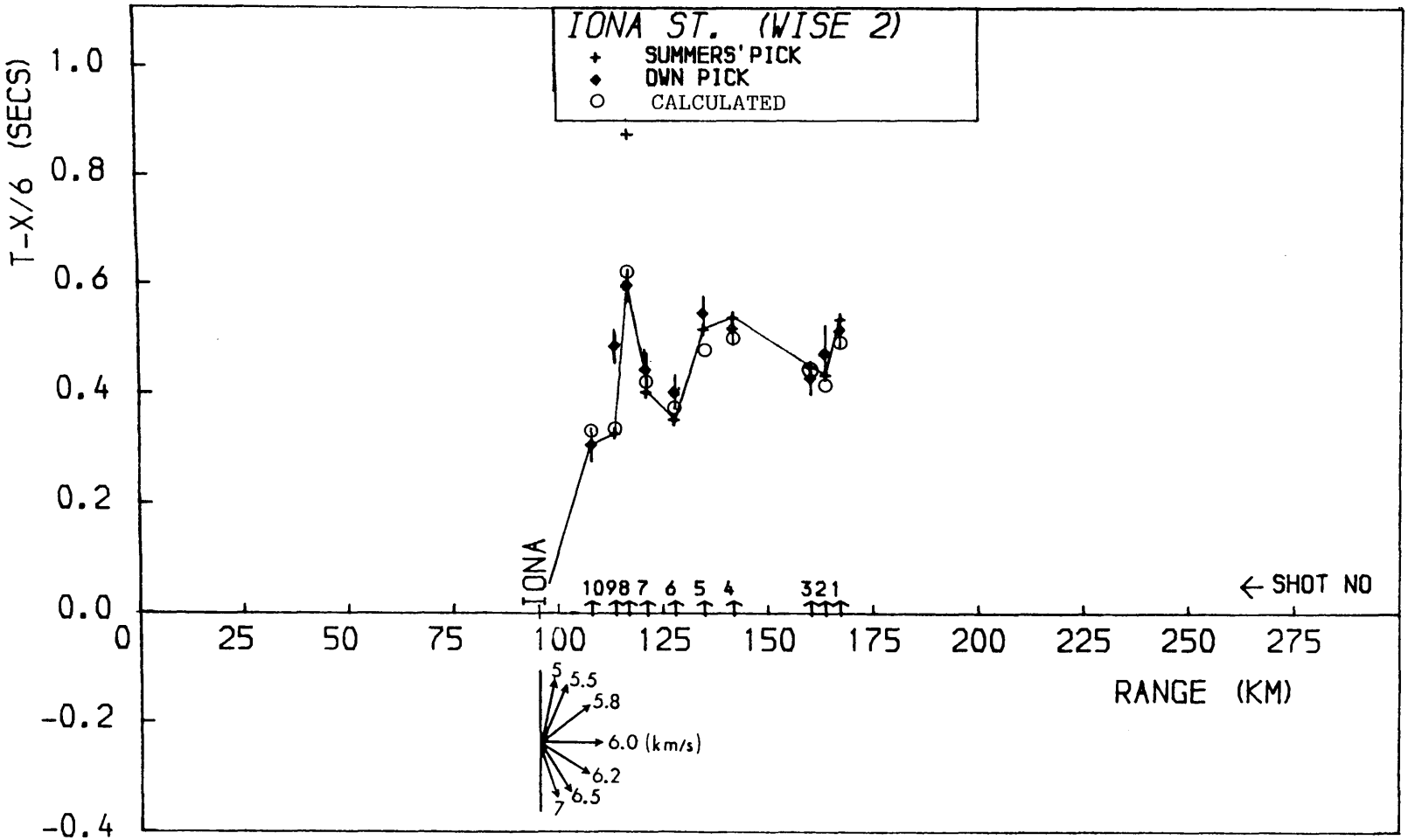

Fig. 5.12: Goodness-of-fit plot for the explosive data recorded at Iona station (Phase 2).

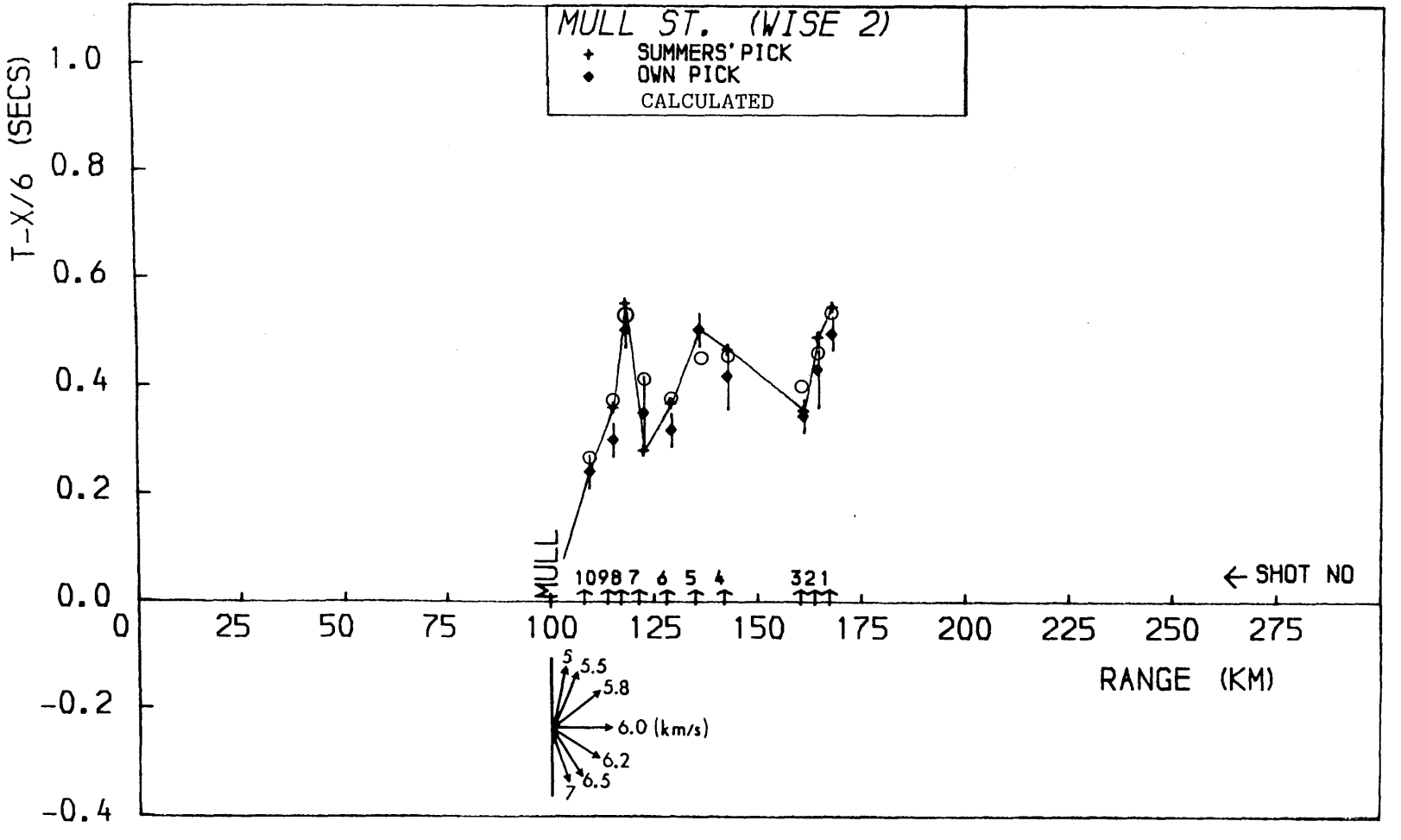

Fig. 5.13: Goodness-of-fit plot for the explosive data recorded at Mull station (Phase 2).

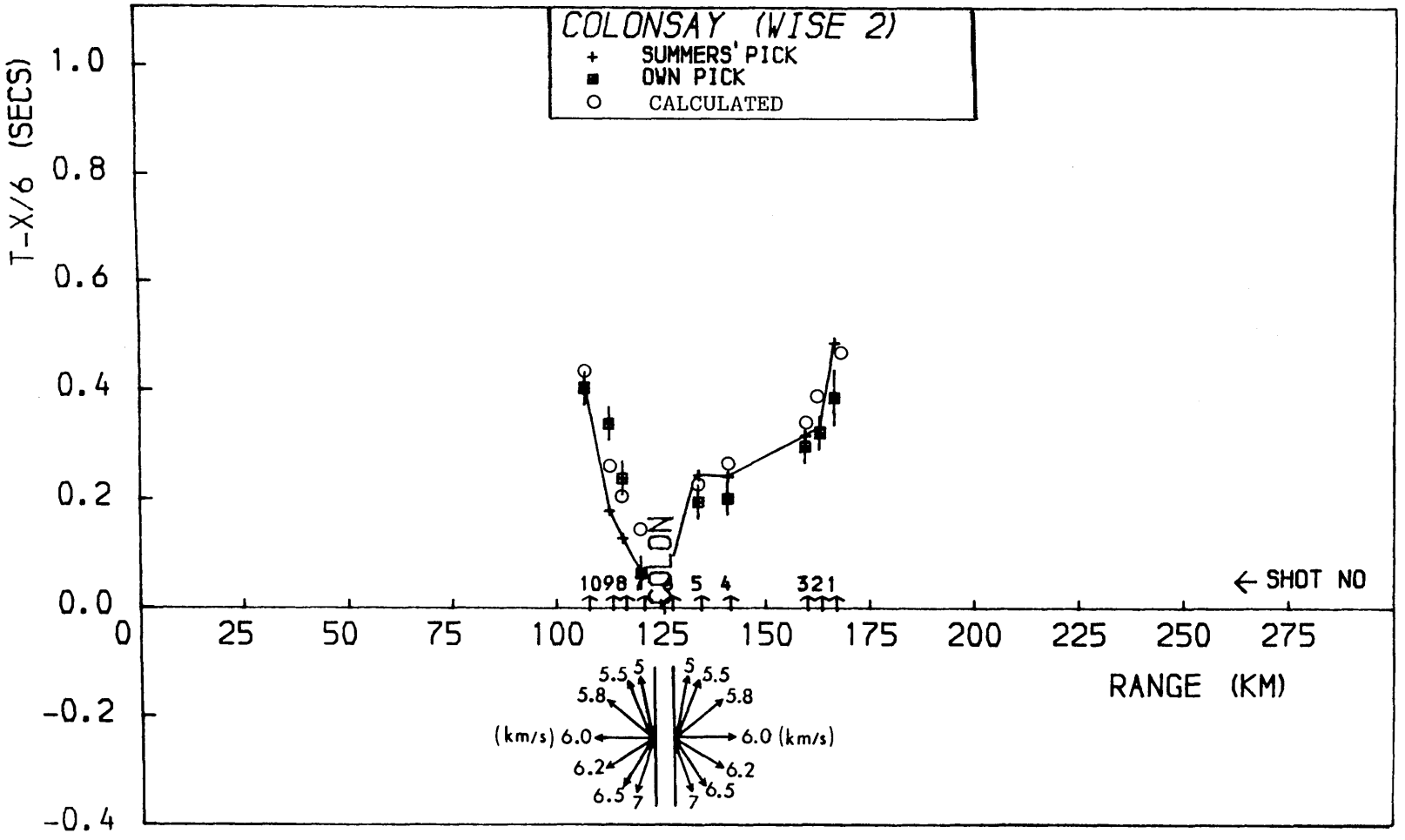

Fig. 5.14: Goodness-of-fit plot for the explosive data recorded at Colonsay station (Phase 2).

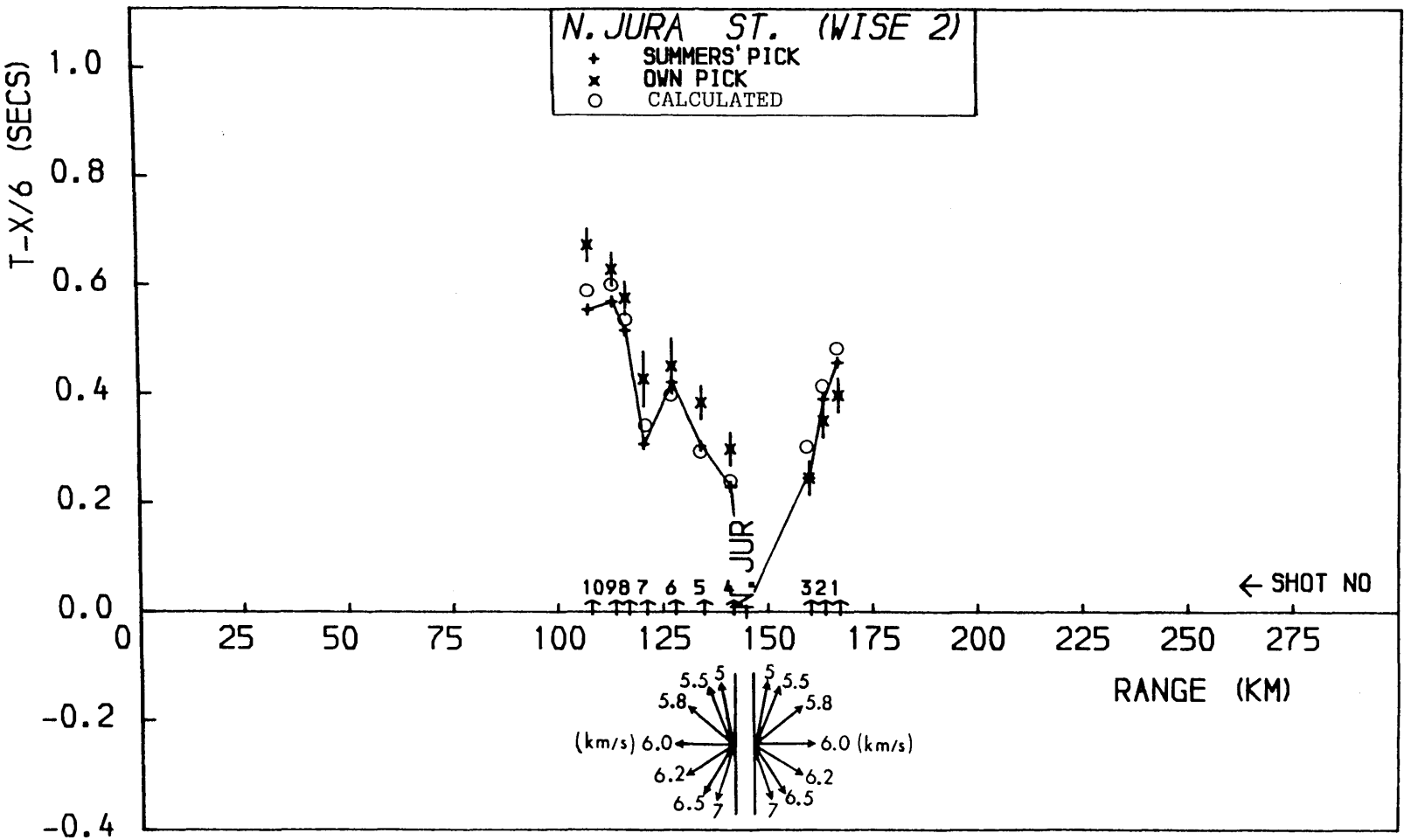

Fig. 5.15: Goodness-of-fit plot for the explosive data recorded at North Jura station (Phase 2).

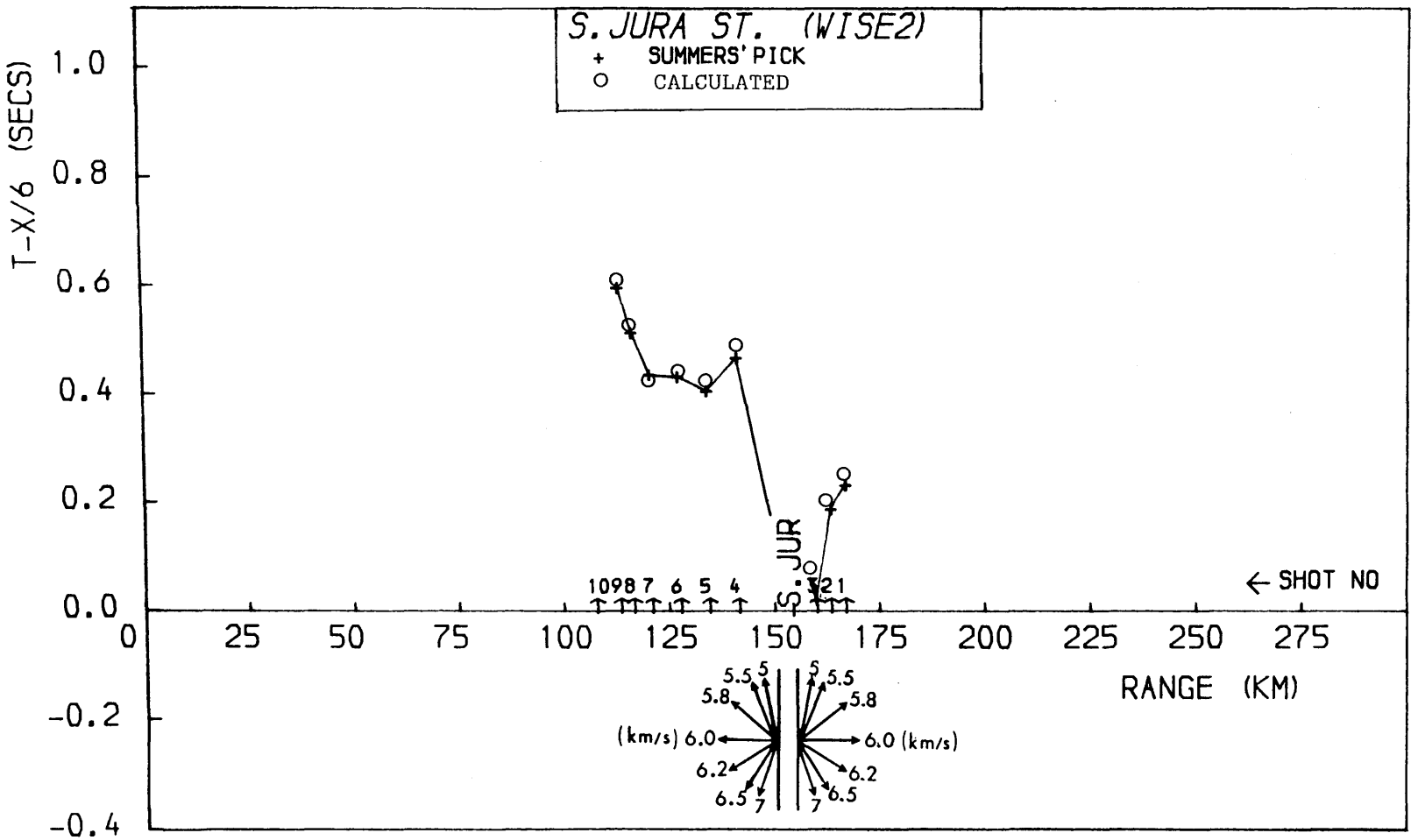

Fig. 5.16: Goodness-of-fit plot for the explosive data recorded at South Jura station (Phase 2).

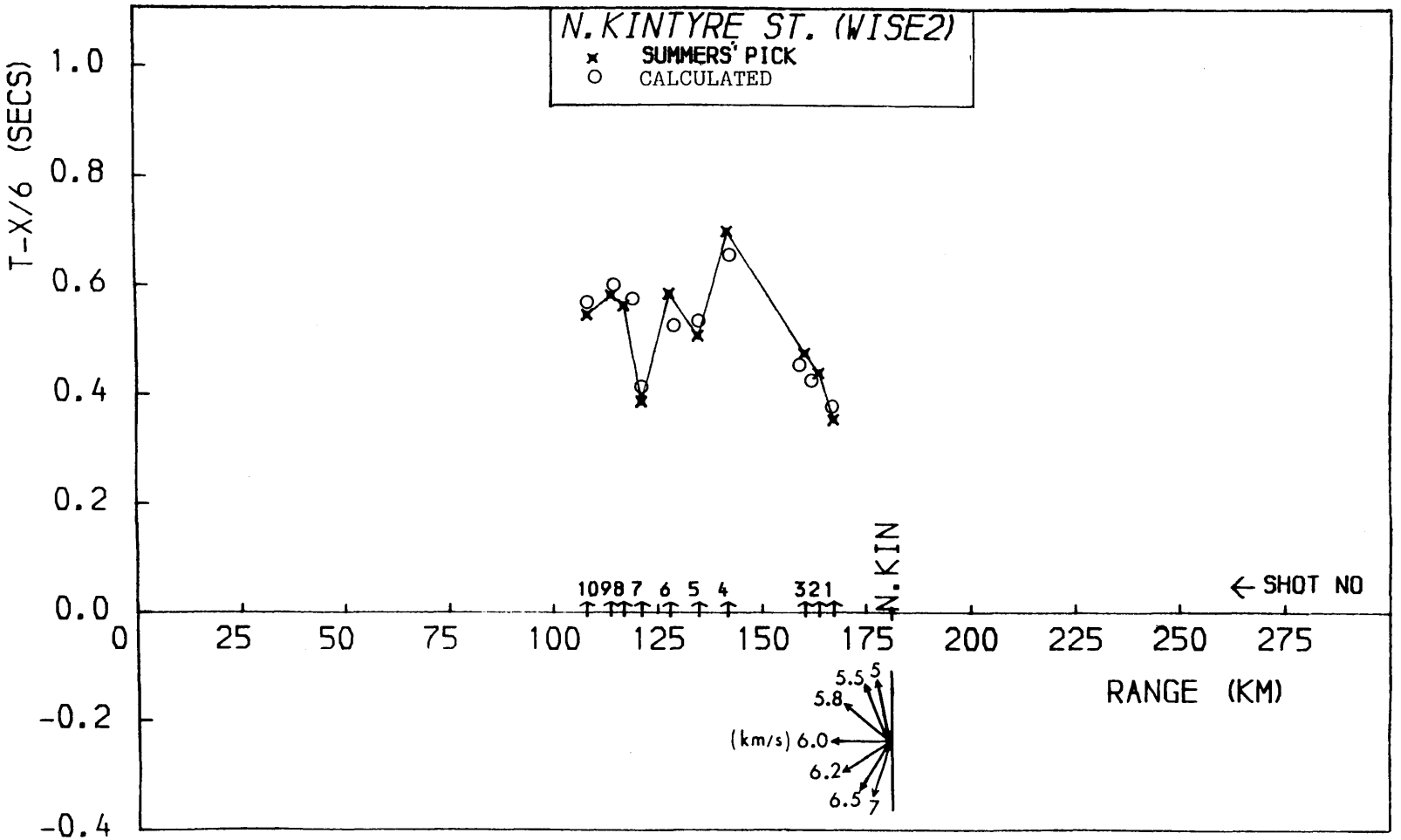

Fig. 5.17: Goodness-of-fit plot for the explosive data recorded at North Kintyre station (Phase 2).

the estimated picking error (Appendix 1), but the subsequent onset of Moho arrivals makes the identification of the pick of shot 9 - as a Pg or Pn arrival - ambiguous.

Overall, the structure of the upper crust in the Sea of the Hebrides shows no significant velocity contrasts at shallow levels (4 - 5 km), of the order of 0.30 km/sec or more as it was tentatively proposed by Summers (1982), who suggested shallow amphibolite / granulite transitions under Barra and Tiree in order to explain the small time-terms there.

The above may be true or it may not, and though the gravity field can be modelled in a way that would support the existence of granulite ridges under Barra, Tiree and Iona (e.g. Shaw 1978; Fig. 5.18), the resolution and accuracy of the model that the seismic data can support does not justify any definite conclusions. As the joint uncertainty due to the basins structure (section 5.2) and the accuracy of the picks (let alone shot positioning and timing uncertainties, Appendix 1), is of the order of 0.15 sec and a granulite ridge under Tiree (assumed velocity contrast of 0.3 km/sec) of 15 - 20 km width would have a similar effect on the travel times, it is obvious that a granulite basement model cannot be supported by shots fired on the basins which account for the majority of the data in the area.

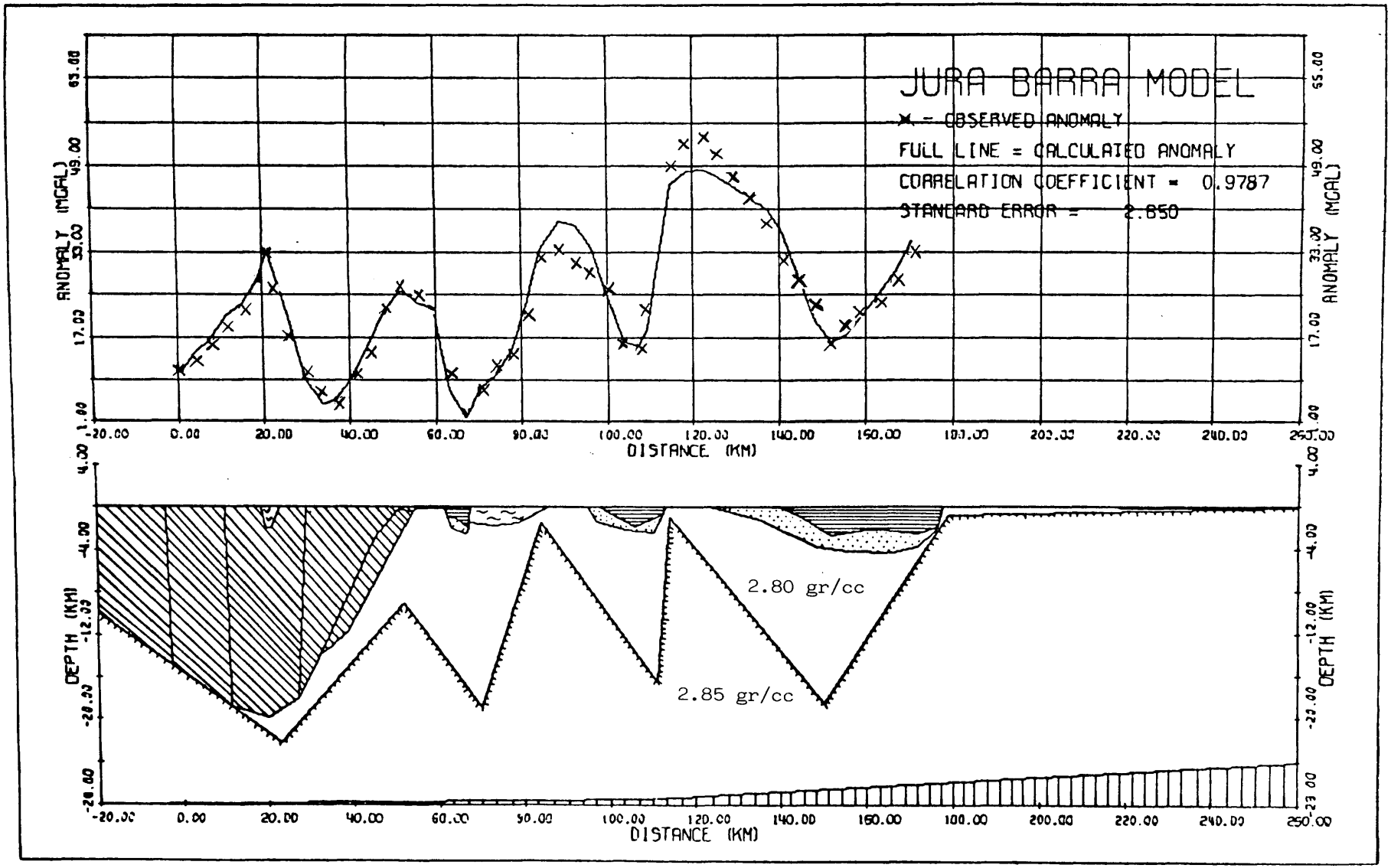

Fig. 5.18: Gravity model between Jura and Barra showing possible granulite ridges (d=2.85 gr/cc) underlying amphibolite facies rocks (d=2.80 gr/cc). After Shaw (1978).

5.4 GREAT GLEN FAULT AND THE DALRADIAN BASIN

As quoted in the previous Chapter and in section 5.3 the velocity structure of the Great Glen Fault zone becomes uncertain at depth greater than 5 - 6 km. The zone has been modelled as being vertical and possessing a constant width of 4 km across the section. Though it is reasonable to assume that the crush zone at shallow depth is merely an extrapolation of its land expression (e.g. Eyles and McGregor, 1952), despite probable rapid velocity changes within the zone that are responsible for some discrepancies of the data recorded during the second Phase at Mull and Iona (Fig. 2.40), its specific structure at depth greater than 3 km or so is not particularly well constrained by the seismic refraction method and it was only adopted for convenience.

Current ideas on the possible modes of downward continuation of major fault zones - based mainly on observations of the rock textures within thrust or fault zones, seismic reflection data and laboratory studies on the behaviour of quartz bearing rocks to deviatoric stress with increasing temperature - show that a number of possible situations might exist (Sibson 1983).

These are shown in Fig. 5.19 and range (for a strike slip fault) from downward continuation of the relatively narrow fault zone from the upper brittle crust (characterized by frictional regime) to the lower ductile crust (characterized by quasi-plastic regime), through shear zones that widen with depth into the crust, to an abrupt transition into a sub-horizontal

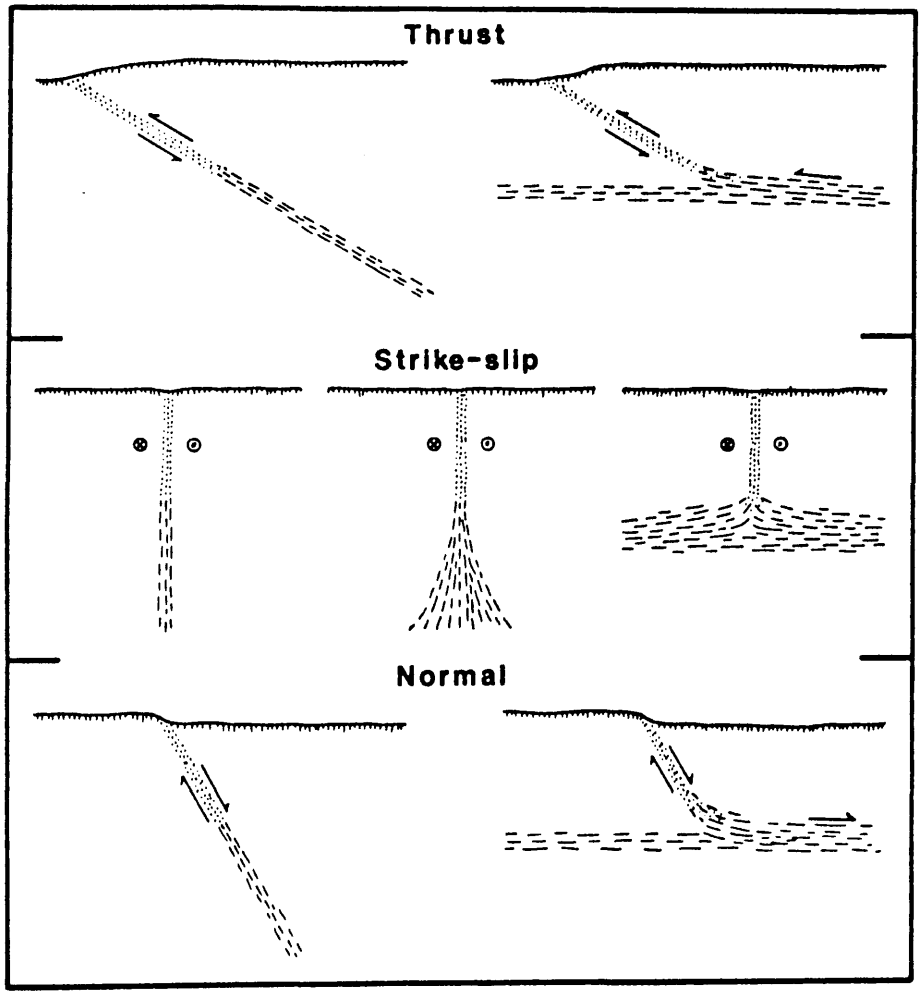

Fig. 5.19: Possible modes of downward extension of major fault zones. Frictional regime dotted, quasi-plastic shear-zones dashed (after Sibson 1983).

decoupling shear zone. (e.g. Prescott and Nur 1981, Lachenbruch and Sass 1980, Watts and Williams 1979). The abundance of shallow earthquake sources and the paucity of lower crustal sources support the possibility for a lower quasi-plastic regime (Jackson and McKenzie 1983, Chen and Molnar 1983).

Though transcurrent gneissose shear zones up to 40 km wide and displacements of the order of 100 km or more have been described (Bak et al, 1975), no seismic evidence on the possible presence of an extensive crustal low velocity zone in California exists (Sibson 1983, Hill 1978), though there is some evidence for the Basin and Range Province (Smith, 1978).

Intra-crystalline quartzo-feldspathic rocks should in general decrease their shear resistance exponentially at temperatures higher than about 300°C, (e.g. Tullis and Yund 1977), thus resulting in plastic behaviour and a somewhat abrupt widening of the fault zone, but it is possible that the downward extension of large earthquake ruptures might disrupt the continuity of the zone within the upper reaches of the quasi-plastic regime (Sibson 1980).

Evidence of unusual fold interference patterns (e.g. Watson 1984) associated with the Strathconon, Killin and Tay faults - which belong to the Great Glen fault set - suggest that the GGF set began to develop when rocks at the present level of erosion were still moderately ductile. The first displacements were thus taken up by broad shear zones but as temperatures started to decline (during the unroofing of the Highland metamorphic complexes produced by the Grampian orogeny, Chapter 1), the movement probably became restricted to discrete fault zones.

The distribution of mineral ages shows (Dewey and Pankhurst 1970) that around 430 Ma blocking temperatures of 300-350°C had been reached over most of the Grampian Highland and thus by 400 Ma the whole Highland region was below these temperatures.

As only a few kilometres at most seem to have remained above the present level of erosion (Watson 1983), and the principal movements of both the Great Glen fault and Highland Boundary fault have been dated between early Devonian and late Carboniferous times (e.g. Smith and Watson 1983 and section 1.5), it seems reasonable to assume - supposing a thermal gradient of 20°C/km at those times, which results in 300°C at depth of 15 km - that at present at least 10 km or so of upper crust remain, where intense frictional regime (and cataclasis) have probably prevailed during the main GGF movements.

The above indicate that the geological evidence so far supports the downward extension of the GGF by a localized low velocity zone (LVZ), down to a depth of about 10 km below the present level of erosion which is well beyond the depth-limit of the resolution that the WISE data can offer.

At lower crustal depths, the structure of the fault will depend on the geothermal gradient, crustal composition, the presence of fluids and the tectonic strain rate. Brittle behaviour will prevail at relatively basic (quartz-poor) dry crust, and high tectonic strain rate.

No vertical LVZ was observed by the LISPB profile in the north-eastern extension of GGF to the Grampian Highlands (Bamford et al 1977, Bamford et al 1978) probably due to the low

quality of the data there and extensive granitization of the crust (Dimitropoulos 1981). Also, the WINCH profile shows that the GGF zone does not continue sub-vertically through the lower crust into the upper mantle and is probably confined to the upper crust (Hall 1986).

The Dalradian basin area (up to Kintyre) is well constrained mainly due to the use of the airgun data during modelling of the shallow structure (Chapter 4), and due to the good quality of the WISE2 explosive shots. The metasediments usually show basement velocities < 5.5 km/sec apart from the high-velocity structures interpreted as the core of the Islay Anticline and the Port Ellen phyllites / Crinan conglomerates (intruded by numerous epidiorite sills).

The latter feature has been modelled as being vertical but that was adopted for convenience and can be considered as a compromise amongst a number of slightly contradicting pieces of evidence. These are, the structural evidence according to which the Jura quartzite strata dip to the SE at about 30° (Anderton 1976), the gravity model of Fig. 4.21 requiring an oppositely dipping high density zone, and the magnetic model of Westbrook and Borradaile (1979) for the Tayvallich volcanics, requiring a similar dip of about 20° to the NW. Because of the small dips involved, considering the geometry of the rays during refraction propogation (Fig. 5.1, 5.2) the real dip of the zone at shallow depths (0 - 2 km) cannot be constrained, while at greater depth the zone is considered to be vertical as the structural evidence of section 1.6 suggests.

Velocity contrasts within the Dalradian quartzites probably

persist to a depth of at least 7 - 8 km, but though the general picture of the structures is believed to be correct, the actual thicknesses of the high velocity zones are not very well constrained by this method and structural considerations of the known geology suggest that they might vary a lot, both along the strike (Roberts and Treagus 1977) and across the strike (e.g. Anderton 1979, Soper and Anderton 1982).

The current work is in agreement with the interpretation of the magnetic field in the area suggesting the general shape of the Lewisian / Dalradian interface (Westbrook and Borradaile 1979), though no definite answer can be given to their suggestion that highly magnetic Lewisian granulites underlie Colonsay at a depth of about 5 km, mainly due to relative uncertainty on the exact magnitude of the GGF zone delay and on the exact shape and velocity structure of the Dalradian basin at this depth. The gravity interpretation in this area (Fig. 4.21) also suggests that there is no need for the introduction of a dense body, (interpreted as the probable core of the Islay Anticline) deep in the basement between Colonsay and Jura, as was found to be necessary by Westbrook and Borradaile (1979) under Islay.

The structure under the Kintyre peninsula remains uncertain, mainly due to the lack of a recording station at the South Kintyre (along the WISE profile) and more shots in the area, but Dalradian basement velocities do not seem to vary much towards Kintyre.

5.5 KINTYRE TO GIRVAN: THE MIDLAND VALLEY

As no detailed information on the basin structure across the basin was available, the shown interfaces and velocities, though believed to be broadly accurate (section 4.7), have been slightly modified in order to produce the required basin delays that would seem to fit the data best. Since the Girvan stations have a considerable areal distribution and the geology of the area is very complicated in 3 dimensions, only the Letterpin station data were used.

Though the structure of the Highland border remains elusive, and the simple shape of the LORS / basement interface towards Kintyre might consist of a series of "en echelon" faults which effectively displace the Highland Boundary Fault to the SE (Hall et al 1984), the general shape of the basin is believed to be correct as the agreement between calculated / observed TT's suggests.

The interpretation of the shots in the area, recorded at Letterpin and at a few other stations, shows that the crystalline basement refractor of the Midland Valley (velocity about 6.1 km/sec) probably underlies directly the LORS strata of the Arran basin and is very shallow under Girvan (1-2 km).

Under shot 4 (just off Kintyre) the high velocity basement rises considerably as Fig. 5.3 shows and thus gives rise to a local increase of the gravity field of about 5 mGal (Fig. 4.2).

5.6 MOHO ARRIVALS

Due to the low quality of the WISE 1 data only shots 1 to 8 recorded at Barra station (Fig. 2.4) and shot 23 recorded at the Jura station (Fig. 2.7, 2.8) produced reliable Moho arrivals. As those arrivals are considered too few to constrain the depth to the Moho in a crustal model along the profile, especially after the complicated structure of the lower crust and upper mantle in the area shown by the interpretation of the WINCH profile (Hall et al 1984), modelling of these arrivals was not attempted.

5.7 THE COMPOSITE GEOLOGICAL SECTION

All the above quoted features of the model (sections 5.2 - 5.5) can be seen in the composite geological section of Fig. 5.20 (Back pocket). In addition the Figure shows all the existing information (mainly on shallow structure) along the profile as explained or referred to in Chapters 4 and 5. That information was used to constrain the models of the shallow structure (both seismic and gravitic; sections 4.4, 4.5 and 4.6) which are also shown in the Figure.

The basin interfaces in the Sea of the Hebrides lie within the general limits of the controls quoted in section 4.3, while the shallow structure between Mull and Girvan is constrained as described in sections 4.4 - 4.7. Within the basement, interfaces have replaced the high lateral velocity gradients between Lewisian / Dalradian and Dalradian / Dalradian formations, though as depth increases the interfaces can only

denote the approximate position of lithological transitions. That is particularly possible for the formation of Port Ellen phyllites to the SE of Jura, where a dense / high velocity body does not probably coincide with the geological boundaries but is formed due to the intrusion of Dalradian sills into the phyllites and, to a lesser extent, into the Jura quartzites.

5.8 GENERAL DISCUSSION AND COMPARISON WITH ADJACENT AREAS

The interpretation along the profile has been impeded by data of variable quality and availability.

In the Sea of the Hebrides, ray-tracing has not distinguished any strong lateral velocity variations within the basement as envisaged by Summers (1982) when trying to explain the small magnitude of the time-terms under Barra and Tiree. A number of probable late picks (due to high noise or low frequency content), corresponding to shots in the Inner Hebrides basin, have probably imbalanced the time-term solution by over-estimating the basin shot delays and thus under-estimating the time-terms under Tiree (and to a lesser extent under Barra), calculated using the least-squares criterion. The effect on the Iona - Mull time-term was minimal due to the extra control provided by the better quality WISE2 shots. An example of the sensitivity of the time-term solution to incorrect assumptions is given by Bamford (1973).

Current ideas on the structure of the region consider the reactivation of Caledonian thrusts as normal faults during the Mesozoic extension, as the dominant mode of basin formation (eg.

Smythe et al 1983, Brewer and Smythe 1984, Hall et al 1984). As tilting of crustal blocks is implied during normal faulting, one would expect low velocity basement to underlie deep basins and that should have been confirmed with an upper crustal experiment if the velocity gradient prior to rifting was high enough for seismic detection. A velocity contrast of about 0.25 km/sec at a depth of 3-4 km under exposed basement ridges and basins would have been sufficient for a positive identification by the WISE experiment. But according to Armour (1977), who could not distinguish any mid-crustal refractions in the HMSP data, the average velocity for the greatest part of the crust in the Hebridean craton is only about 6.2 km/sec. This suggests that, if we accept a fundamental similarity between the crustal structure beyond the Outer Hebrides and the one in the Sea of the Hebrides e.g. WINCH profile, Hall et al 1984, the upper crust does not exhibit any considerable large-scale velocity contrast and the small time-terms under the Hebridean basement ridges come partly from an overestimation of basin delays and partly from velocity contrasts in the lower crust.

In the Dalradian area, the low basement velocities have been shown to persist at great depth, probably 8-10 km in accordance with the interpretation of the upper crust of the WINCH profile (Hall et al 1984). Though it is probable that the crustal structures under the WISE and WINCH profiles are similar (Hall 1985), extrapolation to the NE is much more tentative due to the shallowing of the Dalradian basin and probable extensive granitization of the upper crust (e.g. Hipkin and Hussain 1981)

to the north of the Cruachan Lineament. The high diversity along the Dalradian is shown in geophysical (Hall 1985), geochemical, metamorphic and stratigraphical patterns which have been interpreted as reflecting the formation of pull-apart basins during the extensional phase of the orogeny, bound by transcurrent faults of strike perpendicular to the Caledonoid one (Fettes et al 1986, Graham and Borradaile 1984).

Compared with the interpretation of the LISPB profile in the area where it crosses the Dalradian outcrop (velocity of 5.8 km/sec at surface rising slowly to 6.05 km/sec at 10 km depth), significantly different velocities and velocity contrasts have been revealed by the WISE profile in the SW Highlands. The best established contrasts are due to the Jura Quartzite, but some contrast also occurs between the Dalradian of Jura / Kintyre and those under LISPB especially at shallow depths. Though it is tempting to attribute that contrast to the different grade of metamorphism (of greenschist facies in the SW Highlands / mainly of amphibolite facies in the Central Highlands, Fettes et al 1986), it is possible that it stems from the lack of adequate control under the uppermost 3 km or so along the LISPB profile.

The Dalradian area appears to be isostatically adjusted following the post-orogenic period, and Hall et al (1984) have envisaged a zig-zag sort of obduction during which the upper part of the Dalradian was cleaved off the lower part by the Lewisian basement, probably along the Loch Skerrols thrust.

CHAPTER 6

Conclusions

The extensive use of ray tracing is considered to have succeeded in producing much clearer models than those produced by direct inversion techniques (Time-term / Plus-minus), though a serious drawback was found to be the long execution time of the ray tracing program.

Apart from the detailed conclusions on the shallow structure (sections 4.4.4, 4.5.4 and 4.6.4) the main conclusions of Chapters 4 and 5 can be summarized into the following:

1. In the Sea of the Hebrides, no concrete evidence exists in the data for a shallow transition (1 - 5 km depth) from amphibolite to granulite facies rocks.
2. The Great Glen Fault coincides with a low velocity zone which can be confidently traced to a depth of 5 - 6 km and whose structure at greater depth cannot be quantified by the data.
3. A Mesozoic sedimentary cover of a maximum thickness of about 500 m lies on Dalradian basement rocks between Colonsay and Jura while no such cover exists on the Dalradian rocks between Jura and Kintyre.
4. The Lewisian / Dalradian interface and the inter-Dalradian velocity contrasts persist to a depth of about 7 - 9 km and they show a general shape and disposition compatible with existing ideas on the structure of the area.

REFERENCES

ANDERTON R. 1971. Dalradian Palaeocurrents from the Jura Quartzite. SCOTT J GEOL 7, 175-178.

ANDERTON R. 1976. Tidal-shelf sedimentation: an example from the Scottish Dalradian. SEDIMENTOLOGY 23, 429-458.

ANDERTON R. 1977. The Dalradian rocks of Jura. SCOTT J GEOL 13, 135-42.

ANDERTON R. 1979. Slopes,submarine fans and syn-depositional faults: sedimentology of parts of the middle and upper Dalradian in the SW Highlands of Scotland. In: The Caledonides of the British Isles - reviewed, edited by Harris A.L., Holland C.H. and Leake B.E., SPEC PUBL GEOL SOC LOND 8, 483-8.

ANDERTON R. 1980a. Distinctive pebbles as indicators of Dalradian provenance. SCOTT J GEOL 16, 143-52.

ANDERTON R. 1980b. Did Iapetus start to open during the Cambrian? NATURE, LONDON, 286, 706-8.

ANDERTON R. 1982. Dalradian deposition and the late Precambrian-Cambrian history of the N. Atlantic region: a review of the early evolution of the Iapetus Ocean. J GEOL SOC LOND 139, 421-431.

ANDREWS I.J. 1985. The deep structure of the Moine thrust northwest of Scotland. SCOTT J GEOL 21, 213-217.

ARMOUR A.R. 1977. A seismic refraction study of the crustal structure of the Northwest Scotland and adjacent continental margins. Ph.D. thesis, University of Durham.

ATREE M.C. 1982. Seismic refraction study between Colonsay and Mull. B.Sc. thesis, University of Durham.

BAILEY E.B. 1917. The Islay anticline, Inner Hebrides. Q J GEOL SOC 72,132-164.

BAK J., GROCOTT J., KORSTGARD J.A., SORENSON K., NASH D.F. AND WATTERSON J. 1975. Tectonic implications of Precambrian shear belts in western Greenland. NATURE, LOND 254, 566-569.

BAMFORD D. 1973. An example of the iterative approach to time-term analysis. GEOPHYS J R ASTRON SOC 31, 365-372.

BAMFORD D., NUNN K., PRODEHL C. AND JACOB B. 1977. LISPB-III: Upper crustal structure of northern Britain. J GEOL SOC LOND 133, 481-488.

BAMFORD D., NUNN K., PRODEHL C. AND JACOB B. 1978. LISPB IV: Crustal structure of northern Britain. GEOPHYS J R ASTRON

SOC 54, 43-60.

BAMFORD D. 1979. Seismic constraints on the deep geology of the Caledonides of northern Britain. In: Harris A.L., Holland C.H. and Leake B.E.(eds), The Caledonides of the British Isles -reviewed, SPEC PUBL GEOL SOC LOND 8, 93-98.

BARBER P.L., DOBSON M.R. AND WHITTINGTON R. 1979. The geology of the Firth of Lorne, as determined by seismic and dive sampling methods. SCOTT J GEOL 15, 217-230.

BARRY K.M. 1967. Delay time and its application to refraction profile interpretation. In: Seismic Refraction Prospecting, edited by A.W. Musgrave, Society of Exploration Geophysicists, Tulsa, Oklahoma, pp. 348-361.

BECKINSALE R.D. AND OBRADOVICH J.D. 1973. Potassium - Argon ages for minerals from the Ross of Mull, Argyllshire, Scotland. SCOTT J GEOL 9, 147-156.

BERRY M.J. AND WEST G.F. 1966. An interpretation of the first arrival data of the Lake Superior experiment by the time-term method. BULL SEISMOL SOC AMER 56, 141-171.

BINNS P.E., MCQUILLIN R., KENOLTY N. 1973. The geology of the Sea of the Hebrides. IGS REP 73/14.

BINNS P.E., MCQUILLIN R., FANNIN N.T.G., KENOLTY N. AND ARDUS D.A. 1975. Structure and stratigraphy of sedimentary basins in the Sea of the Hebrides and the Minches. In: Petroleum and the continental shelf of North-Western Europe, edited by Woodland P.

BIRTLES R.G. 1980. Filtering techniques for the enhancement of refraction data from the Western Isles. M.Sc. thesis. University of Durham.

BLUNDELL D.J. 1981. The nature of the continental crust beneath Britain. In: Petroleum geology of the continental shelf of Northwest Europe, Institute of Petroleum, pp. 58-64.

BLUCK B.J., HALLIDAY A.N., AFTALION M. AND MACINTIRE R.M. 1980. Age and origin of Ballantrae ophiolite and its significance to the Caledonian orogeny and the Ordovician time scale. GEOLOGY 8, 492-495.

BORRADAILE G.J. 1973. Dalradian structure and stratigraphy of the northern Loch Awe district, Argyllshire. TRANS R SOC EDINB 69, 1-21.

BORRADAILE G.J. 1979. Pre-tectonic reconstruction of the Islay anticline: implications for the depositional history of the Dalradian rocks in the SW Highlands. In: The Caledonides of the British Isles - reviewed, edited by Harris A.L., Holland C.H., and Leake B.E. SPEC PUBL GEOL SOC 8, 229-237.

BOTT M.H.P. AND MASSON SMITH D. 1960. A gravity survey of the Criffel Granodiorite and the New Red Sandstone deposits near Dumfries. PROC YORKSHIRE GEOL SOC 32, 317-332.

BOTT M.H.P., HOLLAND J.G., STORRY P.G. AND WATTS A.B. 1972. Geophysical evidence concerning the structures of the Lewisian of Sutherland, NW Scotland. J GEOL SOC LOND 128, 599-612.

BOTT M.H.P. AND TUSON J. 1973. Deep structure beneath the Tertiary volcanic regions of Skye, Mull and Ardnamurchan, Northwest Scotland. NATURE PHYS SCI 242, 114-116.

BOTT M.H.P. 1978. The origin and development of continental margins in northwestern Britain. In: Bowes D.R. and Leake B.E.(eds), Crustal evolution in northwestern Britain and adjacent regions. GEOL J SPEC ISSUE NO 10.

BOTT M.H.P., ARMOUR A.R., HIMSWORTH E.M., MURPHY T. AND WYLIE G. 1979. An explosion seismology investigation of the continental margin west of the Hebrides, Scotland, at 58° N. TECTONOPHYSICS 59, 217-231.

BOTT M.H.P. 1982. The interior of the Earth. Second edition, Edward Arnold Ltd.

BOWES D.R. 1968. An orogenic interpretation of the Lewisian of Scotland. In: Report of the 23rd session of the International Geological Congress, Chechoslovakia, Proceedings of Section 4, Geology of Precambrian, 225-236.

BRADBURY H.J., HARRIS A.L. AND SMITH R.A. 1979. Geometry and emplacement of nappes in the Central Scottish Highlands. In: Harris A.L., Holland C.H. and Leake B.E.(eds), The Caledonides of the British Isles -reviewed, SPEC PUBL GEOL SOC LOND 8, 213-220.

BREEMEN O. VAN, AFTALION M. AND PIDGEON R.T. 1971. The age of the granitic injection complex of Harris, Outer Hebrides. SCOTT J GEOL 7, 139-152.

BREWER J.A., MATHEWS D.H., WARNER M.R., HALL J., SMYTHE D.K. AND WHITTINGTON R.J. 1983. BIRPS deep seismic reflection studies of the British Caledonides. NATURE 305, 206-210.

BREWER J.A. AND SMYTHE D.K. 1984. MOIST and the continuity of crustal reflector geometry along the Caledonian Appalachian orogen. J GEOL SOC LOND 141, 105-120.

BROWITT C.W.A. 1972. Seismic refraction investigation of deep sedimentary basins in the continental shelf west of Shetlands. NATURE PHYS SCI 236, 161-163.

BRUCK P.M., DEDMAN R.E. AND SMITH A.G. 1967. The New Red

Sandstone of Raasay and Scalpay, Inner Hebrides. SCOTT J GEOL 3, 168-180.

BULLERWELL W. 1961. In Fowler A. and Robbie J.A., Geology of the country around Dungannon. MEM GEOL SURV NORTH IREL.

CASSON N. 1982. A seismic refraction investigation between the Hebridean Isles of Colonsay and Jura. B.Sc. thesis, University of Durham.

CERVENY V., LANGER J. AND PSENCIK I. 1974. Computation of geometric spreading of seismic body waves in laterally inhomogeneous media with curved inerfaces. GEOPHYS J R ASTRON SOC 38, 9-20.

CERVENY V. 1983. Synthetic body wave seismograms for laterally varying layered structures by the Gaussian beam method. GEOPHYS J R ASTRON SOC 73, 389-426.

CERVENY V. 1984. Ray synthetic seismograms for complex two-dimensional and three-dimensional structures; 5th course in synthetic seismograms: generation and use. International School of Applied Geophysics, Erice, Sicily.

CERVENY V. 1985. The application of ray-tracing to the numerical modelling of seismic wavefields in complex structures. In: Handbook of Geophysical Exploration, section I: Seismic exploration (K. Helbig and S. Treitel, eds.), the volume on Seismic Shear Waves (G.Dohr,ed.), Geophysical Press,London.

CHEN W.P. AND MOLNAR P. 1983. Focal depths of intracontinental and intraplate earthquakes and their implications for the thermal and mechanical properties of the lithosphere. J GEOPHYS RES 88, 4183-4214.

CHESHER J.A. AND BACON M. 1975. A deep seismic survey in the Moray Firth. IGS REP 75/11.

CHINNER G.A. 1978. Metamorphic zones and fault displacements in the Scottish Highlands. GEOL MAG 115, 37-45.

CLAERBOUT J.F. AND MUIR F. 1973. Robust modelling with erratic data. GEOPHYSICS 38, 826-844.

COOK A.H. AND MURPHY T. 1952. Measurements of gravity in Ireland - gravity survey of Ireland north of the line Sligo-Dundalk. GEOPHYS MEM DUBL No 2, Pt 4, 5-36.

COWARD M.P., FRANCIS P.W., GRAHAM R.H. AND WATSON J. 1970. Large-scale Laxfordian structures of the Outer Hebrides in relation to those of the Scottish Mainland. TECTONOPHYSICS 10, 425-435.

COWARD M.P. 1980. The Caledonian thrust and shear zones in NW Scotland. J STRUCT GEOL 2, 11-17.

COWARD M.P 1984. Major shear zones in the Precambrian crust; examples from N.W. Scotland and Southern Africa and their significance. In: Precambrian Tectonics Illustrated, edited by A. Kroner and R. Greiling, pp. 207-235.

DAVIDSON K.A.S., SOLA M., POWELL D.W. AND HALL J. 1984. Geophysical model for the Midland Valley of Scotland. TRANS R.SOC. EDIN 75, 175-181

DEARNLEY R. 1962. An outline of the Lewisian complex of the Outer Hebrides in relation to that of the Scottish mainland. Q J GEOL SOC LOND 118, 143-176.

DEWEY J.F. 1969. Evolution of the Appalachian-Caledonian orogen. NATURE 222, 124-129.

DEWEY J.F. 1982. Plate tectonics and the evolution of the British Isles. J GEOL SOC LOND 139, 371-412.

DEWEY J.F. AND SHACKLETON R.M. 1984. A model for the evolution of the Grampian tract in the early Caledonides and Appalachians. NATURE 312, 115-121.

DIMITROPOULOS K. 1981. Caledonian granites as the cause of uncertainty in LISPB interpretation in the Grampian Highlands area. GEOPHYS J R ASTRON SOC 65, 695-702.

DOBRIN M.B. 1976. Introduction to Geophysical Prospecting, 3rd edition, McGraw-Hill.

DOBSON M.R. AND EVANS D. 1974. Geological structure of the Malin Sea. J GEOL SOC LOND 130, 475-478.

DOBSON M.R., EVANS D. AND WHITTINGTON R. 1975. The offshore extension of the Loch Gruinart Fault, Islay. SCOTT J GEOL 11, 23-35.

DRURY S.A. 1972. The tectonic evolution of a Lewisian complex on Coll, Inner Hebrides. SCOTT J GEOL 8, 309-334.

DURRANCE E.M. 1976. A gravity survey of Islay, Scotland. GEOL MAG 113, 251-261.

ELLIOT D. AND JOHNSON M.R.W. 1980. Structural evolution in the northern part of the Moine thrust belt, NW Scotland. TRANS R SOC EDINBURGH EARTH SCI 71, 69-96.

EVANS D., KENOLTY N., DOBSON M.R. AND WHITTINGTON R.J. 1980. The geology of the Malin Sea. IGS REP 79/15.

EYLES V.A. AND MACGREGOR A.G. 1952. The Great Glen crush belt. GEOL MAG 89, 426-436.

FETTES D.J., LONG C.B., BEVINS R.E., MAX M.D., OLIVER G.J.H.,

PRIMMER T.J., THOMAS L.J. AND YARDLEY B.W.D. 1985. Grade and time of metamorphism in the Caledonide orogen of Britain and Ireland. In: The Nature and Timing of orogenic activity in the Caledonian rocks of the British Isles, edited by A.L. Harris, Memoir no 9, GEOL SOC LOND.

FETTES D.J., GRAHAM C.M., HARTE B. AND PLANT J.A. 1986. Lineaments and basement domains: an alternative view of Dalradian evolution. J GEOL SOC LOND 143, 453-464.

FLINN D., FRANK P.L., BROOK M. AND PRINGLE I.R. 1979. Basement cover relations in Shetland. In: Harris A.L., Holland C.H. and Leake B.E. (eds), The Caledonides of the British Isles - reviewed SPEC PUBL GEOL SOC 8, 109-115.

FRANCIS E.H. 1983. Carboniferous. In: Geology of Scotland, edited by G.Y. Graig, pp. 253-291.

FRANCIS P.W. 1973. Scourian-Laxfordian relationships in the Barra Isles. J GEOL SOC LOND 129, 161-189.

GARDNER L.W. 1939. An areal plan of mapping subsurface structure by refraction shooting. GEOPHYSICS 4, 247-259.

GARDNER L.W. 1967. Refraction Seismograph Profile Interpretation. In: Seismic Refraction Prospecting, edited by A.W. Musgrave, Society of Exploration Geophysicists, Tulsa, Oklahoma, pp. 338-347.

GARSON M.S. AND PLANT J. 1972. Possible dextral movements on Great Glen and Minch faults in Scotland. NATURE PHYS SCI 240, 31-35.

GRAHAM C.M. 1976. Petrochemistry and tectonic significance of Dalradian metabalsatic rocks of the S.W. Scottish Highlands. J GEOL SOC LOND 132, 61-84.

GRAHAM C.M. AND BRADBURY H.J. 1981. Cambrian and late Precambrian basaltic igneous activity in the Scottish Dalradian: a review. GEOL MAG 118, 27-37.

GRAHAM C.M. 1983. High pressure greenshist to epidote-amphibolite facies metamorphism of Dalradian rocks of the S.W. Scottish Highlands: isograds and P-T conditions. GEOL SOC LOND NEWSLETT 12/4, 19.

GRAHAM C.M. AND BORRADAILE G.J. 1984. The petrology and structure of Dalradian metabasaltic dykes of Jura: implications for early Dalradian evolution. SCOTT J GEOL 20, 257-270.

HAGEDOORN J.G. 1959. The plus-minus method of interpreting seismic refraction sections. GEOPHYS PROSPECT 7, 158-182.

HALL J. 1969. The correlation of seismic velocities with formations in the south-west of Scotland. GEOPHYS PROSPECT 18,

134-148.

HALL J. AND AL-HADDAD F.M. 1976. Seismic velocities in the Lewisian metamorphic complex, northwest Britain-in situ measurements. SCOTT J CEOL 12, 305-313.

HALL J. 1978a. "LUST"- a seismic refraction survey of the Lewisian basement complex in North-West Scotland. J GEOL SOC LOND 135, 555-563.

HALL J. 1978b. Seismic refraction studies in the Firth of Clyde. In: The solid geology of the Clyde sheet 55°N/6°W. IGS REP 78/9.

HALL J. 1978c. Crustal structure of the eastern North Atlantic seaboard. In: Bowes D.R. and Leake B.E. (eds), Crustal evolution in Northwestern Britain and Adjacent Regions. SPEC ISSUE GEOL J 10, 23-38.

HALL J. AND AL-HADDAD F.M. 1979. Variation of effective seismic velocities of minerals with pressure and its use in velocity prediction. GEOPHYS J R ASTRON SOC 57, 107-118.

HALL J. AND SIMMONS G. 1979. Seismic velocities of Lewisian metamorphic rocks at pressures to 8 kbar: relation to crustal layering in North Britain. GEOPHYS J R ASTRON SOC 58, 337-357.

HALL J., BREWER J.A., MATTHEWS D.H. AND WARNER M.R. 1984. Crustal structure across the Caledonides from the WINCH deep seismic reflection profile: influences on Midland Valley evolution.TRANS R SOC EDINBURGH EARTH SCI 75,97-109.

HALL J. 1985. Geophysical constraints on crustal structure in the Dalradian region of Scotland. J GEOL SOC LOND 142, 149-155.

HALL J. 1986. Geophysical lineaments and deep continental structure. PHIL TRANS R SOC LOND 317, 33-44.

HARLAND W.B. AND GAYER R.A. 1972. The Arctic Caledonides and earlier oceans. GEOL MAG 109, 289-314.

HARRIS A.L. AND PITCHER W.S. 1975. The Dalradian Supergroup. In Harris A.L. et al: A correlation of the Precambrian rocks in the British Isles. SPEC REP GEOL SOC LOND 6,52-75.

HARRIS A.L., BALDWIN C.T., BRADBURY H.J., JOHNSON H.D. AND SMITH R.A. 1978. Ensialic basin sedimentation: the Dalradian Supergroup. In: Bowes D.R. and Leake B.E.(eds), Crustal Evolution in Northwestern Britain and Adjacent Regions, SPEC ISSUE GEOL J 10, 115-38.

HICKMAN A.H. 1975. The stratigraphy of late Precambrian metasediments between Glen Roy and Lismore. SCOTT J GEOL

11, 117-142.

HIPKIN R.G. AND HUSSAIN A. 1983. Regional gravity anomalies. 1 Northern Britain. IGS REP 82/10.

HILL D.P. 1978. Seismic evidence for the structure and Cenozoic tectonics of the Pacific Coast States. In: Smith R.B. and Eaton G.P. (eds). Cenozoic Tectonics and Regional Geophysics of the Western Cordillera. MEM GEOL SOC AM 152, 145-174.

HOBBS R.W. 1985. Processing of a multichanel seismic reflection survey in the Hebridean region with special emphasis on improvements in velocity analysis. Ph.D. thesis, University of Durham.

HOLGATE N. 1969. Paleozoic and Tertiary transcurrent movements on the Great Glen fault. SCOTT J GEOL 5, 97-139.

JACKSON J.A AND MCKENZIE D.P. 1983. The geometrical evolution of normal fault systems. J STRUCT GEOL 5, 471-481.

JOHNSON M.R.W. 1983. Dalradian. In: The Geology of Scotland, edited by G.Y. Craig. Scottish Academic Press, Edinburgh.

JONES E.J.W. 1978. Seismic evidence for sedimentary troughs of Mesozoic age on the Hebridean continental margin. NATURE 272, 789-92.

JONES E.J.W. 1981. Seismic refraction shooting on the continental margin west of the Outer Hebrides, North-West Scotland. J GEOPHYS RES 86, 11553-11574.

KENNEDY W.Q. 1946. The Great Glen Fault. Q J GEOL SOC LOND 102, 41-72.

KERN H. 1978. The effect of high temperature and high confining pressure on compressional wave velocities in quartz-bearing and quartz-free igneous and metamorphic rocks. TECTONOPHYSICS 44, 185-203.

KENT P.E. 1978. Mesozoic vertical movements in Britain and the surrounding continental shelf. In: Crustal evolution in northwest Britain and adjacent regions, edited by Bowes D.R. and Leake B.E., SPEC ISSUE GEOL J 10, 309-324.

KRAMER F.S., PETERSON R.A. AND WALTER W.C. (eds) 1968. Seismic Energy Sources - Handbook, Pasadena, Bendix United Geophysical.

LACHENBRUCH A.H. AND SASS J.H. 1980. Heat flow and energetics of the San Andreas fault zone. J GEOPHYS RES 85, 6185-6222.

LAMBERT R.St J. AND MCKERROW W.S. 1976. The Grampian orogeny. SCOTT J GEOL 12, 271-292.

LUNN S.F. 1984. The use of refracted arrivals from multichanel seismic reflection data to investigate the geological structure of the Iona platform. M.Sc. thesis, University of Durham.

MCCLAY K.R. AND COWARD M.P. 1981. The Moine Thrust Zone: an overview. In: Thrust and Nappe Tectonics, edited by K.R. MacClay and N.J. Price, SPEC PUBL GEOL SOC LOND 9, 241-260.

MCLEAN A.C. 1978. Evolution of fault-controlled ensialic basins in northwestern Britain. In: Bowes D.R. and Leake B.E. (eds), Crustal Evolution in Northwestern Britain and adjacent regions. SPEC ISSUE GEOL J 10, 325-46.

MCLEAN A.C. AND DEEGAN C.E. 1978.The solid geology of the Clyde Sheet 55°N / 6°W. IGS REP 78/9.

MCLEAN A.C. AND WREN A.E. 1978. Gravity and magnetic studies in the lower Firth of Clyde. In: The solid geology of the Clyde Sheet 55°N / 6°W. IGS REP 78/9.

MCQUILLIN R. AND BINNS P.E. 1973. Geological structure in the Sea of The Hebrides. NATURE PHYS SCI 241, 2-4.

MCQUILLIN R. AND WATSON J. 1973. Large-scale Basement srtuctures of the Outer Hebrides in the light of Geophysical Evidence. NATURE PHYS SCI 245, 1-3.

MCQUILLIN R. AND BINNS P.E. 1975. Geological structure in the Minches, the Sea of The Hebrides and the adjacent North West British Continental Shelf. In: Canada's Continental Margins and offshore Petroleum exploration, eds. C.J. Yorath, E.R. Parker and D.J. Glass; CAN SOC PETROL GEOL, MEMOIR 4, 283-293.

MCQUILLIN R. AND ARDUS D.A. 1977. Exploring the geology of shelf areas, Graham and Trotman Limited.

MENKE W. 1984. Geophysical data analysis: discrete inverse theory, Academic Press.

MILLER H. AND GEBRANDE H. 1976. Crustal structure in Southeastern Bavaria derived from seismic refraction measurements by ray-tracing methods. In: Explosion seismology in Central Europe, edited by P. Giese, C. Prodehl and A. Stein, Springer-Verlag, Berlin.

MOOD M.A., GRAYBILL F.A. AND BOES D.C. 1985. Introduction to the theory of statistics, International student edition, McGraw Hill.

MOORBATH S. 1969. Evidence for the age of deposition of the Torridonian sediments of north-west Scotland. SCOTT J GEOL 5, 154-170.

MOORBATH S., WELKE H. AND GALE N.H. 1969. The significance of lead isotope studies in ancient high grade metamorphic complexes, as exemplified by the Lewisian rocks of northwest Scotland. EARTH PLANET SCI LETT 6, 245-256.

MULLER G. AND FUCHS K. 1976. Inversion of seismic records with the aid of synthetic seismograms. In: Explosion Seismology in Central Europe, edited by P. Giese, C. Prodehl and A. Stein, Springer-Verlag, Berlin.

MURPHY T., YOUNG D.G. AND BRUCK G. 1971. The post - Dalradian strata along the north-west coast of Lough Foyle, Inishowen, Co. Donegal. PROC R IR ACAD 71b, 171-182.

MYKURA W. 1975. Possible large scale sinistral displacement along the Great Glen fault in Scotland. GEOL MAG 112,91-94.

MYKURA W. 1983. Old Red Sandstone. In: Geology of Scotland, edited by G.Y. Graig, pp. 205-242.

NORTHWOOD E.J. 1967. Notes on errors in refraction interpretation. In: Seismic Refraction Prospecting, edited by A.W. Musgrave, Society of Exploration Geophysicists, Tulsa, Oklahoma.

O'BRIEN P.N.S. 1968. Lake Superior crustal structure/a reinterpretation of the 1963 seismic experiment. J GEOPHYS RES, 2669.

PANKHURST R.J. AND SUTHERLAND D.S. 1982. Caledonian granites and diorites of Scotland and Ireland. In: Sutherland D.S. (ed), Igneous rocks of the British Isles, Wiley, 149-190.

PARK R.G. 1970. Observations on Lewisian chronology. SCOTT J GEOL 6, 379-399.

PEDDY C.P. 1984. Displacement of the Moho by the Outer Isles Thrust as shown by seismic modelling. NATURE 312, 628-630.

PHILLIPS W.E.A.,STILLMAN C.J., AND MURPHY T. 1976. A Caledonian plate tectonic model. J GEOL SOC LOND 132, 579-609.

POWELL D. AND PHILLIPS W.E.A. 1985. Time of deformation in the Caledonian orogen of Britain and Ireland. In: The Nature and Timing of orogenic activity in the Caledonian rocks of the British Isles, edited by A.L. Harris, Memoir no 9, GEOL SOC LOND.

POWELL D.W. 1970. Magnetised rocks under the Lewisian of western Scotland and under the Southern Uplands. SCOTT J GEOL 6, 353-369.

POWELL D.W. 1978. Gravity and magnetic anomalies attributable to basement sources under the northern Britain. In: Crustal

evolution in northwest Britain and adjacent regions, edited by Bowes D.R. and Leake B.E., SPEC ISSUE GEOL J 10,107-114.

PRESCOTT W.H. AND NUR A. 1981. Accommodation of relative motion at depth on the San Andreas fault system in California. J GEOPHYS RES 86, 999-1004.

RASHID B.M. 1978. Interpretation of geophysical data in the Firth of Lorne. M.Sc. thesis, University of Glasgow.

RICHEY J.E., ANDERSON E.M. AND MACGREGOR A.G. 1930. The geology of north Ayrshire. MEM GEOL SURV UK.

ROBERTS J.L. 1974. The structure of the Dalradian rocks in the southwest Highlands of Scotland.J GEOL SOC LOND 130,93-124.

ROBERTS J.L. AND TREAGUS J.E. 1977a. The Dalradian rocks of the southwest Highlands - Introduction. SCOTT J GEOL 13, 87-99.

ROBERTS J.L. AND TREAGUS J.E. 1977b. Polyphase generation of nappe structures in the Dalradian rocks of southwest Highlands of Scotland. SCOTT J GEOL 13, 237-254.

SCHEIDEGGER A.E. AND WILLMORE P.L. 1957. The use of least squares method for the interpretation of data from seismic surveys, GEOPHYSICS 22, 9-22.

SCRUTTON R.A. 1973. The age relationship of igneous activity and continental break-up. GEOL MAG 110, 227-234.

SHACKLETON R.M. 1979. The British Caledonides: comments and summary. In: Harris A.L., Holland C.H. and Leake B.E.(eds), The Caledonides of the British Isles -reviewed, SPEC PUBL GEOL SOC LOND 8, 299-304.

SHAW B.H. 1978. The structure of the crust between Jura and Barra. M.Sc. thesis, University of Durham.

SHERIFF R.E. AND GELDART L.P. 1982. Exploration seismology, Cambridge University Press.

SIBSON R.H. 1977. Fault rocks and fault mechanisms. J GEOL SOC LOND 133, 191-214.

SIBSON R.H. 1980. Transient discontinuities in ductile shear zones. J STRUCT GEOL 2, 165-171.

SIBSON R.H. 1982. Fault zone models, heat flow, and the depth distribution of earthquakes in the continental crust of the United States. BULL SEISM SOC AM 72, 151-163.

SIBSON R.H. 1983. Continental fault structure and the shallow earthquake source. J GEOL SOC LOND 140, 741-767.

SMITH D.I. AND WATSON J. 1983. Scale and timing of movements of

the Great Glen Fault, Scotland. GEOLOGY 11, 523-526.

SMITH P.J. AND BOTT M.H.P. 1975. Structure of the crust beneath the Caledonian Foreland and Caledonian belt of the North Scottish shelf region. GEOPHYS J R ASTRON SOC 40, 187-205.

SMITH R.B. 1978. Seismicity, crustal structure and intra-plate tectonics of the interior of the western Cordillera. In: Smith R.B and Eaton G.P. (Eds), Cenozoic Tectonics and Regional Geophysics of the Western Cordillera. MEM GEOL SOC AM 152, 111-114.

SMYTHE D.K., SOWERBUTTS W.T.C., BACON M. AND MCQUILLIN R. 1972. Deep sedimentary basin beneath northern Skye and the Little Minch. NATURE PHYS SCI 236, 87-89.

SMYTHE D.K. AND KENOLTY N. 1975. Tertiary sediments in the Sea of the Hebrides. J GEOL SOC LOND 131, 227-233.

SMYTHE D.K., DOBINSON A., MCQUILLIN R., BREWER J.A., MATHEWS D.H., BLUNDELL D.J. AND KELK B. 1982. Deep structure of the Scottish Caledonides revealed by the MOIST reflection profile. NATURE 299, 338-340.

SOPER N.J. AND ANDERTON R. 1984. Did the Dalradian slides originate as extensional faults? NATURE 307, 357-359.

SOPER N.J. AND BARBER A.J. 1982. A model for the deep structure of the Moine Thust zone. J GEOL SOC LOND 130, 127-138.

STEEL R.J. 1971. New Red Sandstone movement on the Minch fault. NATURE PHYS SCI 234, 158-159.

STEEL R.J. 1974. New Red Sandstone floodplain and alluvial fan sedimentation in the Hebridean province of Scotland. J SEDIM PETROL 44, 336-357.

STEWART A.D. 1976. Torridonian rocks of western Scotland. In: A correlation of Precambrian rocks in the British Isles edited by Harris et al., GEOL SOC SPEC REP NO 6, 43-52.

STEWART A.D. 1982. Late Proterozoic rifting in northwest Scotland: the genesis of the "Torridonian". J GEOL SOC LOND 139, 415-422.

STURT B.A. 1961. The geological structure of the area south of Loch Tummel. Q JL GEOL SOC LOND 117, 131-156.

SUMMERS T.P. 1982. A seismic study of crustal structure in the region of the Western Isles of Scotland. Ph.D. thesis Universityof Durham.

SUTTON J. AND WATSON J.V. 1951. The pre-Torridonian history of the Loch Torridon and Scourie areas in the Northwestern Highlands and its bearing on the chronological classifica-

tion of the Lewisian. Q J GEOL SOC LOND 106, 241-307.

SUTTON J. AND WATSON J.V. 1955. The deposition of the Upper Dalradian rocks of the Banffshire coast. PROC GEOL ASSOC 66, 101-133.

TALWANI M., WORZEL J.L. AND LANDISMAN M. 1959. Rapid gravity calculations for two-dimensional bodies with application to the Mendocino submarine fracture zone. J GEOPHYS RES 64, 49-59.

TELFORD W.M., GELDART L.P., SHERIFF R.E. AND KEYS D.A. 1976. Applied Geophysics. Cambridge University Press.

THOMAS P.R. 1979.New evidence for a Central Highland Root Zone. In: Harris A.L., Holland C.H. and Leake B.E.(eds), The Caledonides of the British Isles -reviewed, SPEC PUBL GEOL SOC LOND 8, 205-211.

TROSTLE M.E. 1967. Some aspects of refraction shooting through screening layers.In: Seismic Refraction Prospecting, edited by A.W. Musgrave, Society of Exploration Geophysicists, Tulsa, Oklahoma, pp. 469-481.

TULLIS J. AND YUND R.A. 1977. Experimental deformation of dry Westerly Granite. J GEOPHYS RES 82, 5705-5718.

TUSON J. 1959. A geophysical investigation of the Tertiary volcanic districts of western Scotland. Ph.D. thesis University of Durham.

URUSKI C.I. 1982. Geological studies of the continental shelf of Northwest Scotland between 56° - 57° N. Ph.D. thesis University of Durham.

VAN DER VOO R. AND SCOTESE C. 1981. Paleomagnetic evidence for a large (>2000 km) sinistral offset along the Great Glen fault during the Carboniferous. GEOLOGY 9, 583-589.

WARREN R.D. 1981. Signal processing techniques applied to refraction data. M.Sc. thesis, University of Durham.

WATSON J. 1975. The Lewisian complex. In: A correlation of Precambrian rocks in the British Isles. SPEC REP GEOL SOC LOND 6, 15-30.

WATSON J. AND DUNNING F.W. 1979. Basement cover relations in the British Caledonides. In: The Caledonides of the British Isles - reviewed, edited by Harris A.L., Holland C.H. and Leake B.E. SPEC PUBL GEOL SOC LOND 8, 683-97.

WATSON J. 1984. The ending of the Caledonian orogeny in Scotland J GEOL SOC LOND 141, 193-214.

WATTS M.J. AND WILLIAMS G.D. 1979. Fault rocks as indicators

of progressive shear deformation in the Guicamp region, Brittany. J STRUCT GEOL 1, 323-332.

WESTBROOK G.K. 1972. Structure and metamorphism of the Lewisian of East Tiree, Inner Hebrides. SCOTT J GEOL 8, 309-334.

WESTBROOK G.K. AND BORRADAILE G.J. 1978. The geological significance of magnetic anomalies in the region of Islay. SCOTT J GEOL 14, 213-224.

WILLMORE P.L. AND BANCROFT A.M. 1960. The time-term approach to refraction seismology. GEOPHYS J 3, 419-432.

WILSON C.D.V. 1978. A geophysical survey of south Kintyre. SCOTT J GEOL 14, 171-183.

WILSON H.E. AND MANNING P.I. 1978. Geology of the Causeway Coast. MEM GEOL SURV NORTH IREL

WILSON M. 1979. Geophysical surveys around Mull, western Scotland. Ph.D. thesis, University of Glasgow.

WINCHESTER J.A. 1974.The zonal pattern of regional metamorphism in the Scottish Caledonides. J GEOL SOC LOND 130, 509-524.

WINCHESTER J.A. 1978. The zonal pattern of metamorphism in the Scottish Highlands and the displacement along the Great Glen fault; discussion of paper by G.A. Chinner, GEOL MAG 115, 453-460.

WHITBREAD D.R. 1975. Geology and petroleum possibilities west of the United Kingdom. In: Petroleum and the continental shelf of Northwest Europe, edited by Woodland A.W. 1,45-59.

WRIGHT A.E. 1976. Alternating subduction direction and the evolution of the Atlantic Caledonides. NATURE LOND 264, 156-160.

ZERVOS F. 1986. A compilation and regional interpretation of the northern North Sea gravity map. (In press).

ZIEGLER P.A. 1981. Evolution of sedimentary basins in northwest Europe, In: Proceedings of conference on petroleum geology of continental shelf of northwest Europe, London, Institute of Petroleum, p. 3-39.

APPENDIX 1

TABLES

TABLE A.1: LOCATION OF STATIONS IN WISE

Station	Latitude (North)	Longitude (West)
Barra (G + D)	56° 58.11'	7° 26.39'
Ruaig	56° 31.92'	6° 45.66'
Vaul	56° 32.35'	6° 48.48'
Mull (G)	56° 19.14'	6° 19.59'
Mull (D)	56° 17.50'	6° 15.51'
Mull (W2)	56° 19.19'	6° 19.66'
Iona (W1)	56° 20.02'	6° 24.13'
Iona (W2)	56° 20.08'	6° 23.79'
Colonsay (W1 + W2)	56° 04.92'	6° 10.09'
N. Jura (W1 + W2)	55° 57.01'	5° 58.92'
M. Jura (1)	55° 53.57'	5° 55.19'
M. Jura (2)	55° 53.49'	5° 54.83'
S. Jura (W1 + W2)	55° 52.53'	5° 53.87'
N. Kintyre (W1 + W2)	55° 41.95'	5° 37.43'
S. Kintyre (W1 + W2)	55° 34.77'	5° 27.84'
Arran	55° 30.49'	5° 21.19'
Girvan Stns.		
Letterpin	55° 11.41'	4° 50.28'
Lendalfoot	55° 10.55'	4° 55.67'
Cundry Mains	55° 10.68'	4° 54.15'
Knockbrain	55° 10.14'	4° 53.28'
Breaker Hill	55° 09.77'	4° 51.67'
Bargain Hill	55° 09.41'	4° 50.47'
Millenderdale	55° 10.70'	4° 51.70'
Currarie	55° 10.87'	4° 50.28'

G Geostore Recorder

D Durham Mk. 3 Recorder

W1 Phase 1

W2 Phase 2

TABLE A.2

WESTERN ISLES SEISMIC EXPERIMENT

Positions and times of detonation of large explosive shots

No	Weight	Latitude	Longitude	Water Depth	Date	Time ± .03s
1	125 Kg	55°10.0'	04°58.4'	20.1 m	12.11.79	1532 05.79
2	125	55°18.1'	05°08.0'	46.6 m	12.11.79	1332 20.33
3	125	55°26.45'	05°18.1'	18.3 m	12.11.79	1132 01.39
4	125	55°34.08'	05°27.25'	38.4 m	12.11.79	0939 40.57
5	87.5	55°42.54'	05°38.21'	11.9 m	13.11.79	0818 12.40
6	87.5	55°46.05'	05°43.79'	73.2 m	13.11.79	0911 29.47
7	87.5	55°47.04'	05°50.75'	181.1 m	18.11.79	1142 48.86
8	87.5	55°51.84'	05°53.54'	31.1 m	18.11.79	1047 10.14
9	37.5	55°57.5'	06°00.00'	21.0 m	13.11.79	1316 47.90
10	37.5	56°00.0'	06°03.5'	17.4 m	13.11.79	1346 56.62
11	37.5	56°02.9'	06°07.9'	36.6 m	13.11.79	1416 35.19
12	37.5	56°06.9'	06°11.7'	30.2 m	13.11.79	1531 40.83
13	37.5	56°09.6'	06°14.95'	81.4 m	13.11.79	1611 49.85
14	37.5	56°12.5'	06°16.35'	73.2 m	13.11.79	1641 51.46
15	125	56°15.7'	06°18.5'	29.3 m	19.11.79	0948 51.02
16	87.5	56°19.2'	06°27.7'	25.6 m	19.11.79	1117 08.26
17	87.5	56°23.38'	06°32.96'	100.6 m	19.11.79	1211 49.27
18	87.5	56°27.48'	06°39.02'	82.3 m	19.11.79	1311 52.48
19	125	56°32.9'	06°49.3'	23.0 m	15.11.79	0911 51.16
20	125	56°41.15'	07°01.55'	157.3 m	15.11.79	1048 43.38
21	50	56°44.77'	07°07.38'	197.5 m	15.11.79	1126 50.81
22	125	56°49.09'	07°14.10'	155.4 m	15.11.79	1216 59.26
23	125	56°56.65'	07°26.25'	21.0 m	15.11.79	1347 16.37

TABLE A.3

1000 cu.in. AIRGUN PROFILE - PHASE 1

Station Pair	Start		End	
Colonsay-Mull	11.06	14.11.79	18.39	14.11.79
Mull-Tiree	18.42	14.11.79	23.03	14.11.79
Barra-Tiree	22.18	15.11.79	01.44	16.11.79
Barra-Tiree (2)	21.15	16.11.79	08.48	17.11.79
Jura-Kintyre	13.21	18.11.79	16.54	18.11.79
Kintyre-Girvan	21.24	20.11.79	11.21	21.11.79
Kintyre-Jura (2)	09.21	23.11.79	12.54	23.11.79
Jura-Colonsay	15.30	23.11.79	18.00	23.11.79
Shot 21 - Tiree	17.39	26.11.79	22.06	26.11.79
Shot Firing - 3 minute intervals				

TABLE A.4

WESTERN ISLES EXPERIMENT 1

POSITIONS AND TIMES OF DETONATION OF GEOFLEX SHOTS

No.	Length	Latitude	Longitude	Shot Depth	Water Depth	Date	Time
G1	20 m	55°42.5'	5°38.2'	b	8 m	20.11.79	0830 29.416
G2	20 m	55°42.85'	5°38.75'	b	9 m	20.11.79	0844 37.587
G3	20 m	55°43.22'	5°39.30'	b	10 m	20.11.79	0850 57.833
G4	30 m	55°43.63'	5°39.92'	b	23 m	20.11.79	0857 44.397
G5	30 m	55°43.98'	5°40.41'	b	31 m	20.11.79	0903 32.440
G6	30 m	55°44.38'	5°41.00'	b	27 m	20.11.79	0910 23.467
G7	30 m	55°44.80'	5°42.00'	10 m	17 m	20.11.79	0949 48.407
G8	30 m	55°45.38'	5°42.98'	10 m	27 m	20.11.79	0956 00.051
G9	40 m	55°46.11'	5°44.28'	12 m	60 m	20.11.79	1002 45.135
G10	50 m	55°46.88'	5°45.32'	17 m	70 m	20.11.79	1010 30.549
G12	50 m	55°48.42'	5°47.60'	17 m	157 m	20.11.79	1025 05.703

10 m of Geoflex contains 0.41 Kg. of explosive.

For Shot G12 two 50 m lengths were exploded.

TABLE A.5

WESTERN ISLES SEISMIC EXPERIMENT - PHASE 2

Positions and detonation times of explosive shots - 31.8.81

No.	LATITUDE	LONGITUDE	WATER DEPTH	TIME ±0.03
10	56° 14.16'	6° 17.55'	49.5 m	0915 22.03
9	56° 11.32'	6° 15.25'	75.8 m	0948 10.35
8	56° 9.80'	6° 13.94'	75.9 m	1018 17.02
7	56° 7.65'	6° 12.27'	31.1 m	1043 40.89
6	56° 4.42'	6° 9.35'	20.1 m	1138 51.42
5	56° 1.45'	6° 5.23'	31.3 m	1220 00.59
4	55° 58.37'	6° 1.38'	22.5 m	1245 45.64
3	55° 50.52'	5° 50.22'	56.4 m	1515 48.83
2	55° 49.00'	5° 48.31'	180.8 m	1544 10.80
1	55° 47.56'	5° 46.04'	69.6 m	1616 43.09

All shots 50 kg weight

TABLE A.6

2 x 1000 cu.in. AIRGUN PROFILE - PHASE 2

(1.9.81)

Station Pair	Start	End
Kintyre-Jura	10.00	11.36
Juran-Colonsay	15.12	17.54
Colonsay-Mull	19.30	20.06
Shot Firing - 2 minute intervals		

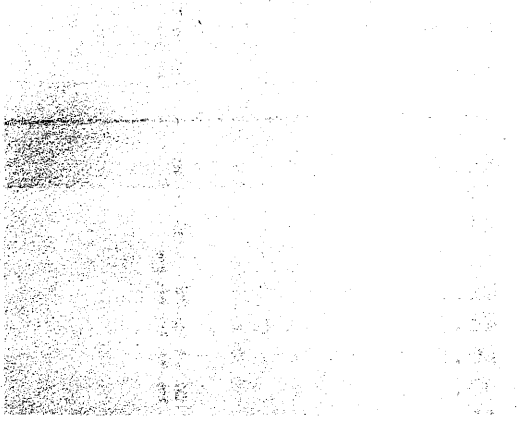

TABLE A.7

TRAVEL TIMES AND RANGES FOR SHOTS RECEIVED - PHASE 1

Station	Shot	Travel Time (sec)	Range (km)
Barra	1	36.51	252.65
	2	34.52	234.52
	3	32.32	215.72
	4	30.05	198.62
	5	27.62	179.16
	6	26.67	170.43
	8	24.82	155.71
	9	23.71	143.28
	10	22.99	137.38
	11	21.64	130.33
	12	20.66	122.05
	13	19.79	116.03
	15	17.51	104.98
	16	15.65	93.89
	17	14.27	84.46
	18	12.76	74.63
	19	10.10	60.16
	20	7.07	40.37
	21	5.90	31.41
	22	4.10	20.88
Ruaig	2	26.86	170.64
	15	7.11	41.08
	16	5.35	29.98
	17	3.77	20.53
	18	2.32	10.69
	21	6.03	32.59
	22	7.78	43.12
	23	10.51	61.81
Vaul	6	18.42	108.96
	19	0.28	1.32
	18	3.02	13.27
Mull	2	22.93	135.74
	3	20.43	116.93
	4	16.92	99.81
	14	2.33	12.77
	15	1.20	6.48
	16	1.59	8.36
	17	3.04	15.86
	18	5.00	25.29
	19	6.84	39.82
	20	10.14	59.36
	21	11.83	68.30
	22	13.66	78.79
	23	16.20	97.44

Station	Shot	Travel Time (sec)	Range (km)
Iona	15	1.80	9.90
	16	0.95	3.98
	17	2.24	11.03
	18	3.93	20.65
	19	6.13	35.23
	20	9.46	54.88
	22	12.80	74.37
	23	15.55	93.04
Colonsay	1	21.23	126.69
	4	12.48	72.65
	9	3.32	17.31
	10	2.18	11.41
	11	0.86	4.39
	17	7.50	41.62
	18	9.36	51.43
	22	18.08	105.10
M. Jura	1	17.00	100.20
	2	14.26	82.06
	3	11.27	63.26
	4	8.10	46.17
	5	4.94	26.73
	6	3.34	17.99
	8	0.57	3.35
	9	1.78	9.19
	10	3.04	15.08
	11	4.17	22.13
	12	5.51	30.45
	13	6.51	36.48
	14	7.56	41.76
	15	8.45	47.98
	16	10.28	58.64
	17	11.83	68.10
	18	13.59	77.92
	19	15.48	92.31
	20	18.76	112.09
	21	20.50	121.05
	22	22.10	131.59
	23	23.95	150.27

Station	Shot	Travel Time (sec)	Range (km)
S. Jura	1	16.62	98.17
	2	13.90	80.03
	3	10.90	61.24
	4	7.72	44.15
	5	4.57	24.73
	6	2.97	15.99
	8	0.18	1.33
	11	4.52	24.16
	12	5.87	32.48
	13	6.92	38.52
	14	7.89	43.80
	15	8.80	50.02
	16	10.65	60.67
	17	12.18	70.13
	18	13.91	79.95
	19	15.84	94.33
	20	19.15	114.11
	21	20.87	123.07
	22	22.46	133.61
	23	24.31	152.29
Letterpin	1	1.77	9.01
	2	4.34	22.51
	3	7.35	40.56
	4	9.63	57.40
	5	13.06	76.76
	6	14.54	85.51
	8	16.93	100.30
	15	24.41	150.88
	16	26.11	161.91
	20	33.61	215.44
Cundry Mains	1	1.00	3.07
	2	3.99	19.16
	3	7.05	37.87
	4	9.40	54.95
	5	12.89	74.41
	6	14.32	83.13
	8	16.62	97.88
Knockbain	1	1.08	4.69
	2	4.21	20.13
	3	7.30	38.71
	5	13.03	75.20
	6	14.52	83.93
Currarie	1	1.36	6.11
	2	4.07	20.93
	3	7.11	39.37
	4	9.56	56.35
	6	14.40	84.52

Station	Shot	Travel Time (sec)	Range (km)
Breaker Hill	1	1.37	7.16
	2	4.42	23.21
	3	7.46	41.72
	4	9.78	58.73
	5	13.29	78.15
	6	14.70	86.89
Bargain Hill	1	1.61	8.50
	2	4.62	24.61
	3	7.46	43.07
	4	9.96	60.05
	6	14.88	88.21
Lendalfoot	1	0.64	3.07
	2	3.78	19.16
	3	6.92	37.87
	4	9.20	54.95
	6	14.16	83.13
	8	16.51	97.88
LOWNET STNS			
Achinoon	8	25.80	152.67
	14	29.86	180.29
	17	32.47	201.82
	18	33.67	210.00
	20	36.83	240.26
Aberfoyle	19	25.73	158.52
	20	28.36	174.70
	21	29.51	182.44
	22	30.63	191.57
	23	31.68	208.19
Black Hill	8	31.12	197.47
	9	26.99	158.38
	12	27.70	167.51
	17	30.50	188.84
	18	31.40	195.65
	20	33.78	220.22
Broadlaw	5	27.60	136.02
	6	27.74	168.58
	17	36.10	228.77
	20	40.04	267.02
Dundee	2	30.30	191.79
	4	29.03	187.07
	6	29.69	189.77

CONTD..

TABLE A.8

TRAVEL TIMES AND RANGES FOR SHOTS RECEIVED - PHASE 2

Station	Shot	Travel Time (sec)	Range (km)
Mull	1	11.93	68.29
	2	11.29	64.79
	3	10.58	61.35
	4	7.64	43.03
	5	6.53	36.15
	6	5.27	29.41
	7	4.07	22.74
	8	3.62	18.40
	9	2.91	15.30
	10	1.84	9.59
Iona	1	12.53	71.96
	2	11.84	68.43
	3	11.28	64.98
	4	8.29	46.50
	5	7.11	39.55
	6	5.80	32.68
	7	4.73	25.96
	8	4.51	21.62
	9	3.41	18.50
	10	2.43	12.74
Colonsay	1	7.29	40.81
	2	6.54	37.24
	3	5.95	33.79
	4	2.77	15.16
	5	1.61	8.18
	7	0.99	5.55
	8	1.78	9.90
	9	2.35	13.02
	10	3.55	18.81
N. Jura	1	4.14	22.09
	2	3.48	18.53
	3	2.76	15.08
	4	0.83	3.60
	5	2.06	10.53
	6	3.34	17.51
	7	4.33	24.13
	8	5.25	28.40
	9	5.82	31.50
	10	6.76	37.23
S. Jura	1	2.30	12.41
	2	1.66	8.84
	3	0.92	5.41
	4	2.68	13.28
	5	3.78	20.25
	6	4.97	27.23
	7	6.08	33.87
	8	6.87	38.15
	9	7.47	41.25

Station	Shot	Travel Time (sec)	Range (km)
N. Kintyre	1	2.65	13.77
	2	3.33	17.34
	3	3.94	20.78
	4	7.27	39.42
	5	8.24	46.38
	6	9.48	53.36
	7	10.38	59.94
	8	11.26	64.17
	9	11.79	67.24
	10	12.70	72.91

APPENDIX A.9

Mull to Tiree Airgun Line

Mull station

Travel time (sec)	Range (km)
1.67	8.54
1.70	8.76
1.75	8.98
1.77	9.13
1.80	9.27
1.81	9.40
1.84	9.54
1.86	9.66
1.87	9.70
1.90	9.91
1.95	10.04
2.01	10.20
2.06	10.36
2.12	10.54
2.20	10.72
2.24	10.92
2.29	11.12
2.35	11.33
2.42	11.54
2.46	11.77
2.50	11.99
2.57	12.22
2.62	12.44
2.67	12.69
2.73	12.95
2.77	13.21
2.82	13.47
2.89	13.72
2.95	13.96
3.65	17.17
3.72	17.53
3.80	17.81
3.90	18.09
3.93	18.44
4.00	18.78
4.05	19.12
4.13	19.45
4.20	19.81
4.26	20.16
4.34	20.51
4.43	20.86
4.50	21.24
4.60	21.61
4.65	21.98
4.70	22.35
4.86	23.13

Iona station

Travel time (sec)	Range (km)
0.94	4.37
0.97	4.50
1.00	4.63
1.01	4.69
1.02	4.75
1.05	4.83
1.08	4.92
1.10	4.90
1.13	5.06
1.14	5.17
1.17	5.28
1.20	5.42
1.24	5.56
1.30	5.73
1.40	5.90
1.47	6.09
1.50	6.28
1.55	6.49
1.61	6.70
1.68	6.92
1.75	7.15
1.81	7.38
1.87	7.61
1.92	7.86
1.98	8.10
2.03	8.37
2.09	8.63
2.13	8.88
2.16	9.13
2.20	9.37
2.24	9.61

Tiree station

Travel time (sec)	Range (km)
0.53	3.10
0.80	3.77
0.86	4.02
0.94	4.29
0.99	4.57
1.05	4.81
1.10	5.05
1.16	5.28
1.24	5.52
1.31	5.87
1.48	6.22
1.46	6.45
1.55	6.68
1.60	6.95
1.66	7.21
1.75	7.47
1.80	7.72
1.86	7.98

Mull to Colonsay Airgun Line

Mull station Travel time (sec)	Corrected TT (sec)	Calculated TT (sec)	Range (km)
1.50	1.46	1.46	7.80
1.52	1.48	1.49	7.94
1.56	1.52	1.53	8.15
1.61	1.57	1.58	8.39
1.65	1.61	1.63	8.61
1.71	1.67	1.68	8.81
1.79	1.75	1.74	8.92
1.85	1.81	1.79	9.13
1.90	1.86	1.87	9.37
1.96	1.92	1.91	9.59
2.03	1.99	1.97	9.89
2.08	2.04	2.02	10.14
2.13	2.09	2.05	10.32
2.20	2.16	2.09	10.48
2.23	2.19	2.16	10.70
2.26	2.22	2.22	10.93
2.30	2.26	2.25	11.11
2.32	2.28	2.28	11.35
2.35	2.31	2.31	11.61
2.37	2.33	2.34	11.81
2.40	2.36	2.37	11.01
2.43	2.39	2.40	12.25
2.46	2.42	2.41	12.51
2.49	2.45	2.46	12.74
2.51	2.47	2.49	13.00
2.57	2.53	2.53	13.23
2.63	2.59	2.58	13.48
2.68	2.64	2.62	13.70
2.73	2.69	2.68	13.98
2.78	2.74	2.72	14.17
2.84	2.80	2.77	14.42
2.87	2.83	2.82	14.68
2.92	2.88	2.87	14.95
2.94	2.90	2.92	15.21
3.00	2.96	2.96	15.38
3.10	3.06	3.08	15.91
3.18	3.14	3.14	16.13
3.27	3.23	3.21	16.37
3.35	3.31	3.27	16.64
3.38	3.34	3.32	16.88
3.41	3.37	3.36	17.12
3.47	3.43	3.42	17.36
3.54	3.50	3.46	17.60
3.57	3.53	3.51	17.85
3.59	3.55	3.54	18.05
3.67	3.63	3.59	18.24
3.73	3.69	3.63	18.52
3.73	3.69	3.69	18.80
3.75	3.71	3.72	19.07
3.95	3.91	3.89	20.24
4.05	4.01	3.95	20.52
4.07	4.03	3.99	20.79
4.11	4.07	4.03	20.97

4.13	4.09	4.06	21.16
4.21	4.17	4.11	21.34
4.24	4.20	4.13	21.65
4.32	4.28	4.22	22.02
4.36	4.32	4.23	22.16

Colonsay to North Jura Airgun Line

North Jura station

Travel time (sec)	Corrected TT (sec)	Calculated TT (sec)	Range (km)
0.72	0.68	0.67	3.07
0.78	0.74	0.72	3.33
0.82	0.78	0.78	3.60
0.87	0.83	0.84	3.87
0.93	0.89	0.90	4.15
1.00	0.96	0.96	4.45
1.02	0.98	1.02	4.70
1.10	1.06	1.07	4.95
1.14	1.10	1.12	5.19
1.19	1.15	1.17	5.42
1.26	1.22	1.22	5.65
1.31	1.27	1.28	5.90
1.35	1.31	1.33	6.15
1.43	1.39	1.38	6.37
1.50	1.46	1.44	6.64
1.54	1.50	1.49	6.85
1.60	1.56	1.55	7.10
1.65	1.61	1.60	7.34
1.71	1.67	1.66	7.60
1.77	1.73	1.72	7.85
1.86	1.82	1.79	8.10
1.90	1.86	1.84	8.35
1.95	1.91	1.88	8.60
1.97	1.93	1.91	8.85
1.98	1.94	1.92	9.10
2.00	1.96	1.94	9.35
2.02	1.98	1.97	9.60
2.05	2.01	1.99	9.84
2.08	2.04	2.04	10.07
2.11	2.07	2.06	10.35
2.14	2.10	2.09	10.56
2.16	2.12	2.12	10.85
2.17	2.13	2.14	11.07
2.22	2.18	2.18	11.34
2.26	2.22	2.23	11.58
2.30	2.26	2.27	11.85
2.36	2.32	2.32	12.10
2.43	2.39	2.37	12.35
2.50	2.46	2.43	12.60
2.54	2.50	2.49	12.85
2.60	2.56	2.55	13.10
2.65	2.61	2.59	13.35
2.70	2.66	2.64	13.60
2.75	2.71	2.69	13.85
2.81	2.77	2.74	14.05
2.88	2.84	2.80	14.33
2.92	2.88	2.83	14.55

2.96	2.92	2.86	14.80
3.01	2.97	2.91	15.05
3.08	3.04	2.96	15.30
3.11	3.07	3.00	15.53
3.15	3.11	3.05	15.75
3.19	3.15	3.10	16.00

Colonsay station

Travel time (sec)	Corrected TT (sec)	Calculated TT (sec)	Range (km)
0.25	0.21	0.22	1.00
0.30	0.26	0.28	1.23
0.34	0.30	0.33	1.47
0.42	0.38	0.40	1.73
0.47	0.43	0.46	2.00
0.50	0.46	0.49	2.21
0.57	0.53	0.55	2.50
0.66	0.62	0.61	2.75
0.70	0.66	0.66	3.00
0.72	0.68	0.70	3.21
0.76	0.72	0.75	3.48
0.81	0.77	0.79	3.70
0.85	0.81	0.84	3.92
0.88	0.84	0.89	4.20
0.94	0.90	0.94	4.42
0.98	0.94	0.99	4.70
1.03	0.99	1.02	4.90
1.08	1.04	1.07	5.15
1.12	1.08	1.12	5.40
1.19	1.15	1.17	5.65
1.25	1.21	1.22	5.90
1.30	1.26	1.27	6.15
1.33	1.29	1.30	6.40
1.34	1.30	1.34	6.65
1.38	1.34	1.37	6.90
1.44	1.40	1.41	7.17
1.49	1.45	1.44	7.41
1.52	1.48	1.48	7.68
1.56	1.52	1.52	7.90
1.62	1.58	1.58	8.19
1.68	1.64	1.62	8.40
1.73	1.69	1.69	8.68
1.76	1.72	1.71	8.91
1.79	1.75	1.76	9.15
1.86	1.82	1.81	9.40
1.90	1.86	1.85	9.65
1.95	1.91	1.90	9.90
2.01	1.97	1.96	10.15
2.06	2.02	2.00	10.40
2.10	2.06	2.06	10.65
2.18	2.14	2.10	10.90
2.25	2.21	2.16	11.15
2.28	2.24	2.20	11.40
2.31	2.27	2.25	11.65
2.33	2.29	2.30	11.90
2.37	2.33	2.33	12.11
2.40	2.36	2.37	12.38

2.46	2.42	2.41	12.60
2.50	2.46	2.46	12.85
2.52	2.48	2.50	13.10
2.55	2.51	2.53	13.33
2.59	2.55	2.58	13.56
2.62	2.58	2.61	13.80
2.64	2.60	2.63	14.05
2.68	2.64	2.68	14.30
2.74	2.70	2.74	14.60
2.80	2.76	2.80	14.88
2.86	2.82	2.85	15.15
2.93	2.89	2.90	15.42
2.99	2.95	2.95	15.68

South Jura to North Kintyre Airgun Line

S. Jura station

Travel time (sec)	Corrected TT (sec)	Calculated TT (sec)	Range (km)
0.53	0.49	0.51	2.30
0.61	0.57	0.57	2.63
0.62	0.58	0.59	2.77
0.64	0.60	0.61	2.95
0.68	0.64	0.65	3.10
0.72	0.68	0.67	3.25
0.75	0.71	0.69	3.40
0.77	0.73	0.73	3.60
0.79	0.75	0.76	3.75
0.82	0.78	0.78	3.90
0.84	0.80	0.80	4.05
0.87	0.83	0.82	4.15
0.89	0.85	0.86	4.35
0.92	0.88	0.89	4.55
0.95	0.91	0.93	4.75
1.00	0.96	0.97	4.95
1.00	0.96	1.00	5.15
1.05	1.01	1.04	5.32
1.07	1.03	1.06	5.45
1.13	1.09	1.10	5.62
1.18	1.14	1.13	5.74
1.22	1.18	1.19	5.95
1.29	1.25	1.25	6.15
1.32	1.28	1.29	6.35
1.35	1.31	1.33	6.55
1.42	1.38	1.39	6.80
1.45	1.41	1.45	7.05
1.52	1.48	1.49	7.25
1.55	1.51	1.52	7.40
1.57	1.53	1.55	7.55
1.67	1.63	1.64	7.91
1.70	1.66	1.67	8.12
1.76	1.72	1.73	8.40
1.79	1.75	1.76	8.60
1.82	1.78	1.80	8.82
1.87	1.83	1.84	9.00
1.91	1.87	1.88	9.20
1.94	1.90	1.91	9.37

1.95	1.91	1.94	9.56
2.00	1.96	1.97	9.73
2.03	1.99	2.00	9.90
2.07	2.03	2.04	10.14
2.10	2.06	2.07	10.30
2.11	2.07	2.10	10.52
2.15	2.11	2.13	10.71
2.19	2.15	2.17	10.91
2.21	2.17	2.20	11.12
2.26	2.22	2.23	11.33
2.28	2.24	2.26	11.54
2.32	2.28	2.29	11.70
2.33	2.29	2.34	11.95
2.36	2.32	2.39	12.20
2.41	2.37	2.42	12.43
2.47	2.43	2.46	12.65
2.52	2.48	2.49	12.85
2.55	2.51	2.52	13.05
2.57	2.53	2.55	13.27
2.62	2.58	2.59	13.50
2.65	2.61	2.63	13.75
2.70	2.66	2.67	14.00
2.74	2.70	2.72	14.25
2.78	2.74	2.76	14.50
2.81	2.77	2.78	14.65
2.85	2.81	2.81	14.83
2.90	2.86	2.84	15.00
2.94	2.90	2.87	15.20
2.96	2.92	2.91	15.40
3.01	2.97	2.94	15.55
3.06	3.02	2.99	15.82
3.10	3.06	3.04	16.05
3.12	3.08	3.06	16.31
3.13	3.09	3.10	16.55
3.16	3.12	3.14	16.80
3.19	3.15	3.16	16.95

N. Kintyre station

Travel time (sec)	Corrected TT (sec)	Calculated TT (sec)	Range (km)
1.84	1.88	1.91	9.39
1.86	1.90	1.94	9.54
1.88	1.92	1.98	9.79
1.93	1.97	2.02	10.03
2.01	2.05	2.07	10.29
2.05	2.09	2.10	10.52
2.09	2.13	2.16	10.79
2.12	2.16	2.19	10.94
2.17	2.21	2.23	11.14
2.22	2.26	2.26	11.34
2.27	2.31	2.30	11.51
2.30	2.34	2.33	11.69
2.34	2.38	2.36	11.84
2.38	2.42	2.41	12.09
2.43	2.47	2.46	12.34
2.46	2.50	2.50	12.59

2.50	2.54	2.54	12.84
2.54	2.58	2.59	13.07
2.59	2.63	2.63	13.29
2.63	2.67	2.67	13.49
2.66	2.70	2.71	13.69
2.70	2.74	2.75	13.91
2.74	2.78	2.79	14.14
2.77	2.81	2.84	14.39
2.81	2.85	2.89	14.64
2.87	2.91	2.92	14.80
2.89	2.93	2.96	15.01
2.95	2.99	3.01	15.22
2.97	3.01	3.05	15.43
3.03	3.07	3.07	15.63
3.06	3.10	3.10	15.82
3.10	3.14	3.16	16.04
3.16	3.20	3.20	16.20
3.18	3.22	3.24	16.44
3.22	3.26	3.27	16.61
3.27	3.31	3.30	16.78
3.31	3.35	3.34	16.97
3.34	3.39	3.37	17.14
3.38	3.42	3.41	17.34
3.39	3.43	3.44	17.52
3.44	3.48	3.48	17.74
3.47	3.51	3.52	17.94
3.52	3.56	3.57	18.22
3.54	3.60	3.61	18.43
3.63	3.67	3.67	18.59
3.65	3.69	3.70	18.94
3.69	3.73	3.72	19.09
3.73	3.77	3.75	19.29
3.79	3.83	3.79	19.54
3.81	3.85	3.82	19.79
3.82	3.86	3.85	19.99
3.85	3.89	3.88	20.19
3.87	3.91	3.91	20.39
3.88	3.92	3.93	20.60
3.91	3.95	3.94	20.72
3.91	3.95	3.95	20.89
3.92	3.96	3.97	21.02
3.96	4.00	4.00	21.19
3.98	4.02	4.02	21.39
4.01	4.05	4.04	21.59
4.04	4.08	4.07	21.79
4.07	4.11	4.10	21.99
4.07	4.11	4.12	22.19
4.09	4.13	4.13	22.29
4.10	4.14	4.16	22.44
4.12	4.16	4.17	22.59
4.15	4.19	4.20	22.74
4.16	4.20	4.23	22.94
4.21	4.25	4.25	23.09
4.20	4.24	4.27	23.24
4.25	4.29	4.29	23.39
4.28	4.32	4.32	23.57
4.29	4.33	4.34	23.71
4.34	4.38	4.37	23.88
4.37	4.41	4.43	24.04

APPENDIX 10

JURA GEOFLEX SHOTS

S. Jura station

Shot No	Travel Time (sec)	Corrected TT (sec)	Calculated TT (sec)	Range (km)
1	4.48	4.44	4.46	24.80
2	4.40	4.36	4.33	23.93
3	4.25	4.21	4.18	23.03
4	4.07	4.03	4.01	22.03
5	3.91	3.87	3.86	21.21
6	3.74	3.70	3.70	20.24
9	2.99	2.95	2.96	15.58
10	2.65	2.61	2.58	13.78
12	2.02	1.98	1.94	10.06

APPENDIX 11

PICKING ERRORS, TOTAL MAXIMUM ERRORS OBSERVED TRAVEL TIMES AND CALCULATED TRAVEL TIMES OF THE EXPLOSIVE SHOTS.

Errors (absolute) were calculated according to the formulae:

Total error = Picking error + shot timing error + shot pos. error
0.03 (0.03 Barra - Mull
0.02 Mull - Kintyre
0.01 Kintyre-Girvan)

Observed travel times are the travel times of the explosive shots of Tables A.7 and A.8.

Barra station

Shot No.	Picking error (sec)	Total error (sec)	Observ.TT (sec)	Calcul. TT (sec)
22	0.05	0.11	4.10	4.13
21	0.05	0.11	5.90	5.91
20	0.05	0.11	7.07	7.13
19	0.05	0.11	10.10	10.07
18	0.05	0.11	12.76	12.80
17	0.05	0.11	14.27	14.27
16	0.05	0.11	15.65	15.70
15	0.05	0.10	17.51	17.51
12	0.10	0.15	20.66	-----
11	0.10	0.15	21.64	21.74
10	0.10	0.15	22.99	22.95
9	0.10	0.15	23.71	23.90
8	0.10	0.15	24.82	-----
6	I.10	0.15	26.67	-----
5	0.15	0.20	27.62	-----
4	0.10	0.14	30.05	-----
3	0.10	0.14	32.32	-----
2	0.10	0.14	34.52	-----
1	0.10	0.14	36.51	-----

Tiree (Ruaig) station

Shot No.	Picking error (sec)	Total error (sec)	Observ. TT (sec)	Calcul. TT (sec)
23	-----	-----	10.51	10.45
22	0.05	0.11	7.78	7.83
21	0.05	0.11	6.03	6.03
18	0.05	0.11	2.32	2.29
17	0.05	0.11	3.77	3.74
16	0.03	0.09	5.35	5.28
15	0.07	0.11	7.11	7.08
2	0.10	0.14	26.86	----

Iona station (WISE1)

Shot No.	Observ. TT (sec)	Calcul. TT (sec)
15	1.80	1.82
16	6.95	0.96
17	2.24	2.20
18	3.93	3.97
19	6.13	6.09
20	9.46	9.47
22	12.80	12.88
23	15.55	15.57

Mull station (WISE 1)

Shot No.	Picking error (sec)	Total error (sec)	Observ. TT (sec)	Calcul. TT (sec)
23	0.07	0.13	16.20	16.22
22	0.03	0.09	13.66	13.69
21	0.03	0.09	11.83	11.86
20	0.03	0.09	10.14	10.18
19	0.03	0.09	6.84	6.84
18	0.07	0.13	5.00	4.81
17	0.03	0.09	3.04	2.91
16	0.03	0.09	1.59	1.58
15	0.03	0.08	1.20	1.20
14	0.05	0.10	2.33	2.29
4	0.07	0.11	16.92	16.97
3	0.07	0.11	20.43	20.05
2	0.10	0.14	22.93	22.96

Colonsay station (WISE1)

Shot No. (sec)	Observ. TT (sec)	Calcul. TT (sec)
1	21.23	21.18
4	12.48	12.52
9	3.32	3.27
10	2.18	2.17
11	0.86	0.85
17	7.50	7.29
18	9.36	9.13
22	18.08	18.04

Mid Jura station (WISE 1)

Shot No.	Picking error (sec)	Total error (sec)	Observ. TT (sec)	Calcul. TT (sec)
23	0.05	0.11	23.95	———
22	0.05	0.11	22.10	22.20
21	0.05	0.11	20.50	20.48
20	0.05	0.11	18.76	18.77
19	0.05	0.11	15.48	15.45
18	0.03	0.09	13.59	13.53
17	0.03	0.09	11.83	11.82
16	0.03	0.09	10.28	10.28
15	0.03	0.08	8.45	8.48
14	0.03	0.08	7.56	7.51
13	0.03	0.08	6.51	6.47
12	0.03	0.08	5.51	5.47
11	0.05	0.10	4.17	4.15
10	0.05	0.10	3.04	3.01
9	0.05	0.10	1.78	1.80
8	0.05	0.10	0.57	0.58
6	0.05	0.10	3.34	3.32
5	0.05	0.10	4.94	4.88
4	0.05	0.09	8.10	8.13
3	0.05	0.09	11.27	11.23
2	0.05	0.09	14.26	14.23
1	0.05	0.09	17.00	16.95

South Jura station (WISE 1)

Shot No.	Picking error (sec)	Total error (sec)	Observ. TT (sec)		Calcul. TT (sec)
23	0.07	0.13	24.31		———
22	0.07	0.13	22.46		
21	0.05	0.11	20.87		22.40
20	0.05	0.11	19.15		20.84
19	0.05	0.11	15.84	15.82	19.11
18	0.05	0.11	13.91		13.80
17	0.03	0.09	12.18		12.17
16	0.05	0.11	10.65		10.62
15	0.05	0.10	8.80		8.84
14	0.05	0.10	7.89		7.89
13	0.05	0.10	6.92		6.94
12	0.05	0.10	5.87		5.84
11	0.05	0.10	4.52		4.50
6	0.05	0.10	2.97		2.95
5	0.05	0.10	4.57		4.51
4	0.05	0.09	7.72		7.72
3	0.05	0.09	10.90		10.85
2	0.05	0.09	13.90		13.87
1	0.05	0.09	16.62		16.57

Letterpin station

Shot No.	Picking error (sec)	Total error (sec)	Observ. TT (sec)	Calcul. TT (sec)
1	0.03	0.07	1.77	1.76
2	0.03	0.07	4.34	4.35
3	0.03	0.07	7.35	7.35
4	———	———	9.63	9.67
5	0.03	0.08	13.06	13.03
6	0.03	0.08	14.54	14.54
8	0.03	0.08	16.93	16.90
15	0.10	0.15	24.41	———
16	0.07	0.12	26.11	———
20	0.07	0.12	33.61	———

APPENDIX 12

Mull station (WISE 2)

Shot No.	Picking error (sec)	Total error (sec)	Observ. TT (sec)	Calcul. TT (sec)
10	0.03	0.08	1.84	1.86
9	0.03	0.08	2.91	2.93
8	0.03	0.08	3.62	3.59
7	0.08	0.13	4.07	4.22
6	0.03	0.08	5.27	5.27
5	0.03	0.08	6.53	6.47
4	0.05	0.10	7.64	7.64
3	0.03	0.08	10.58	10.63
2	0.07	0.12	11.29	11.26
1	0.03	0.08	11.93	11.92

Iona station (WISE 2)

Shot No.	Picking error (sec)	Total error (sec)	Observ. TT (sec)	Calcul. TT (sec)
10	0.03	0.08	2.43	2.45
9	0.03	0.08	3.41	3.41
8	0.03	0.08	4.51	4.20
7	0.03	0.08	4.73	4.75
6	0.03	0.08	5.80	5.81
5	0.03	0.08	7.11	7.06
4	0.03	0.08	8.29	8.25
3	0.03	0.08	11.28	11.26
2	0.05	0.10	11.84	11.83
1	0.03	0.08	12.53	12.48

Colonsay station (WISE 2)

Shot No.	Picking error (sec)	Total error (sec)	Observ. TT (sec)	Calcul. TT (sec)
10	0.03	0.08	3.55	3.55
9	0.03	0.08	2.35	2.45
8	0.03	0.08	1.78	1.70
7	0.03	0.08	0.99	1.08
5	0.03	0.08	1.61	1.59
4	0.03	0.08	2.77	2.80
3	0.03	0.08	5.95	5.98
2	0.03	0.08	6.54	6.59
1	0.05	0.10	7.29	7.28

North Jura station (WISE 2)

Shot No.	Picking error (sec)	Total error (sec)	Observ. TT (sec)	Calcul. TT (sec)
10	0.03	0.08	6.76	6.79
9	0.03	0.08	5.82	5.84
8	0.03	0.08	5.25	5.26
7	0.05	0.10	4.33	4.37
6	0.05	0.10	3.34	3.34
5	0.03	0.08	2.06	2.05
4	0.03	0.08	0.83	0.83
3	0.03	0.08	2.76	2.81
2	0.03	0.08	3.48	3.52
1	0.03	0.08	4.14	4.16

South Jura station (WISE2)

Shot No	Observ. TT (sec)	Calcul. TT (sec)
9	7.47	7.49
8	6.87	6.90
7	6.08	6.06
6	4.97	4.99
5	3.78	3.81
4	2.68	2.69
3	0.92	0.97
2	1.66	1.67
1	2.30	2.33

North Kintyre station (WISE2)

Shot No	Observ. TT (sec)	Calcul. TT (sec)
10	12.70	12.72
9	11.79	11.80
8	11.26	11.26
7	10.38	10.41
6	9.48	9.42
5	8.24	8.26
4	7.27	7.29
3	3.94	3.93
2	3.33	3.33
1	2.65	2.67

APPENDIX 2

List of computer programs

```
      PROGRAM SEIS81A
C
C     ***************
C
C     PROGRAM SEIS81 IS DESIGNED FOR A TWO POINT RAY TRACING AND
C     RAY SYNTHETIC SEISMOGRAM COMPUTATION IN A 2-D LATERALLY
C     INHOMOGENEOUS MEDIA WITH CURVED INTERFACES AND BLOCK STRUCTURES.
C
C     WRITTEN BY CERVENY, 1981 / EXTENDED BY P.TSOUMAKOS 1984-85
C     ***********************************************************************
C
C
C
C
C
      CHARACTER*6 IPLOT
      INTEGER CODE
      DIMENSION MTEXT(17),VEL(8),Y(3),DST1(100)
      COMMON/DIST/DST(100),NDST,IDIST,ASTART,ASTEP,AFIN,REPS
      COMMON/COD/CODE(50),KREF,KC
      COMMON/INTRF/A1(100,20),B1(100,20),C1(100,20),D1(100,20),
     1 X1(100,20),BRD(2),III(100,20),NPNT(20),NINT
      COMMON/RAY/AY(10,4000),DS(9,50),KINT(50),ROS,MREG,N,IREF,IND,IND1
      COMMON/AUXI/INTR,INT1,IOUT,IREFR,LAY,ITYPE,NDER,IPRINT,MPRINT,NTR,
     1IVEL(19)
      COMMON/DEN/RHO1(19),RHO2(19),NRHO
      COMMON/MOD1/IREV,XREV,IERR,EANG1,ZERO1
       COMMON/VMOD/BMIN,BMAX
       COMMON/PPI/PI
         COMMON/DRCON/KOKO
C
      DO 11 I=1,4000
      DO 11 J=1,10
   11 AY(J,I)=0.0
      IRUN=0
      LU3=7
      ONE=1.000
      PI=ATAN(ONE)*4.00
      CALL ICL9HEMASK (64,IRES)
C      CALL ICL9HEMASK (128,IRES)
C
      IRUN=0
C
C   IPLOT CHOOSES PLOTTING DEVICE FOR CONTOURING SECTION
C   -ROUTINE "GRIDCONT"
C   MTEXT  WILL APPEAR AS A TITLE ON THE TOP OF THE PLOT .
C
    1 READ(5,110)LU1,LU2,MPRINT,IPLOT,MTEXT
      WRITE(6,110)LU1,LU2,MPRINT,IPLOT,MTEXT
      READ(5,100) IREV,IERR,IVX,IVZ,KOKO
      WRITE(6,101) IREV,IERR,IVX,IVZ,KOKO
      READ(5,103) XREV,EANG1,ZERO1
      WRITE(6,103) XREV,EANG1,ZERO1
      IF(IRUN.EQ.0.AND.LU1.NE.0)REWIND LU1
C     IF(IRUN.EQ.0.AND.LU2.NE.0)REWIND LU2
```

```
      IRUN=1
      REWIND LU2
C
C     SPECIFICATION OF THE MODEL
C
      CALL MODEL(MTEXT,LU3,IVX,IVZ,IPLOT)
      IF(IVX.LT.1) GO TO 212
C      WRITE(LU3,222)
C
C     SPECIFICATION OF THE SYNTHETIC SEISMOGRAMS
C
  212 NAUX=0
    2 READ(5,100)ICONT,MEP,MOUT,MDIM,METHOD,IBP,IBS,IDP,IDS,IREAD,MREG,
     1MPSOUR,MSSOUR,ITMAX,NLAY
      IF(NAUX.EQ.0) WRITE(6,101)ICONT,MEP,MOUT,MDIM,METHOD,IBP,IBS,IDP,
     1IDS,IREAD,MREG,MPSOUR,MSSOUR,ITMAX,NLAY
      IF(NAUX.EQ.1) WRITE(6,102)ICONT,MEP,MOUT,MDIM,METHOD,IBP,IBS,IDP,
     1IDS,IREAD,MREG,MPSOUR,MSSOUR,ITMAX,NLAY
      IF(ICONT.EQ.(-1))GO TO 1
      IF(LU1.NE.0.AND.ICONT.EQ.0) WRITE(LU1,100)ICONT
      IF(ICONT.EQ.0)GO TO 99
      IF(NRHO.EQ.1)MREG=1
      NAUX=1
      IF(ITMAX.EQ.0)ITMAX=20
      IREC=1
      IUP=0
      IUS=0
      NLAYER=NINT-NLAY
      MREG=0
      NDR=7
      NDER=0
      IF(MDIM.NE.0)NDER=1
      IF(MDIM.NE.0)NDR=10
C
      IF(MEP.GT.0)GO TO 3
      NDST=-MEP
      READ(5,104)(DST(I),I=1,NDST)
      WRITE(6,104)(DST(I),I=1,NDST)
C NEXT, SOME OF BEN'S EFFORT FOR AUTO REVERSE OF THE LINE
      DO 7 I=1,NDST
      IF(IREV.NE.0) DST1(I)=DST(I)
      IF(IREV.NE.0) DST(I)=XREV-DST1(I)
  7   CONTINUE
      IF(IREV.NE.0) WRITE(6,104) (DST(I),I=1,NDST)
C   IF ONLY ONE RECEIVER , NO STEP  CAN BE DEFINED AND THE PROGRAM
C    FAILS DUE TO THE NEXT LINE.
C       RSTEP=(DST(NDST)-DST(1))/FLOAT(NDST-1)
      GO TO 4
    3 NDST=MEP
      READ(5,104)RMIN,RSTEP
      WRITE(6,104)RMIN,RSTEP
      A=RMIN
      DO 13 I=1,MEP
      DST(I)=A
   13 A=A+RSTEP
```

```
C +++++++++++++++++++++++++++++++++++++++++++++++++++++++++++++++
    4 READ(5,104)XSOUR,ZSOUR,TSOUR,REPS,ASP
      WRITE(6,104)XSOUR,ZSOUR,TSOUR,REPS,ASP
      IF(IREV.NE.0)XSOUR1=XSOUR
      IF(IREV.NE.0)  XSOUR=XREV-XSOUR1
      IF(IREV.NE.0) WRITE(6,104)  XSOUR,ZSOUR,TSOUR,REPS,ASP
      IF(IREAD.EQ.0)
     1READ(5,104)DT,AMIN1,ASTEP1,AMAX1,AMIN2,ASTEP2,AMAX2,AC
      IF(IREAD.EQ.0)
     1WRITE(6,104)DT,AMIN1,ASTEP1,AMAX1,AMIN2,ASTEP2,AMAX2,AC
      IF(IREAD.NE.0)  READ(5,104)DT,AMIN1,AC
      IF(IREAD.NE.0)  WRITE(6,104)DT,AMIN1,AC
      CALL SOURCE(0,1,MPSOUR,ANGLE,AMSOUR,PHSOUR)
      CALL SOURCE(0,2,MSSOUR,ANGLE,AMSOUR,PHSOUR)
      IF(DT.LT.0.0000001)DT=1.
      IF(AC.LT.0.0000001)AC=0.0001
      TMAX=10000.
      IF(ASP.LT..00001)ASP=2.
      IF(REPS.LT..00001)REPS=.05
      IND=-1
      CALL RAY2(XSOUR,ZSOUR,TSOUR,AMIN1,X,Z,T,FI,TMAX,DT,AC)
      IF(IND.EQ.10) WRITE(6,111)IND
      IF(IND.EQ.10)GO TO 99
      LAY=IND
      ISOUR=IND
      Y(1)=XSOUR
      Y(2)=ZSOUR
      Y(3)=AMIN1
      CALL VCHECK(Y,VEL)
      ROS=RHO1(IND)+RHO2(IND)*VEL(1)
C
C
C     GENERATE FILE LU2 FOR PLOTTING OF SYNTHETIC SEISMOGRAMS
C
      IF(LU2.EQ.0)GO TO 25
      WRITE(LU2,115)MTEXT
      WRITE(LU2,100)NDST
      WRITE(LU2,104)XSOUR,ZSOUR,TSOUR,RSTEP
      WRITE(LU2,104)(DST(I),I=1,NDST)
   25 CONTINUE
C
C    LOOP FOR ELEMENTARY WAVES
C
      NAWX=0
      IF(MOUT.EQ.0) WRITE(6,105)
   20 CALL GENER(NAWX,IDP,IDS,IBP,IBS,IUP,IUS,IREAD,ISOUR,IREC,NLAYER,
     1IFIN,NCODE)
      NAWX=1
      IF(IFIN.EQ.1)GO TO 49
      IF(MOUT.NE.0) WRITE(6,107)
      WRITE(6,106)NCODE,KC,KREF,(CODE(I),I=1,KREF)
      IF(MOUT.NE.0) WRITE(6,108)
      IF(IFIN.EQ.(-1))GO TO 20
C
C     GENERATE FILE LU1 FOR PLOTTING OF RAY DIAGRAMS,TRAVEL TIMES AND
```

```
C       AMPLITUDES
C
        IF(LU1.EQ.0)GO TO 21
        WRITE(LU1,100)ICONT
        WRITE(LU1,100)NINT,(NPNT(I),I=1,NINT)
        DO 22 IIJ=1,NINT
        NI=NPNT(IIJ)-1
     22 WRITE(LU1,116)(A1(J,IIJ),B1(J,IIJ),C1(J,IIJ),D1(J,IIJ),
       1X1(J,IIJ),III(J,IIJ),J=1,NI)
        WRITE(LU1,116)XSOUR,ZSOUR
     21 CONTINUE
C
C
        IF(IREAD.NE.0)
       1READ(5,104) AMIN1,ASTEP1,AMAX1,AMIN2,ASTEP2,AMAX2
        IF(IREAD.NE.0)
       1WRITE(6,104) AMIN1,ASTEP1,AMAX1,AMIN2,ASTEP2,AMAX2
        ASTART=AMIN1
        ASTEP=ASTEP1
        AFIN=AMAX1
        IF(KC.LT.0)ASTART=AMIN2
        IF(KC.LT.0)ASTEP=ASTEP2
        IF(KC.LT.0)AFIN=AMAX2
        CALL TRAMP(XSOUR,ZSOUR,TSOUR,DT,AC,TMAX,ASP,ITMAX,MOUT,
       1MDIM,MPSOUR,MSSOUR,NCODE,LU1,LU2,METHOD)
        GO TO 20
C
C       END OF LOOP FOR ELEMENTARY WAVES
C
     49 JJ=0
        A=0.
        IF(LU2.NE.0) WRITE(LU2,112)JJ,JJ,A,A,A,A,A
C
        GO TO 2
C
    100 FORMAT(26I3)
    101 FORMAT(2X,26I3)
    102 FORMAT(1H1,////,2X,26I3)
    103 FORMAT(F10.5,2F12.10)
    104 FORMAT(8F10.5)
    105 FORMAT(//2X,'LISTING OF WAVE CODES'//2X,'INT.CODE',5X,'E  T E R N
       1 A L   C O D E')
    106 FORMAT(I10,5X,31I3/18X,30I3)
    107 FORMAT(//2X,'INT.CODE',5X,'E X T E R N A L   C O D E')
    108 FORMAT(//)
    110 FORMAT(3I2,A6,17A4)
    111 FORMAT(/2X,'IND=',I5,/)
    112 FORMAT(2I5,1F10.5,2E15.9,2F10.5)
    115 FORMAT(17A4)
    116 FORMAT(5F10.5,I3)
    222   FORMAT('999.')
     99 STOP
        END
C
C       ***************************************************************
```

```
C
CSUB1
      SUBROUTINE TRAMP(XSOUR,ZSOUR,TSOUR,DT,AC,TMAX,ASTOP,ITMAX,MOUT,
     1MDIM,MPSOUR,MSSOUR,NCODE,LU1,LU2,METHOD)
C
C     TWO-POINT RAY TRACING
C
      INTEGER CODE
      DIMENSION TIME(4000),XCOOR(4000),AMPX(4000),AMPZ(4000),INDI(4000),
     1ZCOOR(4000),IND1I(4000)
      COMMON/RAY/AY(10,4000),DS(9,50),KINT(50),ROS,MREG,N,IREF,IND,IND1
      COMMON/DIST/DST(100),NDST,IDIST,ASTART,ASTEP,AFIN,REPS
      COMMON/COD/CODE(50),KREF,KC
C
C
       AA=ASTART-ASTEP
      INDEX=0
      INUM=0
      INDS=0
C
C     LOOP IN RAY PARAMETERS AA, FROM ASTART TO AFIN, WITH THE STEP
C     ASTEP
C
    1 AA=AA+ASTEP
      IF(ASTEP.GT.0..AND.AA.GT.AFIN)GO TO 99
      IF(ASTEP.LT.0..AND.AA.LT.AFIN)GO TO 99
      IND=INDS
      CALL RAY2(XSOUR,ZSOUR,TSOUR,AA,X,Z,T,FI,TMAX,DT,AC)
      IF(MOUT.EQ.2) WRITE(6,100)IND,IND1,X,T,AA
      IF(INUM.NE.0)GO TO 2
      AOLD=AA
      IOLD=IND
      XOLD=X
      INUM=1
      GO TO 1
C
C     PARAMETERS FOR THE PRECEDING RAY: AA=AOLD, X=XOLD, IND=IOLD
C     PARAMETERS FOR THE NEW RAY: AA=ANEW, X=XNEW, IND=INEW
C
    2 INEW=IND
      ANEW=AA
      XNEW=X
      IF(INEW.EQ.3.AND.IOLD.EQ.3)GO TO 40
      IF(INEW.EQ.3)GO TO 50
      IF(IOLD.EQ.3)GO TO 55
      IF(INEW.EQ.9.AND.IOLD.NE.9)GO TO 30
      IF(INEW.NE.9.AND.IOLD.EQ.9)GO TO 35
C
C     NO ITERATIONS, TAKE A NEW RAY IN THE LOOP
C
    3 IOLD=INEW
      XOLD=XNEW
      AOLD=ANEW
      GO TO 1
C
```

```
C       REGULAR CASE: IOLD=3, INEW=3
C
   40 XXNEW=XNEW
      XXOLD=XOLD
      AANEW=ANEW
      AAOLD=AOLD
   41 IF(XXNEW.GT.XXOLD)GO TO 46
C
C       REGULAR CASE: XXNEW.LE.XXOLD, ITREND=-1 (REVERSE BRANCH)
C
      ITREND=-1
      DO 42 I=1,NDST
      NDD=NDST-I+1
      IF(DST(NDD).GT.XXOLD)GO TO 42
      IF(DST(NDD).LT.XXNEW)GO TO 3
      DD=DST(NDD)
      II=NDD
      GO TO 43
   42 CONTINUE
      GO TO 3
C
C       REGULAR CASE: XXNEW.GT.XXOLD, ITREND=1 (REGULAR BRANCH)
C
   46 ITREND=1
      DO 44 I=1,NDST
      IF(DST(I).LT.XXOLD)GO TO 44
      IF(DST(I).GT.XXNEW)GO TO 3
      DD=DST(I)
      II=I
      GO TO 43
   44 CONTINUE
      GO TO 3
   43 P1=AAOLD
      P2=AANEW
      X1=XXOLD
      X2=XXNEW
C
C       I T E R A T I O N S
C
   60 ITER=0
      ISIGN=1
   61 ITER=ITER+1
      ISIGN=-ISIGN
      PNEW=0.5*(P1+P2)
      IF(ISIGN.GT.0.AND.METHOD.EQ.1)PNEW=P1+(DD-X1)*(P2-P1)/
     1(X2-X1)
      IF(METHOD.EQ.0)PNEW=P1+(DD-X1)*(P2-P1)/(X2-X1)
      IF(ITER.GT.ITMAX)GO TO 80
      IND=INDS
      CALL RAY2(XSOUR,ZSOUR,TSOUR,PNEW,X,Z,T,FI,TMAX,DT,AC)
      IF(MOUT.EQ.2) WRITE(6,101)IND,IND1,ITER,DD,X,T,PNEW
      IF(IND.NE.3)P2=PNEW
      IF(IND.NE.3)GO TO 61
      IF(ABS(X-DD).LT.REPS)GO TO 65
      IF(X1.LT.X2.AND.DD.GT.X)GO TO 63
```

```
      IF(X1.GT.X2.AND.DD.LT.X)GO TO 63
      P2=PNEW
      X2=X
      GO TO 61
   63 P1=PNEW
      X1=X
      GO TO 61
C
C     SUCCESSFUL ITERATIONS
C
   65 INDEX=INDEX+1
      IF(MOUT.EQ.2) WRITE(6,102)IND,IND1,ITER,II,INDEX,DD,X,T,PNEW
      IF(MOUT.EQ.2.AND.MDIM.EQ.0) WRITE(6,114)
      IF(MOUT.EQ.1.AND.MDIM.EQ.0) WRITE(6,113)DD,X,Z,T,PNEW,IND,
     1IND1,ITER,II,INEW
      IF(LU1.NE.0) WRITE(LU1,116)N,IND
C
C     ARRAY AY(I,J) OUTPUT WITH J=1,7 ONLY SINCE SOMETIMES
C     THE ELEMENTS AY(8,I),AY(9,I),AY(10,I) BECOME VERY BIG NUMBERS
C     AND THE W-PART OF THE FORMAT IS INCREASED WHITCH CREATES
C     PROBLEMS WITH THE PLOTTING.    SEE ALSO COMENTS IN LINES  490 - 49
C
      IF(LU1.NE.0) WRITE(LU1,117)((AY(J,I),J=1,7),I=1,N)
      TIME(INDEX)=T
      XCOOR(INDEX)=X
      ZCOOR(INDEX)=Z
      INDI(INDEX)=IND
      IND1I(INDEX)=IND1
      IF(MDIM.NE.0) GOTO 9
      AMPZ(INDEX)=0.0
      AMPX(INDEX)=0.0
      GO TO 80
    9 IF(MDIM.EQ.1)SPR=1.
      IF(MDIM.EQ.1)GO TO 10
      N=0
      Q0=0.
      P0=1./AY(5,1)
      CALL JPAR(Q0,P0,SPR,P,0)
   10 CALL AMPL(SPR,AX,AZ,PHX,PHZ)
      MWAVE=1
      IF(CODE(1).LT.0)MWAVE=2
      MTYPE=MPSOUR
      IF(CODE(1).LT.0)MTYPE=MSSOUR
      CALL SOURCE(1,MWAVE,MTYPE,PNEW,AMSOUR,PHSOUR)
      AX=AX*AMSOUR
      AZ=AZ*AMSOUR
      PHX=PHX+PHSOUR
      PHZ=PHZ+PHSOUR
      IF(MDIM.LT.3)GO TO 12
      AUX=0.
      DO 11 I=2,N
      TDIF=AY(1,I)-AY(1,I-1)
      VAVER=0.5*(AY(5,I)+AY(5,I-1))
      VAVER2=VAVER*VAVER
   11 AUX=AUX+VAVER2*TDIF
```

```
      IF(AUX.LT.0.000001)AUX=0.001
      AUX=SQRT(AY(5,1)/AUX)
      SPR=SPR/AUX
      AX=AX*AUX
      AZ=AZ*AUX
   12 CONTINUE
      IF(CODE(1).LT.0)AX=AX*ASTOP
      IF(CODE(1).LT.0)AZ=AZ*ASTOP
      AMPZ(INDEX)=AZ
      AMPX(INDEX)=AX
      IF(MOUT.EQ.1.AND.MDIM.NE.0) WRITE(6,105)DD,X,Z,T,PNEW,SPR,AX,
     1PHX,AZ,PHZ,IND,IND1,ITER,II,INEW
      IF(MOUT.EQ.2) WRITE(6,110)AX,PHX,AZ,PHZ,SPR
      IF(LU2.NE.0) WRITE(LU2,115)NCODE,II,T,AX,AZ,PHX,PHZ
C
C
C
   80 P1=PNEW
      X1=X
      IF(ITER.GT.ITMAX)P1=AAOLD
      IF(ITER.GT.ITMAX)X1=XXOLD
      P2=AANEW
      X2=XXNEW
      IF(ITREND.EQ.(-1))GO TO 85
      II=II+1
      IF(II.GT.NDST)GO TO 3
      DD=DST(II)
      IF(DD.GT.XXNEW)GO TO 3
      GO TO 60
   85 II=II-1
      IF(II.LT.1)GO TO 3
      DD=DST(II)
      IF(DD.LT.XXNEW)GO TO 3
      GO TO 60
C
C     E N D   O F    I T E R A T I O N S
C
C
C      BOUNDARY RAYS. CASE IOLD.NE.3, INEW=3
C
   50 XXNEW=XNEW
      AANEW=ANEW
      P1=AOLD
      P2=ANEW
   54 IRES=0
      ITER=0
   51 PNEW=0.5*(P1+P2)
      ITER=ITER+1
      IND=INDS
      CALL RAY2(XSOUR,ZSOUR,TSOUR,PNEW,X,Z,T,FI,TMAX,DT,AC)
      IF(MOUT.EQ.2) WRITE(6,103)IND,IND1,ITER,X,T,PNEW
      IF(IND.EQ.3)GO TO 52
      P1=PNEW
      GO TO 53
   52 IRES=1
```

```
      XXOLD=X
      AAOLD=PNEW
      P2=PNEW
   53 IF(ITER.GE.ITMAX.AND.IRES.EQ.1)GO TO 41
      IF(ITER.GE.ITMAX)GO TO 3
      GO TO 51
C
C     BOUNDARY RAYS. CASE IOLD=3, INEW.NE.3
C
   55 XXOLD=XOLD
      AAOLD=AOLD
      P1=AOLD
      P2=ANEW
   59 IRES=0
      ITER=0
   56 PNEW=0.5*(P1+P2)
      ITER=ITER+1
      IND=INDS
      CALL RAY2(XSOUR,ZSOUR,TSOUR,PNEW,X,Z,T,FI,TMAX,DT,AC)
      IF(MOUT.EQ.2) WRITE(6,103)IND,IND1,ITER,X,T,PNEW
      IF(MOUT.EQ.1.AND.ITER.EQ.20) WRITE(6,107)X,Z,T,PNEW,IND,IND1,ITER
      IF(IND.EQ.3)GO TO 57
      P2=PNEW
      GO TO 58
   57 IRES=1
      XXNEW=X
      AANEW=PNEW
      P1=PNEW
   58 IF(ITER.GE.ITMAX.AND.IRES.EQ.1)GO TO 41
      IF(ITER.GE.ITMAX)GO TO 3
      GO TO 56
C
C     CRITICAL RAYS. CASE IOLD.NE.9, IOLD.NE.9, INEW=9
C
   30 ITER=0
      P1=AOLD
      P2=ANEW
      IRES=0
   31 PNEW=0.5*(P1+P2)
      ITER=ITER+1
      IND=INDS
      CALL RAY2(XSOUR,ZSOUR,TSOUR,PNEW,X,Z,T,FI,TMAX,DT,AC)
      IF(MOUT.EQ.2) WRITE(6,104)IND,IND1,ITER,X,T,PNEW
      IF(MOUT.EQ.1.AND.ITER.EQ.20) WRITE(6,111)X,Z,T,PNEW,IND,IND1,ITER
      IF(IND.EQ.9.OR.IND.GT.100)GO TO 32
      IF(IND.EQ.3)GO TO 33
      P1=PNEW
      GO TO 34
   32 P2=PNEW
      GO TO 34
   33 IRES=1
      P1=PNEW
   34 IF(ITER.GE.ITMAX.AND.IRES.EQ.0)GO TO 3
      IF(ITER.LT.ITMAX)GO TO 31
      P2=PNEW
```

```
      XXNEW=X
      AANEW=P2
      P1=AOLD
      GO TO 54
C
C     CRITICAL RAYS. CASE IOLD=9, INEW.NE.9, INEW.NE.3.
C     (THIS VERSION NOT YET  WRITTEN)
C
   35 CONTINUE
      GO TO 3
  100 FORMAT(2I3,2F10.5,F15.10)
  101 FORMAT(1X,'ITERATIONS',5X,3I3,3F10.5,F15.10)
  102 FORMAT(/,1X,'SUCCESSFUL ITERATION',3X,5I3,3F10.5,F15.10)
  103 FORMAT(2X,'BOUNDARY RAY',5X,3I3,2F10.5,F15.10)
  104 FORMAT(2X,'CRITICAL RAY',5X,3I3,2F10.5,F15.10)
  105 FORMAT(4F10.5,F15.10,F15.5,4F10.5,5I3)
  106 FORMAT(2I5,5E15.10)
  107 FORMAT(10X,3F10.5,F15.10,3I3,5X,'BOUNDARY RAY')
  110 FORMAT(25X,4F10.5,F15.5,/)
  111 FORMAT(10X,3F10.5,F15.10,3I3,5X,'CRITICAL RAY')
  113 FORMAT(4F10.5,F15.10,5I3)
  114 FORMAT(/)
  115 FORMAT(2I5,1F10.5,2E15.9,2F10.5)
  116  FORMAT(24I3)
  117 FORMAT(7F10.5)
  118  FORMAT(2I5,4F12.5)
C
C
   79 N=0
      NAUX=0
C     IF(LU1.NE.0) WRITE(LU1,116)N,NAUX
C      IF(LU1.NE.0) WRITE(LU1,116)INDEX
      IF(INDEX.EQ.0)RETURN
C
C     I HAVE LEFT OUT THE AMPZ(I) AT THE END OF THE NEXT "WRITE"
C      STATEMENT SINCE SOMETIMES IS A VERY BIG NUMBER -THE F12.5 FORMAT
C      OF THE F12.5 FORMAT IS INCREASED TO A MINIMUM BY THE COMPUTER-
C      - WHITCH CANNOT BE READ FROM THE FIXED FORMAT OF THE " RAYPLOT "
C     CREATING AN ERROR MESAGE.SEE ALSO COMENTS IN LINES 312 - 317
C
C      IF(LU1.NE.0) WRITE(LU1,118)(INDI(I),IND11(I),XCOOR(I),ZCOOR(I),
C     1TIME(I),AMPX(I),I=1,INDEX)
      RETURN
      END
C
C     ***************************************************************
C
CSUB2
      SUBROUTINE GENER(N,IDP,IDS,IBP,IBS,IUP,IUS,IREAD,IS,IR,NS,IFIN,
     1NCODE)
C
C     THE ROUTINE GENER IS DESIGNED TO GENERATE NUMERICAL CODES OF
C     ELEMENTARY SEISMIC BODY WAVES
C
      DIMENSION JCA(50)
```

```
      COMMON/COD/JC(50),KCA,KC
C
C
      IFIN=0
      IF(N.GT.0)GO TO 1
      NCODE=1
      INEW=1
      INDEX=1
      GO TO 51
    1 NCODE=NCODE+1
      IF(INDEX.GE.11)GO TO 80
      IF(INEW.EQ.1)GO TO 50
      JAUX=0
      DO 20 I=1,KCA
      IF(JCA(I).EQ.JAUX)GO TO 21
      IAUX=I
   20 JAUX=JCA(I)
   21 IF(INDEX.LE.6.AND.JAUX.GE.(NS-1))GO TO 50
      IF(INDEX.GT.6.AND.JAUX.EQ.1)GO TO 50
      IAUX1=IAUX+1
      IAUX2=IAUX+2
      DO 22 I=IAUX1,KCA
      II=KCA+IAUX1-I
      JC(II+2)=JC(II)
   22 JCA(II+2)=JCA(II)
      KCA=KCA+2
      IF(INDEX.GE.7)GO TO 31
      JC(IAUX1)=JAUX+1
      JC(IAUX2)=JAUX+1
      JCA(IAUX1)=JC(IAUX1)
      JCA(IAUX2)=JC(IAUX2)
      IF(INDEX.GE.5)JC(IAUX1)=-JC(IAUX1)
      IF(INDEX.EQ.4.OR.INDEX.EQ.5)JC(IAUX2)=-JC(IAUX2)
       RETURN
   31 JC(IAUX1)=JAUX-1
      JC(IAUX2)=JAUX-1
      JCA(IAUX1)=JC(IAUX1)
      JCA(IAUX2)=JC(IAUX2)
      IF(INDEX.GE.9)JC(IAUX1)=-JC(IAUX1)
      IF(INDEX.EQ.8.OR.INDEX.EQ.9)JC(IAUX2)=-JC(IAUX2)
      RETURN
C
   50 INDEX=INDEX+1
      INEW=1
      IF(INDEX.GE.11)GO TO 80
   51 IF(INDEX.EQ.1.AND.IDP.EQ.0)GO TO 50
      IF(INDEX.EQ.2.AND.IDS.EQ.0)GO TO 50
      IF(INDEX.EQ.3.AND.IBP.EQ.0)GO TO 50
      IF(INDEX.EQ.4.AND.IBP.NE.2)GO TO 50
      IF(INDEX.EQ.5.AND.IBS.EQ.0)GO TO 50
      IF(INDEX.EQ.6.AND.IBS.NE.2)GO TO 50
      IF(INDEX.EQ.7.AND.IUP.EQ.0)GO TO 50
      IF(INDEX.EQ.8.AND.IUP.NE.2)GO TO 50
      IF(INDEX.EQ.9.AND.IUS.EQ.0)GO TO 50
      IF(INDEX.EQ.10.AND.IUS.NE.2)GO TO 50
```

```
      IMIN=IS
      IMAX=IR
      IF(IS.GT.IR)IMIN=IR
      IF(IS.GT.IR)IMAX=IS
      ISUM=IMAX-IMIN+2
      IF(INDEX.LE.2)GO TO 70
      INEW=0
      IF(INDEX.GT.6)GO TO 60
      ISM=IMAX-IS+1
      DO 55 I=1,ISM
      JCA(I)=IS+I-1
      JC(I)=JCA(I)
   55 IF(INDEX.GT.4)JC(I)=-JCA(I)
      ISM2=ISM+1
      DO 56 I=ISM2,ISUM
      JCA(I)=IMAX+ISM2-I
      JC(I)=JCA(I)
   56 IF(INDEX.EQ.4.OR.INDEX.EQ.5)JC(I)=-JCA(I)
      KCA=ISUM
      KC=1
      RETURN
   60 ISM=IS-IMIN+1
      DO 65 I=1,ISM
      JCA(I)=IS+1-I
      JC(I)=JCA(I)
   65 IF(INDEX.GT.8)JC(I)=-JCA(I)
      ISM2=ISM+1
      DO 66 I=ISM2,ISUM
      JCA(I)=IMIN+I-ISM2
      JC(I)=JCA(I)
   66 IF(INDEX.EQ.8.OR.INDEX.EQ.9)JC(I)=-JCA(I)
      KCA=ISUM
      KC=-1
      INEW=0
      RETURN
   70 KCA=IMAX-IMIN+1
      KC=1
      IF(IS.GE.IR)KC=-1
      DO 71 I=1,KCA
      JC(I)=IS+I-1
      IF(IS.GT.IR)JC(I)=IS-I+1
      JCA(I)=JC(I)
      IF(INDEX.EQ.2)JC(I)=-JC(I)
   71 CONTINUE
      RETURN
   80 IF(IREAD.EQ.0)GO TO 101
      READ(5,100)KC,KCA,(JC(I),I=1,KCA),KCAAUX
      IF(KCAAUX.GT.0)GOTO 101
      DO 81 I=1,KCA
   81 JCA(I)=IABS(JC(I))
      IF(KCA.GT.50)GO TO 99
      JAUX=JCA(1)
      IF(JAUX.NE.IS.OR.IS.LE.0.OR.IS.GT.NS)GO TO 99
      IRAUX=IR
      IF(KCA.EQ.1) IR=IS
```

```
      IF(JCA(KCA).NE.IR.OR.IR.LE.0.OR.IR.GT.NS)GO TO 99
      IR=IRAUX
      IF(KCA.EQ.1)RETURN
      ID=1
      IF(KC.LT.0)ID=-1
      DO 103 I=2,KCA
      JJ=JCA(I)
      IF(JJ.LE.0.OR.JJ.GE.NS)GO TO 99
      IF(JJ.EQ.JAUX)GO TO 105
      IF(ID.EQ.1.AND.JJ.EQ.(JAUX+1))GO TO 103
      IF(ID.EQ.(-1).AND.JJ.EQ.(JAUX-1))GO TO 103
      GO TO 99
  105 ID=-ID
  103 JAUX=JJ
      RETURN
   99 IFIN=-1
      RETURN
  101 IFIN=1
      RETURN
  100 FORMAT(24I3)
      END
C
C     ******************************************************************
C
C
C
C      S U B R O U T I N E   R A Y 2
C
C      ********************************************************************
C
CSUB3
      SUBROUTINE RAY2(X0,Z0,T0,FI0,X,Z,T,FI,TMAX,DT,AC)
C
C     RAY TRACING BY THE RUNGE-KUTTA'S METHOD
C
      INTEGER CODE
      DIMENSION Y(3),DERY(3),DIN(3),PRM(5),AUX(8,3)
      COMMON/INTRF/A1(100,20),B1(100,20),C1(100,20),D1(100,20),
     1 X1(100,20), BRD(2),III(100,20),NPNT(20),NINT
      COMMON/AUXI/INTR,INT1,IOUT,IREFR,LAY,ITYPE,NDER,IPRINT,MPRINT,NTR,
     1 IVEL(19)
      COMMON/COD/CODE(50),KREF,KC
      COMMON/RAY/AY(10,4000),DS(9,50),KINT(50),ROS,MREG,N,IREF,IND,IND1
      COMMON/MOD2/IRFRCT
C
C
      Y(1)=X0
      Y(2)=Z0
      Y(3)=FI0
      IREFR=0
      IRFRCT=0
      N=0
      IREF=1
      IOUT=0
      IF(IND.GT.0) GO TO 6
C
```

```
C       FOR IND=-1: DETERMINATION OF THE NUMBER OF THE LAYER, IN WHICH
C       THE INITIAL POINT (X0,Z0) IS SITUATED
C
        IF(Y(1).LT.BRD(1).OR.Y(1).GT.BRD(2)) GO TO 4
        INT1=0
        INTR=1
      1 NL=NPNT(INTR)-1
        DO 2 I=1,NL
        J=I
        IF(Y(1).LT.X1(I+1,INTR)) GO TO 3
      2 CONTINUE
      3 A2=A1(J,INTR)
        B2=B1(J,INTR)
        C2=C1(J,INTR)
        D2=D1(J,INTR)
        X2=X1(J,INTR)
        AU =Y(1)-X2
        ZINT=((D2*AU +C2)*AU +B2)*AU +A2
        IF(Y(2).LT.ZINT.AND.INTR.EQ.1) GO TO 4
        IF(ABS(Y(2)-ZINT).LT..0000001)INT1=INTR
        IF(Y(2).LT.ZINT) GOTO 5
        ISOUR=INTR
        IF(ABS(Y(2)-ZINT).LT..0000001.AND.INTR.EQ.NINT)GO TO 5
        IF(INTR.EQ.NINT)GO TO 4
        INTR=INTR+1
        GO TO 1
      4 IND=10
        RETURN
C
C       DETERMINATION OF THE INITIAL CONDITIONS FOR THE RUNGE-KUTTA
C       PROCEDURE
C
      5 IINT1=INT1
        IF(IND.GE.0) GO TO 6
        IND=ISOUR
        RETURN
C
      6 LAY=ISOUR
        INT1=IINT1
        IF(ISOUR.NE.IABS(CODE(1)))IND=14
        IF(ISOUR.NE.IABS(CODE(1)))RETURN
        IND=0
        ITYPE=ISIGN(1,CODE(1))
        PRM(1)=T0
        PRM(2)=TMAX
        PRM(3)=DT
        PRM(4)=AC
        T=PRM(1)
        DIN(1)=.33
        DIN(2)=.33
        DIN(3)=.34
      9 DO 10 I=1,3
     10 DERY(I)=DIN(I)
C
C       COMPUTATION OF THE RAY
```

```
C
      CALL RKGS(PRM,Y,DERY,3,IHLF,AUX)
      IF(IHLF.EQ.11)IND=5
      IF(IHLF.EQ.12)IND=6
      IF(IHLF.EQ.13)IND=7
      IF(IND.GE.5.AND.IND.LE.7)RETURN
      IF(ABS(PRM(5)).GT..0001) GO TO 11
C
C     INTEGRATION FROM THE POINT OF REFLECTION/TRANSMISSION WITH
C     A SPECIFIED REGULAR TIME STEP
C
      T=AY(1,N)
      DELTT=PRM(3)
      IF(T.GE.TMAX)GO TO 15
      GO TO 14
   11 IF(ABS(PRM(5)-1.1).GT..0001) GO TO 13
C
C     LOOP FOR THE ITERATIVE DETERMINATION OF THE POINT OF
C     INCIDENCE (NOT USED IN THIS VERSION)
C
      PRM(1)=AY(1,N)
      PRM(3)=PRM(3)/(2.**(IHLF+1))
      DO 12 I=1,3
   12 Y(I)=AY(I+1,N)
      T=AY(1,N)
      N=N-1
      GO TO 9
   13 X=Y(1)
      Z=Y(2)
      T=AY(1,N)
      IF(ABS(PRM(5)-2.).GT..0001.AND.IREFR.EQ.1)IND1=-IND1
      IF(ABS(PRM(5)-2.).GT..0001)GO TO 20
C
C     INTEGRATION FROM THE POINT OF REFLECTION/TRANSMISSION TO THE
C     CLOSEST POINT OF THE RAY CORRESPONDING TO THE REGULAR TIME
C     STEP ALONG THE RAY
C
      PRM(1)=AY(1,N)
      I=INT((PRM(1)-T0)/DT)
      PRM(2)=FLOAT(I+1)*DT+T0
      GO TO 9
   14 PRM(1)=PRM(2)
      PRM(2)=TMAX
      PRM(3)=DT
      N=N-1
      GO TO 9
   15 IND=12
      X=Y(1)
      Z=Y(2)
      IF(IREFR.EQ.1)IND1=-IND1
C
C
   20 FI=AY(4,N)
C
      RETURN
```

```
      END
C
C     ******************************************************************
C
CSUB4
      SUBROUTINE OUTP(X,Y,DERY,IHLF,NDIM,PRMT)
C
C     EXTERNAL ROUTINE IN THE RUNGE-KUTTA'S RAY TRACING.
C     PERFORMS VARIOUS COMPUTATIONS AT EACH POINT OF THE RAY.
C
      INTEGER CODE
      DIMENSION Y(3),DERY(3),PRMT(5),YOLD(2),YINT(2),VEL(8),Y1(2)
      COMMON/COD/CODE(50),KREF,KC
      COMMON/INTRF/A1(100,20),B1(100,20),C1(100,20),D1(100,20),
     1X1(100,20), BRD(2),III(100,20),NPNT(20),NINT
      COMMON/RAY/AY(10,4000),DS(9,50),KINT(50),ROS,MREG,N,IREF,IND,IND1
      COMMON/AUXI/INTR,INT1,IOUT,IREFR,LAY,ITYPE,NDER,IPRINT,MPRINT,NTR,
     1  IVEL(19)
      COMMON/DEN/RHO1(19),RHO2(19),NRHO
      COMMON/MOD1/IREV,XREV,IERR,EANG1,ZERO1
      COMMON/MOD2/IRFRCT
       COMMON/PPI/PI
C
C
      INSPL=0
      N=N+1
      NRR=N
      NTR=1
      IF(N.GT.4000)GO TO 50
      INTR=LAY
C
C     CHECK THE POSITION OF THE POINT OF THE RAY
C
      NL=NPNT(INTR)-1
      DO 2 I=1,NL
      J=I
      IF(Y(1).LT.X1(I+1,INTR)) GOTO 3
    2 CONTINUE
    3 IF(IREF.EQ.1)GO TO 27
      IF(KINT(IREF-1).EQ.(N-1))GO TO 21
   27 A2=A1(J,INTR)
      B2=B1(J,INTR)
      C2=C1(J,INTR)
      D2=D1(J,INTR)
      X2=X1(J,INTR)
      AUX=Y(1)-X2
      ZINT=((D2*AUX+C2)*AUX+B2)*AUX+A2
      IF(Y(2).LT.ZINT) GO TO 9
      INTR=LAY+1
      NL=NPNT(INTR)-1
      DO 4 I=1,NL
      J=I
      IF(Y(1).LT.X1(I+1,INTR)) GO TO 5
    4 CONTINUE
    5 A2=A1(J,INTR)
```

```
      B2=B1(J,INTR)
      C2=C1(J,INTR)
      D2=D1(J,INTR)
      X2=X1(J,INTR)
      AUX=Y(1)-X2
      ZINT=((D2*AUX+C2)*AUX+B2)*AUX+A2
      IF(Y(2).GT.ZINT) GO TO 9
   21 IF(Y(1).LT.BRD(1).OR.Y(1).GT.BRD(2))GO TO 7
C
C     THE RAY DID NOT CROSS AN INTERFACE
C
   99 IF(IRFRCT.EQ.2) IRFRCT=0
      IF(IRFRCT.EQ.1) IRFRCT=2
      AY(1,N)=X
      DO 6 I=1,3
    6 AY(I+1,N)=Y(I)
      IF(IERR.EQ.1.AND.EANG1.LT.AY(4,1)) WRITE(6,100) (AY(I,N),I=1,4)
      YAN=Y(3)
      Y(3)=101.
      CALL VCHECK(Y,VEL)
      Y(3)=YAN
      RETURN
C
C     THE RAY CROSSED ONE OF THE VERTICAL BOUNDARIES
C
    7 IF(Y(1).LT.BRD(1)) IND=1
      IF(Y(1).GT.BRD(2)) IND=2
   33 AUX=(BRD(IND)-AY(2,N-1))/(Y(1)-AY(2,N-1))
      AY(1,N)=AY(1,N-1)+AUX*(X-AY(1,N-1))
      DO 8 I=2,3
    8 AY(I+1,N)=AY(I+1,N-1)+AUX*(Y(I)-AY(I+1,N-1))
      AY(2,N)=BRD(IND)
      X=AY(1,N)
      Y(1)=AY(2,N)
      Y(2)=AY(3,N)
      Y(3)=AY(4,N)
      PRMT(5)=3.
      KINT(IREF)=N
      NTR=2
      GO TO 32
C
C     THE RAY MIGHT HAVE CROSSED AN INTERFACE.
C
C     DETERMINE THE POINT OF INCIDENCE
C
    9 YOLD(1)=AY(2,N-1)
      YOLD(2)=AY(3,N-1)
      IRR=IREF
      IF(IERR.EQ.1.AND.EANG1.LT.AY(4,1)) WRITE(6,100) YOLD(1),YOLD(2)
      CALL ROOT(YOLD,Y,YINT,ANYX,ANYZ,RC,J,IROOT)
      IF(IERR.EQ.1.AND.EANG1.LT.AY(4,1)) WRITE(6,100) YINT(1),YINT(2)
  100 FORMAT(8F10.5)
      IF(IRFRCT.EQ.0) GO TO 98
      IF(YINT(1).LT.AY(2,N-1)+ZERO1) GO TO 99
   98 CONTINUE
```

```
C       RAY CROSSED INTERFACE
        IRFRCT=1
        IF(IND.EQ.1.OR.IND.EQ.2)GO TO 33
        IND1=INTR
        IF(IROOT.EQ.100)GO TO 30
C
C       THE LOOP FOR THE ITERATIVE DETERMINATION OF THE POINT
C       OF INCIDENCE (NOT USED IN THIS VERSION)
C
        IF(IOUT.NE.0)GO TO 11
   10   N=N-1
        Y1(1)=YINT(1)
        Y1(2)=YINT(2)
        PRMT(5)=1.1
        IOUT=1
        RETURN
   11   IAC=IAC+1
        IF(IAC.EQ.10)GO TO 30
        AUX1=Y1(1)-YINT(1)
        AUX2=Y1(2)-YINT(2)
        AUX=AUX1*AUX1+AUX2*AUX2
        IF(AUX.GT..00001) GO TO 10
C
C       DETERMINATION OF PARAMETERS OF INCIDENT WAVE AT THE POINT
C       OF INCIDENCE
C
   30   IAC=0
        IOUT=0
        AY(2,N)=YINT(1)
        AY(3,N)=YINT(2)
        XDIF=Y(1)-AY(2,N-1)
        YDIF=Y(2)-AY(3,N-1)
        IF(ABS(XDIF).LT.0.001)GO TO 60
        AUX=(AY(2,N)-AY(2,N-1))/XDIF
        GO TO 62
   60   IF(ABS(YDIF).LT.0.001)GO TO 61
        AUX=(AY(3,N)-AY(3,N-1))/YDIF
        GO TO 62
   61   AUX=0.
   62   CONTINUE
        AY(1,N)=AY(1,N-1)+AUX*(X-AY(1,N-1))
        AY(4,N)=AY(4,N-1)+AUX*(Y(3)-AY(4,N-1))
        IF(IERR.EQ.1.AND.EANG1.LT.AY(4,1)) WRITE(6,100) (AY(I,N),I=1,4)
        X=AY(1,N)
        DO 12 I=1,3
   12   Y(I)=AY(I+1,N)
        IF(IERR.EQ.1.AND.EANG1.LT.AY(4,1)) WRITE(6,101) IREF
  101   FORMAT(I10)
        NTR=3
        IF(IREF.EQ.1.AND.KC.EQ.1.AND.LAY.EQ.INTR)GO TO 26
        NTR=4
        IF(IREF.EQ.1.AND.KC.EQ.(-1).AND.LAY.NE.INTR)GO TO 26
        IF(IREF.EQ.1)GO TO 49
        NNN=KINT(IREF-1)
        IF(NNN.LE.0)GO TO 49
```

```
      IF(ABS(AY(2,NNN)-YINT(1)).GT.0.0001.OR.INTR.NE.INT1)GOTO 49
      IRR=IRR-1
        NTR=5
      IF(AINDEX.GT.1)GO TO 28
        NTR=6
      GO TO 26
C
C
   49 ITYPE1=ITYPE
      ITYPE=1
      CALL VCHECK(Y,VEL)
      DS(4,IREF)=VEL(1)
      DS(8,IREF)=RHO1(LAY)+RHO2(LAY)*VEL(1)
      ITYPE=-1
      CALL VCHECK(Y,VEL)
      DS(5,IREF)=VEL(1)
      ITYPE=ITYPE1
      DS(1,IREF)=0.
      DS(3,IREF)=0.
      DS(6,IREF)=0.
      DS(7,IREF)=0.
      DS(9,IREF)=0.
      IF(KREF.GT.1)IC1=CODE(IREF)
      LAY1=LAY
      PX=COS(Y(3))
      PZ=SIN(Y(3))
      YAN=Y(3)
      AUX=ANYX*PX+ANYZ*PZ
      TANG=-1.57079632
      IF(-ANYX*ANYZ.GT.0)TANG=-TANG
      IF(ABS(ANYZ).GT.0.000000001*ABS(ANYX))TANG=ATAN(-ANYX/ANYZ)
      TANG=ATAN(-ANYX/ANYZ)
      IF(AUX.LE.0.) GO TO 13
      TANG=TANG+3.14159265
      ANYX=-ANYX
      ANYZ=-ANYZ
      AUX=-AUX
      RC=-RC
   13 AA=3.14159265-TANG+Y(3)
      DS(2,IREF)=AA
      IF(AA.GT.3.14159265)DS(2,IREF)=AA-6.2831852
      IF(KREF.LE.1)GO TO 31
C
C     MULTIPLY REFLECTED WAVE
C
      NTR=7
      IF((IREF+1).GT.KREF) GO TO 24
      NCD=CODE(IREF+1)-CODE(IREF)
      NTR=8
      IF(INTR.EQ.INT1.AND.NCD.NE.0)GO TO 26
      IF(INTR.NE.INT1.OR.NCD.NE.0)GO TO 46
      IREFR=1
      KINT(IREF)=0
      IREF=IREF+1
      IRR=IREF
```

```
      DS(2,IREF)=DS(2,IREF-1)
      DS(4,IREF)=DS(4,IREF-1)
      DS(5,IREF)=DS(5,IREF-1)
      DS(8,IREF)=DS(8,IREF-1)
      DO 53 I=1,9
   53   DS(I,IREF-1)=0.
      NCD=CODE(IREF+1)-CODE(IREF)
      NTR=9
      IF((IREF+1).GT.KREF) GO TO 24
   46 INT1=INTR
      NTR=10
      IF(IREF.EQ.1.AND.KC.EQ.(-1).AND.INTR.NE.LAY) GO TO 26
      NTR=11
      IF(IREF.EQ.1.AND.KC.EQ.1.AND.INTR.EQ.LAY) GO TO 26
      J11=J
      I11=INTR
      L11=LAY1
      IF(NCD.NE.0) GO TO 22
C
C     REFLECTION OF UNCONVERTED WAVE
C
      IIII=III(J,INTR)
      NTR=12
      IF(IIII.EQ.(-2))GO TO 48
      Y(3)=101.
      CALL VCHECK(Y,VEL)
      Y(3)=YAN
      AUX2=PZ-2.*AUX*ANYZ
      AUX1=PX-2.*AUX*ANYX
      IREF=IREF+1
      V1=VEL(1)
      V2=V1
      AINDEX=1.
      GO TO 18
C
C     REFRACTED WAVE
C
   31 NTR=13
      IF(INTR.EQ.LAY.AND.LAY.EQ.1) GO TO 24
      NTR=14
      IF(INTR.GT.LAY.AND.INTR.EQ.NINT) GO TO 24
      NCD=1
      GO TO 14
C
C     REFRACTION OR REFLECTION OF CONVERTED WAVE
C
   22 NCD=IABS(CODE(IREF+1))-IABS(CODE(IREF))
      IIII=III(J,INTR)
      NTR=15
      IF(NCD.EQ.0.AND.IIII.EQ.(-2)) GO TO 48
      IC2=CODE(IREF+1)
   14 Y(3)=101.
      CALL VCHECK(Y,VEL)
      Y(3)=YAN
      V1=VEL(1)
```

```
   45 IREF=IREF+1
C
C      CHECK FOR TRANSMISSION AT AN INTERFACE WHICH COINCIDES
C      WITH ANOTHER INTERFACE
C
       IF(KREF.GT.1)ITYPE=ISIGN(1,CODE(IREF))
       IF(NCD.EQ.0)GO TO 16
       IF(INTR.EQ.LAY)GO TO 15
       NTR=16
       IF(NCD.LT.0)GO TO 26
       NTR=17
       IF(INTR.EQ.NINT) GO TO 26
       LAY=LAY+1
       GO TO 29
   15 NTR=18
         IF(NCD.GT.0.AND.KREF.GT.1)GO TO 26
       IF(LAY.EQ.1.AND.KREF.EQ.1)GO TO 24
       NTR=19
       IF(LAY.EQ.1)GO TO 26
       LAY=LAY-1
   29  INTRA=INTR
       JA=J
       IF(INTR.EQ.LAY1)GO TO 36
       NC=NPNT(INTR+1)
       DO 34 I=1,NC
       JJ1=I
       II1=III(I,INTR+1)
       IF(J.EQ.II1)GO TO 35
   34 CONTINUE
       GO TO 16
   35 INTR=INTR+1
       J=JJ1
       GO TO 37
   36 II1=III(J,INTR)
       IF(II1.LE.0)GO TO 16
       INTR=INTR-1
       J=II1
C
C      TRANSMISSION AT AN INTERFACE WHICH COINCIDES WITH
C      ANOTHER INTERFACE
C
   37  NTR=20
       IF((N+1).GT.4000) GO TO 50
       NDR=7
       IF(NDER.EQ.1)NDR=10
       LAY1=LAY
       IND1=INTR
       KINT(IREF)=-1
       DO 47 I=1,9
   47 DS(I,IREF)=0.
       NTR=21
       IF(KREF.GT.1.AND.(IREF+1).GT.KREF)GO TO 24
       INT1=INTR
       IF(KREF.GT.1)NCD=IABS(CODE(IREF+1))-IABS(CODE(IREF))
       NTR=22
```

```
      IF(NCD.EQ.0.AND.III(J,INTR).GT.0)GO TO 23
      IF(KREF.GT.1)IC2=CODE(IREF+1)
      GO TO 45
   16 LAY2=LAY
      CALL VCHECK(Y,VEL)
      V2=VEL(1)
      IF(KREF.GT.1)NCD=IABS(IC2)-IABS(IC1)
      AINDEX=V2/V1
      AUX1=1.-AINDEX*AINDEX*(1.-AUX*AUX)
      IF(AUX1.GT.0.) GO TO 17
      NTR=23
      GO TO 28
   17 IF(NCD.EQ.0)AUX1=AINDEX*AUX-SQRT(AUX1)
      IF(NCD.NE.0)AUX1=AINDEX*AUX+SQRT(AUX1)
      AUX2=AINDEX*PZ-AUX1*ANYZ
      AUX1=AINDEX*PX-AUX1*ANYX
      INSPL=0
   18 IF(ABS(AUX1).GT..000001) GO TO 19
      Y(3)=1.57079632*SIGN(1.,PZ)
      IF(KREF.LE.1.OR.NCD.NE.0) GO TO 20
      Y(3)=-Y(3)
      GO TO 20
   19 Y(3)=ATAN2(AUX2,AUX1)
C
   20 PRMT(5)=2.
      KINT(IRR)=NRR
      DS(1,IRR)=RC
      AUX=3.14159265-TANG+Y(3)
      DS(3,IRR)=AUX
      IF(AUX.GT.3.14159265)DS(3,IRR)=AUX-6.2831852
C
C     DETERMINATION OF PARAMETERS OF GENERATED WAVES AT A
C     POINT OF INCIDENCE
C
      IF(NCD.NE.0)GO TO 52
C
C     CHECK WHETHER THE REFLECTING INTERFACE COINCIDES WITH
C     ANOTHER INTERFACE
C
      JA=J11
      INTRA=I11
      LAY2=L11
      IF(INTRA.EQ.L11)GO TO 43
   40 LAY2=LAY2+1
      NTR=24
      IF(INTRA.EQ.NINT.AND.NDER.NE.0)GO TO 51
      IF(INTRA.EQ.NINT)RETURN
      NC=NPNT(INTRA+1)
      DO 41 I=1,NC
      JJ1=I
      II1=III(I,INTRA+1)
      IF(JA.EQ.II1)GO TO 42
   41 CONTINUE
      GO TO 44
   42 INTRA=INTRA+1
```

```
      JA=JJ1
      GO TO 40
   43 LAY2=LAY2-1
      II1=III(JA,INTRA)
      IF(II1.LE.0)GO TO 44
      INTRA=INTRA-1
      JA=II1
      GO TO 43
   44 IF(LAY2.NE.0)GO TO 52
      DS(6,IRR)=0.
      DS(7,IRR)=0.
      DS(9,IRR)=0.
      RETURN
   52 ITYPE1=ITYPE
      ITYPE=1
      L11=LAY
      LAY=LAY2
      CALL VCHECK(Y,VEL)
      DS(6,IRR)=VEL(1)
      DS(9,IRR)=RHO1(LAY2)+RHO2(LAY2)*VEL(1)
      ITYPE=-1
      CALL VCHECK(Y,VEL)
      DS(7,IRR)=VEL(1)
      ITYPE=ITYPE1
      LAY=L11
      RETURN
C
C     TERMINATION OF COMPUTATION
   48 IND=16
      GO TO 25
   51 IND=15
      GO TO 25
   23 IND=17
      GO TO 25
   26 IND=8
      GO TO 25
   24 IND=INTR+100
      IF(INTR.EQ.1)IND=3
      IF(INTR.EQ.NINT)IND=4
      GO TO 25
   28 IND=9
   25 PRMT(5)=3.
      KINT(IRR)=NRR
      IREF=IRR
      IF(IND.EQ.3.OR.IND.EQ.4)GO TO 32
      DS(1,IRR)=RC
      AA=3.14159265-TANG+Y(3)
      DS(2,IRR)=AA
      IF(AA.GT.3.14159265)DS(2,IRR)=AA-6.2831852
      DS(3,IRR)=0.
      GO TO 32
   50 IND=13
      PRMT(5)=3.
   32 IF(IND.EQ.9.OR.IND.EQ.8)RETURN
      YAN=Y(3)
```

```
      Y(3)=101.
      CALL VCHECK(Y,VEL)
      Y(3)=YAN
      RETURN
      END
C
C     ***************************************************************
C
CSUB5
      SUBROUTINE FCT(X,Y,DERY,NDIM)
C
C     COMPUTATION OF THE RIGHT-HAND SIDES IN THE RAY TRACING SYSTEM
C
      DIMENSION VEL(8),Y(3),DERY(3)
C
      CALL VCHECK(Y,VEL)
      DERY(1)=VEL(1)*COS(Y(3))
      DERY(2)=VEL(1)*SIN(Y(3))
      DERY(3)=VEL(2)*SIN(Y(3))-VEL(3)*COS(Y(3))
      RETURN
      END
C
C     ***************************************************************
C
CSUB6
      SUBROUTINE ROOT(YOLD,YNEW,YINT,ANYX,ANYZ,RC,J,IROOT)
C
C     DETERMINATION OF THE POINT OF INCIDENCE AT AN INTERFACE
C     (INTERSECTION OF THE RAY WITH THE INTERFACE).
C
      DIMENSION YOLD(2),YNEW(3),YINT(2)
      COMMON/INTRF/A1(100,20),B1(100,20),C1(100,20),D1(100,20),
     1  X1(100,20),BRD(2),III(100,20),NPNT(20),NINT
      COMMON/AUXI/INTR,INT1,IOUT,IREFR,LAY,ITYPE,NDER,IPRINT,MPRINT,NTR,
     1  IVEL(19)
      COMMON/RAY/AY(10,4000),DS(9,50),KINT(50),ROS,MREG,N,IREF,IND,IND1
      COMMON/MOD1/IREV,XREV,IERR,EANG1,ZERO1
C
      SH(X9)=(EXP(X9)-EXP(-X9))/2.
      CH(X9)=(EXP(X9)+EXP(-X9))/2.
      ARCCOS(X9)=ATAN(SQRT(1.-X9*X9)/X9)
      ARCCH(X9)=ALOG(X9+SQRT(X9*X9-1.))
      ARCSH(X9)=ALOG(X9+SQRT(X9*X9+1.))
C
C
      IROOT=100
C
C     DETERMINATION OF THE ELEMENT OF THE INTERFACE WITH THE P   IT
C     OF INCIDENCE
C
      IF(IERR.EQ.1.AND.EANG1.LT.AY(4,1)) WRITE(6,101)
  101 FORMAT('  POINT 1 REACHED')
      NC=NPNT(INTR)
      XA=YOLD(1)
      XB=YNEW(1)
```

```
      AUX=XB-XA
      X2=X1(J,INTR)
      A2=A1(J,INTR)
      IF(ABS(AUX).GT..000001)GO TO 1
      YINT(1)=YOLD(1)
      GO TO 2
    1 P=(YNEW(2)-YOLD(2))/AUX
      Q=YOLD(2)-P*XA
      IF(AUX.LT.0.)GO TO 21
      IF(XA.GE.X2)GO TO 2
      X3=X1(J+1,INTR)
      A3=A1(J+1,INTR)
      Y2=P*X2+Q
      Y3=P*X3+Q
   20 AUX1=(Y3-A3)*(Y2-A2)
      IF(AUX1.LE.0.)GO TO 2
      J=J-1
      X3=X2
      X2=X1(J,INTR)
      A3=A2
      A2=A1(J,INTR)
      IF(XA.GE.X2)GO TO 2
      Y3=Y2
      Y2=P*X2+Q
      GO TO 20
   21 X3=X1(J+1,INTR)
      IF(XA.LE.X3)GO TO 2
      A3=A1(J+1,INTR)
      Y2=P*X2+Q
      Y3=P*X3+Q
   22 AUX1=(Y3-A3)*(Y2-A2)
      IF(AUX1.LE.0.)GO TO 2
      J=J+1
      X2=X3
      X3=X1(J+1,INTR)
      A2=A3
      IF(XA.LE.X3)GO TO 2
      A3=A1(J+1,INTR)
      Y2=Y3
      Y3=P*X3+Q
      GO TO 22
C
    2 B2=B1(J,INTR)
      C2=C1(J,INTR)
      D2=D1(J,INTR)
      IF(ABS(AUX).LE.0.0001)GO TO 17
      XA=X2
      XB=X1(J+1,INTR)
      AUX=XB-XA
C
C     DETERMINATION OF COEFFICIENTS OF CUBIC EQUATION D*X**3+C*X**2+B*X+
C     ROOTS ARE LOOKED FOR IN INTERVAL (0,1)
C
      D=D2*AUX*AUX*AUX
      C=C2*AUX*AUX
```

```
      B=(B2-P)*AUX
      A=A2-P*XA-Q
C
      IF(ABS(D).LT..000001)GO TO 10
C
C     TRANSFORMATION OF CUBIC EQUATION INTO FORM Y**3+3*P*Y+Q
C     SUBSTITUTING Y=X+C/(3*D)
C
      AUX1=C/(3.*D)
      Q=AUX1*AUX1*AUX1-.5*(B*AUX1-A)/D
      P=B/(3.*D)-AUX1*AUX1
      DISKR=Q*Q+P*P*P
      IF(Q.EQ.0.) GO TO 8
      IF(P.EQ.0.) GO TO 7
      R=SIGN(1.,Q)*SQRT(ABS(P))
      AX=Q/(R*R*R)
      IF(P.GT.0.) GO TO 6
      IF(DISKR)3,3,5
C
C     P.LT.0.AND.DISKR.LE.0
C
    3 D=ARCCOS(AX)/3.
      XR=-2.*R*COS(D)-AUX1
      XR1=2.*R*COS(1.047198-D)-AUX1
      XR2=2.*R*COS(1.047198+D)-AUX1
   25 NRT=3
      IF(XR.GE.0..AND.XR.LE.1.)GO TO 18
      NRT=NRT-1
      XR=XR2
   18 IF(XR1.GE.0..AND.XR1.LE.1.)GO TO 19
      NRT=NRT-1
      XR1=XR2
   19 IF(XR2.GE.0..AND.XR2.LE.1.)GO TO 4
      NRT=NRT-1
    4 IF(NRT.EQ.1)GO TO 15
      RR=XA+XR*AUX-YOLD(1)
      IF(ABS(RR).LT..001)RR=1000000.
      RR1=XA+XR1*AUX-YOLD(1)
      IF(ABS(RR1).LT..001)RR1=1000000.
      IF(ABS(RR1).LT.ABS(RR))XR=XR1
      IF(ABS(RR1).LT.ABS(RR))RR=RR1
      IF(NRT.EQ.2)GO TO 15
      RR1=XA+XR2*AUX-YOLD(1)
      IF(ABS(RR1).LT..001)RR1=1000000.
      IF(ABS(RR1).LT.ABS(RR))XR=XR2
      GO TO 15
C
C     P.LT.0..AND.DISKR.GT.0.
C
    5 XR=-2.*R*CH(ARCCH(AX)/3.)-AUX1
      GO TO 15
C
C     P.GT.0
C
    6 XR=-2.*R*SH(ARCSH(AX)/3.)-AUX1
```

```
      GO TO 15
C
C     P.EQ.0.
C
    7 XR=-SIGN(1.,Q)*EXP(ALOG(2.*ABS(Q))/3.)-AUX1
      GO TO 15
C
C     Q.EQ.0
C
    8 XR=-AUX1
      IF(P)9,15,15
C
C     Q.EQ.0..AND.P.LT.0.
C
    9 XR1=SQRT(-3.*P)-AUX1
      XR2=-XR1-2.*AUX1
      GO TO 25
C
C     REDUCTION OF CUBIC EQUATION TO QUADRATIC EQUATION
C
   10 IF(ABS(C).LT..000001) GO TO 14
      DISKR=B*B-4.*C*A
      P=-B/(2.*C)
      IF(DISKR)11,11,12
C
   11 XR=P
      GO TO 15
C
   12 Q=SQRT(DISKR)/(2.*C)
      XR=P+Q
      XR1=P-Q
   13 NRT=2
      IF(XR.GE.0..AND.XR.LE.1.)GO TO 23
      NRT=NRT-1
      XR=XR1
   23 IF(XR1.GE.0..AND.XR1.LE.1.)GO TO 24
      NRT=NRT-1
   24 IF(NRT.EQ.1)GO TO 15
      RR=XA+XR*AUX-YOLD(1)
      IF(ABS(RR).LT..001)RR=1000000.
      RR1=XA+XR1*AUX-YOLD(1)
      IF(ABS(RR1).LT..001)RR1=1000000.
      IF(ABS(RR1).LT.ABS(RR))XR=XR1
      GO TO 15
C
C     REDUCTION OF CUBIC EQUATION TO LINEAR EQUATION
C
   14 XR=-A/B
   15 YINT(1)=XA+XR*(XB-XA)
      IF(YINT(1).LT.BRD(1))IND=1
      IF(YINT(1).GT.BRD(2))IND=2
      IF(IND.EQ.1.OR.IND.EQ.2)RETURN
   17 AUX=YINT(1)-X2
      IF(IERR.EQ.1.AND.EANG1.LT.AY(4,1)) WRITE(6,100) AUX
  100 FORMAT(8F10.5)
```

```
      YINT(2)=((D2*AUX+C2)*AUX+B2)*AUX+A2
      AUX1=(3.*D2*AUX+2.*C2)*AUX+B2
      AUX2=1./(AUX1*AUX1+1.)
      AUX2=SQRT(AUX2)
      ANYX=-AUX1*AUX2
      ANYZ=AUX2
      RC=6.*D2*AUX+2.*C2
      RC=RC*ANYZ*ANYZ*ANYZ
      RETURN
      END
C
C     ******************************************************************
C
CSUB7  SUBROUTINE MODEL
C    ******************************************************************
C SUB8
      SUBROUTINE BIAP(MX1,MX,MY1,MY,MXY1)
C
C
C     THIS ROUTINE PERFORMS THE DETERMINATION OF COEFFICIENTS OF
C     THE BICUBIC SPLINE INTERPOLATION
C
      DIMENSION X(150),FX(150)
      COMMON/MEDIM/V(30000),SX(499),SY(499),NX(20),NY(20),NVS(19),
     1PTOS(19)
      COMMON/VCOEF/A02(2000),A20(2000),A22(2000)
C
      DO 1 J=1,MX
      L=MX1+J-1
    1 X(J)=SX(L)
      DO 3 I=1,MY
      DO 2 J=1,MX
      K=MXY1+(J-1)*MY+I-1
    2 FX(J)=V(K)
      CALL SPLIN(X,FX,1,MX)
      DO 3 J=1,MX
      K=MXY1+(J-1)*MY+I-1
    3 A20(K)=FX(J)
C
      DO 4 I=1,MY
      L=MY1+I-1
    4 X(I)=SY(L)
      DO 6 J=1,MX
      DO 5 I=1,MY
      K=MXY1+(J-1)*MY+I-1
    5 FX(I)=V(K)
      CALL SPLIN(X,FX,1,MY)
      DO 6 I=1,MY
      K=MXY1+(J-1)*MY+I-1
    6 A02(K)=FX(I)
C
      DO 7 J=1,MX
      L=MX1+J-1
    7 X(J)=SX(L)
      DO 9 I=1,MY
```

```
      DO 8 J=1,MX
      K=MXY1+(J-1)*MY+I-1
    8 FX(J)=A02(K)
      CALL SPLIN(X,FX,1,MX)
      DO 9 J=1,MX
      K=MXY1+(J-1)*MY+I-1
    9 A22(K)=FX(J)
C
      RETURN
      END
C
C     ******************************************************************
C
CSUB9
      SUBROUTINE VELOC(Y,VEL)
C
C     DETERMINATION OF VELOCITY AND ITS DERIVATIVES
C     FOR BICUBIC POLYNOMIAL APPROXIMATION
C
      DIMENSION Y(3),VEL(8)
      COMMON/MEDIM/V(30000),SX(499),SY(499),NX(20),NY(20),NVS(19),
     1IPTOS(19)
      COMMON/VCOEF/A02(2000),A20(2000),A22(2000)
      COMMON/RAY/AY(10,4000),DS(9,50),KINT(50),ROS,MREG,N,IREF,IND,IND1
      COMMON/AUXX/MMX(20),MMY(20),MMXY(20),MAUX
      COMMON/AUXI/INTR,INT1,IOUT,IREFR,LAY,ITYPE,NDER,IPRINT,MPRINT,NTR,
     1 IVEL(19)
      COMMON /DEN/RHO1(19),RHO2(19),NRHO
C
C          CALL ICL9HEMASK(128,IRES)
      MX=NX(LAY)
      MY=NY(LAY)
      DO 1 I=2,MX
      K=MMX(LAY)+I-1
      IF(Y(1).LT.SX(K))GO TO 2
    1 CONTINUE
    2 I1=K
      DO 3 I=2,MY
      K=MMY(LAY)+I-1
      IF(Y(2).LT.SY(K))GO TO 4
    3 CONTINUE
    4 J1=K
      IF(MAUX.EQ.0)GO TO 5
      IF(I1.EQ.I2.AND.J1.EQ.J2)GO TO 6
    5 I=I1-MMX(LAY)
      J=J1-MMY(LAY)
      I2=I1
      J2=J1
      XX=SX(I1-1)
      YY=SY(J1-1)
      MM=MMXY(LAY)-1
      K=MM+(I-1)*MY+J
      B20=A20(K)
      B02=A02(K)
      B22=A22(K)
```

```
      B00=V(K)
      K=MM+I*MY+J
      C20=A20(K)
      C02=A02(K)
      C22=A22(K)
      C00=V(K)
      K=MM+(I-1)*MY+J+1
      D20=A20(K)
      D02=A02(K)
      D22=A22(K)
      D00=V(K)
      K=MM+I*MY+J+1
      E20=A20(K)
      E02=A02(K)
      E22=A22(K)
      E00=V(K)
      HX=SX(I1)-XX
      HY=SY(J1)-YY
      XA=3.*HX
      YA=3.*HY
      XB=HX/3.
      YB=HY/3.
      D32=(E22-D22)/XA
      D30=(E20-D20)/XA
      B30=(C20-B20)/XA
      B32=(C22-B22)/XA
      D12=(E02-D02)/HX-XB*(E22+2.*D22)
      D10=(E00-D00)/HX-XB*(E20+2.*D20)
      B10=(C00-B00)/HX-XB*(C20+2.*B20)
      B12=(C02-B02)/HX-XB*(C22+2.*B22)
      B03=(D02-B02)/YA
      B13=(D12-B12)/YA
      B23=(D22-B22)/YA
      B33=(D32-B32)/YA
      B01=(D00-B00)/HY-YB*(D02+2.*B02)
      B11=(D10-B10)/HY-YB*(D12+2.*B12)
      B21=(D20-B20)/HY-YB*(D22+2.*B22)
      B31=(D30-B30)/HY-YB*(D32+2.*B32)
      MAUX=1
    6 AX=Y(1)-XX
      AZ=Y(2)-YY
      AUX1=((B33*AZ+B32)*AZ+B31)*AZ+B30
      AUX2=((B23*AZ+B22)*AZ+B21)*AZ+B20
      AUX3=((B13*AZ+B12)*AZ+B11)*AZ+B10
      AUX4=((B03*AZ+B02)*AZ+B01)*AZ+B00
      VEL(1)=((AUX1*AX+AUX2)*AX+AUX3)*AX+AUX4
      VEL(2)=(3.*AUX1*AX+2.*AUX2)*AX+AUX3
      IF(NDER.EQ.0)GO TO 7
      VEL(4)=6.*AUX1*AX+2.*AUX2
    7 AUX1=(3.*B33*AZ+2.*B32)*AZ+B31
      AUX2=(3.*B23*AZ+2.*B22)*AZ+B21
      AUX3=(3.*B13*AZ+2.*B12)*AZ+B11
      AUX4=(3.*B03*AZ+2.*B02)*AZ+B01
      VEL(3)=((AUX1*AX+AUX2)*AX+AUX3)*AX+AUX4
      IF(NDER.EQ.0)GO TO 8
```

```
      VEL(5)=(3.*AUX1*AX+2.*AUX2)*AX+AUX3
      AUX1=3.*B33*AZ+B32
      AUX2=3.*B23*AZ+B22
      AUX3=3.*B13*AZ+B12
      AUX4=3.*B03*AZ+B02
      VEL(6)=2.*(((AUX1*AX+AUX2)*AX+AUX3)*AX+AUX4)
    8 IF(ITYPE.GT.0.AND.NVS(LAY).EQ.0)VEL(7)=VEL(1)/PTOS(LAY)
      IF(ITYPE.GT.0.AND.NVS(LAY).EQ.0)VEL(8)=RHO1(LAY)+RHO2(LAY)*VEL(1)
      IF(ITYPE.GT.0.AND.NVS(LAY).EQ.0)GO TO 10
      IF(ITYPE.LT.0.AND.NVS(LAY).EQ.1)GO TO 10
      IF(ITYPE.GT.0.AND.NVS(LAY).EQ.1)GO TO 9
      IF(PTOS(LAY).GE.100.)GO TO 12
      VEL(1)=VEL(1)/PTOS(LAY)
      VEL(2)=VEL(2)/PTOS(LAY)
      VEL(3)=VEL(3)/PTOS(LAY)
      IF(NDER.EQ.0)GO TO 10
      VEL(4)=VEL(4)/PTOS(LAY)
      VEL(5)=VEL(5)/PTOS(LAY)
      VEL(6)=VEL(6)/PTOS(LAY)
      GO TO 10
   12 VEL(1)=0.
      VEL(2)=0.
      VEL(3)=0.
      IF(NDER.EQ.0)GO TO 10
      VEL(4)=0.
      VEL(5)=0.
      VEL(6)=0.
      VEL(7)=0.0
      VEL(8)=0.0
      GO TO 10
    9 VEL(1)=VEL(1)*PTOS(LAY)
      VEL(2)=VEL(2)*PTOS(LAY)
      VEL(3)=VEL(3)*PTOS(LAY)
      IF(NDER.EQ.0)GO TO 10
      VEL(4)=VEL(4)*PTOS(LAY)
      VEL(5)=VEL(5)*PTOS(LAY)
      VEL(6)=VEL(6)*PTOS(LAY)
   10 IF(Y(3).LT.100.)RETURN
      AY(5,N)=VEL(1)
      AY(6,N)=VEL(2)
      AY(7,N)=VEL(3)
      IF(NDER.EQ.0)RETURN
      AY(8,N)=VEL(4)
      AY(9,N)=VEL(5)
      AY(10,N)=VEL(6)
      RETURN
      END
C
C     ******************************************************************
C
CSUB9
      SUBROUTINE VELOC1(Y,VEL)
C
C     DETERMINATION OF VELOCITY AND ITS DERIVATIVES
C      FOR LINEAR INTERPOLATION
```

```
C
C          VEL(1)=V(X,Y) VELOCITY AT RAY-POINT (X,Y)FOUND VIA ROUTUNE "RAY
C          VEL(2)= FIRST DERIVATIVE OF V(X,Y) IN RESPEKT TO X
C          VEL(3)=    "        "        "     "     "    "      TO Y
C          VEL(4)=SECOND       "        "     "     "    "      TO X AND Y
C          VEL(5), VEL(6) FICTICIOUS VALUES FOR THE OTHER TWO 2ND
C             DERIVATIVES SINCE THEY WERE USED ONLY IN THE SPLINE APROXIMA

C
      DIMENSION Y(3),VEL(8)
      COMMON/MEDIM/V(30000),SX(499),SY(499),NX(20),NY(20),NVS(19),
     1PTOS(19)
C       COMMON/VCOEF/A02(2000),A20(2000),A22(2000)
      COMMON/RAY/AY(10,4000),DS(9,50),KINT(50),ROS,MREG,N,IREF,IND,IND1
      COMMON/AUXX/MMX(20),MMY(20),MMXY(20),MAUX
      COMMON/AUXI/INTR,INT1,IOUT,IREFR,LAY,ITYPE,NDER,IPRINT,MPRINT,NTR,
     1  IVEL(19)
      COMMON /DEN/RHO1(19),RHO2(19),NRHO
C
C
C     FIND THE WINDOW OF THE NETWORK WHERE THE GIVEN POINT OF THE RAY IS
      MX=NX(LAY)
      MY=NY(LAY)
      DO 1 I=2,MX
      K=MMX(LAY)+I-1
      IF(Y(1).LT.SX(K))GO TO 2
    1 CONTINUE
    2 I1=K
      DO 3 I=2,MY
      K=MMY(LAY)+I-1
      IF(Y(2).LT.SY(K))GO TO 4
    3 CONTINUE
    4 J1=K
      IF(MAUX.EQ.0)GO TO 5
      IF(I1.EQ.I2.AND.J1.EQ.J2)GO TO 6
    5 I=I1-MMX(LAY)
      J=J1-MMY(LAY)
      I2=I1
      J2=J1
      XX=SX(I1-1)
      YY=SY(J1-1)
C
C        FIND VELOCITIES AND THEIR DERIVATIVES
      MM=MMXY(LAY)-1
      K=MM+(I-1)*MY+J
      VA=V(K)
      K=MM+I*MY+J
      VB=V(K)
      K=MM+(I-1)*MY+J+1
      VC=V(K)
      K=MM+I*MY+J+1
      VD=V(K)
      HX=SX(I1)-XX
      HY=SY(J1)-YY
       PET9=(VB-VA)/HX
       PET10=(VC-VA)/HY
```

```
      PET11=(VD-VC-VB+VA)/(HX*HY)
      MAUX=1
    6 PET7=Y(1)-XX
      PET8=Y(2)-YY
      VEL(1)=VA+PET9*PET7+PET10*PET8+PET11*PET7*PET8
      VEL(2)= PET9+ PET11*PET8
      VEL(3)=PET10+ PET11*PET7
      IF(NDER.EQ.0)GO TO 7
      VEL(4)=PET11
    7 IF(NDER.EQ.0)GO TO 8
      VEL(5)=4.0
      VEL(6)=5.0
    8 IF(ITYPE.GT.0.AND.NVS(LAY).EQ.0)VEL(7)=VEL(1)/PTOS(LAY)
      IF(ITYPE.GT.0.AND.NVS(LAY).EQ.0)VEL(8)=RHO1(LAY)+RHO2(LAY)*VEL(1)
      IF(ITYPE.GT.0.AND.NVS(LAY).EQ.0)GO TO 10
      IF(ITYPE.LT.0.AND.NVS(LAY).EQ.1)GO TO 10
      IF(ITYPE.GT.0.AND.NVS(LAY).EQ.1)GO TO 9
      IF(PTOS(LAY).GE.100.)GO TO 12
      VEL(1)=VEL(1)/PTOS(LAY)
      VEL(2)=VEL(2)/PTOS(LAY)
      VEL(3)=VEL(3)/PTOS(LAY)
      IF(NDER.EQ.0)GO TO 10
      VEL(4)=VEL(4)/PTOS(LAY)
      VEL(5)=VEL(5)/PTOS(LAY)
      VEL(6)=VEL(6)/PTOS(LAY)
      GO TO 10
   12 VEL(1)=0.
      VEL(2)=0.
      VEL(3)=0.
      IF(NDER.EQ.0)GO TO 10
      VEL(4)=0.
      VEL(5)=0.
      VEL(6)=0.
         VEL(7)=0.0
         VEL(8)=0.0
      GO TO 10
    9 VEL(1)=VEL(1)*PTOS(LAY)
      VEL(2)=VEL(2)*PTOS(LAY)
      VEL(3)=VEL(3)*PTOS(LAY)
      IF(NDER.EQ.0)GO TO 10
      VEL(4)=VEL(4)*PTOS(LAY)
      VEL(5)=VEL(5)*PTOS(LAY)
      VEL(6)=VEL(6)*PTOS(LAY)
   10 IF(Y(3).LT.100.)RETURN
      AY(5,N)=VEL(1)
      AY(6,N)=VEL(2)
      AY(7,N)=VEL(3)
      IF(NDER.EQ.0)RETURN
      AY(8,N)=VEL(4)
      AY(9,N)=VEL(5)
      AY(10,N)=VEL(6)
      RETURN
      END
C
C     ****************************************************************
```

```
C
CSUB10
      SUBROUTINE SPLIN(X,FX,NMIN,NMAX)
C
C     CUBIC SPLINE INTERPOLATION WITH ZERO CURVATURES AT
C     THE END POINTS
C
      DIMENSION A(150),B(150),H(150),F(150),X(150),FX(150)
C
      IF((NMAX-NMIN).EQ.1)GO TO 4
      NMIN1=NMIN+1
      NMAX1=NMAX-1
      H(NMIN1)=X(NMIN1)-X(NMIN)
      D2=(FX(NMIN1)-FX(NMIN))/H(NMIN1)
      DO 1 I=NMIN1,NMAX1
      H(I+1)=X(I+1)-X(I)
      D1=D2
      D2=(FX(I+1)-FX(I))/H(I+1)
      B(I)=H(I)+H(I+1)
      FX(I)=3.*(D2-D1)/B(I)
      A(I)=H(I)/B(I)
    1 B(I)=H(I+1)/B(I)
    4 FX(NMIN)=0.
      FX(NMAX)=0.
      IF((NMAX-NMIN).EQ.1)RETURN
      H(NMIN)=0.
      F(NMIN)=0.
      DO 2 I=NMIN1,NMAX1
      XPOM=2.+A(I)*H(I-1)
      H(I)=-B(I)/XPOM
    2 F(I)=(FX(I)-A(I)*F(I-1))/XPOM
      DO 3 I=NMIN,NMAX1
      J=NMAX1-(I-NMIN)
    3 FX(J)=H(J)*FX(J+1)+F(J)
      RETURN
      END
C
C     ***************************************************************
C
CSUB11
      SUBROUTINE AMPL(FJ,AX,AZ,PHX,PHZ)
C
C     COMPUTATION OF AMPLITUDES
C
      INTEGER CODE
      COMMON/COD/CODE(50),KREF,KC
      COMMON/RAY/AY(10,4000),DS(9,50),KINT(50),ROS,MREG,N,IREF,IND,IND1
         COMMON/PPI/PI
C
      PH=0.
      Q=1.
      V=1.
      AL=1.
   13 I1=KINT(IREF)
      IF(I1.LE.0)IREF=IREF-1
```

```
      IF(I1.LE.0)GO TO 13
      DST=AY(2,I1)-AY(2,1)
      IREF1=IREF-1
      IF(IREF1.EQ.0)GO TO 10
C
C     LOOP FOR INTERFACES
C
      DO 5 I=1,IREF1
      I1=KINT(I)
      IF(I1.LE.0)GO TO 5
      SN1=DS(2,I)
      SN2=DS(3,I)
      P=COS(SN1)
      VP1=DS(4,I)
      VS1=DS(5,I)
      RO1=DS(8,I)
      VP2=DS(6,I)
      VS2=DS(7,I)
      RO2=DS(9,I)
      IF(KREF.LE.1)IC1=CODE(1)
      IF(KREF.LE.1)IC2=CODE(1)
      IF(KREF.LE.1)GO TO 11
      IC1=CODE(I)
      II=I
   12 II=II+1
      IF(KINT(II).LE.0)GO TO 12
      IC2=CODE(II)
      IF((IABS(IC2)-IABS(IC1)).EQ.0)GO TO 2
   11 IF(IC1.LT.0)GO TO 1
      P=ABS(P/VP1)
      AV=RO1*VP1
      IF(IC2.GT.0)NC=3
      IF(IC2.GT.0)AV=(RO2*VP2)/AV
      IF(IC2.LT.0)NC=4
      IF(IC2.LT.0)AV=(RO2*VS2)/AV
      GO TO 4
    1 P=ABS(P/VS1)
      AV=RO1*VS1
      IF(IC2.GT.0)NC=7
      IF(IC2.GT.0)AV=(RO2*VP2)/AV
      IF(IC2.LT.0)NC=8
      IF(IC2.LT.0)AV=(RO2*VS2)/AV
      GO TO 4
    2 IF(ABS(VP2).LT..00001)RO2=0.
      IF(IC1.LT.0)GO TO 3
      P=ABS(P/VP1)
      IF(IC2.GT.0)NC=1
      IF(IC2.GT.0)AV=1.
      IF(IC2.LT.0)NC=2
      IF(IC2.LT.0)AV=VS1/VP1
      GO TO 4
    3 P=ABS(P/VS1)
      IF(IC2.GT.0)NC=5
      IF(IC2.GT.0)AV=VP1/VS1
      IF(IC2.LT.0)NC=6
```

```
      IF(IC2.LT.0)AV=1.
      GO TO 4
    4 V=V*AV
      ND=0
      IF(SN1.GT.1.57079632)ND=1
      CALL COEF8(P,VP1,VS1,RO1,VP2,VS2,RO2,NC,ND,R,PHS)
      Q=Q*R
      PH=PH+PHS
      SN1=SIN(SN1)
      SN2=SIN(SN2)
      AL=AL*ABS(SN1/SN2)
    5 CONTINUE
C
C     END OF LOOP
C
   10 V0=AY(5,1)
      V=V*ROS*V0
      RO1=DS(8,IREF)
      IF(RO1.LT.0.5)RO1=1.7+0.2*V0
      I=KINT(IREF)
      V=V/(RO1*AY(5,I))
      V=SQRT(V)
      IF(FJ.LT.0.)PH=PH-1.57079632
      AUX=ABS(FJ)
      AL=AL*AUX
      FJ=SQRT(AL)
      U=(V*Q)/FJ
C
C
      IF(MREG.GE.0)GO TO 20
      AX=0.
      AZ=U
      PHX=0.
      PHZ=PH
      RETURN
   20 CONTINUE
C
      IF(IND.NE.3)GO TO 8
      IF(MREG.EQ.1)GO TO 8
      VP1=DS(4,IREF)
      VS1=DS(5,IREF)
      RO2=0.
      SN1=DS(2,IREF)
      P=COS(SN1)
      ND=0
      IF(SN1.LT.1.57079632.AND.DST.GE.0.)ND=1
      IF(SN1.GT.1.57079632.AND.DST.LT.0.)ND=1
      IF(IC2.LT.0)GO TO 6
      P=ABS(P/VP1)
      CALL COEF8(P,VP1,VS1,RO1,VP2,VS2,RO2,5,ND,RX,PHX)
      CALL COEF8(P,VP1,VS1,RO1,VP2,VS2,RO2,6,ND,RZ,PHZ)
      GO TO 7
    6 P=ABS(P/VS1)
      CALL COEF8(P,VP1,VS1,RO1,VP2,VS2,RO2,7,ND,RX,PHX)
      CALL COEF8(P,VP1,VS1,RO1,VP2,VS2,RO2,8,ND,RZ,PHZ)
```

```
     / AX=U*RX
       AZ=U*RZ
       PHX=PHX+PH
       PHZ=PHZ+PH
       GO TO 9
     3 AY=U*COS(AY(4,I))
       AZ=-U*SIN(AY(4,I))
       AX=PH
       PHZ=PH
     9 RETURN
       END
C
C      ********************************************************************
C
SUBROUTINE IPAR(GO,F0,G,F,IFBUNT)
C
C      DYNAMIC ARRAY TRACING
C
       INTEGER CODE
       DIMENSION Y(2)
       COMMON/PARY/AY(10,4000),DS(9,90),KIN(30),ROS,MPRS,N,IREF,IND,IND1
       COMMON/IPC/CODE(90),IREF,IC
          COMMON/PP(/PP
C
       IPF=0
       G=AY(1,I)
       Y(1)=G0
       Y(2)=F0
    2    IC=KIN(IREF)
         G0=DS(1,IREF)-REF=IREF
         IF(G0.GE.0)GO TO 2
C
    3    G=AY(1,I)
         F=AY(2,I)-PI
         IF(F.LT.0.)F=F+6.28318
         IF(F.GT.6.28318)F=F-6.28318
         CALL RK(Y,F,IRF,IPSINT)
         IF(N.EQ.KINT(IREF))GO TO 4
         D11=0.5*DS(1,IRF)
         IF(KREF.LE.1)GO TO 6
         IC1=CODE(IRF)
    6    ALFA=DS(2,IRF)
         CS1=COS(ALFA)
         SN1=SIN(ALFA)
         BETA=DS(3,IRF)
         SN2=SIN(BETA)
         DELTA=1.570796-AY(4,I1)
         CS=COS(DELTA)
         SN=SIN(DELTA)
         V1=AY(5,I1)
         VX=AY(6,I1)
         VY=AY(7,I1)
         AKAPA1=(VX*CS-VY*SN)/V1
         VS1=VX*SN+VY*CS
```

```
      DELTA=1.57079632-AY(4,I2)
      CS=COS(DELTA)
      SN=SIN(DELTA)
      V2=AY(5,I2)
      VX=AY(6,I2)
      VY=AY(7,I2)
      AKAPA2=(VX*CS-VY*SN)/V2
      VS2=VX*SN+VY*CS
      S1=2.*(AKAPA1*SN1-AKAPA2*SN2)*CS1/V1
      S1=S1+2.*D11*(SN1/V1-SN2/V2)
      S1=S1+(VS1-VS2)*(CS1*CS1/(V1*V1))
      Y(2)=(Y(2)*SN1-Y(1)*S1/SN1)/SN2
      Y(1)=Y(1)*SN2/SN1
    7 IRF=IRF+1
      I1=KINT(IRF)
      IF(I1.LE.0)GO TO 7
      IF(KREF.LE.1)GO TO 1
      IC2=CODE(IRF)
      IF(IABS(IC2).NE.IABS(IC1))GO TO 1
      Y(1)=-Y(1)
      Y(2)=-Y(2)
      GO TO 1
C
    4 Q=Y(1)
      P=Y(2)
      RETURN
      END
C
C     ******************************************************************
C
CSUB13
      SUBROUTINE RK(X,Y,IRF,IPRINT)
C
C     MODIFIED EULER'S METHOD TO SOLVE A SYSTEM OF OF ORDINARY
C     DIFFERENTIAL EQUATIONS OF FIRST ORDER
C
      DIMENSION Y(2),DERY(2),Y1(2),Y2(2)
      COMMON/RAY/AY(10,4000),DS(9,50),KINT(50),ROS,MREG,N,IREF,IND,IND1
C
      IF(IPRINT.EQ.3) WRITE(6,100)X,Y(1),Y(2)
      I1=KINT(IRF)
      N=N+1
    1 H=AY(1,N+1)-AY(1,N)
      X=X+H
      CALL FCTA(Y,DERY,2)
      DO 2 I=1,2
      Y1(I)=DERY(I)
    2 Y2(I)=Y(I)+H*Y1(I)
      N=N+1
      CALL FCTA(Y2,DERY,2)
      DO 3 I=1,2
    3 Y(I)=Y(I)+.5*H*(Y1(I)+DERY(I))
      IF(IPRINT.EQ.3) WRITE(6,100)X,Y(1),Y(2)
  100 FORMAT(2X,3F15.7)
      IF(N.EQ.I1) GO TO 4
```

```
      GO TO 1
    4 RETURN
      END
C
C     ******************************************************************
C
CSUB14
      SUBROUTINE FCTA(Y,DERY,NDIM)
C
C     COMPUTATION OF THE RIGHT-HAND SIDES OF THE DYNAMIC RAY TRACING
C     SYSTEM
C
      DIMENSION Y(NDIM),DERY(NDIM)
      COMMON/RAY/AY(10,4000),DS(9,50),KINT(50),ROS,MREG,N,IREF,IND,IND1
         COMMON/PPI/PI
C
      V=AY(5,N)
      DELTA=1.57079632-AY(4,N)
      CS=COS(DELTA)
      SN=SIN(DELTA)
      VXX=AY(8,N)
      VXY=AY(9,N)
      VYY=AY(10,N)
      V22=VXX*CS*CS-2.*VXY*CS*SN+VYY*SN*SN
      DERY(1)=V*V*Y(2)
      DERY(2)=-(V22*Y(1))/V
      RETURN
      END
C
C     ******************************************************************
C
CSUB15
      SUBROUTINE COEFS(P,VP1,VS1,RO1,VP2,VS2,RO2,NCODE,ND,RMOD,RPH)
C
C     THE ROUTINE COEFS IS DESIGNED FOR THE COMPUTATION OF REFLECTION
C     AND TRANSMISSION COEFFICIENTS AT A PLANE INTERFACE BETWEEN TWO
C     HOMOGENEOUS SOLID HALFSPACES OR AT A FREE SURFACE OF A HOMOGENEOUS
C     SOLID HALFSPACE.
C
C     THE CODES OF INDIVIDUAL COEFFICIENTS ARE SPECIFIED BY THE
C     FOLLOWING NUMBERS
C     A/ INTERFACE BETWEEN TWO SOLID HALFSPACES
C     P1P1...1        P1S1...2        P1P2...3        P1S2...4
C     S1P1...5        S1S1...6        S1P2...7        S1S2...8
C     B/ FREE SURFACE (FOR RO2.LT.0.00001)
C     PP.....1        PX.....5        PX,PZ...X- AND Z- COMPONENTS OF THE
C     PS.....2        PZ.....6        COEF.OF CONVERSION,INCIDENT P WAVE
C     SP.....3        SX.....7        SX,SZ...X- AND Z- COMPONENTS OF THE
C     SS.....4        SZ.....8        COEF.OF CONVERSION,INCIDENT S WAVE
C
C     I N P U T   P A R A M E T E R S
C           P....RAY PARAMETER
C           VP1,VS1,RO1...PARAMETERS OF THE FIRST HALFSPACE
C           VP2,VS2,RO2...PARAMETERS OF SECOND HALFSPACE. FOR THE FREE
C                     SURFACE TAKE RO2.LT.0.00001,EG.RO2=0., AND
```

```
C                    ARBITRARY VALUES OF VP2 AND VS2
C            NCODE...CODE OF THE COMPUTED COEFFICIENT
C            ND...=0  WHEN THE POSITIVE DIRECTION OF THE RAY
C                     AND THE X-AXIS MAKE AN ACUTE ANGLE
C                 =1  WHEN THE WAVE IMPINGES ON THE INTERFACE
C                     AGAINST THE POSITIVE DIRECTION OF THE X-AXIS
C
C     O U T P U T   P A R A M E T E R S
C            RMOD,RPH...MODUL AND ARGUMENT OF THE COEFFICIENT
C
C     N O T E S
C     1/ POSITIVE P...IN THE DIRECTION OF PROPAGATION
C     2/ POSITIVE S...TO THE LEFT FROM P
C     3/ TIME FACTOR OF INCIDENT WAVE ... EXP(-I*OMEGA*T)
C     4/ FORMULAE ARE TAKEN FROM CERVENY ,MOLOTKOV, PSENCIK, RAY METHOD
C        IN SEISMOLOGY, PAGES 30-35. DUE TO THE NOTE 2, THE SIGNS AT
C        CERTAIN COEFFICIENTS ARE OPPOSITE
C
C       WRITTEN BY V.CERVENY,1976
C
      COMPLEX B(4),RR,C1,C2,C3,C4,H1,H2,H3,H4,H5,H6,H,HB,HC
      DIMENSION PRMT(4),D(4),DD(4)
C
      IF(RO2.LT.0.000001)GO TO 150
      PRMT(1)=VP1
      PRMT(2)=VS1
      PRMT(3)=VP2
      PRMT(4)=VS2
      A1=VP1*VS1
      A2=VP2*VS2
      A3=VP1*RO1
      A4=VP2*RO2
      A5=VS1*RO1
      A6=VS2*RO2
      Q=2.*(A6*VS2-A5*VS1)
      PP=P*P
      QP=Q*PP
      X=RO2-QP
      Y=RO1+QP
      Z=RO2-RO1-QP
      G1=A1*A2*PP*Z*Z
      G2=A2*X*X
      G3=A1*Y*Y
      G4=A4*A5
      G5=A3*A6
      G6=Q*Q*PP
      DO 21 I=1,4
      DD(I)=P*PRMT(I)
   21 D(I)=SQRT(ABS(1.-DD(I)*DD(I)))
      IF(DD(1).LE.1..AND.DD(2).LE.1..AND.DD(3).LE.1..AND.DD(4).LE.1.)
     1GO TO 100
C
C     COMPLEX COEFFICIENTS
      DO 22 I=1,4
      IF(DD(I).GT.1.)GO TO 23
```

```
      B(I)=CMPLX(D(I),0.)
      GO TO 22
   23 B(I)= CMPLX(0.,D(I))
   22 CONTINUE
      C1=B(1)*B(2)
      C2=B(3)*B(4)
      C3=B(1)*B(4)
      C4=B(2)*B(3)
      H1=G1
      H2=G2*C1
      H3=G3*C2
      H4=G4*C3
      H5=G5*C4
      H6=G6*C1*C2
      H=1./(H1+H2+H3+H4+H5+H6)
      HB=2.*H
      HC=HB*P
      GO TO (1,2,3,4,5,6,7,8),NCODE
    1 RR=H*(H2+H4+H6-H1-H3-H5)
      GO TO 26
    2 RR=VP1*B(1)*HC*(0*Y*C2+A2*X*Z)
      IF(ND.NE.0)RR=-RR
      GO TO 26
    3 RR=A3*B(1)*HB*(VS2*B(2)*X+VS1*B(4)*Y)
      GO TO 26
    4 RR=-A3*B(1)*HC*(0*C4-VS1*VP2*Z)
      IF(ND.NE.0)RR=-RR
      GO TO 26
    5 RR=-VS1*B(2)*HC*(0*Y*C2+A2*X*Z)
      IF(ND.NE.0)RR=-RR
      GO TO 26
    6 RR=H*(H2+H5+H6-H1-H3-H4)
      GO TO 26
    7 RR=A5*B(2)*HC*(0*C3-VP1*VS2*Z)
      IF(ND.NE.0)RR=-RR
      GO TO 26
    8 RR=A5*B(2)*HB*(VP1*B(3)*Y+VP2*B(1)*X)
      GO TO 26
C     REAL COEFFICIENTS
  100 E1=D(1)*D(2)
      E2=D(3)*D(4)
      E3=D(1)*D(4)
      E4=D(2)*D(3)
      S1=G1
      S2=G2*E1
      S3=G3*E2
      S4=G4*E3
      S5=G5*E4
      S6=G6*E1*E2
      S=1./(S1+S2+S3+S4+S5+S6)
      SB=2.*S
      SC=SB*P
      GO TO (101,102,103,104,105,106,107,108),NCODE
  101 R=S*(S2+S4+S6-S1-S3-S5)
      GO TO 250
```

```
  102 R=VP1*D(1)*SC*(Q*Y*E2+A2*X*Z)
      IF(ND.NE.0)R=-R
      GO TO 250
  103 R=A3*D(1)*SB*(VS2*D(2)*X+VS1*D(4)*Y)
      GO TO 250
  104 R=-A3*D(1)*SC*(Q*E4-VS1*VP2*Z)
      IF(ND.NE.0)R=-R
      GO TO 250
  105 R=-VS1*D(2)*SC*(Q*Y*E2+A2*X*Z)
      IF(ND.NE.0)R=-R
      GO TO 250
  106 R=S*(S2+S5+S6-S1-S3-S4)
      GO TO 250
  107 R=A5*D(2)*SC*(Q*E3-VP1*VS2*Z)
      IF(ND.NE.0)R=-R
      GO TO 250
  108 R=A5*D(2)*SB*(VP1*D(3)*Y+VP2*D(1)*X)
      GO TO 250
C
C     EARTHS SURFACE,COMPLEX COEFFICIENTS AND COEFFICIENTS OF CONVERSION
  150 A1=VS1*P
      A2=A1*A1
      A3=2.*A2
      A4=2.*A1
      A5=A4+A4
      A6=1.-A3
      A7=2.*A6
      A8=2.*A3*VS1/VP1
      A9=A6*A6
      DD(1)=P*VP1
      DD(2)=P*VS1
      DO 151 I=1,2
  151 D(I)=SQRT(ABS(1.-DD(I)*DD(I)))
      IF(DD(1).LE.1..AND.DD(2).LE.1.)GO TO 200
      DO 154 I=1,2
      IF(DD(I).GT.1.)GO TO 155
      B(I)=CMPLX(D(I),0.)
      GO TO 154
  155 B(I)= CMPLX(0.,D(I))
  154 CONTINUE
      H1=B(1)*B(2)
      H2=H1*A8
      H=1./(A9+H2)
      GO TO (161,162,163,164,165,166,167,168),NCODE
  161 RR=(-A9+H2)*H
      GO TO 26
  162 RR=A5*B(1)*H*A6
      IF(ND.NE.0)RR=-RR
      GO TO 26
  163 RR=A5*B(2)*H*A6*VS1/VP1
      IF(ND.NE.0)RR=-RR
      GO TO 26
  164 RR=-(A9-H2)*H
      GO TO 26
  165 RR=A5*H1*H
```

```
      IF(ND.NE.0)RR=-RR
      GO TO 26
  166 RR=A7*B(1)*H
      GO TO 26
  167 RR=A7*B(2)*H
      GO TO 26
  168 RR=-A5*VS1*H1*H/VP1
      IF(ND.NE.0)RR=-RR
   26 Z2=REAL(RR)
      Z3=AIMAG(RR)
      IF(Z2.EQ.0..AND.Z3.EQ.0.)GO TO 157
      RMOD=SQRT(Z2*Z2+Z3*Z3)
      RPH=ATAN2(Z3,Z2)
      RETURN
  157 RMOD=0.
      RPH=0.
      RETURN
C
C     EARTHS SURFACE,REAL COEFFICIENTS AND COEFFICIENTS OF CONVERSION
  200 S1=D(1)*D(2)
      S2=A8*S1
      S=1./(A9+S2)
      GO TO (201,202,203,204,205,206,207,208),NCODE
  201 R=(-A9+S2)*S
      GO TO 250
  202 R=A5*D(1)*S*A6
      IF(ND.NE.0)R=-R
      GO TO 250
  203 R=A5*D(2)*S*A6*VS1/VP1
      IF(ND.NE.0)R=-R
      GO TO 250
  204 R=(S2-A9)*S
      GO TO 250
  205 R=A5*S1*S
      IF(ND.NE.0)R=-R
      GO TO 250
  206 R=A7*D(1)*S
      GO TO 250
  207 R=A7*D(2)*S
      GO TO 250
  208 R=-A5*VS1*S1*S/VP1
      IF(ND.NE.0)R=-R
  250 IF(R.LT.0.)GO TO 251
      RMOD=R
      RPH=0.
      RETURN
  251 RMOD=-R
      RPH=-3.14159
      RETURN
      END
C
C     ******************************************************************
C
CSUB16
      SUBROUTINE RKGS(PRMT,Y,DERY,NDIM,IHLF,AUX)
```

```
      DIMENSION Y(3),DERY(3), AUX(8,3),A(4),B(4),C(4),PRMT(5)
      COMMON/RAY/AY(10,4000),DS(9,50),KINT(50),ROS,MREG,N,IREF,IND,IND1
      COMMON/MOD1/IREV,XREV,IERR,EANG1,ZERO1
C
C     STANDARD IBM SSP ROUTINE TO SOLVE A SYSTEM OF ORDINARY
C     DIFFERENTIAL EQUATIONS OF THE FIRST ORDER BY THE RUNGE-
C     KUTTA'S METHOD
C
      DO 1 I=1,NDIM
    1 AUX(8,I)=.0666667*DERY(I)
      X=PRMT(1)
      XEND=PRMT(2)
      H=PRMT(3)
      PRMT(5)=0.
      CALL FCT(X,Y,DERY,NDIM)
      IF(H*(XEND-X))38,37,2
    2 A(1)=.5
      A(2)=.2928932
      A(3)=1.707107
      A(4)=.1666667
      B(1)=2.
      B(2)=1.
      B(3)=1.
      B(4)=2.
      C(1)=.5
      C(2)=.2928932
      C(3)=1.707107
      C(4)=.5
      DO 3 I=1,NDIM
      AUX(1,I)=Y(I)
      AUX(2,I)=DERY(I)
      AUX(3,I)=0.
    3 AUX(6,I)=0.0
      IREC=0
      H=H+H
      IHLF=-1
      ISTEP=0
      IEND=0
    4 IF((X+H-XEND)*H)7,6,5
    5 H=XEND-X
    6 IEND=1
    7 CALL OUTP(X,Y,DERY,IREC,NDIM,PRMT)
      IF(IERR.EQ.1.AND.EANG1.LT.AY(4,1)) WRITE(6,100)
  100 FORMAT('  POINT 2A REACHED')
      IF(PRMT(5))40,8,40
    8 ITEST=0
    9 ISTEP=ISTEP+1
      J=1
   10 AJ=A(J)
      BJ=B(J)
      CJ=C(J)
      DO 11 I=1,NDIM
      R1=H*DERY(I)
      R2=AJ*(R1-BJ*AUX(6,I))
      Y(I)=Y(I)+R2
```

```
      R2=R2+R2+R2
   11 AUX(6,I)=AUX(6,I)+R2-CJ*R1
      IF(J-4)12,15,15
   12 J=J+1
      IF(J-3)13,14,13
   13 X=X+.5*H
   14 CALL FCT(X,Y,DERY,NDIM)
      GO TO 10
   15 IF(ITEST)16,16,20
   16 DO 17 I=1,NDIM
   17 AUX(4,I)=Y(I)
      ITEST=1
      ISTEP=ISTEP+ISTEP-2
   18  IHLF=IHLF+1
      X=X-H
      H=.5*H
      DO 19 I=1,NDIM
      Y(I)=AUX(1,I)
      DERY(I)=AUX(2,I)
   19 AUX(6,I)=AUX(3,I)
      GO TO 9
   20 IMOD=ISTEP/2
      IF(ISTEP-IMOD-IMOD)21,23,21
   21 CALL FCT(X,Y,DERY,NDIM)
      DO 22 I=1,NDIM
      AUX(5,I)=Y(I)
   22 AUX(7,I)=DERY(I)
      GO TO 9
   23 DELT=0.
      DO 24 I=1,NDIM
   24 DELT=DELT+AUX(8,I)*ABS(AUX(4,I)-Y(I))
      IF(DELT-PRMT(4))28,28,25
   25 IF(IHLF-10)26,36,36
   26 DO 27 I=1,NDIM
   27 AUX(4,I)=AUX(5,I)
      ISTEP=ISTEP+ISTEP-4
      X=X-H
      IEND=0
      GO TO 18
   28 CALL FCT(X,Y,DERY,NDIM)
      DO 29 I=1,NDIM
      AUX(1,I)=Y(I)
      AUX(2,I)=DERY(I)
      AUX(3,I)=AUX(6,I)
      Y(I)=AUX(5,I)
   29 DERY(I)=AUX(7,I)
      CALL OUTP(X-H,Y,DERY,IHLF,NDIM,PRMT)
      IF(IERR.EQ.1.AND.EANG1.LT.AY(4,1)) WRITE(6,101)
  101 FORMAT('  POINT 2B REACHED')
      IF(PRMT(5))40,30,40
   30 DO 31 I=1,NDIM
      Y(I)=AUX(1,I)
   31 DERY(I)=AUX(2,I)
      IREC=IHLF
      IF(IEND)32,32,39
```

```
   32 IHLF=IHLF-1
      ISTEP=ISTEP/2
      H=H+H
      IF(IHLF)4,33,33
   33 IMOD=ISTEP/2
      IF(ISTEP-IMOD-IMOD)4,34,4
   34 IF(DELT-.02*PRMT(4))35,35,4
   35 IHLF=IHLF-1
      ISTEP=ISTEP/2
      H=H+H
      GO TO 4
   36 IHLF=11
      CALL FCT(X,Y,DERY,NDIM)
      GO TO 39
   37 IHLF=12
      GO TO 39
   38 IHLF=13
   39 CALL OUTP(X,Y,DERY,IHLF,NDIM,PRMT)
      IF(IERR.EQ.1.AND.EANG1.LT.AY(4,1)) WRITE(6,102)
  102 FORMAT('  POINT 2C REACHED')
   40 RETURN
      END
C
C     ************************************************************
C
CSUB17
      SUBROUTINE SOURCE(NUM,MWAVE,MTYPE,ANGLE,AMSOUR,PHSOUR)
C
      DIMENSION IPPAR(4),PPAR(6),ISPAR(4),SPAR(6),
     1APSOUR(200),PPSOUR(200),ASSOUR(200),PSSOUR(200)
C
C     RADIATION PATTERNS OF THE SOURCE
C
C     FOR NUM=0, READ THE INPUT DATA FOR RADIATION PATTERNS
C
      IF(NUM.EQ.1)GO TO 1
      IF(MTYPE.LE.0) RETURN
      IF(MWAVE.EQ.2)GO TO 95
      READ(5,100)IPPAR,PPAR
      WRITE(6,100)IPPAR,PPAR
      IF(MTYPE.NE.1)RETURN
      NPP=IPPAR(2)
      READ(5,101)(APSOUR(I),I=1,NPP)
      WRITE(6,101)(APSOUR(I),I=1,NPP)
      IF(IPPAR(1).EQ.0)RETURN
      READ(5,101)(PPSOUR(I),I=1,NPP)
      WRITE(6,101)(PPSOUR(I),I=1,NPP)
      RETURN
   95 READ(5,100)ISPAR,SPAR
      WRITE(6,100)ISPAR,SPAR
      IF(MTYPE.NE.1)RETURN
      NPP=ISPAR(2)
      READ(5,101)(ASSOUR(I),I=1,NPP)
      WRITE(6,101)(ASSOUR(I),I=1,NPP)
      IF(ISPAR(1).EQ.0)RETURN
```

```
      READ(5,101)(PSSOUR(I),I=1,NPP)
      WRITE(6,101)(PSSOUR(I),I=1,NPP)
      RETURN
  100 FORMAT(4I5,6F10.5)
  101 FORMAT(8F10.5)
C
C     FOR NUM=1, COMPUTE THE RADIATION PATTERNS
C
C     THE RADIATION PATTERN DOES NOT DEPEND ON THE RAY
C     PARAMETER (MTYPE=0)
C
    1 IF(MTYPE.LT.0)RETURN
      AMSOUR=1.
      PHSOUR=0.
      IF(MTYPE.EQ.0)RETURN
C
C     THE RADIATION PATTERNS OF THE SOURCE IS GIVEN BY A TABLE
C     (MTYPE=1)
C
      PI=4.*ATAN(1.)
      IF(ANGLE.LT.(-PI))ANGLE=ANGLE+2.*PI
      IF(ANGLE.GT.PI)ANGLE=ANGLE-2.*PI
      ALPHA=180.*ANGLE/PI
      IF(MTYPE.GT.1)GO TO 10
      IF(MWAVE.EQ.2)GO TO 5
C
C     THE P WAVE RADIATION PATTERN
C

      NPOM=IPPAR(2)
      IF(ALPHA.GT.PPAR(1))GO TO 2
      AMSOUR=APSOUR(1)
      IF(IPPAR(1).EQ.1)PHSOUR=PPSOUR(1)
      RETURN
    2 PARM=PPAR(1)+PPAR(2)*FLOAT(NPOM-1)
      IF(ALPHA.LT.PARM)GO TO 3
      AMSOUR=APSOUR(NPOM)
      IF(IPPAR(1).EQ.1)PHSOUR=PPSOUR(NPOM)
      RETURN
    3 PARM=PPAR(1)
      NPOM=NPOM-1
      DO 4 I=1,NPOM
      PARM=PARM+PPAR(2)
      IF(ALPHA.GT.PARM)GO TO 4
      PAR=PARM-PPAR(2)
      AMSOUR=APSOUR(I)+(ALPHA-PAR)*(APSOUR(I+1)-APSOUR(I))/
     1PPAR(2)
      IF(IPPAR(1).EQ.1)PHSOUR=PPSOUR(I)+(ALPHA-PAR)*(PPSOUR(I+
     1PPSOUR(I))/PPAR(2)
    4 CONTINUE
      RETURN
C
C     THE S WAVE RADIATION PATTERN
C
    5 NPOM=ISPAR(2)
```

```
      IF(ALPHA.GT.SPAR(1))GO TO 6
      AMSOUR=ASSOUR(1)
      IF(ISPAR(1).EQ.1)PHSOUR=PSSOUR(1)
      RETURN
    6 PARM=SPAR(1)+SPAR(2)*FLOAT(NPOM-1)
      IF(ALPHA.LT.PARM)GO TO 7
      AMSOUR=ASSOUR(NPOM)
      IF(ISPAR(1).EQ.1)PHSOUR=PSSOUR(NPOM)
      RETURN
    7 PARM=SPAR(1)
      NPOM=NPOM-1
      DO 8 I=1,NPOM
      PARM=PARM+SPAR(2)
      IF(ALPHA.GT.PARM)GO TO 8
      PAR=PARM-SPAR(2)
      AMSOUR=ASSOUR(I)+(ALPHA-PAR)*(ASSOUR(I+1)-ASSOUR(I))
     1/SPAR(2)
      IF(ISPAR(1).EQ.1)PHSOUR=PSSOUR(I)+(ALPHA-PAR)*(PSSOUR(I+1)
     1-PSSOUR(I))/SPAR(2)
    8 CONTINUE
      RETURN
   10 CONTINUE
C
C     THIS IS TO PLACE TO INCLUDE ANY ANALYTICALLY GIVEN
C     RADIATION PATTERNS OF THE SOURCE.
C     NO ANALYTICAL FORMULAE ARE GIVEN IN THIS VERSION, BUT THE
C     USER IS FREE TO ADD HERE ANY DIRECTIONAL PATTERN HE LIKES.
C
      RETURN
      END
C
C       ****************************************************************
      SUBROUTINE VCHECK(Y,VEL)
C
C     ROUTINE SIMPLY USES IVEL  TO CALL LINEAR (VELOC1) OR BICUBIC SPLINE
C     INTERPOLATION (VELOC) ,ROUTINES
C
      DIMENSION Y(3),VEL(8)
      COMMON/AUXI/INTR,INT1,IOUT,IREFR,LAY,ITYPE,NDER,IPRINT,MPRINT,NTR,
     1 IVEL(19)
C
      IF(IVEL(LAY).EQ.0) CALL VELOC(Y,VEL)
      IF(IVEL(LAY).EQ.1) CALL VELOC1(Y,VEL)
C
      RETURN
      END
C
C  ++++++++++++++++++++++++++++++++++++++++++++++++++++++++++++++++++++++
      SUBROUTINE MODEL(MTEXT,LU3,IVX,IVZ,IPLOT)
C
C     APPROXIMATION OF INTERFACES AND VELOCITY DISTRIBUTION IN
C     INDIVIDUAL LAYERS.
C
      CHARACTER*6 IPLOT
      DIMENSION IPR(201),X(100),FX(100),AUX(12),VEL(8),Y(3),MTEXT(17)
```

```
      DIMENSION SXA(100),CHIPR(101),ARRIPR(11)
      COMMON/INTERPOL/PET(201,101,3),ZVEL(201,3),PWAVE(201,101),
     1 SWAVE(201,101),DENSITY(201,101),W(1111000)
      COMMON/MEDIM/V(30000),SX(499),SY(499),NX(20),NY(20),NVS(19),
     1PTOS(19)
      COMMON/INTRF/A1(100,20),B1(100,20),C1(100,20),D1(100,20),
     1X1(100,20), BRD(2),III(100,20),NPNT(20),NINT
      COMMON/DEN/RHO1(19),RHO2(19),NRHO
      COMMON/AUXI/INTR,INT1,IOUT,IREFR,LAY,ITYPE,NDER,IPRINT,MPRINT,NTR,
     1 IVEL(19)
      COMMON/AUXX/MMX(20),MMY(20),MMXY(20),MAUX
      COMMON/MOD1/IREV,XREV,IERR,EANG1,ZERO1
        COMMON/VMOD/BMIN,BMAX
      COMMON/DRCON/KOKO
      CHARACTER*1 ARRIPR,CHIPR
      DATA ARRIPR/1H1,1H2,1H3,1H4,1H5,1H6,1H7,1H8,1H9,1H0,1H*/
C          DO 34 I=1,201
C             ZVEL(I,2)=0.0
C  34      CONTINUE
C          DO 35 I=1,101
C                PET(I,K,2)=0.0
C  35      CONTINUE
C
C     INPUT OF DATA - INTERFACES
C
      READ(5,102)NINT,(NPNT(I),I=1,NINT)
      WRITE(6,102)NINT,(NPNT(I),I=1,NINT)
      DO 11 I=1,NINT
      NC=NPNT(I)
      READ(5,104) (X(J),FX(J),J=1,NC)
      IF(IREV.EQ.0) GO TO 42
      DO 40 L=1,NC
      X1(L,I)=X(L)
   40 A1(L,I)=FX(L)
      DO 41 L=1,NC
      X(L)=XREV-X1(NC-L+1,I)
   41 FX(L)=A1(NC-L+1,I)
   42 READ(5,100) (III(J,I),J=1,NC)
      WRITE(6,103)(X(J),FX(J),III(J,I),J=1,NC)
C
C     DETERMINATION OF COEFFICIENTS OF CUBIC PARABOLAS
C     APPROXIMATING INTERFACES
C
      DO 1 J=1,NC
      X1(J,I)=X(J)
    1 A1(J,I)=FX(J)
      J1=1
      NMIN=1
    2 DO 3 J=J1,NC
      J2=J
      IF(III(J,I))4,3,6
    3 CONTINUE
    4 IF(NMIN.EQ.J2)GO TO 5
      FX(NMIN)=A1(NMIN,I)
      CALL SPLIN(X,FX,NMIN,J2)
```

```
      KEY=0
      GO TO 8
    5 IF(J2.EQ.NC)GO TO 11
      J1=J2+1
      NMIN=J2
      GO TO 2
    6 IF(NMIN.EQ.J2)GO TO 7
      FX(NMIN)=A1(NMIN,I)
      CALL SPLIN(X,FX,NMIN,J2)
      KEY=1
      GO TO 8
    7 IN=III(J2,I)
      X1(J2,I)=X1(IN,I-1)
      A1(J2,I)=A1(IN,I-1)
      B1(J2,I)=B1(IN,I-1)
      C1(J2,I)=C1(IN,I-1)
      D1(J2,I)=D1(IN,I-1)
      IF(J2.EQ.(NC-1))GO TO 11
      J1=J2+1
      NMIN=J1
      GO TO 2
    8 IF((J2-NMIN).EQ.1)GO TO 10
      J3=J2-1
      DO 9 J=NMIN,J3
      H=X(J+1)-X(J)
      D=(A1(J+1,I)-A1(J,I))/H
      D1(J,I)=(FX(J+1)-FX(J))/(3.*H)
      C1(J,I)=FX(J)
    9 B1(J,I)=D-.333333*H*(FX(J+1)+2.*FX(J))
      IF(KEY)5,5,7
   10 D1(NMIN,I)=0.
      C1(NMIN,I)=0.
      B1(NMIN,I)=(A1(J2,I)-A1(NMIN,I))/(X(J2)-X(NMIN))
      IF(KEY)5,5,7
   11 CONTINUE
C
      NC=NPNT(1)
      BRD(1)=X1(1,1)
      BRD(2)=X1(NC,1)
C
C     INPUT DATA - VELOCITY DISTRIBUTION IN INDIVIDUAL
C     LAYERS
C
      MX2=0
      MY2=0
      MXY2=0
      NC=NINT-1
C  ARRAY IVEL CONTROLS THE KIND OF INTERPOLATION THRU VCHECK
C
         READ(5,102) (IVEL(I),I=1,NC)
         WRITE(6,102) (IVEL(I),I=1,NC)
      DO 13 I=1,NC
      MX1=MX2+1
      MY1=MY2+1
      MXY1=MXY2+1
```

```
      READ(5,102)MX,MY
      WRITE(6,102)MX,MY
      NX(I)=MX
      NY(I)=MY
      MX2=MX1+MX-1
      MY2=MY1+MY-1
      MXY2=MXY1+MX*MY-1
      READ(5,99)(SX(J),J=MX1,MX2)
      IF(IREV.EQ.0) GO TO 52
      DO 50 L=1,MX
   50 SXA(L)=SX(MX1+L-1)
      DO 51 L=1,MX
   51 SX(MX1+L-1)=XREV-SXA(MX-L+1)
   52 READ(5,98) (SY(J),J=MY1,MY2)
      WRITE(6,104)(SX(J),J=MX1,MX2)
      WRITE(6,104)(SY(J),J=MY1,MY2)
      M1=MXY1
      M2=MXY2
      DO 12 L=1,MX
      IF(IREV.EQ.0) M2=M1+MY-1
      IF(IREV.NE.0) M1=M2-MY+1
      READ(5,98)(V(J),J=M1,M2)
      WRITE(6,104)(V(J),J=M1,M2)
      IF(IREV.EQ.0) M1=M2+1
   12 IF(IREV.NE.0) M2=M1-1
C
C     DETERMINATION OF COEFFICIENTS OF BICUBIC PARABOLAS
C     APPROXIMATING VELOCITY DISTRIBUTION
C
        CALL BIAP(MX1,MX,MY1,MY,MXY1)
      MMX(I)=MX1
      MMY(I)=MY1
      MMXY(I)=MXY1
   13 CONTINUE
C
C     DENSITIES AND S VELOCITIES
C
      READ(5,102)NRO,(NVS(I),I=1,NC)
      WRITE(6,102)NRO,(NVS(I),I=1,NC)
      IF(NRO.EQ.0)GO TO 30
      READ(5,104)(RHO1(I),RHO2(I),I=1,NC)
      WRITE(5,104)(RHO1(I),RHO2(I),I=1,NC)
      GO TO 31
   30 DO 32 IRHO=1,NC
      RHO1(IRHO)=1.7
      RHO2(IRHO)=0.2
   32 CONTINUE
   31 CONTINUE
      READ(5,104)(PTOS(I),I=1,NC)
      WRITE(6,104)(PTOS(I),I=1,NC)
      DO 33 IRHO=1,NC
   33 IF(PTOS(IRHO).LT.SQRT(2.))PTOS(IRHO)=1.732
      IF(PTOS(1).GE.100.)RHO1(1)=1.
      IF(PTOS(1).GE.100.)RHO2(1)=0.
      NRHO=0
```

```
      IF(PTOS(1).GE.100.)NRHO=1
C
CC    PRINTER PLOT OF THE VELOCITY DISTRIBUTION
C
      READ(5,104)VMIN,VMAX,BMIN,BMAX
      WRITE(6,104)VMIN,VMAX,BMIN,BMAX
      IF(ABS(BMIN).LT..00001)BMIN=A1(1,1)
      IF(ABS(BMAX).LT..00001)BMAX=A1(1,NINT)
C
CC    NUMERICAL FORM OF INTERFACES
C
   14 AUX1=(BRD(2)-BRD(1))/25.
      IF(MPRINT.GT.0) WRITE(6,101)MTEXT
      IF(MPRINT.GE.2) WRITE(6,105)NINT
      IF(MPRINT.GE.2) WRITE(6,107)
      DO 19 I=1,NINT
      NC=NPNT(I)-1
      IF(MPRINT.GE.2) WRITE(6,112)
      IF(MPRINT.GE.2) WRITE(6,108)I
      DO 15 J=1,NC
      IF(MPRINT.GE.2)
     1WRITE(6,109)D1(J,I),C1(J,I),B1(J,I),A1(J,I),X1(J,I),X1(J+1,I),III(
     2J,I)
   15 CONTINUE
      IF(MPRINT.GE.2) WRITE(6,110)
      AUX2=BRD(1)
      AUX3=AUX2
      AUX(1)=AUX2
      L=1
      J=1
   16 AUX3=AUX3+AUX1
      IF(AUX3.GT.BRD(2))GO TO 17
      L=L+1
      AUX(L)=AUX3
      IF(L.LT.12)GO TO 16
   17 IF(MPRINT.GE.2) WRITE(6,111)(AUX(M),M=1,L)
      K=1
   18 IF(AUX(K).GT.X1(J+1,I))J=J+1
      IF(AUX(K).GT.X1(J+1,I))GO TO 18
      AUX4=AUX(K)-X1(J,I)
      AUX(K)=((D1(J,I)*AUX4+C1(J,I))*AUX4+B1(J,I))*AUX4+A1(J,I
      K=K+1
      IF(K.LE.L)GO TO 18
      IF(MPRINT.GE.2) WRITE(6,111)(AUX(M),M=1,L)
      IF(MPRINT.GE.2) WRITE(6,112)
      IF((AUX3+AUX1).GT.BRD(2))GO TO 19
      L=0
      GO TO 16
   19 CONTINUE
C
CC    NUMERICAL FORM OF VELOCITY DISTRIBUTION
C
      LAY=1
      ITYPE=1
      Y(3)=1.
```

```
      VMM=VMAX-VMIN
      VMMM=VMM/10.
      IF(MPRINT.GE.1) WRITE(6,114)VMIN,VMAX,VMMM
      DY=(BMAX-BMIN)/50.
      DX=(BRD(2)-BRD(1))/5.
      Y(2)=BMIN-DY
      K1=1
      AUX(1)=BRD(1)
      DO 20 I=2,6
   20 AUX(I)=AUX(I-1)+DX
      IF(MPRINT.GE.1) WRITE(6,113)(AUX(I),I=1,6)
      DX=(BRD(2)-BRD(1))/100.
C
         IF(IVX.EQ.0.OR.IVX.EQ.1) GOTO 66
C         DY=0.500
         DY=(BMAX-BMIN)/FLOAT(IVZ-1)
         DX=(BRD(2)-BRD(1))/FLOAT(IVX-1)
      Y(2)=BMIN-DY
C    THE SMALL NUMBER 0.0001 IN THE NEXT STATEMENT HELPS ROUNDING TO THE
C    NEAREST INTEGER ,OTHERWISE 2.99999 BECOMES 3.00009  AND  AFTER TRUNC
                                                                    TION
C    USING IFIX , WE GET 3 INSTEAD OF 2 .
C         IZINC=IFIX((BMAX-BMIN)/DY+0.0001)+1
         IXINC=IVX
         IZINC=IVZ
         GO TO 202
C
C    IF IVX<1 , SET DEFAULT VELOCITY MATRIX VALUES.
C
   66    IZINC=21
         IXINC=51
  202    MAUX=0
         NDER=0
C
C    IF SPECIFIED THEN WRITE THE NUMBER OF X & Z  GRID-LINES
C    FOR THE V-Z-R MATRIX OUTPUT TO LU3
C
         IF(IVX.LT.1)GOTO 199
C         WRITE(LU3,102)IXINC,IZINC
  199   DO 29 K=1,IZINC
      Y(2)=Y(2)+DY
C SINCE Y(2) CAN BE < 0 (SEE THE PREVIOUS 30 LINES), MAKE IT = 0.0
            IF(Y(2).LT.0.0) Y(2)=0.0
      Y(1)=BRD(1)-DX
      DO 28 L=1,IXINC
      Y(1)=Y(1)+DX
               IF(Y(1).LT.0.0)  Y(1)=0.0
      IF(LAY.GE.NINT)GOTO 24
   21 LAY1=LAY+1
      NC=NPNT(LAY1)-1
      DO 22 I=1,NC
      J=I
      IF(Y(1).LT.X1(I+1,LAY1))GO TO 23
   22 CONTINUE
   23 A2=A1(J,LAY1)
      B2=B1(J,LAY1)
```

```
      C2=C1(J,LAY1)
      D2=D1(J,LAY1)
      X2=X1(J,LAY1)
      AUX1=Y(1)-X2
      ZINT=((D2*AUX1+C2)*AUX1+B2)*AUX1+A2
      IF(Y(2).GE.ZINT)LAY=LAY+1
      IF(LAY.GE.NINT)GO TO 27
      IF(Y(2).GT.ZINT)GO TO 21
      IF(LAY.LE.0)GO TO 27
   24 NC=NPNT(LAY)-1
      DO 25 I=1,NC
      J=I
      IF(Y(1).LT.X1(I+1,LAY))GO TO 26
   25 CONTINUE
   26 A2=A1(J,LAY)
      B2=B1(J,LAY)
      C2=C1(J,LAY)
      D2=D1(J,LAY)
      X2=X1(J,LAY)
      AUX1=Y(1)-X2
      ZINT=((D2*AUX1+C2)*AUX1+B2)*AUX1+A2
      IF(Y(2).LT.ZINT)LAY=LAY-1
      IF(LAY.LE.0)GO TO 27
      IF(Y(2).LT.ZINT)GO TO 24
   27 IF(LAY.LE.0.OR.LAY.GE.NINT)IPR(L)=11
      IF(LAY.LE.0.OR.LAY.GE.NINT)GO TO 28
C
C    CALCULATE Vp,Vs AND DENSITY DISTRIBUTIONS ACROSS MATRIX
C
      CALL VCHECK(Y,VEL)
         ZVEL(L,1)=VEL(1)
         ZVEL(L,2)=VEL(7)
         ZVEL(L,3)=VEL(8)
C ARRAY " PET " WIL BE USED FOR CONTOURING  ************************
            PET(L,K,1)=VEL(1)
            PET(L,K,2)=VEL(7)
            PET(L,K,3)=VEL(8)
C      ***************************************************
      AUX1=10.*(VEL(1)-VMIN)/VMM
      IPR(L)=IFIX(AUX1)
      IF(AUX1.LT.0..OR.AUX1.GT.10.)IPR(L)=11
      ITYPE=1
   28 CONTINUE
      DO 282 I=1,101
      IF(IPR(I).LT.1.OR.IPR(I).GT.9) GOTO 281
      CHIPR(I)=ARRIPR(IPR(I))
      GOTO 282
  281 IF(IPR(I).EQ.0)                CHIPR(I)=ARRIPR(10)
      IF(IPR(I).LT.0.OR.IPR(I).GT.9) CHIPR(I)=ARRIPR(11)
  282 CONTINUE
C +++++++ REMOVE THE NEXT TWO C'S IN ORDER TO GET THHE 0-9 REPRES. OF TH
                                                                  MODEL
C       IF(K1.EQ.K.AND.MPRINT.GE.1) WRITE(6,115)Y(2),CHIPR
C       IF(K1.NE.K.AND.MPRINT.GE.1) WRITE(6,116)CHIPR
      IF(K1.EQ.K)K1=K1+10
         IF(IVX.LT.1)GOTO 29
```

```
C
C  OUTPUT velocity/density  MATRIX ON LU3
C
C          WRITE(LU3,117)  Y(2),(ZVEL(I,1),I=1,IXINC)
C          WRITE(LU3,117)  Y(2),(ZVEL(I,2),I=1,IXINC)
C          WRITE(LU3,117)  Y(2),(ZVEL(I,3),I=1,IXINC)
   29 CONTINUE
C    ******************************************************
C  Extract P-wave, S-wave,Densities from array PET for contouring.
C
        DO 129 KD=1,IZINC
            DO 128  L=1,IXINC
                  PWAVE(L,KD)=PET(L,IZINC+1-KD,1)
                  SWAVE(L,KD)=PET(L,IZINC+1-KD,2)
                  DENSITY(L,KD)=PET(L,IZINC+1-KD,3)
  128         CONTINUE
  129     CONTINUE
      PWAVE(1,101)=5.21
C
       IF(KOKO.EQ.1.OR.KOKO.EQ.2.OR.KOKO.EQ.3)
      1 CALL GRIDCONT(MTEXT,IPLOT)
C      1 CALL GRIDCONT(IXINC,IZINC,PWAVE,SWAVE,DENSITY,MTEXT,IPLOT)
C
C
   98  FORMAT(16F5.2)
   99  FORMAT(2X,10F7.3)
  100 FORMAT(40I2)
  101 FORMAT('1'/20A4)
  102 FORMAT(16I5)
  103 FORMAT(3(2F10.5,I5))
  104 FORMAT(8F10.5)
  105 FORMAT(////1X,'M O D E L   O F   M E D I U M'/2X,'NUMBER OF INTERF
     1ACES = ',I3)
  107 FORMAT(///////1X,'I N T E R F A C E S'///1X,'INTERFACES ARE APPROX
     1IMATED BY CUBIC PARABOLAS  Z=D*(X-X1)**3+C*(X-X1)**2+B*(X-X1)+A  B
     2ETWEEN  X1  AND  X2'/1X,'COEFFICIENTS OF PARABOLAS ARE DETERMINED
     3BY CUBIC SPLINE INTERPOLATION'///)
  108 FORMAT(/1X,'COEFFICIENTS OF PARABOLAS APPROXIMATING INTERFACE',I3/
     1/15X,'D',14X,'C',14X,'B',14X,'A',2X,'IN INTERVAL',5X,'FROM X1',
     27X,'TO X2',5X,'INDEX')
  109 FORMAT(1X,4E15.5,15X,F10.5,F12.5,I10)
  110 FORMAT(////1X,'NUMERICAL FORM OF INTERFACE'/1X,'UPPER ROW - X-COOR
     1DINATES OF POINTS OF INTERFACE, LOWER ROW - CORRESPONDING Y-COORDI
     2NATES OF POINTS OF INTERFACE'//)
  111 FORMAT(1X,13F9.4)
  112 FORMAT(/)
  113 FORMAT(5X,5(F7.3,13X),F7.3)
  114 FORMAT(1H1,1X,'VELOCITY DISTRIBUTION'/1X,'ISOLINES CONSTRUCTED FRO
     1M',F10.5,'  TO ',F10.5,'  WITH INCREMENT',F10.5//)
  115 FORMAT(1X,F5.2,2X,101A1)
  116 FORMAT(8X,101A1)
  117   FORMAT(F6.2,1X,101F5.2)
C
      RETURN
        END
```

```
      SUBROUTINE GRIDCONT(MTEXT,IPLOT)
         CHARACTER*6 IPLOT
      DIMENSION ITI(7),MTEXT(17)
      COMMON/INTERPOL/PET(201,101,3),ZVEL(201,3),PWAVE(201,101),
     1 SWAVE(201,101),DENSITY(201,101),W(1111000)
      COMMON/INTRF/A1(100,20),B1(100,20),C1(100,20),D1(100,20),
     1X1(100,20), BRD(2),III(100,20),NPNT(20),NINT
         COMMON/VMOD/BMIN,BMAX
         COMMON/DRCON/KOKO
      DATA IAN/1/,IFULL/1/,ANIN/40.0/,IBR/0/,NP/221/,
     1 XCR/2.0/,YCR/0.5/,IDF/1/,NCONT/25/,IS/1/
      NW=1111000
C
C SET UP PLOT.
C
      IF(IPLOT.EQ.'T4010 ') CALL T4010
      IF(IPLOT.EQ.'T4014 ') CALL T4014
      IF(IPLOT.EQ.'ADM3AG') CALL ADM3AG
      IF(IPLOT.EQ.'HP747 ') CALL HP747
      IF(IPLOT.EQ.'HP2647') CALL HP2647
      IF(IPLOT.EQ.'GP39  ') CALL GP39
      IF(IPLOT.EQ.'GP39W ') CALL GP39W
      IF(IPLOT.EQ.'ST5680') CALL ST5680
      IF(IPLOT.EQ.'BBC   ') CALL BBC
C
      IF(BRD(2).GT.200.0)CALL WINDO2(0.0,1300.0,10.0,300.0)
      IF(BRD(2).LT.200.0)CALL WINDO2(0.0,280.0,10.0,150.0)
C      CALL DEVPAP(250.0,150.0,1)
C         CALL UNITS(0.5)
C        CALL WINDOW(2)
      CALL TITLE(4,17,MTEXT)
       CALL LABCON(IAN,IFULL,ANIN,IBR)
      IF(BRD(2).GT.200.0) XCR=5.0
      CALL SETSCA(XCR,YCR,IDF)
         IF(KOKO.EQ.1)
     1CALL DRACON(201,BRD(1),BRD(2),101,-BMAX,BMIN,PWAVE,NCONT,IS,
     2NW,W)
         IF(KOKO.EQ.2)
     1CALL DRACON(201,BRD(1),BRD(2),101,-BMAX,BMIN,SWAVE,NCONT,IS,NW,W)
         IF(KOKO.EQ.3)
     1CALL DRACON(201,BRD(1),BRD(2),101,-BMAX,BMIN,DENSITY,NCONT,IS,
     2NW,W)
        CALL DEVEND
       RETURN
        END
```

```
      PROGRAM TXWISE
      IMPLICIT REAL*4(A-H,O-Z)
      REAL MIN1,MIN2,MAX1,MAX2
      DIMENSION TOBS(99),TMODEL(99),X(99),TXOBS(99),TXMODEL(99),
     1 XSHOT(99),NOSHOT(99),Y(99),AA(99),BB(99),XX(99),ESTERR(99),
     2 TX1(99),TX2(99)
      CHARACTER *10 STNAME(8)
C
C        THE NEXT TWO SHITCHES (SW1  , SW2 ) CONTROL THE WAY
C         THE VARIOUS PLOTS FOR THE VARIOUS RECORDING STATIONS
C         ARE PLOTTED :
C  1 :      IF SW1 NON 0.0 AND SW2 =0.0  THEN WE GET DIFFERENT FRAME
C                   WITH THE SAME Y-SCALE (THE SCALE BEING DEFINED
C                   BY THE MIN. AND MAX. VALUE AMONGST ALL THE DATA SETS.
C  2 :      IF SW1 NON 0.0 AND SW2 NON 0.0  THEN WE GET SEPARATE PLOTS WITH
C                   DIFFERENT SCALE FOR EACH (THE SCALE DEPENDING ON
C                   THE MIN. AND MAX. VALUE OF THE INDIVIDUAL DATA SET) .
C  3 :      IF SW1 =0.0 AND SW2 =0.0  THEN WE GET EVERYTHING ON THE SAME
C                   PLOT  WITH THE SAME SCALE AS IN CASE 1 .
C  4 :      IF SW1 = 0.0 AND SW2 NON 0.0 THEN WEGET SAME PLOT  AND
C                   DIFFERENT SCALE    [ NOT RECOMENDED ]
C
      DATA SW1/0.0  /,SW2/0.0  /
C
C        FOLLOW DISTANCES OF SHOTS FROM BARRA STATION (SHOT 1 TO 23)
C        AND CORRESPONDING SHOT NOS.
C
      DATA XSHOT/252.65,234.52,215.72,198.62,179.16,170.43,163.00,
     1 155.71,143.28,137.38,130.33,122.05,116.03,110.70,104.98,
     2 93.89,84.86,74.63,60.16,40.37,31.41,20.88,2.72/
      DATA NOSHOT/1,2,3,4,5,6,7,8,9,10,11,12,13,14,15,16,
     1 17,18,19,20,21,22,23/
C
C       DATA XSHOT/167.26,163.73,160.28,141.80,134.85,127.98,121.26,
C      1 116.92,113.8,108.04/
C       DATA NOSHOT/1,2,3,4,5,6,7,8,9,10/
C
C
C        STNPOS = DISTANCE OF STATION FROM  0.0 (X-COORD.) I.E. BARRA ST
C          K ,L  =LIMITS OF A SUBSET  SHOT NUMBER ARRAY TO BE PLOTTED.
C        INDEX = SWITCH CONTROLING PLOTTING OF STANDARD ERRORS
C              OF MY PICKING  OF THE TRAVEL TIMES
C          IF INDEX = 1  , STAND. ERRORS READ IN FOR PLOTTING
C                TOGETHER WITH THE OBS. AND CALC. VALUES .
C          IF INDEX = 2 ,STAND. ERRORS READ IN FOR PLOTTING
C                WITHOUT THE OBS. OR CALC. VALUES .
C          IF INDEX OTHER THAN 1 OR 2 , PLOTS WITHOUT STAND.ERR. PLOTTIN
C
C       FOLLOW MORE DATA : N = NUMBER OF OBSERVED TRVEL TIME      ES
C                                (OR MODEL T.T.V.) TO BE PLOTT     .
C                          NCHAR1 / NCHAR2 / NCHAR3 ARE CHARAC     NOS
C                                FROM VARIOUS CTRSETS .
C
      IP=0
   20 CONTINUE
```

```
      CALL READCS(STNAME)
      READ(5,*,END=21) STNPOS,K,L,INDEX
      READ(5,*) N,NCHAR1,NCHAR2,NCHAR3
      READ(5,*) ((TOBS(I),TMODEL(I),X(I)),I=1,N)
      IF (INDEX.EQ.1.OR.INDEX.EQ.2)   READ(5,*) (ESTERR(I),I=1,N)
 6    FORMAT(3(F7.3))
         DO 8 I=1,N
            TXOBS(I)=TOBS(I)-ABS(X(I))/6.0
            TXMODEL(I)=TMODEL(I)-ABS(X(I))/6.0
 8       CONTINUE
C
C        FIND THE MINIMUM AND MAXIMUM VALUES OF THE Y-COORDINATES
C         OF ALL THE DATA SETS
C        (I.E. THE REDUCED TRAVEL TIMES  T-X/6) AND LEAVE SOME
C        ADDITIONAL SPACE UP & DOWN .
C
               CALL YMINV(TXOBS,MIN1,N)
               CALL YMAXV(TXOBS,MAX1,N)
               CALL YMINV(TXMODEL,MIN2,N)
               CALL YMAXV(TXMODEL,MAX2,N)
            IF(MIN1.GE.MIN2)YYMIN=MIN2-0.20
               IF(MIN1.LT.MIN2) YYMIN=MIN1-0.20
            IF(MAX1.GE.MAX2) YYMAX=MAX1+0.20
               IF(MAX1.LT.MAX2) YYMAX=MAX2+0.20
      IP=IP+1
      AA(IP)=YYMIN
      BB(IP)=YYMAX
      GOTO 20
C
 21   CONTINUE
C
C     NORMALY NEXT LINE SHOULD HAVE IP INSTEAD OF IP-1.
C     WITH IP-1  THE LAST SET OF DATA (NOW LETTERPIN ST.)
C     IS NOT TAKEN INTO ACCOUNT FOR THE CALCULATION OF  THE MINS AND MAXS.
C
      CALL YMINV(AA,AMIN,IP)
         YMIN=AMIN
      CALL YMAXV(BB,BMAX,IP)
         YMAX=BMAX
      REWIND 5
C
C    IFRAME    COUNTS THE FRAMES I.E. NO OF DATA SETS.
C
       IFRAME=0
 26       CALL READCS(STNAME)
       IFRAME=IFRAME+1
      READ(5,*,END=27) STNPOS,K,L,INDEX
      READ(5,*) N,NCHAR1,NCHAR2,NCHAR3
      READ(5,*) ((TOBS(I),TMODEL(I),X(I)),I=1,N)
         IF(INDEX.EQ.1.OR.INDEX.EQ.2) READ (5,*) (ESTERR(I),I=1,N)
         DO 18 I=1,N
            TXOBS(I)=TOBS(I)-ABS(X(I))/6.0
            TXMODEL(I)=TMODEL(I)-ABS(X(I))/6.0
 18       CONTINUE
      IF(SW2.EQ.0.0) GOTO 31
```

```
C
C       FIND THE MINIMUM AND MAXIMUM VALUES OF THE Y-COORDINATES
C       (I.E. THE REDUCED TRAVEL TIMES  T-X/6) AND LEAVE SOME
C       ADDITIONAL SPACE UP & DOWN .
C
              CALL YMINV(TXOBS,MIN1,N)
              CALL YMAXV(TXOBS,MAX1,N)
              CALL YMINV(TXMODEL,MIN2,N)
              CALL YMAXV(TXMODEL,MAX2,N)
           IF(MIN1.GE.MIN2)YMIN=MIN2-0.12
              IF(MIN1.LT.MIN2) YMIN=MIN1-0.12
           IF(MAX1.GE.MAX2) YMAX=MAX1+0.12
              IF(MAX1.LT.MAX2) YMAX=MAX2+0.12
C
C      *******  GRAPHICS CALLS  **********
C
 31         CALL PAPER(1)
C          NEXT 2 LINES FOR LONG T-X DIAGRAMS
C          CALL PSPACE(0.15,2.5,0.10,0.90)
C          CALL CSPACE(0.0,3.0,0.0,1.0)
C       NEXT 2 LINES FOR A4 SIZE DIAGRAMS
        CALL PSPACE(0.15,0.90,0.10,0.60)
        CALL CSPACE(0.0,1.0,0.0,1.0)
        CALL MAP(0.0,300.0,YMIN,YMAX)
        CALL BOX(0.0,300.0,YMIN,YMAX)
C        CALL BORDER
         CALL CTRMAG(13)
C          CALL AXES
        CALL AXESSI(25.0,0.2)
           CALL CTRSET(4)
           CALL CTRMAG(10)
        DO 45 I45=1,N
           XX(I45)=STNPOS-X(I45)
  45    CONTINUE
      IF (INDEX.EQ.2) GOTO 11
              DO 10 I=1,N
                 CALL BLKPEN
                 CALL PLOTNC(XX(I),TXOBS(I),NCHAR1)
C                 CALL REDPEN
C                 CALL PLOTNC(XX(I),TXMODEL(I),NCHAR2)
  10          CONTINUE
           CALL BLKPEN
           CALL POSITN(XX(1),TXOBS(1))
              DO 11 I=2,N
                 CALL JOIN(XX(I),TXOBS(I))
  11          CONTINUE
C
      IF (INDEX.NE.1.AND.INDEX.NE.2)  GOTO 111
         CALL REDPEN
            DO 99 I=1,N
               TX1(I)=TXMODEL(I)+ESTERR(I)
               TX2(I)=TXMODEL(I)-ESTERR(I)
               CALL POSITN(XX(I),TX1(I))
               CALL JOIN(XX(I),TX2(I))
  99        CONTINUE
```

```
 111  CONTINUE
            CALL CTRSET(1)
            CALL BLKPEN
            CALL BOX(100.0,200.0,YMAX-0.15,YMAX)
            CALL CTRMAG(14)
C       IF (SW1.EQ.0.0) GO TO 38
        IF(IFRAME.GE.2)GOTO 39
            CALL ITALIC(1)
            CALL PLOTCS(105.0,YMAX-0.040,STNAME,20)
            CALL CTRMAG(9)
            CALL ITALIC(0)
  38  CONTINUE
            CALL CTRSET(4)
            CALL BLKPEN
            CALL PLOTNC(110.0,YMAX-0.09,NCHAR1)
            CALL CTRSET(1)
            CALL BLKPEN
            CALL PLOTCS(117.0,YMAX-0.09,'  MID JURA STATION',18)
            CALL CTRSET(4)
            CALL REDPEN
            CALL PLOTNC(110.0,YMAX-0.130,NCHAR2)
            CALL CTRSET(1)
            CALL BLKPEN
            CALL PLOTCS(117.0,YMAX-0.130,'  SOUTH JURA STATION',20)
  39      CALL CTRSET(1)
          CALL POSITN(230.0,0.0-0.15)
          CALL CTRMAG(13)
          CALL TYPECS(' RANGE (KM) ',12)
          CALL POSITN(268.0,0.05)
          CALL CTRMAG(10)
          CALL TYPECS(' SHOT NO',8)
          CALL CTRMAG(22)
          CALL PLOTNC(265.0,0.05,NCHAR3)
          CALL CTRMAG(13)
             CALL POSITN(-26.0,YMAX-0.5)
             CALL CTRORI(1.0)
             CALL TYPECS(' T-X/6 (SECS)',13)
          CALL CTRSET(1)
          CALL POSITN(STNPOS,0.0)
          CALL PLOTNC(STNPOS,0.0,44)
          CALL PLOTCS(STNPOS,0.02,STNAME,5)
          CALL CTRORI(0.0)
C
C         PLOT SHOT ARROWS INDICATING POSITIONS OF SHOTS
C         AND PLOT ALSO SHOT NUMBERS
C
      DO 55 I=1,23
         Y(I)=0.0+0.008
  55  CONTINUE
         CALL CTRSET(1)
         CALL CTRMAG(15)
C  NEXT LINE TO BE USED ONLY IN CONJUCTION WITH THE BARRADATA1 OR
C     7 OR 9, TO ADJUST THE SCALE
       IF(IFRAME.GT.2) GO TO 66
         CALL PTPLOT(XSHOT,Y,K,L,54)
```

```
         CALL CTRMAG(8)
      DO 66 I=K,L
         CALL POSITN(XSHOT(I)-4.0,0.04)
         CALL TYPENI(NOSHOT(I))
C     OR   CALL PLOTNI(XSHOT(I),0.05,NOSHOT(I))
 66   CONTINUE
      IF(SW1.EQ.0.0) GOTO 28
      CALL FRAME
 28   CONTINUE
      GO TO 26
 27   CONTINUE
         CALL GREND
      STOP
      END
C
C        THE SUBROUTINE  YMIN  FIMDS THE MINIMUM VALUE OF
C         AN ARRAY A .
C
      SUBROUTINE YMINV(A,MIN,N)
      REAL  MIN,MIN1
      DIMENSION A(N)
      MIN1=A(1)
         DO 33 I=1,N
            IF(A(I).LE.MIN1)  MIN1=A(I)
  33     CONTINUE
      MIN=MIN1
      RETURN
      END
C
C
C        THE SUBROUTINE YMAX FINDS THE MAXIMUM VALUE
C        OF ARRAY B .
C
      SUBROUTINE YMAXV(B,MAX,N)
      DIMENSION B(N)
      REAL MAX,MAX1
      MAX1=B(1)
         DO 22 I=1,N
            IF(B(I).GE.MAX1) MAX1=B(I)
  22     CONTINUE
      MAX=MAX1
      RETURN
      END
```

```
      PROGRAM TXAIRGUN
C  PROGRAM FOR PLOTTING REDUCED OR UNREDUCED AIR GUN DATA FROM THE  WISE
C  TOGETHER WITH THE RELEVANT EXPLOSIVE SHOT DATA
      IMPLICIT REAL*4(A-H,O-Z)
      REAL MIN1,MIN2,MAX1,MAX2
      DIMENSION TOBS(99),TMODEL(99),X(99),TXOBS(99),TXMODEL(99),
     1 XSHOT(99),NOSHOT(99),Y(99),AA(99),BB(99),XX(99),ESTERR(99),
     2 TX1(99),TX2(99)
      CHARACTER *10 STNAME(8)
      CHARACTER *4 NAME(99),PAM*4
C
C        THE NEXT THREE SWITCHES (SW1,SW2,SW3) CONTROL.THE WAY
C         THE VARIOUS PLOTS FOR THE VARIOUS RECORDING STATIONS
C         ARE PLOTTED :
C     1 :     IF SW1 NOT 0.0 AND SW2 =0.0  THEN WE GET DIFFERENT FRAME
C                    WITH THE SAME Y-SCALE (THE SCALE BEING DEFINED
C                    BY THE MIN. AND MAX. VALUE AMONGST ALL THE DATA SETS
C   2 :     IF SW1 NOT 0.0 AND SW2 NOT 0.0  THEN WE GET SEPARATE PLOTS WITH
C                    DIFFERENT SCALE FOR EACH (THE SCALE DEPENDING ON
C                    THE MIN. AND MAX. VALUE OF THE INDIVIDUAL DATA SET)
C     3 :     IF SW1 =0.0 AND SW2 =0.0  THEN WE GET EVERYTHING ON THE SAME
C                    PLOT  WITH THE SAME SCALE AS IN CASE 1 .
C     4 :     IF SW1 = 0.0 AND SW2 NOT 0.0 THEN WEGET SAME PLOT  AND
C                    DIFFERENT SCALE    [ NOT RECOMENDED ]
C      5 :    IF SW3 = 0.0 WE GET THE PLOT OF UNREDUCED TRAVEL TIMES
C              (ONLY WITH THE SAME SCALE IE. SW2=0.0
C
      DATA SW1/0.0  /,SW2/0.0  /,SW3/1.0/
C
C
C
C          STNPOS = DISTANCE OF STATION FROM  0.0 (X-COORD.)
C
C       INDEX = SWITCH CONTROLING PLOTTING OF STANDARD ERRORS
C             OF MY PICKING  OF THE TRAVEL TIMES
C          IF INDEX = 1 , STAND. ERRORS READ IN FOR PLOTTING
C             TOGETHER WITH THE OBS. AND CALC. VALUES .
C          IF INDEX = 2 ,STAND. ERRORS READ IN FOR PLOTTING
C             WITHOUT THE OBS. OR CALC. VALUES .
C          IF INDEX OTHER THAN 1 OR 2 , PLOTS WITHOUT STAND.ERR  PLOTTIN
C
C
C       FOLLOW MORE DATA : N = NUMBER OF OBSERVED TRVEL TIME VALUES
C                            (OR MODEL T.T.V.) TO BE PLOTTED .
C                      NCHAR1 / NCHAR2 /  ARE CHARACTER NOS
C                            FROM VARIOUS CTRSETS .
C
C
      IP=0
      IPP=0
   20 CONTINUE
       CALL READCS(STNAME)
      READ(5,*,END=21) STNPOS,INDEX
      READ(5,*) N,NCHAR1,NCHAR2
      IF(N.LT.10)READ(5,77)((TOBS(I),TMODEL(I),X(I),NAME(I)),I=1,N)
      IF(N.GE.10)READ(5,*) ((TOBS(I),TMODEL(I),X(I)),I=1,N)
      IF (INDEX.EQ.1.OR.INDEX.EQ.2)   READ(5,*) (ESTERR(I),I=1,N)
```

```
 77    FORMAT(2(F6.3),F7.3,1X,A4)
       DO 8 I=1,N
          TXOBS(I)=TOBS(I)-ABS(X(I))/6.0
          TXMODEL(I)=TMODEL(I)-ABS(X(I))/6.0
    8     CONTINUE
C
C        FIND THE MINIMUM AND MAXIMUM VALUES OF THE Y-COORDINATES
C         OF ALL THE DATA SETS
C        (I.E. THE REDUCED OR UNREDUCED TRAVEL TIMES ) AND LEAVE SOME
C        ADDITIONAL SPACE UP & DOWN .
C
      IF(SW3.EQ.0.0) GOTO 14
                CALL YMINV(TXOBS,MIN1,N)
                CALL YMAXV(TXOBS,MAX1,N)
                CALL YMINV(TXMODEL,MIN2,N)
                CALL YMAXV(TXMODEL,MAX2,N)
             IF(MIN1.GE.MIN2)YYMIN=MIN2-0.20
                IF(MIN1.LT.MIN2) YYMIN=MIN1-0.20
             IF(MAX1.GE.MAX2) YYMAX=MAX1+0.20
                IF(MAX1.LT.MAX2) YYMAX=MAX2+0.20
 14       IF(SW3.NE.0.0) GOTO 9
                CALL YMINV(TOBS,MIN1,N)
                CALL YMAXV(TOBS,MAX1,N)
                CALL YMINV(TMODEL,MIN2,N)
                CALL YMAXV(TMODEL,MAX2,N)
             IF(MIN1.GE.MIN2)YYMIN=MIN2-0.20
                IF(MIN1.LT.MIN2) YYMIN=MIN1-0.20
             IF(MAX1.GE.MAX2) YYMAX=MAX1+0.20
                IF(MAX1.LT.MAX2) YYMAX=MAX2+0.20
C
  9      CONTINUE
C
      IP=IP+1
      AA(IP)=YYMIN
      BB(IP)=YYMAX
      GOTO 20
C
  21  CONTINUE
C
C
      CALL YMINV(AA,AMIN,IP)
         YMIN=AMIN
      CALL YMAXV(BB,BMAX,IP)
         YMAX=BMAX
      REWIND 5
 26        CALL READCS(STNAME)
      READ(5,*,END=27) STNPOS,INDEX
      READ(5,*) N,NCHAR1,NCHAR2
      IF(N.LT.10)READ(5,77)((TOBS(I),TMODEL(I),X(I),NAME(I)),I=1,N)
      IF(N.GE.10)READ(5,*) ((TOBS(I),TMODEL(I),X(I)),I=1,N)
         IF(INDEX.EQ.1.OR.INDEX.EQ.2) READ (5,*) (ESTERR(I),I=1,N)
         DO 18 I=1,N
            TXOBS(I)=TOBS(I)-ABS(X(I))/6.0
            TXMODEL(I)=TMODEL(I)-ABS(X(I))/6.0
   18     CONTINUE
```

```
      IF(SW2.EQ.0.0) GOTO 31
C
C         FIND THE MINIMUM AND MAXIMUM VALUES OF THE Y-COORDINATES
C         (I.E. THE REDUCED TRAVEL TIMES  T-X/6) AND LEAVE SOME
C         ADDITIONAL SPACE UP & DOWN .
C
                CALL YMINV(TXOBS,MIN1,N)
                CALL YMAXV(TXOBS,MAX1,N)
                CALL YMINV(TXMODEL,MIN2,N)
                CALL YMAXV(TXMODEL,MAX2,N)
              IF(MIN1.GE.MIN2)YMIN=MIN2-0.12
                IF(MIN1.LT.MIN2) YMIN=MIN1-0.12
              IF(MAX1.GE.MAX2) YMAX=MAX1+0.12
                IF(MAX1.LT.MAX2) YMAX=MAX2+0.12
C
C      *******  GRAPHICS CALLS  **********
C
 31           CALL PAPER(1)
C  FOR A LONG PLOT CHANGE  0.90 TO 3.0 AND 1.0 TO 3.0 BELLOW
           CALL PSPACE(0.15,0.9,0.10,0.60)
           CALL CSPACE(0.0,1.0,0.0,1.0)
         IF(SW3.EQ.0.0) CALL MAP(0.0-4.0,29.0,-0.50,YMAX+0.40)
         IF(SW3.EQ.0.0) CALL BOX(0.0-4.0,29.0,-0.50,YMAX+0.40)
         IF(SW3.NE.0.0) CALL MAP(0.0-4.00,29.0,YMIN,YMAX)
         IF(SW3.NE.0.0) CALL BOX(0.0-4.00,29.0,YMIN,YMAX)
            CALL CTRMAG(13)
           IF(SW3.NE.0.0) CALL AXESSI(5.0,0.05)
           IF(SW3.EQ.0.0) CALL AXESSI(5.0,0.2)
              CALL CTRSET(4)
              CALL CTRMAG(5)
              IF(N.LT.10)CALL CTRMAG(10)
           DO 45 I45=1,N
            XX(I45)=STNPOS-X(I45)
 45        CONTINUE
       IF (INDEX.EQ.2) GOTO 11
                 DO 10 I=1,N
                    CALL CTRSET(4)
                    CALL BLUPEN
                       IF(SW3.EQ.0.0)GOTO 22
                    CALL PLOTNC(XX(I),TXOBS(I),NCHAR1)
                    CALL REDPEN
                    CALL PLOTNC(XX(I),TXMODEL(I),NCHAR2)
         GOTO 10
 22        CONTINUE
                    CALL PLOTNC(XX(I),TOBS(I),NCHAR1)
                    CALL REDPEN
                    CALL PLOTNC(XX(I),TMODEL(I),NCHAR2)
 10              CONTINUE
 11              CONTINUE
           IF(N.GE.10)GOTO 90
                 DO 90 I=1,N
                    CALL BLUPEN
                    CALL CTRMAG(7)
                    CALL CTRSET(1)
                       IF(SW3.EQ.0.0)GOTO 23
```

```
                    PAM=NAME(I)
                    CALL PLOTCS(XX(I)-0.7,TXOBS(I)-0.03,PAM,4)
      GOTO 90
   23   CONTINUE
                    PAM=NAME(I)
                    CALL PLOTCS(XX(I)-0.7,TOBS(I)-0.12,PAM,4)
   90         CONTINUE
            CALL BLKPEN
C
      IF (INDEX.NE.1.AND.INDEX.NE.2)  GOTO 111
         CALL BLUPEN
            DO 99 I=1,N
               TX1(I)=TXMODEL(I)+ESTERR(I)
               TX2(I)=TXMODEL(I)-ESTERR(I)
               CALL POSITN(XX(I),TX1(I))
               CALL JOIN(XX(I),TX2(I))
   99       CONTINUE
  111  CONTINUE
            CALL CTRSET(1)
            CALL BLKPEN
            IF(SW3.EQ.0.0)CALL BOX(0.0,30.0,YMAX-0.1,YMAX+0.40)
            IF(SW3.NE.0.0)CALL BOX(0.0,30.0,YMAX-0.13,YMAX)
          CALL CTRMAG(14)
      IF (SW1.EQ.0.0) GO TO 38
            CALL ITALIC(1)
            IF(SW3.EQ.0.0)CALL PLOTCS(11.0,YMAX+0.10,STNAME,20)
            IF(SW3.NE.0.0)CALL PLOTCS(11.0,YMAX-0.040,STNAME,20)
            CALL CTRMAG(8)
           CALL ITALIC(0)
   38  CONTINUE
C
C  UP TO STATEMENT NO.55 IS DESERVED FOR TITLE AND DATA EXPLANATION
C  FOR THE CASE AL THE DATA ARE ON THE SAME FRAME/SAME SCALE(SW1=0,SW2=0)
C
      IF(SW1.EQ.0.0.AND.SW2.EQ.0.0.AND.IPP.EQ.0) GOTO 54
      GOTO 55
   54 IPP=IPP+1
      CALL CTRSET(1)
         IF(SW3.NE.0) GOTO 63
         CALL ITALIC(1)
         CALL CTRMAG(14)
C         CALL PLOTCS(4.0,YMAX+0.20,'MULL TO COLONSAY    ',29)
C        CALL PLOTCS(3.0,YMAX+0.20,'COLONSAY TO N.JURA ',19)
       CALL PLOTCS(4.0,YMAX+0.20,'S.JURA TO N.KINTYRE',19)
C       CALL PLOTCS(4.0,YMAX+0.20,'    MULL TO TIREE',17)
         CALL ITALIC(0)
         CALL CTRMAG(10)
         CALL TYPECS('- AIR GUNS AND EXPLOSIVE SHOTS',30)
         CALL PLOTCS(7.0,YMAX+0.00,'OBSERVED=',9)
         CALL BLUPEN
         CALL TYPECS(' BLUE',5)
         CALL BLKPEN
         CALL PLOTCS(14.0,YMAX+0.00,'CALCULATED=',11)
         CALL  REDPEN
         CALL TYPECS(' RED',4)
```

```
          GOTO 64
   63     CONTINUE
          CALL ITALIC(1)
          CALL CTRMAG(14)
C          CALL PLOTCS(4.0,YMAX-0.05,'MULL TO COLONSAY    ',19)
C         CALL PLOTCS(3.0,YMAX-0.05,'COLONSAY TO N.JURA ',19)
        CALL PLOTCS(4.0,YMAX-0.05,'S.JURA TO N.KINTYRE',19)
C        CALL PLOTCS(4.0,YMAX-0.05,'     MULL TO TIREE',17)
          CALL ITALIC(0)
          CALL CTRMAG(10)
          CALL TYPECS('- AIR GUNS AND EXPLOSIVE SHOTS',30)
          CALL PLOTCS(7.0,YMAX-0.10,'OBSERVED=',9)
          CALL BLUPEN
          CALL TYPECS(' BLUE',5)
          CALL BLKPEN
          CALL PLOTCS(14.0,YMAX-0.10,'CALCULATED=',11)
          CALL  REDPEN
          CALL TYPECS(' RED',4)
   64     CONTINUE
            CALL CTRSET(4)
             CALL BLKPEN
C             CALL PLOTNC(110.0,YMAX-0.09,NCHAR1)
             CALL CTRSET(1)
             CALL BLKPEN
C             CALL PLOTCS(117.0,YMAX-0.09,' TIM'S PICK',11)
             CALL CTRSET(4)
             CALL REDPEN
C             CALL PLOTNC(110.0,YMAX-0.130,NCHAR2)
             CALL CTRSET(1)
             CALL BLKPEN
C             CALL PLOTCS(115.0,YMAX-0.130,'  MY  PICK ',11)
   55     CALL CTRSET(1)
          IF(SW3.EQ.0.0)CALL POSITN(15.0,0.0-0.40)
          IF(SW3.NE.0.0)CALL POSITN(13.0,0.0-0.09)
          CALL CTRMAG(13)
          CALL TYPECS(' RANGE (KM) ',12)
          CALL CTRMAG(13)
             CALL POSITN(-3.0,YMAX/3.)
             CALL CTRORI(1.0)
            IF(SW3.NE.0.0) CALL TYPECS(' T-X/6 (SECS)',13)
        IF(SW3.EQ.0.0) CALL TYPECS('ARRIVAL TIME (SECS)',19)
          CALL CTRSET(1)
          CALL POSITN(STNPOS,0.0)
          CALL PLOTNC(STNPOS,0.0,44)
          CALL PLOTCS(STNPOS,0.02,STNAME,5)
         CALL CTRORI(0.0)
        IF(SW1.EQ.0.0) GOTO 28
        CALL FRAME
   28   CONTINUE
        GO TO 26
   27   CONTINUE
          CALL GREND
        STOP
        END
C
```

```
C
C        THE SUBROUTINE  YMIN  FIMDS THE MINIMUM VALUE OF
C         AN ARRAY A .
C
      SUBROUTINE YMINV(A,MIN,N)
      REAL  MIN,MIN1
      DIMENSION A(N)
      MIN1=A(1)
         DO 33 I=1,N
            IF(A(I).LE.MIN1)  MIN1=A(I)
   33    CONTINUE
      MIN=MIN1
      RETURN
      END
C
C        THE SUBROUTINE YMAX FINDS THE MAXIMUM VALUE
C        OF ARRAY B .
C
      SUBROUTINE YMAXV(B,MAX,N)
      DIMENSION B(N)
      REAL MAX,MAX1
      MAX1=B(1)
         DO 22 I=1,N
            IF(B(I).GE.MAX1) MAX1=B(I)
   22    CONTINUE
      MAX=MAX1
      RETURN
      END
```